

***The design, synthesis and biological evaluation
of novel compounds against biomarkers of
Alzheimer's disease***

Divan Gerald van Greunen

*Submitted in partial fulfilment of the requirements for the degree
of Doctor of Philosophy
in the Faculty of Natural & Agricultural Sciences
University of Pretoria
Pretoria*

June 2019

*Supervised by Dr D.L. Riley
Co-supervised by Dr J-L. Panayides and Prof V. Steenkamp*

Declaration

I, Divan Gerald van Greunen, declare that the thesis, which I hereby submit for the degree of Doctor of Philosophy at the University of Pretoria, is my own work and has not previously been submitted by me for a degree at this or any other tertiary institution.

Divan Gerald van Greunen

June 2019

Abstract

Alzheimer's disease (AD) is the most common neurodegenerative disease accounting for an estimated 60 – 80 % of dementia cases. The disease affected 5.5 million Americans older than 65 years in 2018 alone, and this number is projected to increase to 13.8 million by 2050. The total cost of care in the United States for people with AD was \$277 billion in 2018, making it one of the costliest diseases to treat. Statistics on the prevalence of dementia in South Africa are very limited and according to a study performed in the rural areas of the Eastern Cape in 2017, it was estimated that 352 000 individuals older than 60 are living with dementia. Unfortunately, there are currently no approved therapies which target AD pathology directly and therefore current treatments focus on relieving symptomatic and behavioral aspects of AD. Thus, a lot of focus has been placed on the development of new drugs for different biomarkers as potential treatment of AD.

This study consists of the design, synthesis and biological evaluation of novel compounds against biomarkers of AD. In this study, four different series of compounds, consisting of ninety-one analogues, were synthesized as novel compounds against biomarkers of AD. These included; (i) series 1: *N*-benzylpiperidine carboxamide derivatives; (ii) series 2: 1-(5,6-dimethoxy-8*H*-indeno[1,2-*d*]thiazole-2-yl)urea derivatives; (iii) series 3: 1-amino-3-(indeno[1,2-*b*]indol-5(10*H*)-yl)propan-2-ol derivatives; and (iv) series 4: 6,7-dimethoxy-1-phenyl-1,4-dihydroindeno[1,2-*c*]pyrazole-3-carboxamide derivatives. All compounds were evaluated for activity against acetylcholinesterase (AChE), the major biomarker of AD. Derivatized compounds of series 1 were assessed for activity against butyrylcholinesterase (BuChE). Derivatized compounds of series 3 were assessed for activity against the amyloid precursor protein cleaving enzyme 1 (BACE1).

The first series of fifteen compounds based upon the skeleton of 5,6-dimethoxy-1-oxo-2,3-dihydro-1*H*-inden-2-yl 1-benzylpiperidine-4-carboxylate, a compound previously synthesized, were synthesized and evaluated for activity against acetylcholinesterase. A second series of thirty-five compounds designed to have dual acetylcholinesterase and glycogen synthase kinase 3 inhibitory activity, were synthesized based upon the skeleton of 1-benzyl-*N*-(5,6-dimethoxy-8*H*-indeno[1,2-*d*]thiazol-2-yl)piperidine-4-carboxamide. A third series of seventeen compounds with potential β -secretase 1 inhibitors were designed and synthesized based upon the skeleton of 1-(3,6-dichloro-9*H*-carbazol-9-yl)-3-(naphthalen-1-ylamino)propan-2-ol, a compound previously reported in literature by Macchia and co-workers. A fourth series consisting of twenty-four potential *N*-methyl-D-aspartate (NMDA) receptor antagonists were designed and synthesized based upon scaffolds previously reported in the literature by the Liotta and Kawai research groups.

In order to prepare large quantities of donepezil for use as a stock reagent for the development of libraries of potential BACE1 inhibitors, the preparation of donepezil using continuous flow conditions was attempted. The highest yield obtained for the benzylation of ethyl isonipecotate was 83% at 90 °C with a residence time of 45 minutes as compared to the batch process which took 3 hours to complete with a yield of 79%. Reduction of the (*E*)-2-[(1-benzylpiperidin-4-yl)methylene]-5,6-dimethoxy-2,3-dihydro-1*H*-inden-1-one to afford the final product donepezil was obtained with a yield of 80% after 4.5 hours, with no observable de-benzylation in flow as compared to the batch process which was completed after 6 hours with a yield of 78%. Due to time constraints, Stage 2 of the flow synthesis of donepezil could not be completed. However, with only two of the three steps completed for the flow process, the yield of the individual steps was already improved, and there was a reduction in the reaction time.

Dedication

***Dedicated to my Family. My mother Soreta,
grandmother Joey, brother Jean and in memory
of my father Max.***

Acknowledgements

I would like to first off thank God for giving me the necessary strength and knowledge to complete this thesis.

My supervisors:

- Dr Darren Riley, thank you for all your guidance and support throughout the years. Thank you for giving me the opportunity to explore organic chemistry and always letting me explore every idea I had.
- Dr Jenny-Lee Panayides, thank you for all your guidance and support. Thank you for your wisdom regarding certain aspects surrounding synthetic as well as biological strategies. Also, for your input regarding the compilation of this thesis.
- Professor Vanessa Steenkamp, thank you for your support and guidance regarding the biological aspect of this project, as well as the compilation of this thesis.

George Kleinhans, Marc Boucher, Ian Strydom, Madelien Wooding and Dominique Buyens. You guys are certainly the best colleagues and friends that an academic can have. Thanks for all our chemistry discussions as well as moral support. It helped a lot!

A special thanks to Ms Naomi Steenkamp. Tannie, thank you for all the admin tasks you have performed for me over the years, for which some were not part of your job description, yet Tannie was always able to complete them.

Dr Werner Cordier, I would like to extend my gratitude for teaching me how to perform the biological assays. Thank you for always making time for when I had any queries.

Ms Margo Nell, you were my lab partner when I always visited the Department of Pharmacology. I am truly grateful for all the cytotoxicity assays you performed as well as learning some new assays with you so that I was not alone.

Ms Madelien Wooding, for always running all of my HRMS spectra, even when you were busy with your own studies. I really appreciate it.

Dr Frederick Malan, thank you for the XRD structure elucidation that you did for me.

And lastly, I would like to thank my family. My mother Soreta le Roux, Mom thank you for all your support from day one. Would not been able to complete my studies if not for your support. My grandmother Joey van der Walt, thank you Ouma for all your support. My brother Jean van Greunen,

boet thank you for all the long talks we had. For taking my mind of my work if it got too much. Gawie le Roux, for all your messages of encouragement during my studies. I appreciate it.

Financial Assistance

The financial assistance of the National Research Foundation of South Africa and the University of Pretoria towards this research project is gratefully acknowledged. Opinions expressed in this thesis and conclusions arrived at, are those of the author, and are not necessarily to be attributed to the National Research Foundation of South Africa or the University of Pretoria.

Quote

“You can find work and sort your life out anytime. The pub closes in 5 hours.”

-Bernard Black, Black Books

Table of contents

| | |
|--------------------------------------|-------------|
| Declaration | I |
| Abstract | II |
| Dedication | IV |
| Acknowledgements | V |
| Financial Assistance | VII |
| Quote | VIII |
| Table of contents | IX |
| Abbreviations | XIII |
| List of abbreviations..... | XIII |
| List of chemical abbreviations | XV |

Chapter 1. General introduction

| | |
|---|----|
| 1.1. Alzheimer’s disease..... | 2 |
| 1.2. Signs and Symptoms | 2 |
| 1.3. Diagnosis | 3 |
| 1.3.1. Magnetic resonance imaging..... | 3 |
| 1.3.2. Positron emission tomography | 5 |
| 1.3.3. Cerebrospinal fluid biomarkers..... | 7 |
| 1.4. Pathogenesis and Treatment of Alzheimer’s Disease..... | 7 |
| 1.4.1. Cholinergic hypothesis | 8 |
| 1.4.2. Amyloid hypothesis..... | 14 |
| 1.4.3. Glycogen synthase kinase 3 hypothesis..... | 21 |
| 1.4.4. N-Methyl-D-aspartate hypothesis | 27 |
| 1.5. BRIEF DESCRIPTION OF Aims and Objectives..... | 32 |
| 1.6. References | 32 |

Chapter 2. Novel *N*-benzylpiperidine carboxamide derivatives as inhibitors of acetylcholinesterase

| | |
|-------------------------|----|
| Abstract..... | 48 |
| 2.1. Introduction | 49 |
| 2.2. Chemistry | 51 |

| | | |
|--------|---|----|
| 2.3. | Structure-activity relationship study | 53 |
| 2.4. | Conclusion..... | 56 |
| 2.5. | Experimental..... | 56 |
| 2.5.1. | Chemistry | 56 |
| 2.5.2. | Bioactivity screening..... | 68 |
| 2.6. | Acknowledgements..... | 70 |
| 2.7. | Conflict of interest | 70 |
| 2.8. | Appendix A. Supplementary information | 70 |
| 2.9. | References | 70 |

Chapter 3. Novel 1-(5,6-dimethoxy-8*H*-indeno[1,2-*d*]thiazol-2-yl)urea derivatives as potential dual acetylcholinesterase and glycogen synthase kinase 3 inhibitors for the potential treatment of Alzheimer’s disease

| | |
|--|-----|
| Abstract..... | 73 |
| 3.1. Introduction | 74 |
| 3.2. Chemistry | 78 |
| 3.3. Structure activity relationship study..... | 82 |
| 3.4. Conclusion..... | 87 |
| 3.5. Experimental..... | 87 |
| 3.5.1. Chemistry | 87 |
| 3.5.2. Bioactivity screening..... | 104 |
| 3.6. Molecular modelling..... | 106 |
| 3.7. Acknowledgements..... | 106 |
| 3.8. Conflict of interest | 107 |
| 3.9. Appendix B. Supplementary information | 107 |
| 3.10. References | 107 |

Chapter 4. Novel 1-amino-3-(indeno[1,2-*b*]indol-5(10*H*)-yl)propan-2-ol derivatives as possible β -secretase inhibitors for the treatment of Alzheimer’s disease

| | |
|---|-----|
| Abstract..... | 113 |
| 4.1. Introduction | 114 |
| 4.2. Chemistry | 118 |
| 4.3. Structure activity relationship study..... | 119 |

| | | |
|--------|--|-----|
| 4.4. | Conclusion..... | 122 |
| 4.5. | Experimental..... | 122 |
| 4.5.1. | Chemistry..... | 122 |
| 4.5.2. | Bioactivity screening..... | 133 |
| 4.6. | Acknowledgements..... | 135 |
| 4.7. | Conflict of interest..... | 135 |
| 4.8. | Appendix C. Supplementary information..... | 135 |
| 4.9. | References..... | 135 |

Chapter 5. Synthesis of novel 6,7-dimethoxy-1-phenyl-1,4-dihydroindeno[1,2-c]pyrazole-3-carboxamide derivatives as potential *N*-methyl-*D*-aspartate receptor antagonists for the treatment of Alzheimer’s disease

| | | |
|---------------|--|-----|
| Abstract..... | 141 | |
| 5.1. | Introduction..... | 142 |
| 5.2. | Chemistry..... | 145 |
| 5.3. | Structure activity relationship study..... | 150 |
| 5.4. | Conclusion..... | 152 |
| 5.5. | Experimental..... | 152 |
| 5.5.1. | Chemistry..... | 152 |
| 5.5.2. | Bioactivity screening..... | 168 |
| 5.6. | Acknowledgements..... | 168 |
| 5.7. | Conflict of interest..... | 168 |
| 5.8. | Appendix D. Supplementary information..... | 169 |
| 5.9. | References..... | 169 |

Chapter 6. Synthesis of donepezil as precursor for the development of β -secretase inhibitors for the treatment of Alzheimer’s disease using flow conditions

| | | |
|---------------|-----------------------------------|-----|
| Abstract..... | 176 | |
| 6.1. | Introduction..... | 177 |
| 6.2. | Results and discussion..... | 179 |
| 6.2.1. | Batch synthesis of donepezil..... | 179 |
| 6.2.2. | Flow synthesis of donepezil..... | 180 |
| 6.3. | Conclusion..... | 190 |

| | | |
|--------|--|-----|
| 6.4. | Experimental..... | 191 |
| 6.4.1. | General methods | 191 |
| 6.4.2. | Batch synthesis of donepezil..... | 192 |
| 6.4.3. | Flow synthesis of donepezil | 195 |
| 6.5. | Acknowledgements..... | 197 |
| 6.6. | Conflict of interest | 197 |
| 6.7. | Appendix E. Supplementary information..... | 197 |
| 6.8. | References | 197 |

Chapter 7. Conclusion, and limitations and future work

| | | |
|------|----------------------------------|-----|
| 7.1. | Thesis conclusion | 200 |
| 7.2. | Limitations and Future work..... | 201 |

Abbreviations

LIST OF ABBREVIATIONS

| | |
|-----------------------|---|
| [¹⁴ C]PIB | Pittsburgh Compound-B |
| ¹³ C NMR | Carbon-13 nuclear magnetic resonance |
| ¹ H NMR | Proton nuclear magnetic resonance |
| Acetyl-CoA | Acetyl coenzyme A |
| ACh | Acetylcholine |
| AChE | Acetylcholinesterase |
| AD | Alzheimer's disease |
| ADME | Absorption, distribution, metabolism and excretion |
| APP | Amyloid Precursor Protein |
| ATD | Amino terminal domain |
| Aβ | Amyloid-β |
| BACE1 | Beta-site APP cleaving enzyme |
| BBB | Blood-brain barrier |
| BOLD | Blood-oxygen level-dependant |
| BPR | Back-pressure regulator |
| BuChE | Butyrylcholinesterase |
| CAS | Catalytic anionic site |
| ChAT | Acetyltransferase |
| CNS | Central nervous system |
| CSF | Cerebrospinal fluid |
| CTD | Carboxyl terminal domain |
| CTF | C-terminal fragment |
| <i>EeAChE</i> | <i>Electrophorus electricus</i> acetylcholinesterase |
| eqBuChE | Equine serum butyrylcholinesterase |
| ESI | Electron spray ionisation |
| FAD | Familial Alzheimer's disease |
| FCS | Foetal calf serum |
| FDG-PET | ¹⁸ F-Fluorodeoxyglucose positron emission tomography |

| | |
|------------------|--|
| fMRI | Functional magnetic resonance imaging |
| GAMII | Gas Addition Module II |
| GSK-3 | Glycogen synthase kinase 3 |
| h | Hour(s) |
| HRMS | High-resolution mass spectrometry |
| IC ₅₀ | 50% Inhibitory concentration |
| IR | Infrared |
| LBD | Ligand binding domain |
| MCI | Mild cognitive impairment |
| MHz | Megahertz |
| mp | Melting point |
| MRI | Magnetic resonance imaging |
| NFTs | Neurofibrillary tangles |
| NMR | Nuclear magnetic resonance |
| PAS | Peripheral anionic site |
| PBR | Packed-bed reactor |
| PDH | Pyruvate dehydrogenase |
| PET | Positron emission tomography |
| P-gp | P-glycoprotein |
| R _f | Retention factor, defined as the distance travelled by the compound divided by the distance travelled by the solvent |
| RoF | Lipinski's rule of five |
| rt | Room temperature |
| SAR | Structure-activity relationship |
| SEM | Standard error of mean |
| SI | Selectivity index |
| sMRI | Structural magnetic resonance imaging |
| <i>Tc</i> | <i>Torpedo californica</i> |
| TLC | Thin layer chromatography |
| TMD | Transmembrane domain |
| tPET | Tau positron emission tomography |
| TPKI | Tau protein kinase I |

| | |
|--------|--|
| TPSA | Topological polar surface area |
| T_R | Retention time |
| US FDA | United States Food and Drug Administration |
| UV | Ultraviolet |

LIST OF CHEMICAL ABBREVIATIONS

| | |
|-------------|--|
| 4-DMAP | 4-(dimethylamino)pyridine |
| ACN | acetonitrile |
| AMPA | (<i>S</i>)-2-amino-3-(3-hydroxy-5-methyl-4-isoxazolyl)propionic acid |
| ATP | adenosine triphosphate |
| CDI | carbonyl diimidazole |
| DCM | dichloromethane |
| DIBAL-H | diisobutylaluminium hydride |
| DMSO | dimethyl sulfoxide |
| DMSO- d_6 | deuterated dimethyl sulfoxide |
| DTNB | 5,5-dithiobis-2-nitrobenzoic acid |
| ECH | (\pm)-epichlorohydrin |
| HEA | hydroxyethylamine |
| KA | kainic acid |
| LDA | lithium diisopropylamide |
| NMDA | <i>N</i> -methyl-D-aspartate |
| SRB | sulforhodamine B |
| TDZD | thiadiazolidinone |
| THF | tetrahydrofuran |
| Tris | trisaminomethane |

Chapter 1. General introduction

1.1. ALZHEIMER'S DISEASE

Since the first description of Alzheimer's disease (AD) by Alois Alzheimer in 1907, seventy years elapsed before AD was recognized as a form of dementia [1]. Today AD is the most common neurodegenerative disease [2] accounting for an estimated 60 – 80 % of dementia cases. This disease affected 5.5 million Americans older than 65 years in 2018 alone, and this number is projected to increase to 13.8 million by 2050 [3]. Upon onset of AD, it is estimated that an individual has a life-expectancy of 4-8 years, however cases of individuals living with AD for up to 20 years have been documented [4-8]. The total cost of care in the United States for people with AD was \$277 billion in 2018, making it one of the costliest diseases to manage [3].

Statistics on the prevalence of dementia in South Africa are very limited and according to a study performed in the rural areas of the Eastern Cape in 2017, it was estimated that 352 000 individuals older than 60 are living with dementia [9]. This number was estimated to double over the next fifteen years [9]. Unfortunately, there are currently no approved therapies which target AD pathology directly and therefore current treatments focus on relieving symptomatic and behavioral aspects of AD [10]. Thus, recent research has centered around the development of new drugs focusing on a selection of different targets in order to identify compounds which possess the potential to be fully developed as treatments for the disease.

1.2. SIGNS AND SYMPTOMS

Alzheimer's first description of the disease was when a 51-year old patient, named August D., presented with signs of progressive memory loss, delusions, hallucinations and focal symptoms such as disorientation [11]. Since then, additional signs and symptoms associated with AD have been described which have been found to change over time. The pace at which these symptoms advance differs between individuals [3]. Common signs and symptoms include:

- Memory loss, such as forgetting newly learned information and difficulty recalling information,
- Difficulty or inability to plan or solve problems, such as trying to solve simple mathematical problems like basic addition or taking noticeably longer to do so than before,
- Misplacing items or losing the ability to retrace steps,
- Having trouble completing routine familiar tasks, such as how to cook a simple meal or driving to a familiar place,
- Withdrawal from social or work activities such as hobbies, work projects or sports because of the mental changes they experience, and

- Behavioural changes such as confusion, suspicion, depression, anxiousness or anger. Anger is normally accounted for when individuals forget simple things or due to confusion.

1.3. DIAGNOSIS

The progression of AD transitions from a normal cognition state to mild cognitive impairment (MCI) [12]. Further cognitive decline gradually transitions into early onset AD [13]. The only definite diagnosis of AD is confirmed *post mortem*, however, due to improved diagnostic techniques and criterion it is now possible to provide an earlier probable diagnosis of MCI and AD [14]. A variety of imaging techniques are available, including magnetic resonance imaging (MRI) and positron emission tomography [15]. Alternative diagnostic techniques include the identification of biomarkers such as amyloid- β_{42} together with hyperphosphorylated tau in the cerebrospinal fluid (CSF) [15].

1.3.1. Magnetic resonance imaging

Techniques such as quantitative MRI are especially useful in identifying the anatomical origins of AD [16]. These techniques have become a unique tool for examining brain anatomy alterations since they are non-invasive procedures [17].

1.3.1.1. Structural magnetic resonance imaging

Structural magnetic resonance imaging (sMRI) is focused at the measurement of brain morphology. The technique can be utilized to capture grey matter atrophy caused by the loss of synapses, neurons and dendritic de-arborization, at a microscopic level. In addition, white matter atrophy due to the loss of structural integrity of white matter tracts (presumably due to demyelination of axonal processes and expansion of CSF spaces) can also be observed [18]. These atrophic processes lead to changes in brain anatomy, such as the thinning of the cortical surface, structural variations in several brain regions and variation in regional tissue densities, and have been demonstrated in several neuroimaging-based studies focused on AD classification [19-22].

Two regions of the medial temporal lobe, the entorhinal cortex and hippocampus, are of special interest in the investigation of the pathophysiology of AD (**Figure 1.1**) [23]. Volume measurements taken of the hippocampus showed that the grey matter in AD and MCI patients is altered, with changes in white matter only presenting in AD patients, which is indicative of a more advanced stage of the disease [17]. Furthermore, the reduction in the volume of the hippocampus was found to vary between 30 and 40% depending on the protocol used to obtain the results as well as the degree of severity of the disease [24].

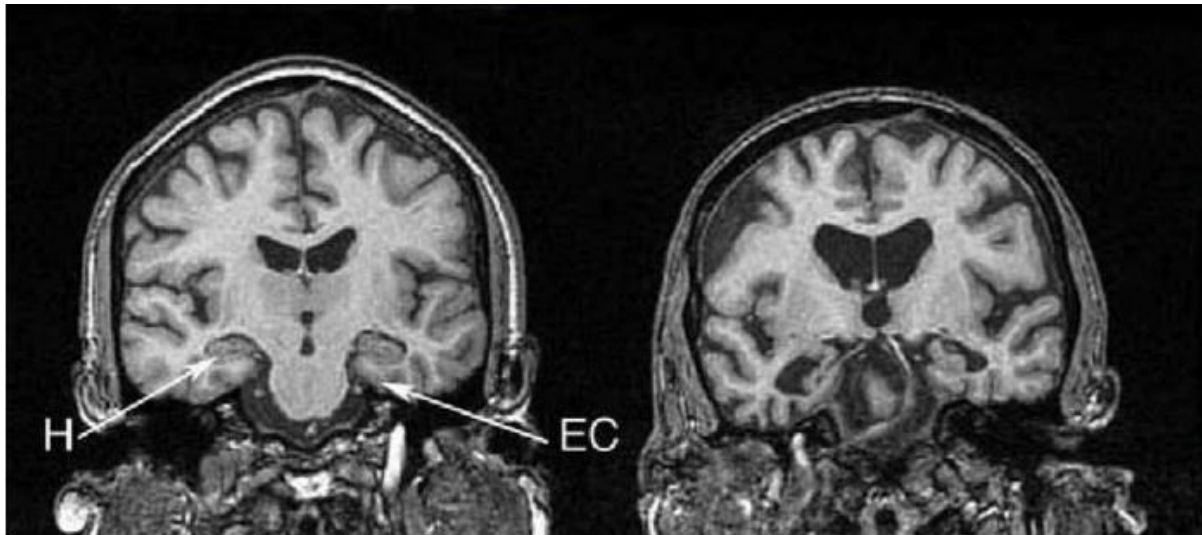


Figure 1.1. sMRI image of a normal older subject (left) and an AD patient (right). The hippocampus (H) and entorhinal cortex (EC) are labelled on the normal subject and shows severe atrophy in the AD patient [19].

Although MRI imaging ‘targets’ the hippocampus to indicate early MCI and AD onset, it is not the site in which the earliest pathology has been identified. *Post mortem* pathological studies rather identify the entorhinal and transentorhinal cortex as the sites of the earliest pathogenesis [12, 16]. Applying sMRI, Pearlson and co-workers demonstrated a 30% reduction in the volume of the entorhinal cortex in AD patients compared to control patients [25]. Due to these changes, early onset AD can potentially be distinguished with the help of sMRI which has successfully been used to monitor the atrophy of the medial temporal lobe, which includes the hippocampus and the entorhinal cortex that are used as AD biomarkers [18, 20, 26, 27].

1.3.1.2. Functional magnetic resonance imaging

Functional magnetic resonance imaging (fMRI) is used to assess alterations in brain function, which are related to the earliest symptoms of AD [28]. This kind of imaging technique relies on the imaging of the endogenous blood-oxygen level-dependent (BOLD) contrast in which changes in cerebral blood flow (CBF), cerebral blood volume (CBV), blood oxygenation and metabolism are monitored [28, 29]. As a result of these physiological changes, functional maps of mental operations can be produced [29].

Due to the clear evidence of neuropathology and structural atrophy in the medial temporal lobe structures of patients within the early stages of AD, fMRI studies focus on utilizing memory tasks and then investigating the alterations in the medial temporal lobe patterns by use of MRI [28]. In a typical fMRI experiment, an MRI signal during one cognitive task (e.g. memory encoding) will be compared to a control task or baseline condition (e.g. visual fixation). In AD patients, an attenuated BOLD

response is noted due to the presence of amyloid- β in the brain, together with altered cholinergic activity and impaired synaptic, neuronal and glial functions [30, 31].

1.3.2. Positron emission tomography

Positron emission tomography (PET) is a functional imaging method in which a positron-emitting radionuclide, such as ^{11}C , ^{15}O or ^{18}F , is used to label ligands of interest in an effort to measure their uptake in a specific region in the body. Due to isotopic decay, a positron is released, which then encounters an electron in the surroundings, causing the two particles to annihilate each other. This then causes a release of energy in the form of two gamma-ray photons, which are then detected by a detector and an image is created [20].

Unfortunately, AD must first reach the stage at which significant cognitive and non-cognitive symptoms are found for this technique to be applied in clinical diagnoses [32]. Recently PET imaging using probes or ligands that bind specifically to amyloid- β ($\text{A}\beta$) and tau aggregates in individuals with MCI or AD have received much attention, due to the feasibility of this technique to possibly provide an earlier diagnosis of MCI and AD [33].

1.3.2.1. ^{18}F -Fluorodeoxyglucose Positron Emission Tomography

^{18}F -Fluorodeoxyglucose PET (FDG-PET) is used to monitor glucose metabolism in the brain. The technique is used in the identification of hypometabolism in the parietal, temporal, posterior cingulate cortices and hippocampus [22]. FDG-PET can differentiate cognitively normal individuals from patients with AD [19] and predict the progression from MCI to AD with high accuracy [34, 35]. Additionally, by coupling PET to MRI it is possible to guide the anatomical sampling, which enables the detection of hippocampal glucose metabolism as well as the regional changes on FDG-PET, which provides a better prediction in the decline from MCI to AD than volumetric MRI [21, 36].

In **Figure 1.2** the FDG-PET scans of a 71-year-old woman, monitored for nine years, is depicted. The patient's cognitive decline from MCI to AD is clearly evident in these scans. The first scan indicates normal cognition in the entorhinal cortex and anterior hippocampal region. A scan taken six years later indicates the decline in cognition to MCI status, which is evident from the reduction in the volume of the entorhinal cortex and anterior hippocampus, as well as by the darkening regions which indicates that less glucose metabolism is occurring. The last scan indicates an even darker region, where almost no glucose metabolism is occurring, resulting in a diagnosis of AD, which was subsequently confirmed during autopsy [37].

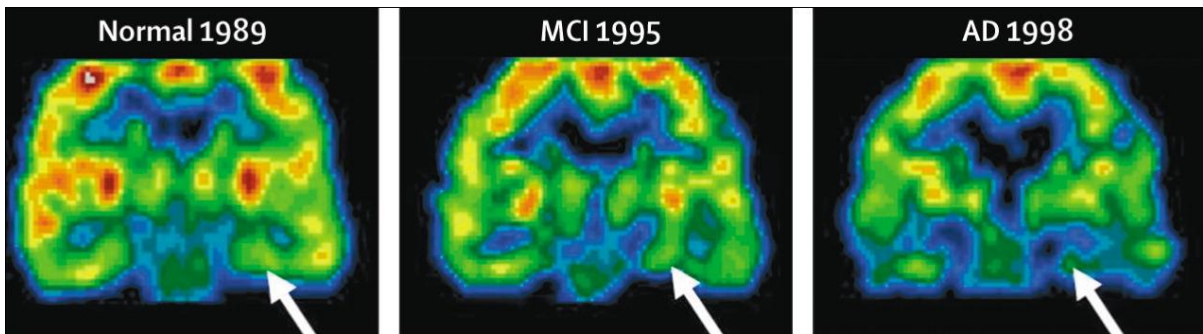


Figure 1.2. Longitudinal metabolic reduction on FDG-PET [37].

1.3.2.2. Amyloid positron emission tomography

Amyloid PET (aPET) is commonly used together with a PET ligand called Pittsburgh Compound-B ($[^{11}\text{C}]\text{PIB}$) which is a ^{11}C radionuclide labelled compound that binds to $\text{A}\beta$ plaques. It has been shown that there is an increased uptake of the ligand in several brain regions in AD patients when compared to healthy patients [38]. A higher uptake of the PET ligand is indicative of an increased presence of $\text{A}\beta$. Kempainen and co-workers reported a higher uptake of $[^{11}\text{C}]\text{PIB}$ in individuals with MCI compared to healthy individuals, suggesting it may be possible to detect early onset AD sooner [39]. Newly designed PET ligands include ^{18}F -florbetapir and ^{18}F -flutemetamol have been shown to be effective in imaging $\text{A}\beta$ fibrillary abnormalities *in vivo* [40]. **Figure 1.3** shows the PET ligand ^{18}F -flutemetamol used in an amyloid PET scan.

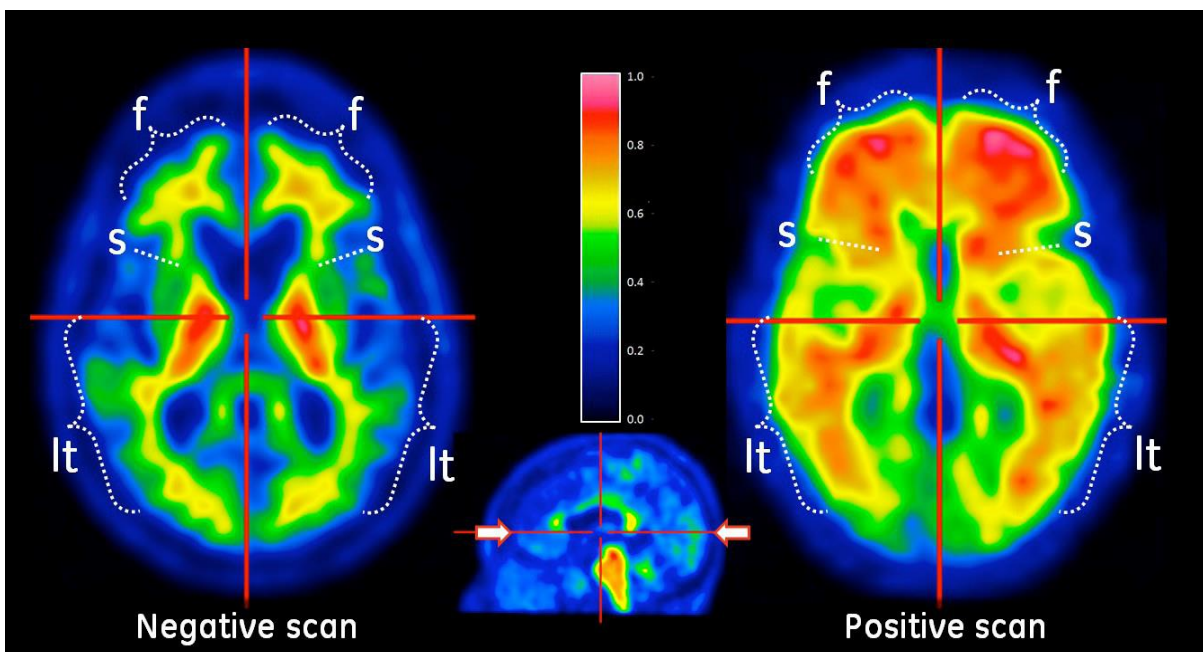


Figure 1.3. Axial view of negative (left) and positive (right) scans. Frontal (f), lateral temporal (lt) and striatal (s) regions of the brain. Positive scan indicating presence of amyloid- β [41].

1.3.2.3. *Tau positron emission tomography*

The tau PET (tPET) ligand, known as [¹⁸F]AV-1451, is used in tPET due to its selectivity towards hyperphosphorylated tau in patients with AD [42, 43]. Xia and co-workers provided evidence that there is a strong association between the severity and distribution of tau pathological findings and the symptoms in patients with typical and atypical AD using [¹⁸F]AV-1451 [44]. Tauopathy has been indicated as the primary determinant of cognitive decline and only tPET has been found to account for significant unique variance in cognition studies using the [¹⁸F]AV-1451 ligand [45].

1.3.3. Cerebrospinal fluid biomarkers

Biomarkers are measurable indicators of a pathological condition. In the case of AD pathology, A β and tau proteins are considered good biomarkers. As AD pathology is restricted to the brain, cerebrospinal fluid (CSF) is an excellent source of these biomarkers as it is in direct contact with the extracellular space of the brain, and biochemical changes in the brain will thus affect the CSF [46, 47]. Therefore, biochemical markers for AD should reflect the central pathogenetic processes such as neuronal degeneration, deposition of A β in plaques as well as hyper-phosphorylation of tau [47].

During the sampling of CSF for A β plaque pathology, a low CSF A β ₄₂ concentration or CSF A β _{42/40} ratio is an indication of A β plaques in the brain due to the selective retention of A β ₄₂ in the brain tissue [48]. As a result of the mis-metabolism of tau due to neurodegeneration and the tangles that form in the brain there will be an increase of both the total tau levels as well as phosphorylated tau [48]. These biomarkers have 85 - 95% specificity for both the MCI and dementia stages of AD [49].

1.4. PATHOGENESIS AND TREATMENT OF ALZHEIMER'S DISEASE

Considered a multifactorial disease, where factors such as age, genetic and/or environmental factors are considered as combinational triggers in the pathological decline in AD, the precise mechanism/s causing the disease are still unknown [50]. However, several hypotheses have been suggested as possible causes of AD. These include the:

- Cholinergic hypothesis,
- Amyloid hypothesis,
- Glycogen synthase kinase 3 hypothesis, and
- *N*-Methyl-D-aspartate hypothesis

The areas of the brain that are affected in AD are the basal forebrain, cortex and amygdala. These areas are involved in attention, learning, memory and emotional regulation. AD is classified as either sporadic or familial (FAD). In sporadic AD there is a severe progressive decline in cognition and increased neuronal cell death occurs. On the other hand, FAD develops much faster and is characterized as being the cause of rare autosomal dominant mutations in three genes namely: the amyloid precursor protein (APP), presenilin-1 and presenilin-2. The latter form of AD accounts for only 2 - 3% of AD cases [10].

1.4.1. Cholinergic hypothesis

In a study carried out in 1976 by Davies and Maloney it was noted that there was a selective loss of activity of choline acetyltransferase (ChAT), the enzyme responsible for the synthesis of the neurotransmitter acetylcholine **1** (ACh) (**Figure 1.4**), in the amygdala, hippocampus and cortex of patients with AD [51]. The authors also noted that there was reduced activity of acetylcholinesterase (AChE), the enzyme responsible for the hydrolysis of ACh **1** into acetic acid **2** and choline **3** (**Figure 1.4**), in the same areas of the cerebral cortex which showed reductions in ChAT activity in individuals with AD compared to healthy individuals with normal brain activity [52].

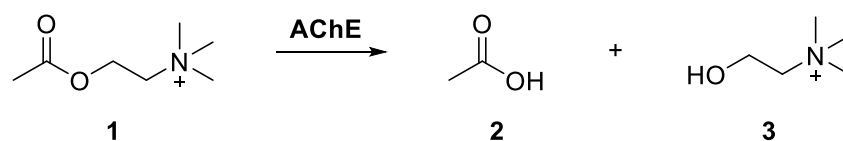


Figure 1.4. Catalytic activity of AChE [51].

This supported the notion that a selective degenerative process had occurred. *Post mortem* studies by other research groups confirmed the decrease in ACh concentrations in cortical tissue due to the reduced activity of ChAT in AD patients [53-57]. Thus, the cholinergic hypothesis postulates that memory impairments in AD patients are the result of a deficit of cholinergic functions [58]. Therefore, research has focused on the enhancement of cortical cholinergic transmission as treatment of AD [59-62]. Two strategies have been proposed to increase ACh levels: (1) the inhibition of AChE to decrease hydrolysis of ACh, and (2) the therapeutic use of directly acting agonists at postsynaptic muscarinic receptors in the cortex [63]. Of these two strategies, the former has been more extensively studied [64] (**Figure 1.5**).

A second enzyme that also hydrolyses ACh, butyrylcholinesterase (BuChE), has been implicated in the pathogenesis of AD (**Figure 1.5**). In *post mortem* samples it was noted that where there was a decrease in AChE, there was a corresponding increase in BuChE activity [65]. It is suggested that the combined cholinesterase abnormalities may be specifically associated with the pathology of senile dementia. It

has been noted that the efficiency with which AChE and BuChE hydrolyze ACh differs depending on the concentration of ACh. BuChE hydrolyses ACh more efficiently when present at high concentrations, whereas AChE has a greater catalytic activity at lower ACh concentrations. Since lower concentrations of ACh are found in AD patients, it is the preferred therapeutic target for increasing ACh concentrations [66].

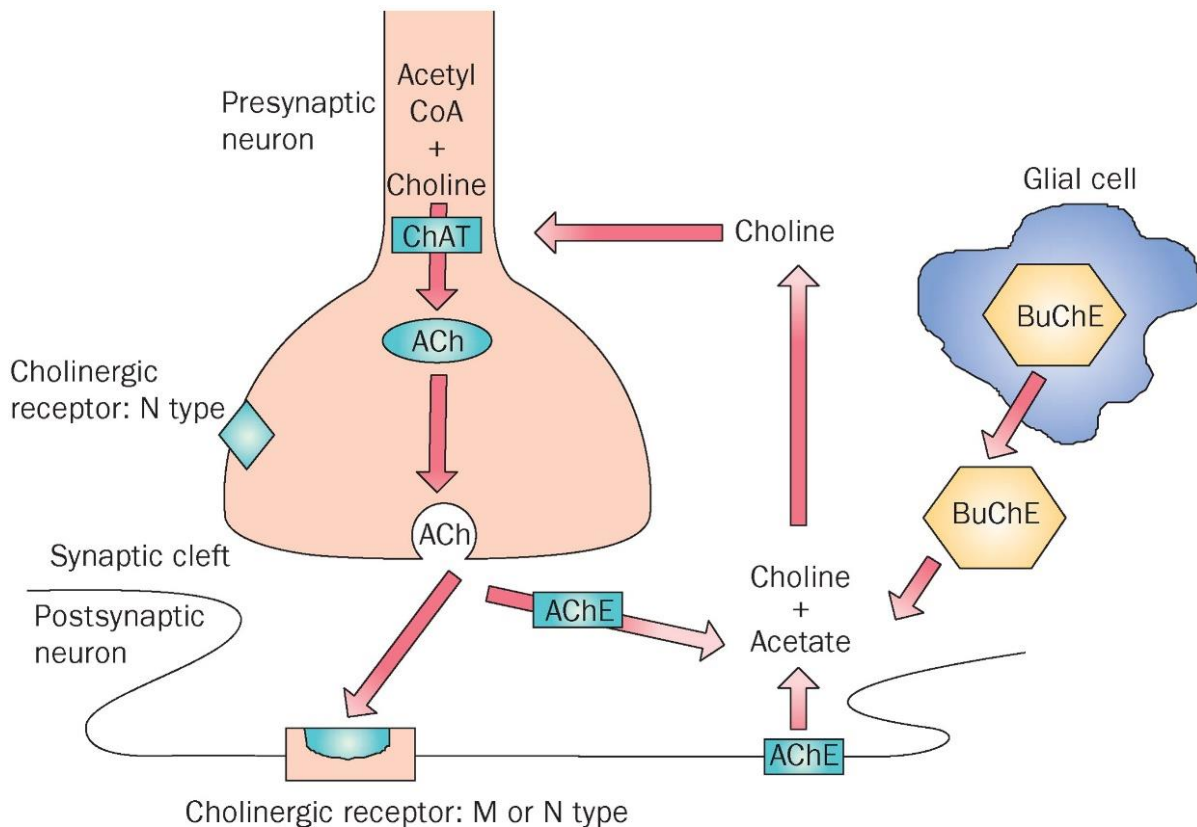


Figure 1.5. The cholinergic functional system [67]. (ACh = acetylcholine, AChE = acetylcholinesterase, ChAT = choline acetyltransferase, BuChE = butyrylcholinesterase, acetyl CoA = acetyl coenzyme A, M = muscarinic, N= nicotinic).

The three-dimensional structure of AChE isolated from the Pacific electric ray *Torpedo californica* (*Tc*), was delineated by Sussman and co-workers in 1991 [68, 69]. This assisted in rational drug design by understanding the ACh-binding site, as well as other sites implicated in the inhibition of AChE [68].

AChE, a serine-protease, contains two main domains; the catalytic anionic site (CAS) and the peripheral anionic site (PAS) which are located approximately 20 Å from each other [68]. In the active site there are three amino acid residues: Ser200, His440 and Glu327, which constitute the catalytic triad. The CAS is located at the bottom of a deep and narrow gorge, which is characterized by several domains:

- (i) the anionic site, where Trp84 is a key residue important for the interaction with the quaternary ammonium group of ACh, as well as other ligands via cation- π interaction through Phe330,
- (ii) the esteratic site, to which nerve agents bind,
- (iii) the oxyanion hole or anionic loci, which is a hydrophobic region that is near the esteratic site and which is important in binding aryl substrates and active site ligands, and the acyl pocket which confers substrate selectivity as shown in **Figure 1.6** [68, 70, 71].

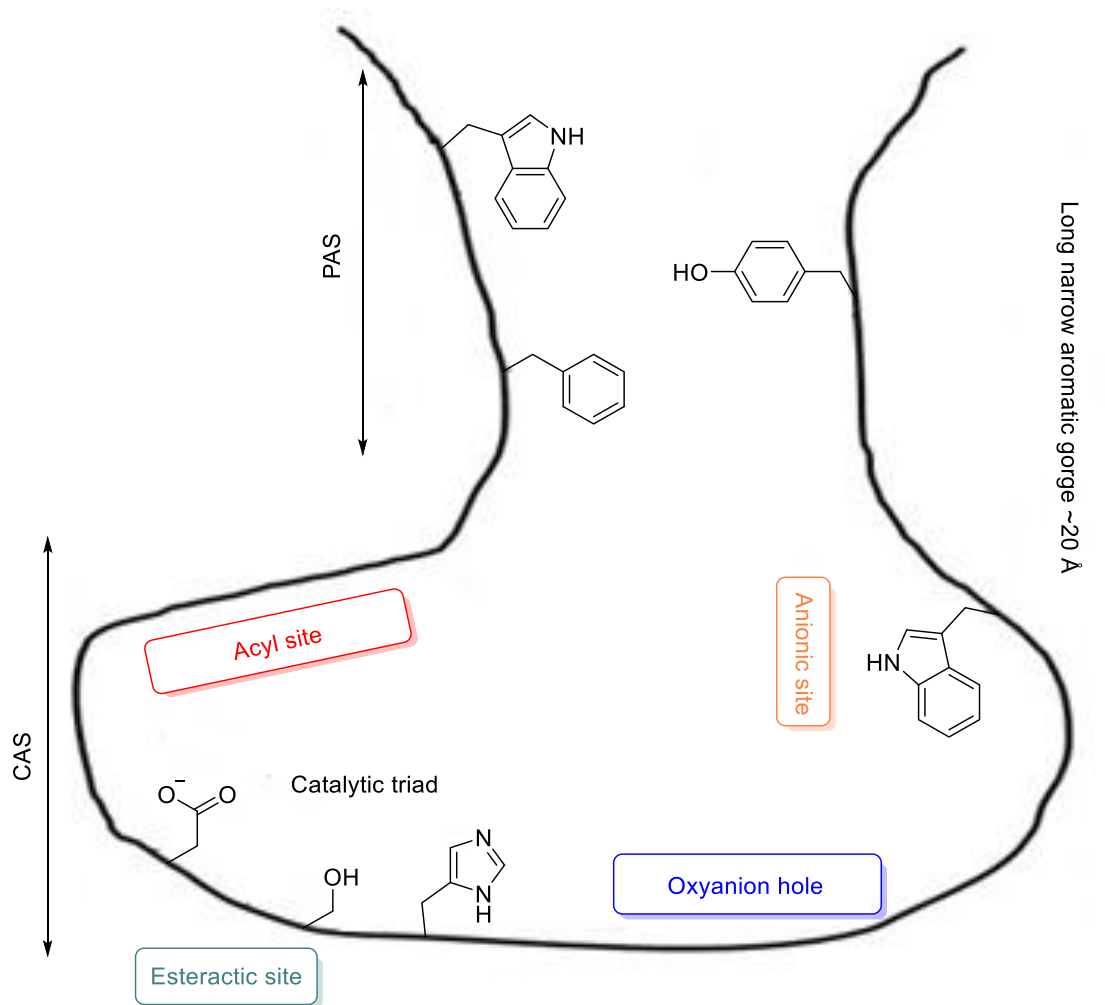


Figure 1.6. Schematic illustration of the active site gorge of *TcAChE* [70, 72].

The PAS is the area that is located at the entrance to the CAS. Although it is still not well defined, the arrangement appears to change frequently during ligand occupation. The active centre contains Tyr70, Asp72, Tyr121, Trp279 and Tyr334, of which Trp279 is responsible for the adhesion function of AChE. The function of the PAS is to bind the substrate in a transient fashion and this is considered the first

step in the catalytic pathway, where it enhances the catalytic efficiency by trapping the substrate on its way to the active site [68, 71].

The use of AChE inhibitors may inhibit AChE through either, (i) a competitive mechanism in which the inhibitor may interact with the CAS, (ii) through a non-competitive mechanism by binding to the PAS, or (iii) by inhibiting AChE through both mechanisms, thus exerting a dual binding inhibition [73]. In recent literature, it has been shown that the PAS also plays a role in non-catalytic actions, such as the aggregating activity of A β . This can also be attributed to AChE, as the PAS provides a seeding location for small molecular weight oligomers, further promoting the aggregation process, as well as the formation of highly toxic AChE-A β complexes [72-75]. Several AChE inhibitors not only facilitate cholinergic transmission, but also interfere with the synthesis, deposition and aggregation of A β [76-80]. Thus, the inhibition of AChE is a critical strategy for the management of AD.

AChE predominates in a healthy brain; this situation, however, changes during AD, where the activity of BuChE progressively increases [70]. It has recently been reported that BuChE prevents A β -fibril formation and thereby delays the formation of A β -aggregation in the brain, which is in contrast to AChE [72]. BuChE possesses several structural similarities in the CAS to AChE, but it lacks three of the four aromatic residues in the PAS, explaining the difference in selectivity between AChE and BuChE [72]. As the role of BuChE in the regulation of cholinergic transmission is not yet fully understood, AChE remains the main target within the cholinergic hypothesis [70]. That being said, in AChE inhibition studies, parallel BuChE inhibition assays are carried out in order to attain selectivity parameters of the compounds being studied [70].

Currently approved drugs for the symptomatic treatment of AD by the United States Food and Drug Administration (US FDA) include the three AChE inhibitors: donepezil **4**, galantamine **5** and rivastigmine **6** (**Figure 1.7**) [50]. Tacrine **7**, the first US FDA approved AChE inhibitor, was discontinued 2013 due to concerns over hepatotoxicity [81].

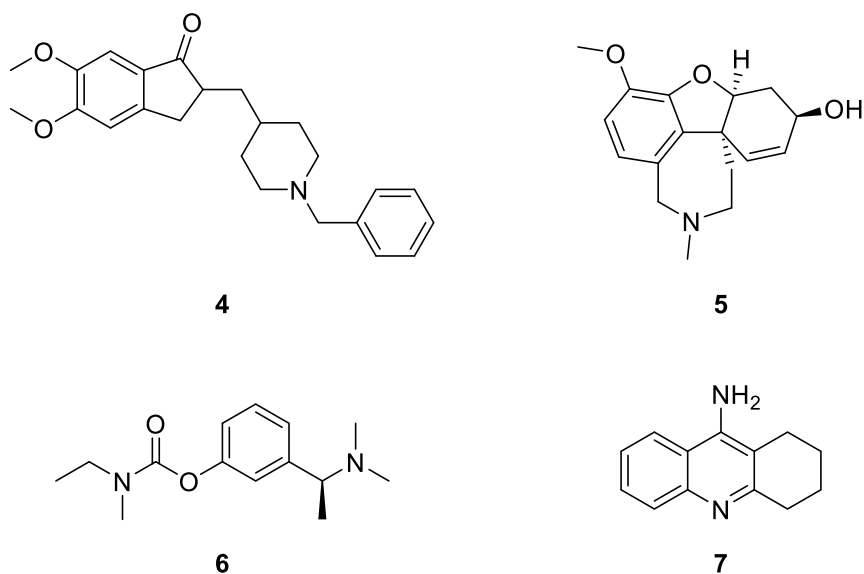


Figure 1.7. Current and former FDA approved AChE inhibitors for the treatment of AD [50, 81].

Inhibitors of AChE can be divided into two categories:

- Natural AChE inhibitors
- Synthetic AChE inhibitors

Due to the extensive amount of research conducted on AChE inhibitors, only select examples will be mentioned in the discussions that follow.

1.4.1.1. Natural AChE inhibitors

Huperzine A **8** (**Figure 1.8**), isolated from the Chinese herb *Huperzia serrata*, is a potent reversible inhibitor of AChE and has been shown to afford significant improvement of memory in aged subjects and patients with AD. Compound **8** has a human AChE IC_{50} of 0.26 μ M (Ellman's assay method) and its use for the treatment of AD has been approved in China [82, 83].

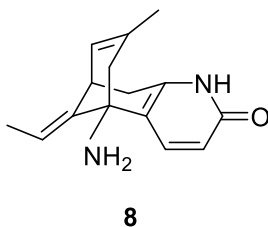


Figure 1.8. Huperzine A **8** [82].

Mahanimbine **9**, a carbazole alkaloid isolated from the *Murraya koenigii* leaves, is one of many carbazole derivatives which have shown bovine AChE inhibition activity (IC_{50} 30 μ g/mL) using Ellman's

assay method. Mahanimbine **9** contains a carbazole core that is regarded crucial for its activity (**Figure 1.9**) [84].

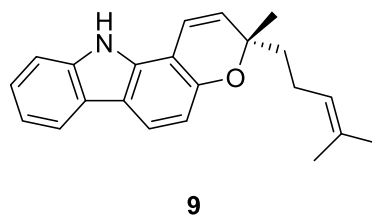


Figure 1.9. Carbazole alkaloid mahanimbine **9** [84].

1.4.1.2. Synthetic AChE inhibitors

In the search for new AChE inhibitors, Liu and co-workers designed and synthesized a series of 7*H*-thiazolo[3,2-*b*]-1,2,4-triazin-7-one derivatives, which interacted with both the CAS and PAS [77]. It was found that compound **10** and compound **11** (**Figure 1.10**) were the most active AChE inhibitors, with an inhibition of 90% and 74% at 10 μ M respectively [78].

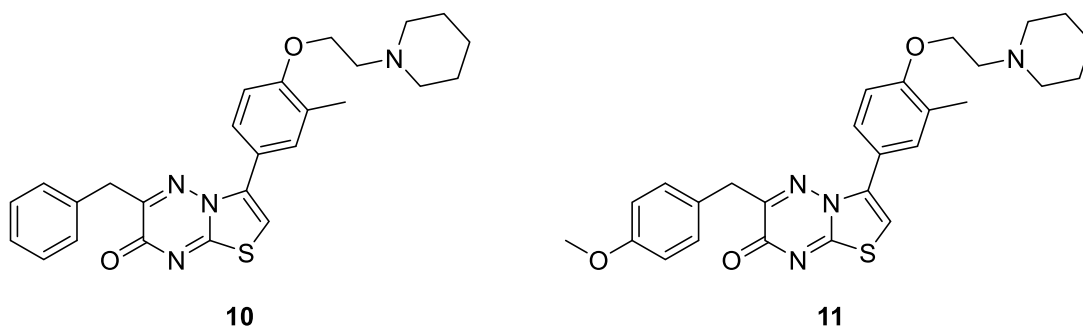


Figure 1.10. 7*H*-Thiazolo[3,2-*b*]-1,2,4-triazin-7-one derivatives [78].

Novel pyrano[3,2-*c*]quinolone derivatives (**Figure 1.11**) were designed and synthesized by the Muñoz-Torrero group. Utilizing molecular docking studies, the derivatives were designed based on the predicted ability of compound **12** to bind to the PAS at the entrance of the catalytic gorge of AChE [79]. Although compound **12** possessed weak inhibition of AChE, of the fourteen derivatives synthesized, compound **13** was the most potent *Electrophorus electricus* AChE inhibitor with an IC_{50} of 4.6 nM using Ellman's assay method. In addition to their AChE inhibition studies, an *in vitro* parallel artificial membrane permeability assay to determine the blood-brain barrier (BBB) permeability was performed, where compound **13** was found to be able to penetrate the BBB [79].

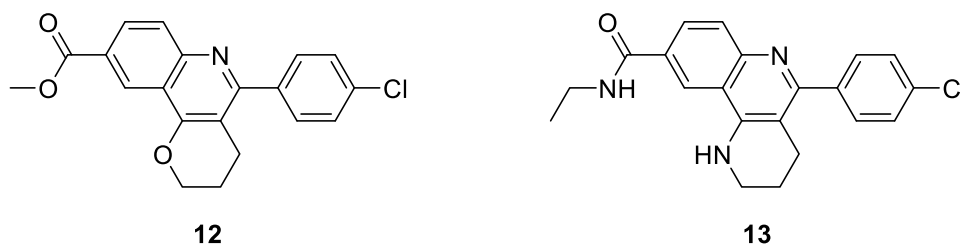


Figure 1.11. Pyrano[3,2-*c*]quinolone derivatives [79].

Xia and co-workers designed and synthesized 2-arylethenyl-*N*-methylquinolinium derivatives as multifunctional agents in which they targeted AChE, BuChE, A β aggregation, anti-oxidant activity and BBB permeability [80]. Compound **14** (**Figure 1.12**) was shown to be a specific inhibitor of the PAS of AChE ($IC_{50} = 1.5 \mu M$), reducing the AChE-induced A β aggregation (93% inhibition), and having a significant effect on the protection of neuronal cells against glutamate-induced cytotoxicity in HT22 cells via inhibition of the formation of reactive oxygen species (ROS). Furthermore, the compound was shown to penetrate the BBB by performing an *in vitro* parallel artificial membrane permeability assay [80].

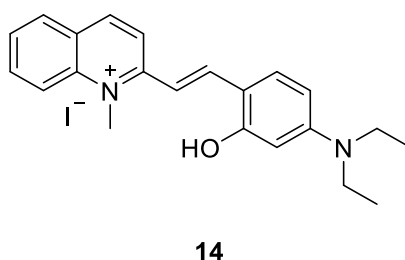


Figure 1.12. 2-Arylethenyl-*N*-methylquinolinium derivative, compound **14** [80].

1.4.2. Amyloid hypothesis

The amyloid hypothesis or amyloid cascade hypothesis revolves around the cascade of events arising during the formation and accumulation of A β fragments in the extracellular matrix of neuronal cells [85]. The A β fragment is cleaved from the transmembrane protein, known as the amyloid precursor protein (APP), found mainly in the neuronal and glial cells of the brain [86]. Although the primary function of APP is not fully understood, it has been found to be crucial in neuronal plasticity as well as synapse formation [74]. The cleavage of the APP is accomplished by a set of proteolytic enzymes, known as the secretase enzymes (α , β and γ secretase). These enzymes cleave APP at different sites of the protein, leading to the formation of different fragments [74]. During the cleavage of APP, there are two types of metabolic pathways: the non-amyloidogenic and the amyloidogenic pathway (**Figure 1.13**). In the non-amyloidogenic pathway, α -secretase initiates pathway events [87].

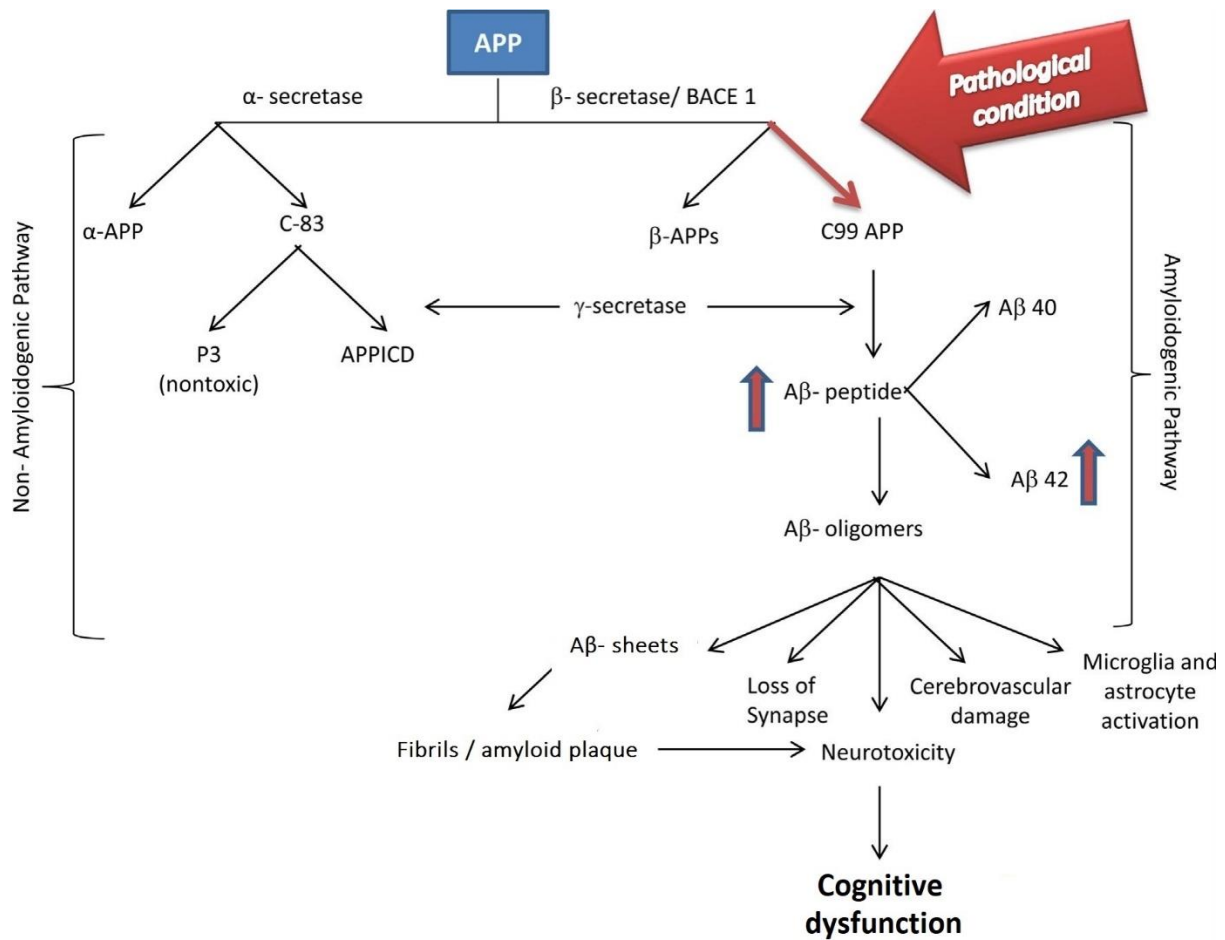


Figure 1.13. Diagrammatic presentation of the amyloid precursor protein metabolic pathways [91].

The APP cleavage site for α -secretase is very close to the cell membrane surface and is situated between the Lys16 and Leu17 amino acid residues. This cleavage site disrupts the release of the full length A β _{1-40/42} peptide fragment. Due to the proteolysis between the specific amino acid residues, the extracellular release of a large soluble APP-alpha fragment (α -APPs) and a membrane-help C-terminal fragment (C-83) is accomplished in which no further secretase metabolism is required [88, 89]. However, the C-83 fragment is further processed by γ -secretase in which an amyloid intracellular domain fragment and a A β _{17-40/42} fragment is released, with both fragments having an impact on neuronal function such as inflammatory glial modulators, thereby playing a role in the development of the immunopathology observed in AD [74, 90].

The amyloidogenic metabolic pathway is initiated by β -secretase; however, γ -secretase also plays a role in this pathway. β -secretase is also referred to as the beta-site APP cleaving enzyme 1 (BACE1) and similar to α -secretase, is a transmembrane protein. Classified as an aspartyl protease, it has a large N-terminal domain which is responsible for the cleavage functionality, although its extracellular domain has a flexible hairpin loop (also called the flap) which plays a crucial role in BACE1's proteolytic

activity by managing substrate binding as well as the active site conformation [92, 93]. The cleavage site on APP for BACE1 is located further upstream to that of α -secretase and consequently has no impact on the A β -peptide sequence. The proteolytic cleavage by BACE1 produces a soluble APP-beta (β -APPs) fragment, as well as a membrane-held C-terminal fragment (C-99), which carries the full-length A β -peptide at the *N*-terminus [74]. In an analogous fashion to C-83, only C-99 is processed further by γ -secretase to release the full A $\beta_{1-40/42}$ fragment [94, 95].

The full A $\beta_{1-40/42}$ fragment released via the amyloidogenic metabolic pathway is a normal process; however, in AD deviation in this process occurs due to a wide range of regulatory mechanisms that start failing, such as the APP metabolism shifts from non-amyloidogenic to amyloidogenic which causes an inefficient clearance of A $\beta_{1-40/42}$ fragments. Thus, a build-up of these monomeric fragments causes them to undergo misfolding arrangements, which results in various levels of aggregate deposits. The oligomeric structures which are formed, are soluble in nature and are considered the most toxic of all the aggregate forms [96, 97]. Due to the maturation of these oligomers, individual filaments are generated which form fibrils that take on an anti-parallel, cross- β -sheet formation, causing the dense plaque deposits seen in neuroimaging [98-100]. As BACE-1 is the initiator of the amyloidogenic metabolic pathway, it is considered a very desirable target for the development of treatments for AD.

β -secretase/BACE1, also known as memapsin 2, was discovered in 1999 and has remained a highly challenging target in drug discovery [101]. As a member of the pepsin-like family of aspartyl proteases, it contains a characteristic dual active site motif (Asp-Thr/Ser-Gly-Thr/Ser) in its ectodomain [102, 103]. Initially formed in the endoplasmic reticulum as an immature, glycosylated pro-peptide referred to as pro-BACE1, the pro-peptide is finally cleaved in the Golgi apparatus into mature BACE1 [104, 105]. As pro-BACE 1, the pro-peptide has both a closed and open conformation, in which the latter can exhibit some enzymatic activity. However, when in the closed conformation, the pro-domain covers the active site therefore inhibiting the activity of pro-BACE1, and acting as a weak inhibitor of BACE1 activity (**Figure 1.14**) [106, 107].

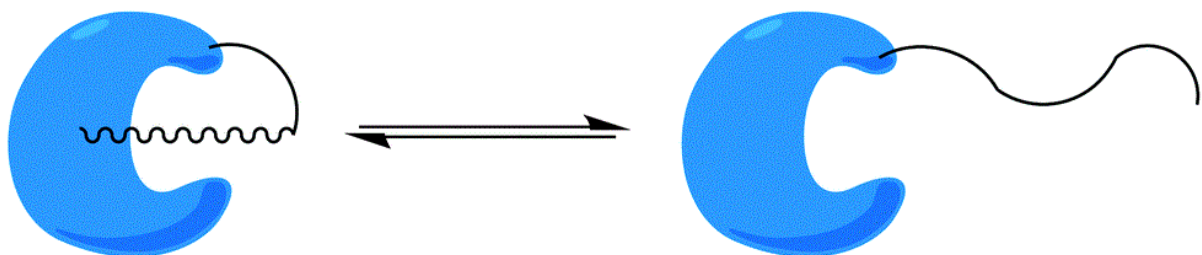


Figure 1.14. Closed (left) and open (right) conformations of pro-BACE1 [107].

The full enzymatic activity of BACE1 is achieved by the cleavage of the pro-domain, thereby allowing the catalytic active site to be fully accessible to the substrate [108]. As a monomeric protein, BACE1 has four *N*-linked glycosylation sites and six luminal cysteines, which allows for the formation of up to three intramolecular disulfide bonds, and therefore, the enzyme is considered to be a type I transmembrane protein in which the active site is on the luminal side of the membrane where it cleaves APP [101, 109]. The disulfide bonds, in particular Cys330/Cys380 are found inside the active site of BACE1 and is important for the stability and activity of the enzyme [110].

BACE1, similarly to pro-BACE1, has two major conformations known as a flap open conformation and a flap closed conformation, as indicated in **Figure 1.15** [107]. The flap open conformation of BACE1 is found when no substrate is bound to the enzyme. The latter is energetically stable and held together by optimal hydrogen bonds.

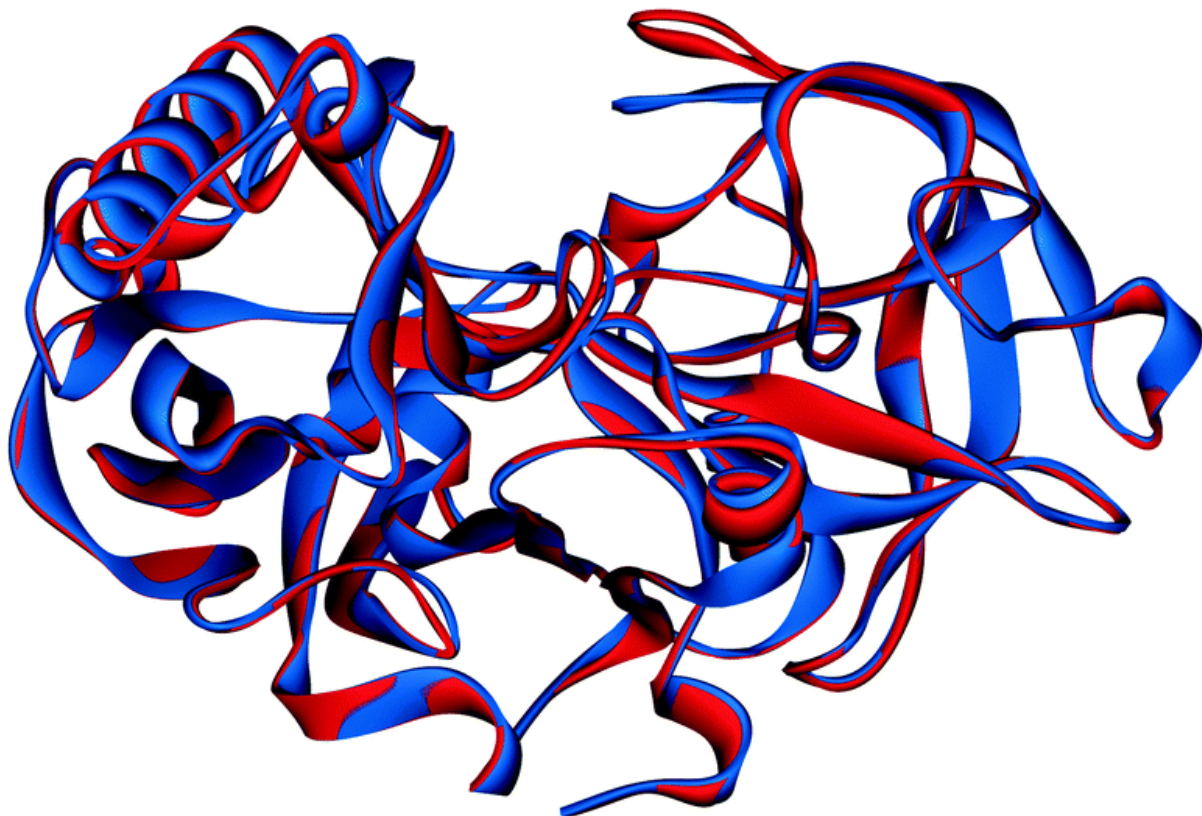


Figure 1.15. Open flap (in red, PDB: 1SGZ) and closed flap (in blue, PDB: 1M4H) conformations of mature BACE1 [107].

The BACE1 adopts a flap closed conformation when bound to the substrate [111]. In order to perform this conformational shift from flap open to flap closed, there is a breakage of hydrogen bonds between the oxygen of Tyr71 and the nitrogen of Gly74, the nitrogen of Lys75 and the oxygen of Glu77, and the hydroxyl of Tyr71 and the oxygen of Lys107. The latter is caused by the interaction between the

substrate and the enzyme [111]. Due to this conformational change, a new interaction occurs between side chain Tyr71, and the indole nitrogen of Trp76. Although substrates can enter through a cleft in the enzyme while in the flap open conformation, a bottleneck occurs which is formed by Thr72, Arg235, Ser328, and Thr329, which requires some flexibility in the substrate [111].

BACE1 has been identified as a significant target in AD intervention, and it is proposed that its inhibition would halt the formation of A β at the initiation of APP processing. Conversely, targeting later stages in the amyloid cascade causes the excess A β generated to be harmful to cognitive function even before neuronal death, which limits synaptic function [112]. Therefore, it would be ideal to slow down the progression of AD by inhibiting A β formation at an early stage.

BACE1 inhibitors can be divided into two categories:

- Peptidomimetic BACE1 inhibitors
- Non-peptidomimetic BACE1 inhibitors

1.4.2.1. Peptidomimetic BACE1 inhibitors

Designed to mimic the natural substrate of the enzyme, peptidomimetic inhibitors ensure that subsite specificity, hydrogen bonding, and hydrophobic interactions are enhanced or conserved [107]. Ghosh and co-workers were the first to demonstrate the druggability of BACE1 by developing the substrate inhibitor OM99-2 **15** and demonstrating the interaction of the substrate with the enzyme by obtaining a crystal structure of the BACE1 and OM99-2 **15** complex [103, 113]. OM99-2 **15** showed potent *in vitro* BACE1 inhibition activity of 1.6 nM [113]. Subsequent development of **15**, in which asparagine and valine were substituted for aspartic acid and leucine respectively, afforded the more potent BACE1 inhibitor **16** with an inhibition activity of 0.3 nM (**Figure 1.16**) [114].

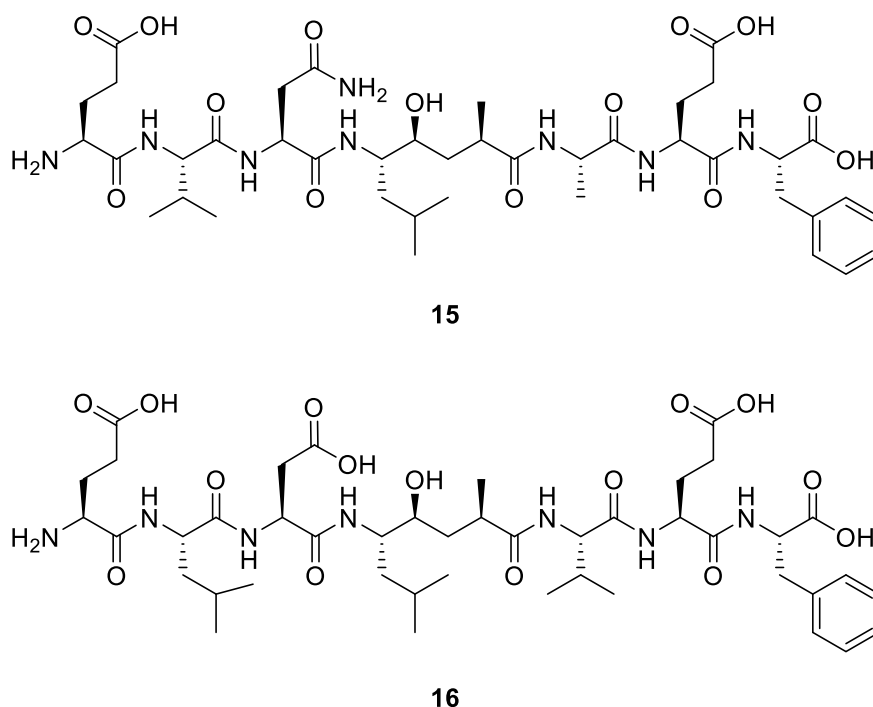


Figure 1.16. Peptidomimetic BACE1 inhibitors OM99-2 **15** and OM00-3 **16** [103, 113, 114].

Milliard and co-workers developed a series of BACE1 inhibitors containing a hydroxyethylamine (HEA) moiety linked to an isophthalamide moiety in which the HEA group has *R*-stereochemistry at the transition state isostere, as well as a 3,5-difluorophenyl fragment at the P1 cleavage site. Compound **17** (**Figure 1.17**) was found to be a highly potent and cell permeable peptidomimetic inhibitor of human BACE1 with an IC_{50} value of 20 nM [115]. Kortum and co-workers substituted the methyl group for an amide group and discovered compound **18** with an IC_{50} value of 11 nM (**Figure 1.17**) [116].

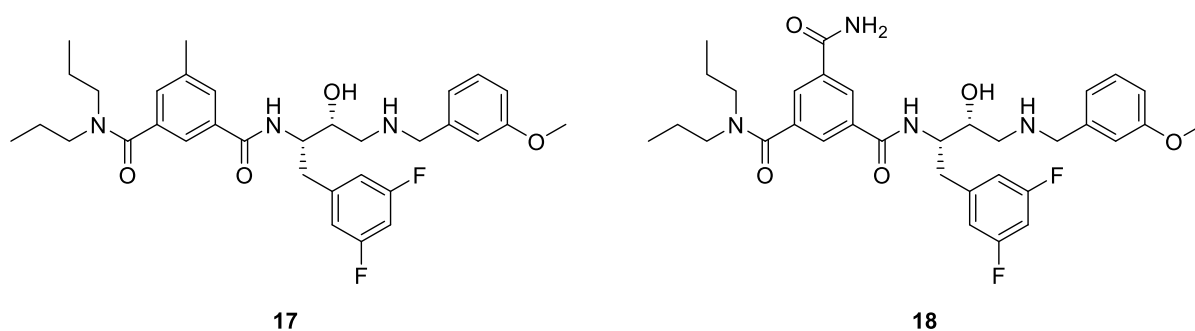


Figure 1.17. Hydroxyethylamine-type peptidomimetic BACE1 inhibitors [115, 116].

1.4.2.2. Non-peptidomimetic BACE1 inhibitors

In an effort to discover novel non-peptidomimetic BACE1 inhibitors, Gerritz and co-workers performed a NMR spectroscopy direct binding structure-based fragment screening search in which they discovered acyl guanidine **19** [117]. Although the K_i value of 3.9 μ M was far less potent than that of

peptide-based inhibitors such as compound **17**, they felt that the unusual structure needed further exploration. Their curiosity was rewarded with improved compound **20** that had a K_i value of 0.005 μM (**Figure 1.18**) [117].

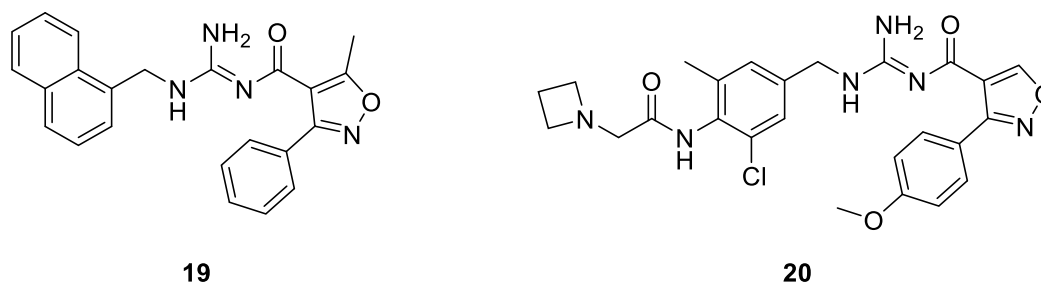


Figure 1.18. Acyl guanidine non-peptidomimetic BACE1 inhibitors [117].

Another highly potent BACE1 non-peptidomimetic inhibitor, lanabecestat **21** (**Figure 1.19**), was developed by AstraZeneca. It was found to have an IC_{50} value of 0.6 pM and by performing an *in vitro* parallel artificial membrane permeability assay it was shown to possess BBB penetration [118]. This inhibitor progressed to phase-III clinical trials [118], but after failing interim futility analyses the trials were halted in mid-2018. Results of the trials are yet to be published [10].

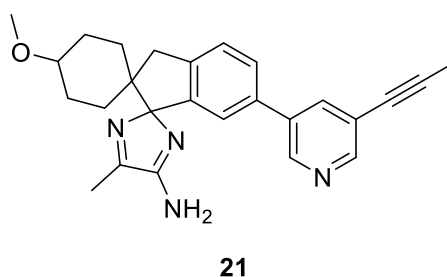


Figure 1.19. Lanabecestat **21** [118].

Brodney and co-workers focused on designing BACE1 inhibitors that contained a spirocyclic sulfamide moiety which interacts through a N-H hydrogen bond with Gln73 in the S1 pocket of BACE1 [119]. Through their exploration, they discovered compound **22**, which showed a weak IC_{50} value of 20.9 μM (**Figure 1.20**). Thereafter, using structure-activity relationship guided studies, which involved varying the aryl and alkyl substituents, they discovered potent compound **23** (**Figure 1.20**), with an IC_{50} value of 0.10 μM [119].

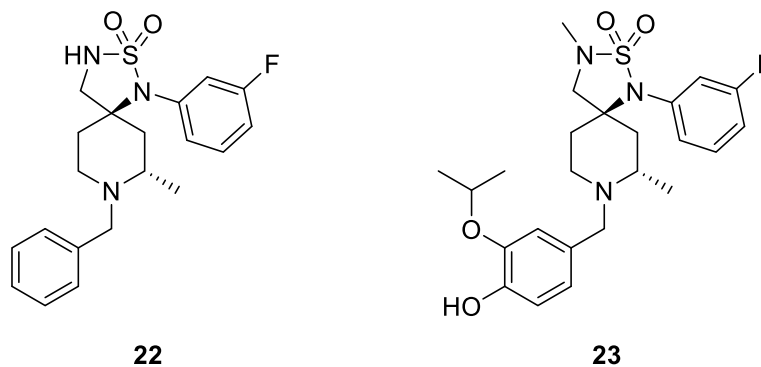


Figure 1.20. Spirocyclic sulfamide non-peptidomimetic BACE1 inhibitors [119].

1.4.3. Glycogen synthase kinase 3 hypothesis

Defined as a proline-directed serine/threonine kinase, glycogen synthase kinase 3 (GSK-3) plays a pivotal and central role in the pathogenesis of both the sporadic and familial forms of AD [121]. There are two types of GSK-3, namely GSK-3 α and GSK-3 β , which are involved in a variety of cellular processes such as glycogen metabolism, gene transcription, apoptosis and microtubule stability [120]. To date, there is not much direct evidence of its involvement in AD pathology, as it is technically difficult to measure the GSK-3 enzymatic activity in *post mortem* brain tissue. There is however indirect evidence, including:

- (i) the co-localization of GSK-3 with dystrophic neurites and NFTs [121, 122],
- (ii) the appearance of active GSK-3 in neurons with pre-tangle changes [123],
- (iii) increased GSK-3 activity in the frontal cortex in AD patients as evidenced by immunoblotting for GSK-3 phosphorylated at its tyrosine-216 residue [124],
- (iv) as well as the up-regulated expression of GSK-3 in the hippocampus of AD patients [125].

GSK-3, a tau phosphorylating kinase, is known to deactivate enzymes by phosphorylation, including as examples glycogen synthase and the insulin receptor substrates. GSK-3 β is abundant in the CNS [126] and it has been shown that granulovascular degenerated neurons contain GSK-3 β [126]. This implies that there is a critical involvement of GSK-3 β in neurodegeneration.

Two microtubule-associated proteins, microtubule-associated protein 1B (MAP 1B) and tau, are both substrates of GSK-3 in neurons, and their microtubule threads are destabilized by GSK-3 phosphorylation [127-129]. In AD patients, GSK-3 β hyper-phosphorylates the microtubule-associated tau protein leading to the detachment of tau from the microtubules in the neurons (**Figure 1.21**). As a result of the accumulation of hyper-phosphorylated tau protein, paired helical filaments are formed, the so-called neurofibrillary tangles (NFTs), which ultimately results in neuronal death. Tau is reported

to be phosphorylated by GSK-3 by at least twelve serine/threonine pro-sites *in vitro* and in transfected cells [130-133]. It is evident that GSK-3 is the key kinase responsible for the hyperphosphorylation of the tau protein.

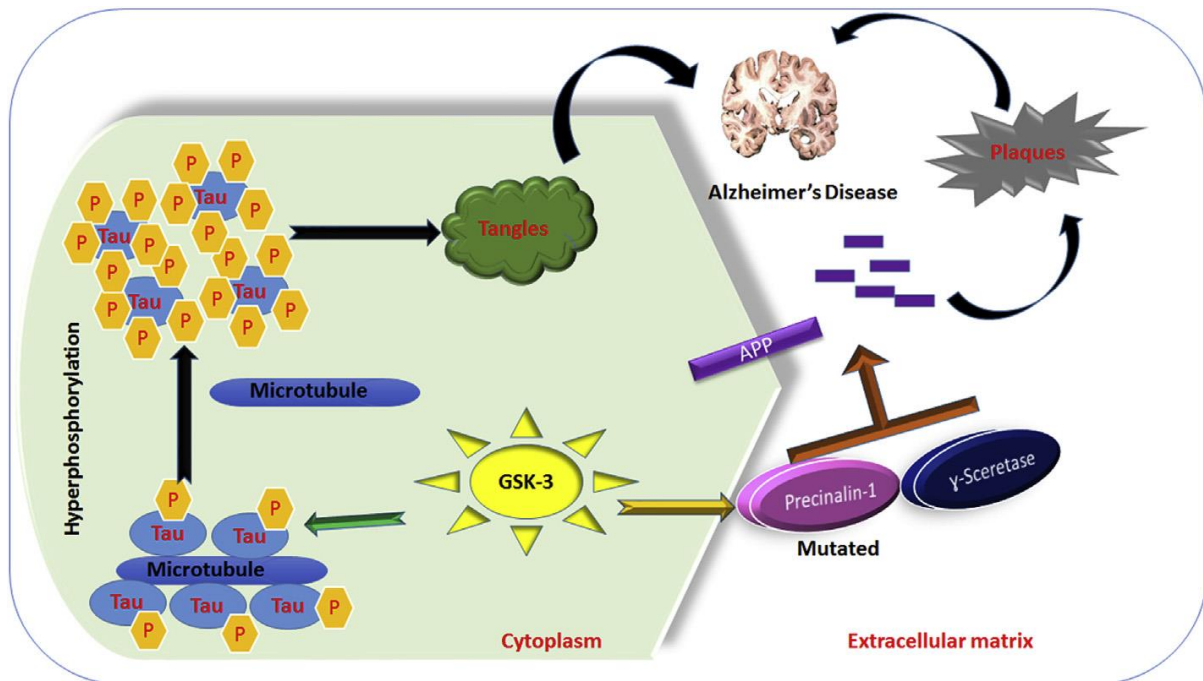


Figure 1.21. Involvement of GSK-3 in the production of A β and tau phosphorylation [134].

GSK-3 α , and not GSK-3 β , regulates the APP cleavage metabolism through its action on γ -secretase [134], resulting in increased production of A β . Although the over activity of GSK-3 is not the primary cause of AD, it would serve to augment A β production. Therefore, also augmenting tau hyperphosphorylation and thus neuronal degeneration would be in line with the amyloid hypothesis of AD [120] (**Figure 1.21**).

Hoshi and co-workers observed the interaction of GSK-3 β with pyruvate dehydrogenase (PDH), the enzyme responsible for the conversion of pyruvate to acetyl-CoA in mitochondria, and found that GSK-3 β phosphorylated the enzyme *in vitro* and also in an A β -treated hippocampal culture. In addition, it was found that the inactivated PDH (due to A β exposure) resulted in the dysfunction of the mitochondria. Thus, contributing to neuronal death through the failure of energy metabolism and thereby leading to reduced ACh levels in cholinergic neurons due to the decreased production of acetyl-CoA. As a result of this, additional insight into the cholinergic hypothesis and the pathogenesis of AD was obtained [135].

Since the discovery of GSK-3 in 1980, the interest in it as a potential drug target has increased substantially. Between 2010 and 2014, sixty-three patents for different therapeutic targets were filed;

however, limited success was obtained in clinical trials [136]. During the structural exploration of GSK-3's adenosine triphosphate (ATP) active binding pocket, it was noted that all of ATP's hydrogen bonds were with the backbone amino acid residues Asp133 and Val135. These residues were found to play a key role in enhancing the affinity towards GSK-3 [136] (**Figure 1.22**).

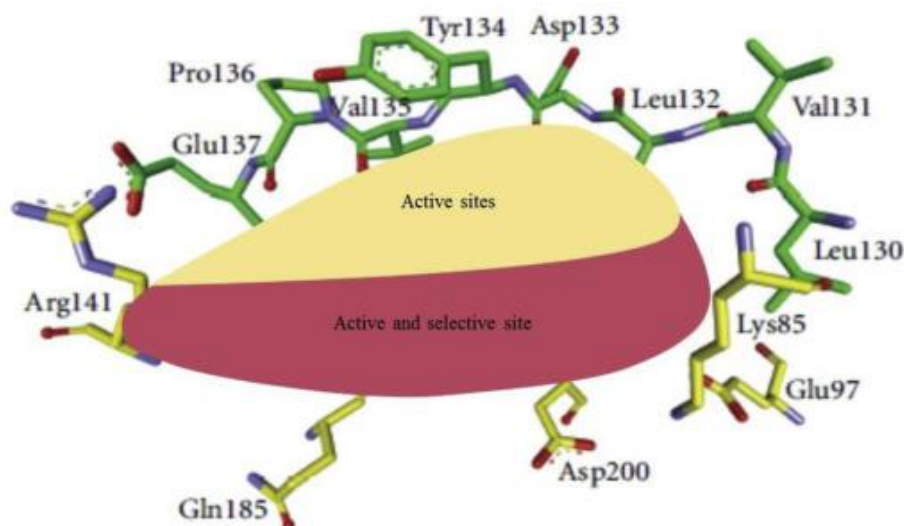


Figure 1.22. The ATP binding pocket of GSK-3 β . Important areas for activity and selectivity are denoted PDB code 1I09 [136].

The binding pocket region of the active and selective site of GSK-3 β contains the amino acids Lys85, Glu97 and Asp200, where Lys85 simultaneously forms a salt bridge with Glu97 and Asp200. That been said, the salt bridge between Lys85 and Asp200 is thought to be less significant and effective than the Lys85 and Glu97 salt bridge. Docking studies have highlighted that interactions with at least two or three areas of the active site would enhance the activity of inhibitors against GSK-3 therefore rendering them active inhibitors [136].

A diverse range of chemical structures showing inhibition of GSK-3 have been identified from both synthetic or natural origin [70]. With regards to inhibitors of natural origin, marine invertebrates have played a prominent role in the generation of GSK-3 inhibitors [136]. These classes include, thiadiazolidinones **24**, halomethylketones **25**, maleimides **26**, indirubines **27** and triazole derivatives, **28** and **29** [136] (**Figure 1.23**).

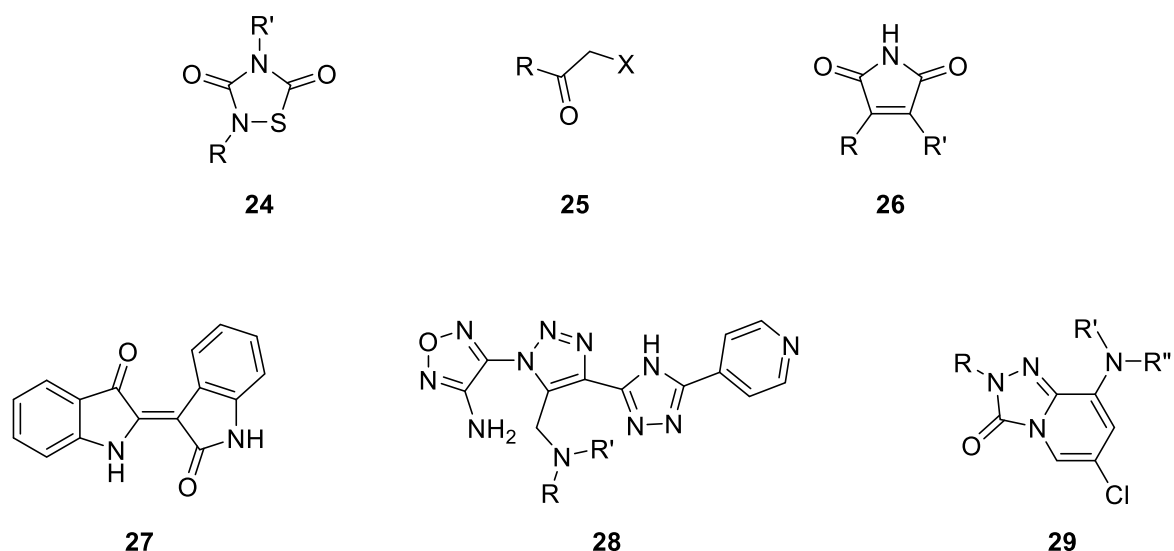


Figure 1.23. Examples of classes of GSK-3 inhibitors [136].

Inhibitors of GSK-3 can be divided into three categories namely:

- Non-ATP-competitive inhibitors
- ATP-competitive inhibitors
- Substrate competitive GSK-3 β inhibitors

1.4.3.1. Non-ATP-competitive inhibitors

The first class of compounds discovered to show non-ATP-competitive inhibition towards GSK-3 β were small heterocyclic thiadiazolidinone **24** (TDZD) derivatives, which demonstrated selectivity to various kinases such as protein kinase A, protein kinase C, casein kinase 2, and cyclin-dependent 1/cyclin B [70]. Compounds **30** and **31** were found to be the most potent, with IC₅₀ values of 2.0 μ M and 1.1 μ M, respectively (**Figure 1.24**) [137, 138]. Tideglusib **32** (**Figure 1.24**) is currently undergoing phase-II clinical trials for the treatment of AD and progressive supranuclear palsy [70].

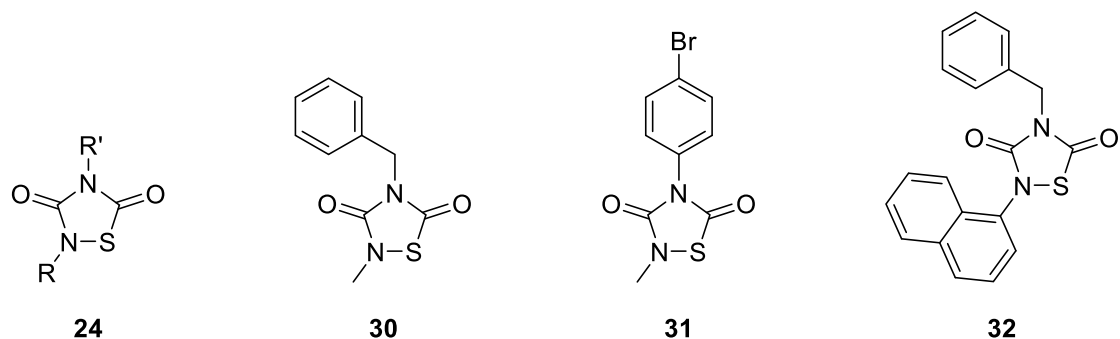


Figure 1.24. Thiadiazolidinone **24** scaffold and derivatives [70, 137, 138].

A second class of non-competitive GSK-3 β inhibitors, known as the halomethylketones **25**, were developed by Martinez and co-workers in 2003 [139]. Compound **33**, a halomethyl thienyl ketone derivative had an IC₅₀ of 0.5 μ M, whereas compound **34**, a halomethyl phenyl ketone derivative, had an IC₅₀ value of 1.0 μ M [139] (**Figure 1.25**). In another study by the same group, an irreversible non-competitive GSK-3 β inhibitor, compound **35** with an IC₅₀ value of 1.0 μ M, was discovered [140] (**Figure 1.25**).

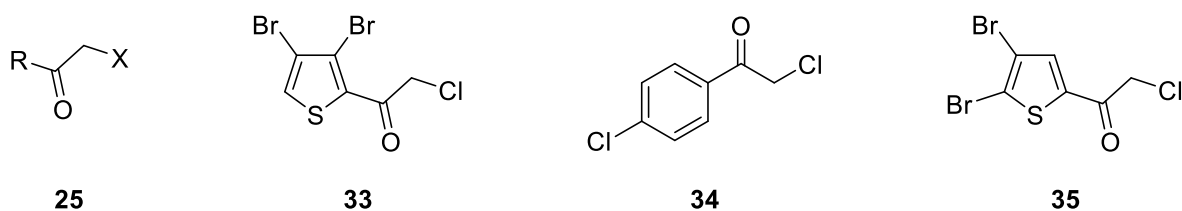


Figure 1.25. Halomethylketone **25** scaffold and derivatives [139, 140].

1.4.3.2. ATP-competitive inhibitors

Maleimide **26**, was identified as a potent ATP-competitive GSK-3 α inhibitor by Smith and co-workers [141], but unfortunately was found not to possess any activity against GSK-3 β . Indolyl-maleimide derivatives with GSK-3 β inhibition have been reported for compounds **36**, **37** and **38** with IC₅₀ values of 340 nM, 13 nM and 0.73 nM, respectively [142-144] (**Figure 1.26**).

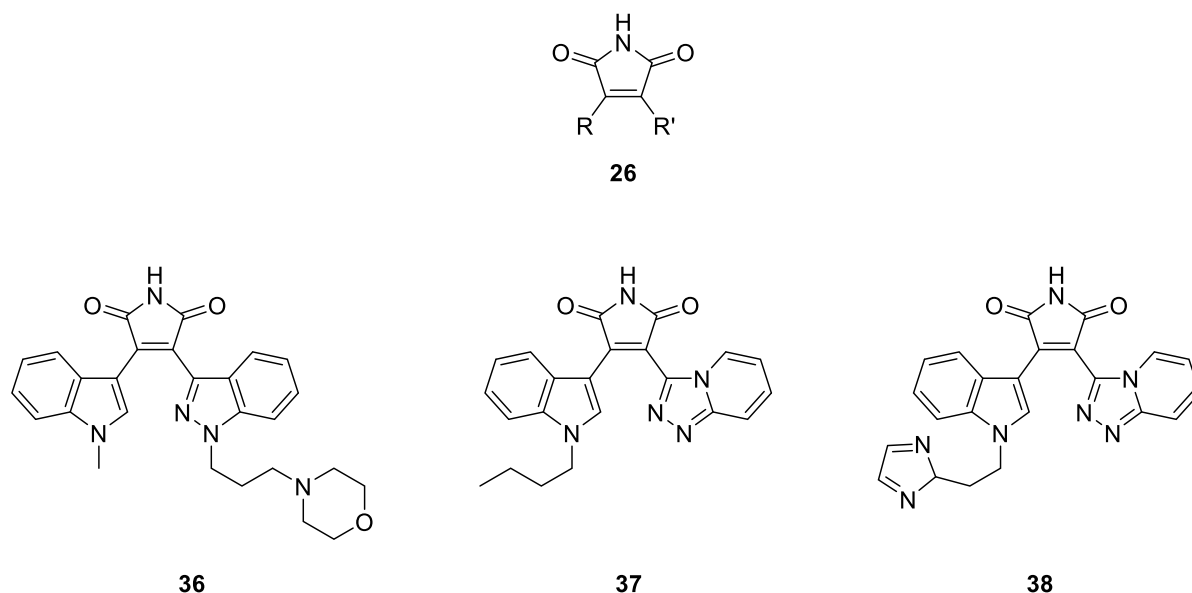


Figure 1.26. Maleimide **26** scaffold and derivatives [142-144].

Indirubin **27** comprises of a bis-indole scaffold and is found in a variety of natural sources. It was initially identified as the active ingredient in a Chinese traditional medicine treatment for leukemia (*Danggui Longhui Wan*). Leclerc *et al.*, synthesized compound **39**, a derivative of **27**, which showed

good inhibition of GSK-3 β with an IC₅₀ value of 9.0 nM [70, 145] (**Figure 1.27**). Subsequently, Polychronopoulos *et al.*, prepared a dichloro derivative of compound **39** (compound **40**) which had an IC₅₀ value of 4.0 nM (**Figure 1.27**) [146].

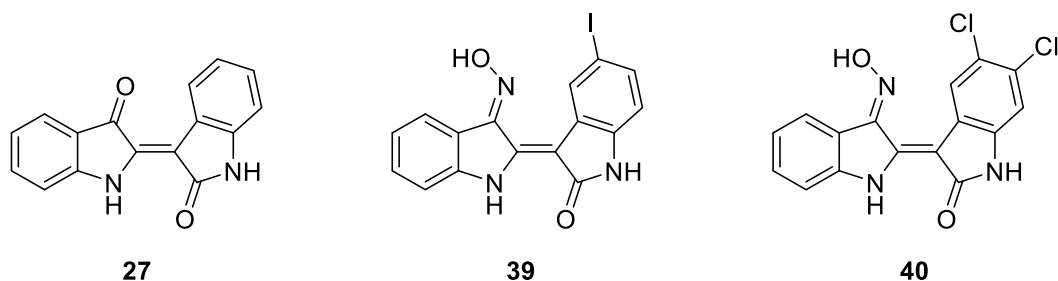


Figure 1.27. Indirubin **27** scaffold and derivatives [145, 146].

Two research groups have taken advantage of the versatility of click chemistry in accessing triazole compounds to develop new GSK-3 β inhibitors. The Kim group developed the 1,2,3-triazole compound **41**, a potent inhibitor with an IC₅₀ value of 0.111 μ M [147]. Olesen and co-workers developed the 1,2,4-triazole compound **42** with an IC₅₀ value of 0.28 μ M (**Figure 1.28**) [148].

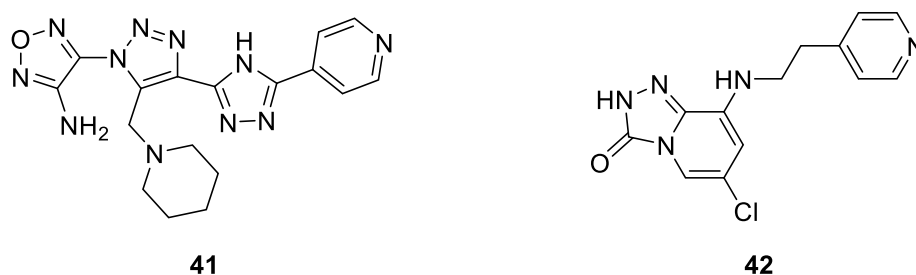


Figure 1.28. Triazole derivatives **42** and **43** [148, 149].

1.4.3.3. Substrate competitive GSK-3 β inhibitors

Non-competitive GSK-3 inhibitors have also been isolated from natural marine sources such as the Indonesian sponge, *Acanthostrongylophora*. Manzamine A **43**, is a β -carboline polycyclic alkaloid which was isolated from this Indo-Pacific sponge and found to possess an IC₅₀ value of 10.2 μ M (**Figure 1.29**) [149].

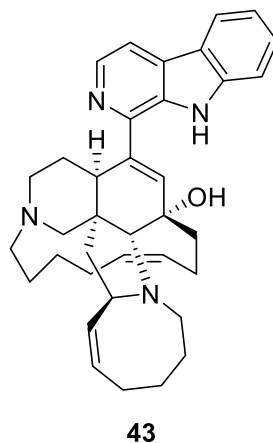


Figure 1.29. Manzamine A **44** [150].

1.4.4. N-Methyl-D-aspartate hypothesis

Glutamate **44** (Figure 1.30), the principal excitatory neurotransmitter in the CNS, stimulates a number of postsynaptic glutamate receptors. Glycine **45** acts as the co-agonist, being responsible for many neurological functions, such as cognition, memory, movement and sensation [150, 151]. Glutamate has been implicated in various pathologic conditions, including stroke and neurological diseases such as AD [150, 152, 153], where overstimulation of glutamate receptors due to glutamate **44** may result in neuronal damage excitotoxicity. Excitotoxicity may be mediated by an excessive influx of calcium into neurons through ionic channels, which are triggered by the activation of glutamate receptors such as the *N*-methyl-D-aspartate (NMDA) receptor. This then results in a voltage-dependent blockage of the ionic channel by Mg^{2+} causing a lower level of postsynaptic intracellular Ca^{2+} . The Mg^{2+} blockade can be removed through the depolarization of the cell plasma membrane, which triggers a pathological influx of Ca^{2+} . Prolonged Ca^{2+} overload then leads to the loss of synaptic function, followed by synaptotoxicity, ultimately leading to cell death which correlates with the loss of memory function as well as the learning ability in AD patients [154].

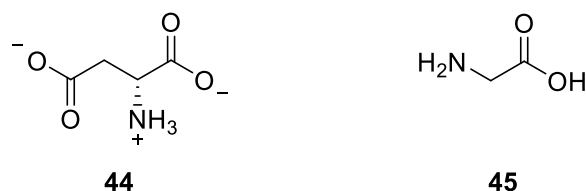


Figure 1.30. NMDA agonists [150].

Glutamate receptors can be divided into two main categories, namely (i) ionotropic glutamate receptors (iGluRs) which are coupled directly to the membrane ion channels, and (ii) metabotropic glutamate receptors (mGluRs) which are coupled to G-proteins and modulate secondary messengers such as calcium [150].

In this section and later, iGluRs with special focus on the NMDA receptor will be discussed. Three different classes of iGluRs have been identified and defined based on their different activating substrates: (i) (*S*)-2-amino-3-(3-hydroxy-5-methyl-4-isoxazolyl)propionic acid **46** (AMPA), (ii) kainic acid **47** (Kainite or KA) and (iii) NMDA **48** (Figure 1.31) [155].

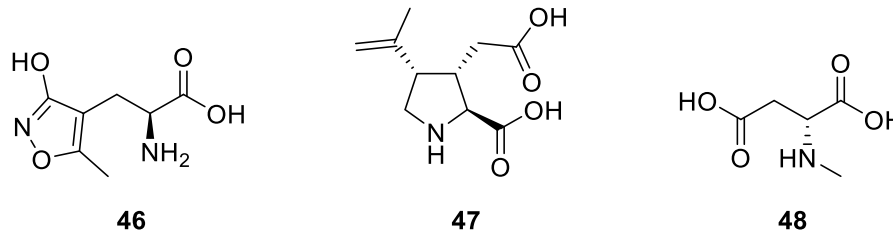


Figure 1.31. Ionotropic glutamate receptor substrates [155].

The iGluRs are homomeric or heteromeric assemblies and can be divided into three subclasses: AMPA (GluA1-4), KA (GluK1-5) and NMDA (GluN1, GluN2A-D, GluN3A-B). Ionotropic receptor subunits are assembled as tetramers, whereas the metabotropic receptor subunits are assembled as dimers (Figure 1.32) [155, 156].

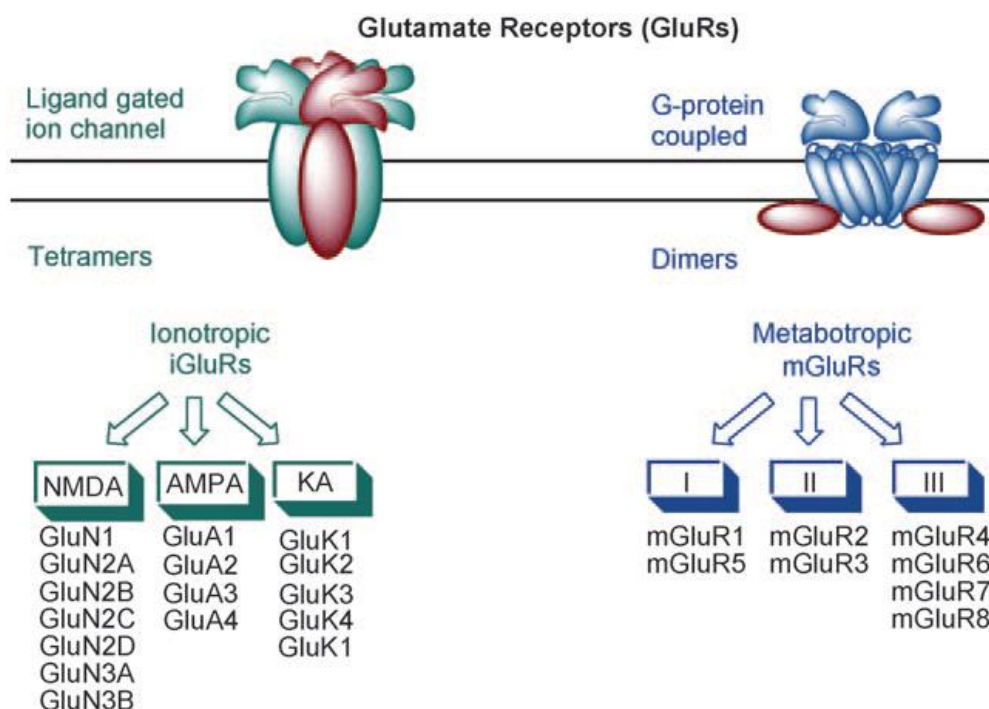


Figure 1.32. Glutamate receptors and their subunits [155].

The pharmacologic properties of NMDA receptors are determined by GluN2 [157]. Among these receptors, the GluN2B subunit, is one of the most highly focused drug targets for drug development [156]. Levels of specific subunits of NMDA are known to be abnormal in patients with AD, with reduced

levels of GluN1 and GluN2B in the hippocampus and of GluN2A and GluN2B in the entorhinal cortex [152].

Neuronal loss in the hippocampus and entorhinal cortex is more prominently seen in advanced AD than at the onset of AD [159, 160]. The changes in NMDA receptors seem to mirror neuronal loss rather than synaptic loss, indicating that the changes are subunit specific. It has been reported that the GluN2B subunit is the most vulnerable subunit, with abnormal levels in both the hippocampus and entorhinal cortex of AD patients, suggesting that neurons with GluN2B may be more sensitive than other neurons to the pathogenic mechanisms in AD. Thus, the severity of decrement in the subunits of NMDA in the hippocampus and entorhinal cortex correlates strongly with the magnitude of cognitive impairment observed in patients with AD [151].

The binding domain of GluN2 is less well understood compared to the other ionotropic receptors, especially the structural mechanism which governs partial and full agonism of the enzyme. Before the availability of XRD, site directed mutagenesis was used to identify the binding residues within the GluN2 subunits [158-162]. In these studies, it was shown that when the binding residues are in direct contact with glutamate **44**, they show high homology with the agonist-binding residues of GluN1 and the AMPA receptor units [155].

All iGluRs subunits contain four individual domains: a carboxyl terminal domain (CTD), an amino terminal domain (ATD), a transmembrane domain (TMD) and a ligand binding domain (LBD) (**Figure 1.33**) [163]. For NMDA, these subunits have been studied independently and in varying detail. The ATD and LBD appear as a single unit, in which there exists a clear divide due to flexible linkers between the two domains. The single ATD/LBD system may explain why the NMDA receptors show a pronounced regulation of ion channel function by the ATD [164]. Three transmembrane helices and a re-entrant pore loop form the ion channel pore of the TMD, which resembles an inverted potassium channel [165]. The residues in the TMD affect the channel pore on the voltage-dependent block of extracellular Mg^{2+} of NMDA [166]. The CTD comprises of a large intracellular portion of glutamate receptors and influences membrane targeting, allowing for multiple sites for post-translational modifications which can alter the receptor function and trafficking [167].

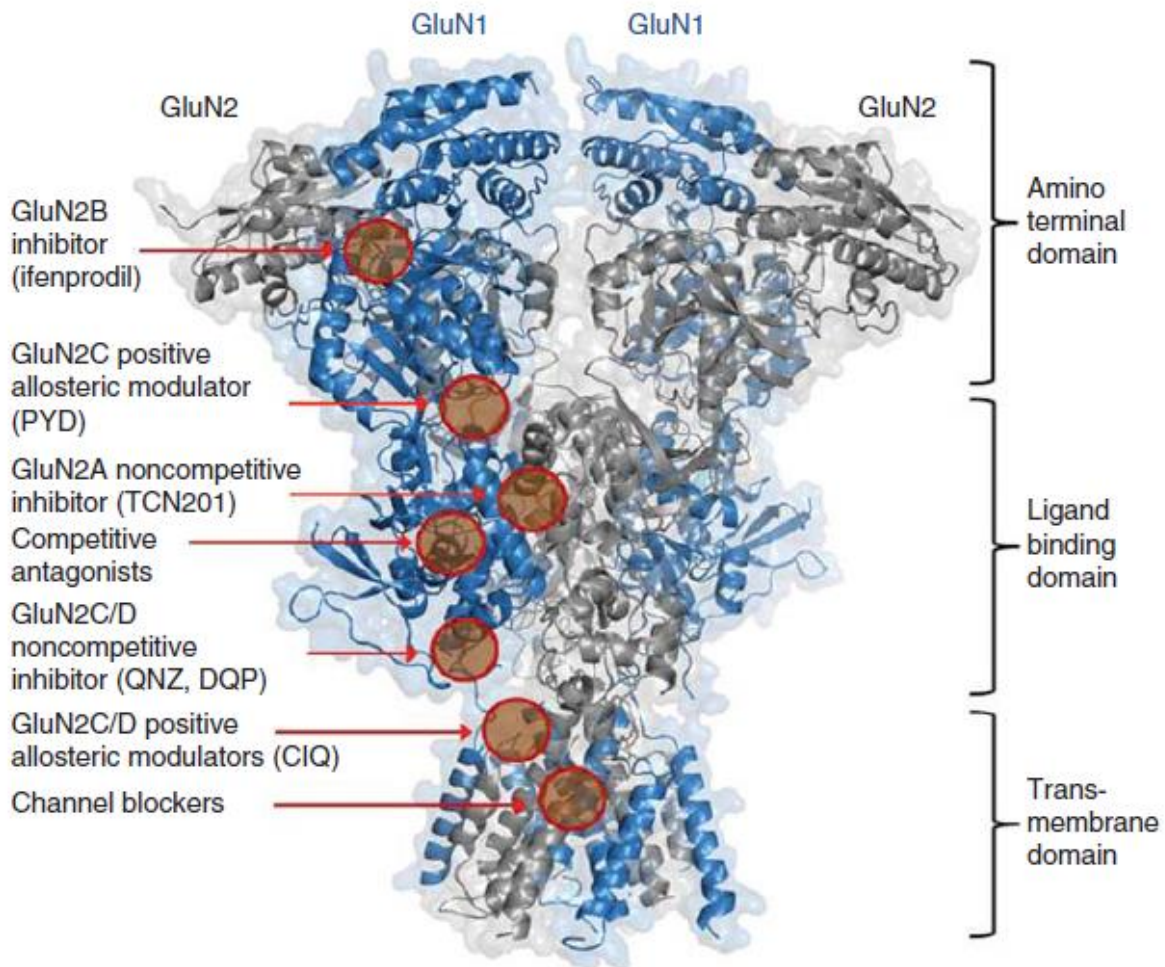
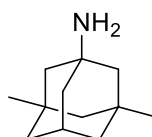


Figure 1.33. NMDA receptor homology model highlighting sites [163].

Each of the four GluN2 subunits (A-D) differ with regards to agonist sensitivity, channel opening probability, channel opening duration and deactivation time course to the GluN2 receptor [168-171]. As an example, the GluN2A-containing receptors are less sensitive to glutamate **44** and glycine **45** and have a much faster deactivation time compared to the other GluN2 subunits [172]. Furthermore, the recombinant GluN2A receptors have a nearly ten-fold higher probability of being open than the GluN2B and GluN2D containing receptors [173]. In terms of channel properties such as Ca^{2+} permeability, Mg^{2+} blockade and single conductance, this varies between the GluN2A/B and GluN2C/D receptors as it is dependent on a single residue in the transmembrane region [174]. Due to the diversity in the functions of the subunits in the NMDA receptor, it makes it a very attractive candidate as a therapeutic target.

Uncompetitive NMDA receptor antagonists or channel blockers require activation of the receptor before the antagonist can bind deep in the ion channel pore [175]. To date, there is only one US FDA approved drug for the treatment of moderate to severe AD, memantine **49** (**Figure 1.34**) [176]. It is an

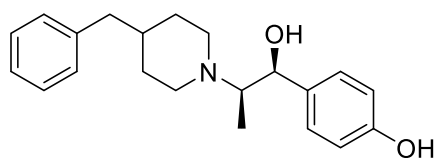
uncompetitive, voltage-dependent NMDA receptor antagonist which has rapid blocking-unblocking receptor kinetics as well as moderate binding affinity [177]. Unfortunately, currently available channel blockers are unable to differentiate between the different GluN2 subunits [178]. Side effects such as decreased motor function, hallucinations and delusions are thought to be a result of this lack of subunit selectivity [179].



49

Figure 1.34. The US FDA approved NMDA antagonist memantine **49** [176].

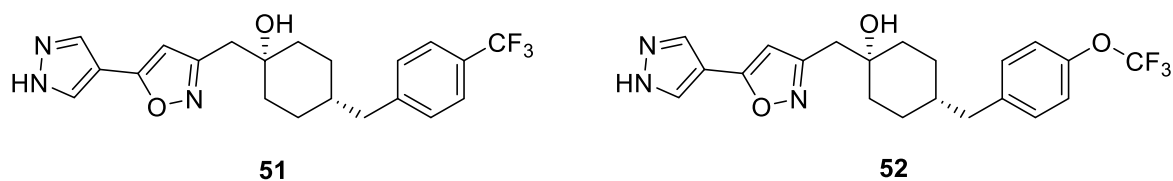
The discovery of the first subunit selective NMDA non-competitive antagonist, ifenprodil **50** (**Figure 1.35**), was a breakthrough, as it was shown to be more than four hundred times more selective for the GluN2B subunit, than the GluN2A, GluN2C and GluN2D subunits [180, 181]. Reported as a neuroprotectant, it has been tested in advanced clinical trials for traumatic brain injury and neuropathic pain. Although further research is required on **50**, the ifenprodil **50** scaffold holds great potential for the exploration of new scaffolds that selectively antagonize GluN2B-containing receptors [163].



50

Figure 1.35. Selective GluN2B antagonist ifenprodil **50** [163].

In the search for new selective subunit antagonists, Anan and co-workers discovered a novel class of cyclohexanol-based GluN2B-selective receptor antagonists. In their efforts to identify potent as well as orally bioavailable antagonists, they discovered compounds **51** ($IC_{50} = 0.85 \mu M$) and **52** ($IC_{50} = 0.85 \mu M$), which additionally were found to contain analgesic activity (**Figure 1.36**) [156].



51

52

Figure 1.36. Cyclohexanol-based GluN2B-selective antagonists [156].

1.5. BRIEF DESCRIPTION OF AIMS AND OBJECTIVES

The aim of this project was to develop a series of novel inhibitors targeting various biomarkers of AD and to assess the activity of these compounds *in vitro*. Some of the various compounds was also evaluated against the respective biomarkers with *in silico* studies.

Objective 1: Synthesize inhibitors targeting AChE based on the modification of (i) the linker between the indanone and piperidine groups of donepezil, and (ii) the exchange of the indanone group with various aryl and aromatic heterocycles.

Objective 2: Incorporating leads identified from objective 1 and expanding on previously reported literature inhibitors for GSK-3, objective 2 is to synthesize urea-based dual inhibitors that will act against both AChE and GSK-3.

Objective 3: Synthesize inhibitors targeting β -secretase/BACE1 through the modification of previously reported indole-based pharmacophores.

Objective 4: Expand upon previously reported literature for the development of NMDA antagonists, by synthesizing novel carboxamide derivatives.

Objective 5 (standalone): Investigate the applicability of flow chemistry for the synthesis of donepezil as a feedstock for future drug discovery projects within the group.

More details regarding the objectives will be provided in the separate chapters.

1.6. REFERENCES

- [1] R. Katzman, The prevalence and malignancy of Alzheimer's disease, *Arch. Neurol.*, 33 (1976) 217-218.
- [2] M. Goedert, M.G. Spillantini, A century of Alzheimer's disease, *Science*, 314 (2006) 777-781.
- [3] Alzheimer's Association. 2018 Alzheimer's disease facts and figures, *Alzheimers Dement.*, 14 (2018) 367-429.
- [4] S.E. Tom, R.A. Hubbard, P.K. Crane, S.J. Haneuse, J. Bowen, W.C. McCormick, S. McCurry, E.B. Larson, Characterization of dementia and Alzheimer's disease in an older population: updated incidence and life expectancy with and without dementia, *Am. J. Public Health*, 105 (2015) 408-413.
- [5] M. Ganguli, H.H. Dodge, C. Shen, R.S. Pandav, S.T. DeKosky, Alzheimer's disease and mortality: a 15-year epidemiological study, *Arch. Neurol.*, 62 (2005) 779-784.

- [6] R. Brookmeyer, M.M. Corrada, F.C. Curriero, C. Kawas, Survival following a diagnosis of Alzheimer's disease, *Arch. Neurol.*, 59 (2002) 1764-1767.
- [7] E.B. Larson, M.-F. Shadlen, L. Wang, W.C. McCormick, J.D. Bowen, L. Teri, W.A. Kukull, Survival after initial diagnosis of Alzheimer's disease, *Ann. Int. Med.*, 140 (2004) 501-509.
- [8] S. Todd, S. Barr, M. Roberts, A.P. Passmore, Survival in dementia and predictors of mortality: a review, *Int. J. Geriatr. Psychiatry.*, 28 (2013) 1109-1124.
- [9] C.A. de Jager, W. Msemburi, K. Pepper, M.I. Combrinck, Dementia Prevalence in a rural region of South Africa: a cross-sectional community study, *J. Alzheimers Dis.*, 60 (2017) 1087-1096.
- [10] P.V. Fish, D. Steadman, E.D. Bayle, P. Whiting, New approaches for the treatment of Alzheimer's disease, *Bioorg. Med. Chem. Lett.*, 29 (2019) 125-133.
- [11] A. Alzheimer, R.A. Stelzmann, H.N. Schnitzlein, F.R. Murtagh, An English translation of Alzheimer's 1907 paper, "Uber eine eigenartige Erkankung der Hirnrinde", *Clin. Anat.*, 8 (1995) 429-431.
- [12] Y. Xu, C.R. Jack, P.C. O'Brien, E. Kokmen, G.E. Smith, R.J. Ivnik, B.F. Boeve, R.G. Tangalos, R.C. Petersen, Usefulness of MRI measures of entorhinal cortex versus hippocampus in AD, *Neurology*, 54 (2000) 1760-1767.
- [13] S.J. Son, J. Kim, H. Park, Structural and functional connective fingerprints in mild cognitive impairment and Alzheimer's disease patients, *PLoS One*, 12 (2017) e0173426.
- [14] C. Ballard, S. Gauthier, A. Corbett, C. Brayne, D. Aarsland, E. Jones, Alzheimer's disease, *Lancet*, 377 (2011) 1019-1031.
- [15] J.E. Morley, S.A. Farr, A.D. Nguyen, Alzheimer's disease, *Clin. Geriatr. Med.*, 34 (2018) 591-601.
- [16] B.C. Dickerson, I. Goncharova, M.P. Sullivan, C. Forchetti, R.S. Wilson, D.A. Bennett, L.A. Beckett, MRI-derived entorhinal and hippocampal atrophy in incipient and very mild Alzheimer's disease, *Neurobiol. Aging*, 22 (2001) 747-754.
- [17] M. Symms, H.R. Jager, K. Schmierer, T.A. Yousry, A review of structural magnetic resonance neuroimaging, *J. Neurol. Neurosurg. Psychiatry.*, 75 (2004) 1235-1244.
- [18] P. Vemuri, C.R. Jack, Jr., Role of structural MRI in Alzheimer's disease, *Alzheimers Res. Ther.*, 2 (2010) 1-10.
- [19] W. Jagust, Positron emission tomography and magnetic resonance imaging in the diagnosis and prediction of dementia, *Alzheimers Dement.*, 2 (2006) 36-42.
- [20] P.J. Nestor, P. Scheltens, J.R. Hodges, Advances in the early detection of Alzheimer's disease, *Nat. Med.*, 10 (2004) 34.
- [21] S. De Santi, M.J. de Leon, H. Rusinek, A. Convit, C.Y. Tarshish, A. Roche, W.H. Tsui, E. Kandil, M. Boppana, K. Daisley, Hippocampal formation glucose metabolism and volume losses in MCI and AD, *Neurobiol. Aging*, 22 (2001) 529-539.

- [22] S. Rathore, M. Habes, M.A. Iftikhar, A. Shacklett, C. Davatzikos, A review on neuroimaging-based classification studies and associated feature extraction methods for Alzheimer's disease and its prodromal stages, *Neuroimage*, 155 (2017) 530-548.
- [23] L. deToledo-Morrell, T.R. Stoub, M. Bulgakova, R.S. Wilson, D.A. Bennett, S. Leurgans, J. Wu, D.A. Turner, MRI-derived entorhinal volume is a good predictor of conversion from MCI to AD, *Neurobiol. Aging*, 25 (2004) 1197-1203.
- [24] K. Juottonen, M.P. Laakso, R. Insausti, M. Lehtovirta, A. Pitkänen, K. Partanen, H. Soininen, Volumes of the entorhinal and perirhinal cortices in Alzheimer's disease, *Neurobiol. Aging*, 19 (1998) 15-22.
- [25] G.D. Pearlson, G.J. Harris, R.E. Powers, P.E. Barta, E.E. Camargo, G.A. Chase, J.T. Noga, L.E. Tune, Quantitative changes in mesial temporal volume, regional cerebral blood flow, and cognition in Alzheimer's disease, *Arch. Gen. Psych.*, 49 (1992) 402-408.
- [26] R.J. Killiany, B.T. Hyman, T. Gomez-Isla, M.B. Moss, R. Kikinis, F. Jolesz, R. Tanzi, K. Jones, M.S. Albert, MRI measures of entorhinal cortex vs hippocampus in preclinical AD, *Neurology*, 58 (2002) 1188-1196.
- [27] A. Chincarini, P. Bosco, G. Gemme, S. Morbelli, D. Arnaldi, F. Sensi, I. Solano, N. Amoroso, S. Tangaro, R. Longo, S. Squarcia, F. Nobili, Alzheimer's disease markers from structural MRI and FDG-PET brain images, *Eur. Phys. J. Plus*, 127 (2012) 1-16.
- [28] M. Pihlajamäki, R.A. Sperling, fMRI: use in early Alzheimer's disease and in clinical trials, *Future Neurol.*, 3 (2008) 409-421.
- [29] K.K. Kwong, J.W. Belliveau, D.A. Chesler, I.E. Goldberg, R.M. Weisskoff, B.P. Poncelet, D.N. Kennedy, B.E. Hoppel, M.S. Cohen, R.T. Turner, Dynamic magnetic resonance imaging of human brain activity during primary sensory stimulation, *Proc. Natl. Acad. Sci.*, 89 (1992) 5675-5679.
- [30] M. D'Esposito, L.Y. Deouell, A. Gazzaley, Alterations in the BOLD fMRI signal with ageing and disease: a challenge for neuroimaging, *Nat Rev Neurosci*, 4 (2003) 863-872.
- [31] C. Iadecola, Neurovascular regulation in the normal brain and in Alzheimer's disease, *Nat. Rev. Neurosci.*, 5 (2004) 347-360.
- [32] G. McKhann, D. Drachman, M. Folstein, R. Katzman, D. Price, E.M. Stadlan, Clinical diagnosis of Alzheimer's disease: Report of the NINCDS-ADRDA Work Group under the auspices of Department of Health and Human Services Task Force on Alzheimer's disease, *Neurology*, 34 (1984) 939-939.
- [33] V. Camus, P. Payoux, L. Barre, B. Desgranges, T. Voisin, C. Tauber, R. La Joie, M. Tafani, C. Hommet, G. Chetelat, K. Mondon, V. de La Sayette, J.P. Cottier, E. Beaufils, M.J. Ribeiro, V. Gissot, E. Vierron, J. Vercouillie, B. Vellas, F. Eustache, D. Guilloteau, Using PET with ¹⁸F-AV-45 (florbetapir) to quantify brain amyloid load in a clinical environment, *Eur. J. Nucl. Med. Mol. Imaging*, 39 (2012) 621-631.

- [34] E. Arnaiz, V. Jelic, O. Almkvist, L.O. Wahlund, B. Winblad, S. Valind, A. Nordberg, Impaired cerebral glucose metabolism and cognitive functioning predict deterioration in mild cognitive impairment, *Neuroreport*, 12 (2001) 851-855.
- [35] G. Chetelat, B. Desgranges, V. de la Sayette, F. Viader, F. Eustache, J.C. Baron, Mild cognitive impairment: Can FDG-PET predict who is to rapidly convert to Alzheimer's disease?, *Neurology*, 60 (2003) 1374-1377.
- [36] M.J. de Leon, A. Convit, O.T. Wolf, C.Y. Tarshish, S. DeSanti, H. Rusinek, W. Tsui, E. Kandil, A.J. Scherer, A. Roche, A. Imossi, E. Thorn, M. Bobinski, C. Caraos, P. Lesbre, D. Schlyer, J. Poirier, B. Reisberg, J. Fowler, Prediction of cognitive decline in normal elderly subjects with 2-[(¹⁸F)fluoro-2-deoxy-D-glucose/positron-emission tomography (FDG/PET), *Proc. Natl. Acad. Sci.*, 98 (2001) 10966-10971.
- [37] K.J. Blennow, M.J.J. de Leon, H.M. Zetterberg, Alzheimer's disease, *Lancet*, 368 (2006) 387-403.
- [38] W.E. Klunk, H. Engler, A. Nordberg, Y. Wang, G. Blomqvist, D.P. Holt, M. Bergström, I. Savitcheva, G.F. Huang, S. Estrada, Imaging brain amyloid in Alzheimer's disease with Pittsburgh Compound-B, *Ann. Neurol.*, 55 (2004) 306-319.
- [39] N.M. Kemppainen, S. Aalto, I.A. Wilson, K. Någren, S. Helin, A. Brück, V. Oikonen, M. Kailajärvi, M. Scheinin, M. Viitanen, PET amyloid ligand [¹¹C] PIB uptake is increased in mild cognitive impairment, *Neurology*, 68 (2007) 1603-1606.
- [40] V.K.N. Shivamurthy, A.K. Tahari, C. Marcus, R.M. Subramaniam, Brain FDG PET and the diagnosis of dementia, *Am. J. Roentgenol.*, 204 (2015) 76-85.
- [41] <http://www.gevizamyl.com/us/wp-content/uploads/2017/02/43-1067C-Vizamy1.pdf> [Accessed 2019/02/21].
- [42] D.T. Chien, S. Bahri, A.K. Szardenings, J.C. Walsh, F. Mu, M.Y. Su, W.R. Shankle, A. Elizarov, H.C. Kolb, Early clinical PET imaging results with the novel PHF-tau radioligand [F-18]-T807, *J. Alzheimers Dis.*, 34 (2013) 457-468.
- [43] M. Marquie, M.D. Normandin, C.R. Vanderburg, I.M. Costantino, E.A. Bien, L.G. Rycyna, W.E. Klunk, C.A. Mathis, M.D. Ikonovic, M.L. Debnath, N. Vasdev, B.C. Dickerson, S.N. Gomperts, J.H. Growdon, K.A. Johnson, M.P. Frosch, B.T. Hyman, T. Gomez-Isla, Validating novel tau positron emission tomography tracer [F-18]-AV-1451 (T807) on postmortem brain tissue, *Ann. Neurol.*, 78 (2015) 787-800.
- [44] C. Xia, S.J. Makaretz, C. Caso, S. McGinnis, S.N. Gomperts, J. Sepulcre, T. Gomez-Isla, B.T. Hyman, A. Schultz, N. Vasdev, K.A. Johnson, B.C. Dickerson, Association of *in vivo* [¹⁸F]AV-1451 tau PET imaging results with cortical atrophy and symptoms in typical and atypical Alzheimer's disease, *JAMA Neurol.*, 74 (2017) 427-436.

- [45] A.J. Aschenbrenner, B.A. Gordon, T.L.S. Benzinger, J.C. Morris, J.J. Hassenstab, Influence of tau PET, amyloid PET, and hippocampal volume on cognition in Alzheimer's disease, *Neurology*, 91 (2018) 859-866.
- [46] C.R. Jack, Jr., D.A. Bennett, K. Blennow, M.C. Carrillo, B. Dunn, S.B. Haeberlein, D.M. Holtzman, W. Jagust, F. Jessen, J. Karlawish, E. Liu, J.L. Molinuevo, T. Montine, C. Phelps, K.P. Rankin, C.C. Rowe, P. Scheltens, E. Siemers, H.M. Snyder, R. Sperling, Toward a biological definition of Alzheimer's disease, *Alzheimers Dement.*, 14 (2018) 535-562.
- [47] K. Blennow, H. Hampel, CSF markers for incipient Alzheimer's disease, *Lancet Neurol.*, 2 (2003) 605-613.
- [48] A.D. Cohen, S.M. Landau, B.E. Snitz, W.E. Klunk, K. Blennow, H. Zetterberg, Fluid and PET biomarkers for amyloid pathology in Alzheimer's disease, *Mol. Cell Neurosci.*, 97 (2019) 3-17.
- [49] H. Zetterberg, Blood-based biomarkers for Alzheimer's disease, *J. Neurosci. Methods*, 319 (2018) 2-6.
- [50] H. Sugimoto, Y. Yamanish, Y. Iimura, Y. Kawakami, Donepezil hydrochloride (E2020) and other acetylcholinesterase inhibitors, *Curr. Med. Chem.*, 7 (2000) 303-339.
- [51] P. Davies, A.J.F. Maloney, Selective loss of central cholinergic neurons in Alzheimer's disease, *Lancet*, 308 (1976) 1403.
- [52] P. Davies, Neurotransmitter-related enzymes in senile dementia of the Alzheimer type, *Brain Res.*, 171 (1979) 319-327.
- [53] E.K. Perry, R.H. Perry, G. Blessed, B.E. Tomlinson, Necropsy evidence of central cholinergic deficits in senile dementia, *Lancet*, 309 (1977) 189.
- [54] T.D. Reisine, H.I. Yamamura, E.D. Bird, E. Spokes, S.J. Enna, Pre- and postsynaptic neurochemical alterations in Alzheimer's disease, *Brain Res.*, 159 (1978) 477-481.
- [55] P. White, M.J. Goodhardt, J.P. Keet, C.R. Hiley, L.H. Carrasco, I.E.I. Williams, D.M. Bowen, Neocortical cholinergic neurons in elderly people, *Lancet*, 309 (1977) 668-671.
- [56] J.A. Richter, E.K. Perry, B.E. Tomlinson, Acetylcholine and choline levels in post-mortem human brain tissue: Preliminary observations in Alzheimer's disease, *Life Sci.*, 26 (1980) 1683-1689.
- [57] N.R. Sims, C.C.T. Smith, A.N. Davison, D.M. Bowen, R.H.A. Flack, J.S. Snowden, D. Neary, Glucose metabolism and acetylcholine synthesis in relation to neuronal activity in Alzheimer's disease, *Lancet*, 315 (1980) 333-336.
- [58] H. Sugimoto, Y. Tsuchiya, H. Sugumi, K. Higurashi, N. Karibe, Y. Iimura, A. Sasaki, Y. Kawakami, T. Nakamura, Novel piperidine derivatives. Synthesis and anti-acetylcholinesterase activity of 1-benzyl-4-[2-(*N*-benzoylamino)ethyl]piperidine derivatives, *J. Med. Chem.*, 33 (1990) 1880-1887.

- [59] W.H. Moos, R.E. Davis, R.D. Schwarz, E.R. Gamzu, Cognition activators, *Med. Res. Rev.*, 8 (1988) 353-391.
- [60] J.H. Growdon, Neuropharmacology of degenerative diseases associated with aging, *Med. Res. Rev.*, 3 (1983) 237-257.
- [61] E. Hollander, R.C. Mohs, K.L. Davis, Cholinergic approaches to the treatment of Alzheimer's disease, *Br. Med. Bull.*, 42 (1986) 97-100.
- [62] F.M. Hershenson, W.H. Moos, Drug development for senile cognitive decline, *J. Med. Chem.*, 29 (1986) 1125-1130.
- [63] H. Sugimoto, Y. Imura, Y. Yamanishi, K. Yamatsu, Synthesis and structure-activity relationships of acetylcholinesterase inhibitors: 1-benzyl-4-[(5,6-dimethoxy-1-oxoindan-2-yl)methyl]piperidine hydrochloride and related compounds, *J. Med. Chem.*, 38 (1995) 4821-4829.
- [64] Y. Kawakami, A. Inoue, T. Kawai, M. Wakita, H. Sugimoto, A.J. Hopfinger, The rationale for E2020 as a potent acetylcholinesterase inhibitor, *Bioorg. Med. Chem.*, 4 (1996) 1429-1446.
- [65] E.K. Perry, R.H. Perry, G. Blessed, B.E. Tomlinson, Changes in brain cholinesterases in senile dementia of Alzheimer type, *Neuropathol. Appl. Neurobiol.*, 4 (1978) 273-277.
- [66] R.M. Lane, S.G. Potkin, A. Enz, Targeting acetylcholinesterase and butyrylcholinesterase in dementia, *Int. J. Neuropsychopharmacol.*, 9 (2006) 101-124.
- [67] E. Scarpini, P. Scheltens, H. Feldman, Treatment of Alzheimer's disease; current status and new perspectives, *Lancet Neurol.*, 2 (2003) 539-547.
- [68] J. Sussman, M. Harel, F. Frolow, C. Oefner, A. Goldman, L. Toker, I. Silman, Atomic structure of acetylcholinesterase from *Torpedo californica*: a prototypic acetylcholine-binding protein, *Science*, 253 (1991) 872-879.
- [69] A. Shafferman, C. Kronman, Y. Flashner, M. Leitner, H. Grosfeld, A. Ordentlich, Y.I. Gozes, S. Cohen, N. Ariel, D. Barak, Mutagenesis of human acetylcholinesterase. Identification of residues involved in catalytic activity and in polypeptide folding, *J. Biol. Chem.*, 267 (1992) 17640-17648.
- [70] T. Silva, J. Reis, J. Teixeira, F. Borges, Alzheimer's disease, enzyme targets and drug discovery struggles: from natural products to drug prototypes, *Ageing Res. Rev.*, 15 (2014) 116-145.
- [71] M. Singh, M. Kaur, H. Kukreja, R. Chugh, O. Silakari, D. Singh, Acetylcholinesterase inhibitors as Alzheimer therapy: from nerve toxins to neuroprotection, *Eur. J. Med. Chem.*, 70 (2013) 165-188.
- [72] A.K. Saxena, R. Saini, The structural hybrids of acetylcholinesterase inhibitors in the treatment of Alzheimer's disease: a review, *J. Alzheimers. Neurodegener. Dis.*, 4 (2018) 1-25.
- [73] A. Samadi, M. de la Fuente Revenga, C. Perez, I. Iriepa, I. Moraleda, M.I. Rodriguez-Franco, J. Marco-Contelles, Synthesis, pharmacological assessment, and molecular modeling of 6-chloro-

pyridonepezils: new dual AChE inhibitors as potential drugs for the treatment of Alzheimer's disease, *Eur. J. Med. Chem.*, 67 (2013) 64-74.

[74] T. Mohamed, A. Shakeri, P.P. Rao, Amyloid cascade in Alzheimer's disease: Recent advances in medicinal chemistry, *Eur. J. Med. Chem.*, 113 (2016) 258-272.

[75] N. Guzior, M. Bajda, M. Skrok, K. Kurpiewska, K. Lewinski, B. Brus, A. Pislak, J. Kos, S. Gobec, B. Malawska, Development of multifunctional, heterodimeric isoindoline-1,3-dione derivatives as cholinesterase and beta-amyloid aggregation inhibitors with neuroprotective properties, *Eur. J. Med. Chem.*, 92 (2015) 738-749.

[76] J.S. Lan, T. Zhang, Y. Liu, J. Yang, S.S. Xie, J. Liu, Z.Y. Miao, Y. Ding, Design, synthesis and biological activity of novel donepezil derivatives bearing *N*-benzyl pyridinium moiety as potent and dual binding site acetylcholinesterase inhibitors, *Eur. J. Med. Chem.*, 133 (2017) 184-196.

[77] F. Belluti, M. Bartolini, G. Bottegoni, A. Bisi, A. Cavalli, V. Andrisano, A. Rampa, Benzophenone-based derivatives: a novel series of potent and selective dual inhibitors of acetylcholinesterase and acetylcholinesterase-induced β -amyloid aggregation, *Eur. J. Med. Chem.*, 46 (2011) 1682-1693.

[78] S. Liu, R. Shang, L. Shi, D.C. Wan, H. Lin, Synthesis and biological evaluation of 7*H*-thiazolo[3,2-*b*]-1,2,4-triazin-7-one derivatives as dual binding site acetylcholinesterase inhibitors, *Eur. J. Med. Chem.*, 81 (2014) 237-244.

[79] O. Di Pietro, E. Viayna, E. Vicente-Garcia, M. Bartolini, R. Ramon, J. Juarez-Jimenez, M.V. Clos, B. Perez, V. Andrisano, F.J. Luque, R. Lavilla, D. Munoz-Torrero, 1,2,3,4-Tetrahydrobenzo[*h*][1,6]naphthyridines as a new family of potent peripheral-to-midgorge-site inhibitors of acetylcholinesterase: synthesis, pharmacological evaluation and mechanistic studies, *Eur. J. Med. Chem.*, 73 (2014) 141-152.

[80] C.L. Xia, N. Wang, Q.L. Guo, Z.Q. Liu, J.Q. Wu, S.L. Huang, T.M. Ou, J.H. Tan, H.G. Wang, D. Li, Z.S. Huang, Design, synthesis and evaluation of 2-arylethenyl-*N*-methylquinolinium derivatives as effective multifunctional agents for Alzheimer's disease treatment, *Eur. J. Med. Chem.*, 130 (2017) 139-153.

[81] E.J. Barreiro, C.A. Camara, H. Verli, L. Brazil-Mas, N.G. Castro, W.M. Cintra, Y. Aracava, C.R. Rodrigues, C.A. Fraga, Design, synthesis, and pharmacological profile of novel fused pyrazolo[4,3-*d*]pyridine and pyrazolo[3,4-*b*][1,8]naphthyridine isosteres: a new class of potent and selective acetylcholinesterase inhibitors, *J. Med. Chem.*, 46 (2003) 1144-1152.

[82] M.M. Alcalá, N.M. Vivas, S. Hospital, P. Camps, D. Muñoz-Torrero, A. Badia, Characterisation of the anticholinesterase activity of two new tacrine–huperzine A hybrids, *Neuropharmacology*, 44 (2003) 749-755.

- [83] A. Badia, J.E. Baños, P. Camps, J. Contreras, D.M. Görbig, D. Muñoz-Torrero, M. Simón, N.M. Vivas, Synthesis and evaluation of tacrine–Huperzine a hybrids as acetylcholinesterase inhibitors of potential interest for the treatment of Alzheimer’s disease, *Bioorg. Med. Chem.*, 6 (1998) 427-440.
- [84] N.S. Kumar, P.K. Mukherjee, S. Bhadra, B.P. Saha, B.C. Pal, Acetylcholinesterase inhibitory potential of a carbazole alkaloid, mahanimbine, from *Murraya koenigii*, *Phytother. Res.*, 24 (2010) 629-631.
- [85] J. Hardy, D.J. Selkoe, The amyloid hypothesis of Alzheimer's disease: progress and problems on the road to therapeutics, *Science*, 297 (2002) 353-356.
- [86] Y. Madav, S. Wairkar, B. Prabhakar, Recent therapeutic strategies targeting β -amyloid and tauopathies in Alzheimer's disease, *Brain Res. Bull.*, 146 (2019) 171-184.
- [87] D.R. Howlett, D.L. Simmons, C. Dingwall, G. Christie, In search of an enzyme: the β -secretase of Alzheimer's disease is an aspartic proteinase, *Trends Neurosci.*, 23 (2000) 565-570.
- [88] R. Cappai, Making sense of the amyloid precursor protein: its tail tells an interesting tale, *J. Neurochem.*, 130 (2014) 325-327.
- [89] G. Thinakaran, E.H. Koo, Amyloid precursor protein trafficking, processing, and function, *J. Biol. Chem.*, 283 (2008) 29615-29619.
- [90] A.M. Szczepanik, D. Rampe, G.E. Ringheim, Amyloid- β peptide fragments p3 and p4 induce pro-inflammatory cytokine and chemokine production *in vitro* and *in vivo*, *J. Neurochem.*, 77 (2008) 304-317.
- [91] A. Kumar, A. Singh, Ekavali, A review on Alzheimer's disease pathophysiology and its management: an update, *Pharmacol. Rep.*, 67 (2015) 195-203.
- [92] S.A. Spronk, H.A. Carlson, The role of tyrosine 71 in modulating the flap conformations of BACE1, *Proteins*, 79 (2011) 2247-2259.
- [93] V. John, J.P. Beck, M.J. Bienkowski, S. Sinha, R.L. Henrikson, Human β -secretase (BACE) and BACE inhibitors, *J. Med. Chem.*, 46 (2003) 4625-4630.
- [94] D.J. Selkoe, Alzheimer's disease: genes, proteins, and therapy, *Physiol. Rev.*, 81 (2001) 741-766.
- [95] Q. Liu, J. Zhang, H. Tran, M.M. Verbeek, K. Reiss, S. Estus, G. Bu, LRP1 shedding in human brain: roles of ADAM10 and ADAM17, *Mol. Neurodegener.*, 4 (2009) 1-7.
- [96] G. Bitan, M.D. Kirkitadze, A. Lomakin, S.S. Vollers, G.B. Benedek, D.B. Teplow, Amyloid β -protein ($A\beta$) assembly: $A\beta$ 40 and $A\beta$ 42 oligomerize through distinct pathways, *Proc. Natl. Acad. Sci.*, 100 (2003) 330-335.
- [97] C.C. Chang, J.C. Althaus, C.J. Carruthers, M.A. Sutton, D.G. Steel, A. Gafni, Synergistic interactions between Alzheimer's $A\beta$ 40 and $A\beta$ 42 on the surface of primary neurons revealed by single molecule microscopy, *PLoS One*, 8 (2013) e82139.

- [98] C.A. Ross, M.A. Poirier, Protein aggregation and neurodegenerative disease, *Nat. Med.*, 10 Suppl (2004) 1-7.
- [99] C. Soto, Unfolding the role of protein misfolding in neurodegenerative diseases, *Nat. Rev. Neurosci.*, 4 (2003) 49-60.
- [100] C. Lee, S. Ham, Characterizing amyloid- β protein misfolding from molecular dynamics simulations with explicit water, *J. Comput. Chem.*, 32 (2011) 349-355.
- [101] R. Vassar, B.D. Bennett, S. Babu-Khan, S. Kahn, E.A. Mendiaz, P. Denis, D.B. Teplow, S. Ross, P. Amarante, R. Loeloff, β -Secretase cleavage of Alzheimer's amyloid precursor protein by the transmembrane aspartic protease BACE, *Science*, 286 (1999) 735-741.
- [102] M. Willem, S. Lammich, C. Haass, Function, regulation and therapeutic properties of β -secretase (BACE1), *Semin. Cell Dev. Biol.*, 20 (2009) 175-182.
- [103] L. Hong, G. Koelsch, X. Lin, S. Wu, S. Terzyan, A.K. Ghosh, X.C. Zhang, J. Tang, Structure of the protease domain of memapsin 2 (β -secretase) complexed with inhibitor, *Science*, 290 (2000) 150-153.
- [104] S. Benjannet, A. Elagoz, L. Wickham, M. Mamarbachi, J.S. Munzer, A. Basak, C. Lazure, J.A. Cromlish, S. Sisodia, F. Checler, M. Chretien, N.G. Seidah, Post-translational processing of β -secretase (β -amyloid-converting enzyme) and its ectodomain shedding. The pro- and transmembrane/cytosolic domains affect its cellular activity and amyloid- β production, *J. Biol. Chem.*, 276 (2001) 10879-10887.
- [105] M. Haniu, P. Denis, Y. Young, E.A. Mendiaz, J. Fuller, J.O. Hui, B.D. Bennett, S. Kahn, S. Ross, T. Burgess, V. Katta, G. Rogers, R. Vassar, M. Citron, Characterization of Alzheimer's β -secretase protein BACE. A pepsin family member with unusual properties, *J. Biol. Chem.*, 275 (2000) 21099-21106.
- [106] X.-P. Shi, E. Chen, K.-C. Yin, S. Na, V.M. Garsky, M.-T. Lai, Y.-M. Li, M. Platchek, R.B. Register, M.K. Sardana, M.-J. Tang, J. Thiebeau, T. Wood, J.A. Shafer, S.J. Gardell, The pro domain of β -secretase does not confer strict zymogen-like properties but does assist proper folding of the protease domain, *J. Biol. Chem.*, 276 (2001) 10366-10373.
- [107] A.K. Ghosh, H.L. Osswald, BACE1 (β -secretase) inhibitors for the treatment of Alzheimer's disease, *Chem. Soc. Rev.*, 43 (2014) 6765-6813.
- [108] J. Ermolieff, J.A. Loy, G. Koelsch, J. Tang, Proteolytic activation of recombinant pro-memapsin 2 (pro- β -secretase) studied with new fluorogenic substrates, *Biochemistry*, 39 (2000) 12450-12456.
- [109] J.T. Huse, D.S. Pijak, G.J. Leslie, V.M. Lee, R.W. Doms, Maturation and endosomal targeting of β -site amyloid precursor protein-cleaving enzyme. , *J. Biol. Chem.*, 275 (2000) 33729-33737.
- [110] F. Fischer, M. Molinari, U. Bodendorf, P. Paganetti, The disulphide bonds in the catalytic domain of BACE are critical but not essential for amyloid precursor protein processing activity, *J. Neurochem.*, 80 (2002) 1079-1088.

- [111] L. Hong, J. Tang, Flap position of free memapsin 2 (β -secretase), a model for flap opening in aspartic protease catalysis, *Biochemistry*, 43 (2004) 4689-4695.
- [112] F. Kamenetz, T. Tomita, H. Hsieh, G. Seabrook, D. Borchelt, T. Iwatsubo, S. Sisodia, R. Malinow, APP processing and synaptic function, *Neuron*, 37 (2003) 925-937.
- [113] A.K. Ghosh, D. Shin, D. Downs, G. Koelsch, X. Lin, J. Ermolieff, J. Tang, Design of potent inhibitors for human brain memapsin 2 (β -secretase), *J. Am. Chem. Soc.*, 122 (2000) 3522-3523.
- [114] L. Hong, R.T. Turner, G. Koelsch, D. Shin, A.K. Ghosh, J. Tang, Crystal structure of memapsin 2 (β -secretase) in complex with an inhibitor OM00-3, *Biochemistry*, 41 (2002) 10963-10967.
- [115] M.C. Maillard, R.K. Hom, T.E. Benson, J.B. Moon, S. Mamo, M. Bienkowski, A.G. Tomasselli, D.D. Woods, D.B. Prince, D.J. Paddock, T.L. Emmons, J.A. Tucker, M.S. Dappen, L. Brogley, E.D. Thorsett, N. Jewett, S. Sinha, V. John, Design, synthesis, and crystal structure of hydroxyethyl secondary amine-based peptidomimetic inhibitors of human β -secretase, *J. Med. Chem.*, 50 (2007) 776-781.
- [116] S.W. Kortum, T.E. Benson, M.J. Bienkowski, T.L. Emmons, D.B. Prince, D.J. Paddock, A.G. Tomasselli, J.B. Moon, A. LaBorde, R.E. TenBrink, Potent and selective isophthalamide S2 hydroxyethylamine inhibitors of BACE1, *Bioorg. Med. Chem. Lett.*, 17 (2007) 3378-3383.
- [117] S.W. Gerritz, W. Zhai, S. Shi, S. Zhu, J.H. Toyn, J.E. Meredith, Jr., L.G. Iben, C.R. Burton, C.F. Albright, A.C. Good, A.J. Tebben, J.K. Muckelbauer, D.M. Camac, W. Metzler, L.S. Cook, R. Padmanabha, K.A. Lentz, M.J. Sofia, M.A. Poss, J.E. Macor, L.A. Thompson, 3rd, Acyl guanidine inhibitors of β -secretase (BACE-1): optimization of a micromolar hit to a nanomolar lead via iterative solid- and solution-phase library synthesis, *J. Med. Chem.*, 55 (2012) 9208-9223.
- [118] S. Eketjall, J. Janson, K. Kaspersson, A. Bogstedt, F. Jeppsson, J. Falting, S.B. Haeberlein, A.R. Kugler, R.C. Alexander, G. Cebers, AZD3293: A novel, orally active BACE1 inhibitor with high potency and permeability and markedly slow off-rate kinetics, *J. Alzheimers Dis.*, 50 (2016) 1109-1123.
- [119] M.A. Brodney, G. Barreiro, K. Ogilvie, E. Hajos-Korcsok, J. Murray, F. Vajdos, C. Ambroise, C. Christoffersen, K. Fisher, L. Lanyon, J. Liu, C.E. Nolan, J.M. Withka, K.A. Borzilleri, I. Efremov, C.E. Oborski, A. Varghese, B.T. O'Neill, Spirocyclic sulfamides as β -secretase 1 (BACE-1) inhibitors for the treatment of Alzheimer's disease: utilization of structure based drug design, WaterMap, and CNS penetration studies to identify centrally efficacious inhibitors, *J. Med. Chem.*, 55 (2012) 9224-9239.
- [120] C. Hooper, R. Killick, S. Lovestone, The GSK3 hypothesis of Alzheimer's disease, *J. Neurochem.*, 104 (2008) 1433-1439.
- [121] H. Yamaguchi, K. Ishiguro, T. Uchida, A. Takashima, C.A. Lemere, K. Imahori, Preferential labeling of Alzheimer neurofibrillary tangles with antisera for tau protein kinase (TPK) I/glycogen synthase kinase-3 β and cyclin-dependent kinase 5, a component of TPK II, *Acta Neuropathol.*, 92 (1996) 232-241.

- [122] J.-J. Pei, T. Tanaka, Y.-C. Tung, E. Braak, K. Iqbal, I. Grundke-Iqbal, Distribution, levels, and activity of glycogen synthase kinase-3 in the Alzheimer's disease brain, *J. Neuropathol. Exp. Neurol.*, 56 (1997) 70-78.
- [123] J.-J. Pei, E. Braak, H. Braak, I. Grundke-Iqbal, K. Iqbal, B. Winblad, R.F. Cowburn, Distribution of active glycogen synthase kinase 3 β (gsk-3 β) in brains staged for Alzheimer's disease neurofibrillary changes, *J. Neuropathol. Exp. Neurol.*, 58 (1999) 1010-1019.
- [124] K. Leroy, Z. Yilmaz, J.P. Brion, Increased level of active GSK-3 β in Alzheimer's disease and accumulation in argyrophilic grains and in neurones at different stages of neurofibrillary degeneration, *Neuropathol. Appl. Neurobiol.*, 33 (2007) 43-55.
- [125] E.M. Blalock, J.W. Geddes, K.C. Chen, N.M. Porter, W.R. Markesbery, P.W. Landfield, Incipient Alzheimer's disease: microarray correlation analyses reveal major transcriptional and tumor suppressor responses, *Proc. Natl. Acad. Sci.*, 101 (2004) 2173-2178.
- [126] R.S. Jope, G.V. Johnson, The glamour and gloom of glycogen synthase kinase-3, *Trends Biochem. Sci.*, 29 (2004) 95-102.
- [127] A.R. Cole, A. Knebel, N.A. Morrice, L.A. Robertson, A.J. Irving, C.N. Connolly, C. Sutherland, GSK-3 phosphorylation of the Alzheimer epitope within collapsin response mediator proteins regulates axon elongation in primary neurons, *J. Biol. Chem.*, 279 (2004) 50176-50180.
- [128] H. Jiang, W. Guo, X. Liang, Y. Rao, Both the establishment and the maintenance of neuronal polarity require active mechanisms: critical roles of GSK-3 β and its upstream regulators, *Cell*, 120 (2005) 123-135.
- [129] T. Yoshimura, Y. Kawano, N. Arimura, S. Kawabata, A. Kikuchi, K. Kaibuchi, GSK-3 β regulates phosphorylation of CRMP-2 and neuronal polarity, *Cell*, 120 (2005) 137-149.
- [130] S. Lovestone, C.H. Reynolds, D. Latimer, D.R. Davis, B.H. Anderton, J.-M. Gallo, D. Hanger, S. Mulot, B. Marquardt, S. Stabel, J.R. Woodgett, C.C.J. Miller, Alzheimer's disease-like phosphorylation of the microtubule-associated protein tau by glycogen synthase kinase-3 in transfected mammalian cells, *Curr. Biol.*, 4 (1994) 1077-1086.
- [131] B.R. Sperber, S. Leight, M. Goedert, V.M.Y. Lee, Glycogen synthase kinase-3 β phosphorylates tau protein at multiple sites in intact cells, *Neurosci. Lett.*, 197 (1995) 149-153.
- [132] J. Zumbunn, K. Kinoshita, A.A. Hyman, I.S. Näthke, Binding of the adenomatous polyposis coli protein to microtubules increases microtubule stability and is regulated by GSK3 β phosphorylation, *Curr. Biol.*, 11 (2001) 44-49.
- [133] E.M. Mandelkow, G. Drewes, J. Biernat, N. Gustke, J. Van Lint, J.R. Vandenheede, E. Mandelkow, Glycogen synthase kinase-3 and the Alzheimer-like state of microtubule-associated protein tau, *FEBS Lett.*, 314 (1992) 315-321.

- [134] M. Maqbool, M. Mobashir, N. Hoda, Pivotal role of glycogen synthase kinase-3: A therapeutic target for Alzheimer's disease, *Eur. J. Med. Chem.*, 107 (2016) 63-81.
- [135] M. Hoshi, A. Takashima, K. Noguchi, M. Murayama, M. Sato, S. Kondo, Y. Saitoh, K. Ishiguro, T. Hoshino, K. Imahori, Regulation of mitochondrial pyruvate dehydrogenase activity by tau protein kinase I/glycogen synthase kinase 3 β in brain, *Proc. Natl. Acad. Sci.*, 93 (1996) 2719-2723.
- [136] I. Khan, M.A. Tantray, M.S. Alam, H. Hamid, Natural and synthetic bioactive inhibitors of glycogen synthase kinase, *Eur. J. Med. Chem.*, 125 (2017) 464-477.
- [137] A. Martinez, M. Alonso, A. Castro, C. Pérez, F.J. Moreno, First non-atp competitive glycogen synthase kinase 3 β (gsk-3 β) inhibitors: thiadiazolidinones (tdzd) as potential drugs for the treatment of Alzheimer's disease, *J. Med. Chem.*, 45 (2002) 1292-1299.
- [138] A. Martinez, M. Alonso, A. Castro, I. Dorronsoro, J.L. Gelpi, F.J. Luque, C. Perez, F.J. Moreno, SAR and 3D-QSAR studies on thiadiazolidinone derivatives: exploration of structural requirements for glycogen synthase kinase 3 inhibitors, *J. Med. Chem.*, 48 (2005) 7103-7112.
- [139] S. Conde, D.I. Perez, A. Martinez, C. Perez, F.J. Moreno, Thienyl and phenyl alpha-halomethyl ketones: new inhibitors of glycogen synthase kinase (GSK-3 β) from a library of compound searching, *J. Med. Chem.*, 46 (2003) 4631-4633.
- [140] D.I. Perez, S. Conde, C. Perez, C. Gil, D. Simon, F. Wandosell, F.J. Moreno, J.L. Gelpi, F.J. Luque, A. Martinez, Thienylhalomethylketones: Irreversible glycogen synthase kinase 3 inhibitors as useful pharmacological tools, *Bioorg. Med. Chem.*, 17 (2009) 6914-6925.
- [141] D.G. Smith, M. Buffet, A.E. Fenwick, D. Haigh, R.J. Iffe, M. Saunders, B.P. Slingsby, R. Stacey, R.W. Ward, 3-Anilino-4-arylmaleimides: potent and selective inhibitors of glycogen synthase kinase-3 (GSK-3), *Bioorg. Med. Chem. Lett.*, 11 (2001) 635-639.
- [142] Q. Ye, M. Li, Y. Zhou, T. Pang, L. Xu, J. Cao, L. Han, Y. Li, W. Wang, J. Gao, J. Li, Synthesis and biological evaluation of 3-benzisoxazolyl-4-indolylmaleimides as potent, selective inhibitors of glycogen synthase kinase-3 β , *Molecules*, 18 (2013) 5498-5516.
- [143] Q. Ye, W. Mao, Y. Zhou, L. Xu, Q. Li, Y. Gao, J. Wang, C. Li, Y. Xu, Y. Xu, H. Liao, L. Zhang, J. Gao, J. Li, T. Pang, Synthesis and biological evaluation of 3-([1,2,4]triazolo[4,3-*a*]pyridin-3-yl)-4-(indol-3-yl)-maleimides as potent, selective GSK-3 β inhibitors and neuroprotective agents, *Bioorg. Med. Chem.*, 23 (2015) 1179-1188.
- [144] Q. Ye, Y. Shen, Y. Zhou, D. Lv, J. Gao, J. Li, Y. Hu, Design, synthesis and evaluation of 7-azaindazolyl-indolyl-maleimides as glycogen synthase kinase-3 β (GSK-3 β) inhibitors, *Eur. J. Med. Chem.*, 68 (2013) 361-371.
- [145] S. Leclerc, M. Garnier, R. Hoessel, D. Marko, J.A. Bibb, G.L. Snyder, P. Greengard, J. Biernat, Y.Z. Wu, E.M. Mandelkow, G. Eisenbrand, L. Meijer, Indirubins inhibit glycogen synthase kinase-3 β and

CDK5/p25, two protein kinases involved in abnormal tau phosphorylation in Alzheimer's disease. , J. Biol. Chem., 276 (2001) 251-260.

[146] P. Polychronopoulos, P. Magiatis, A.L. Skaltsounis, V. Myrianthopoulos, E. Mikros, A. Tarricone, A. Musacchio, S.M. Roe, L. Pearl, M. Leost, P. Greengard, L. Meijer, Structural basis for the synthesis of indirubins as potent and selective inhibitors of glycogen synthase kinase-3 and cyclin-dependent kinases, J. Med. Chem., 47 (2004) 935-946.

[147] K. Chun, J.S. Park, H.C. Lee, Y.H. Kim, I.H. Ye, K.J. Kim, I.W. Ku, M.Y. Noh, G.W. Cho, H. Kim, S.H. Kim, J. Kim, Synthesis and evaluation of 8-amino-[1,2,4]triazolo[4,3-a]pyridin-3(2*H*)-one derivatives as glycogen synthase kinase-3 (GSK-3) inhibitors, Bioorg. Med. Chem. Lett., 23 (2013) 3983-3987.

[148] P.H. Olesen, A.R. Sorensen, B. Urso, P. Kurtzhals, A.N. Bowler, U. Ehrbar, B.F. Hansen, Synthesis and in vitro characterization of 1-(4-aminofurazan-3-yl)-5-dialkylaminomethyl-1*H*-[1,2,3]triazole-4-carboxylic acid derivatives. A new class of selective GSK-3 inhibitors, J. Med. Chem., 46 (2003) 3333-3341.

[149] M. Hamann, D. Alonso, E. Martin-Aparicio, A. Fuertes, M.J. Perez-Puerto, A. Castro, S. Morales, M.L. Navarro, M. Del Monte-Millan, M. Medina, H. Pennaka, A. Balaiah, J. Peng, J. Cook, S. Wahyuono, A. Martinez, Glycogen synthase kinase-3 (GSK-3) inhibitory activity and structure-activity relationship (SAR) studies of the manzamine alkaloids. , J. Nat. Prod., 70 (2007) 1397-1405.

[150] S.A. Lipton, P.A. Rosenberg, Excitatory amino acids as a final common pathway for neurologic disorders, N Engl J Med, 330 (1994) 613-622.

[151] C.-I. Sze, H. Bi, B.K. Kleinschmidt-DeMasters, C.M. Filley, L.J. Martin, *N*-Methyl-D-aspartate receptor subunit proteins and their phosphorylation status are altered selectively in Alzheimer's disease, J. Neurol. Sci., 182 (2001) 151-159.

[152] E. Shimizu, J.P. Tang, C. Rampon, J.Z. Tsien, NMDA receptor-dependent synaptic reinforcement as a crucial process for memory consolidation, Science, 290 (2000) 1170-1174.

[153] S. Ackerley, A.J. Grierson, J. Brownlees, P. Thornhill, B.H. Anderton, P.N. Leigh, C.E. Shaw, C.C.J. Miller, Glutamate slows axonal transport of neurofilaments in transfected neurons, J. Cell Biol., 150 (2000) 165-176.

[154] W. Danysz, C.G. Parsons, Alzheimer's disease, β -amyloid, glutamate, NMDA receptors and memantine, Br. J. Pharmacol., 167 (2012) 324-352.

[155] R. Risgaard, K.B. Hansen, R.P. Clausen, Partial agonists and subunit selectivity at NMDA receptors, Chemistry, 16 (2010) 13910-13918.

[156] K. Anan, M. Masui, S. Hara, M. Ohara, M. Kume, S. Yamamoto, S. Shinohara, H. Tsuji, S. Shimada, S. Yagi, N. Hasebe, H. Kai, Discovery of orally bioavailable cyclohexanol-based NR2B-selective NMDA

receptor antagonists with analgesic activity utilizing a scaffold hopping approach, *Bioorg. Med. Chem. Lett.*, 27 (2017) 4194-4198.

[157] J.A. Kemp, R.M. McKernan, NMDA receptor pathways as drug targets, *Nat. Neurosci.*, 5 Suppl (2002) 1039-1042.

[158] B. Laube, H. Hirai, M. Sturgess, H. Betz, J. Kuhse, Molecular determinants of agonist discrimination by NMDA receptor subunits: analysis of the glutamate binding site on the NR2B subunit, *Neuron*, 18 (1997) 493-503.

[159] L.C. Anson, P.E. Chen, D.J.A. Wyllie, D. Colquhoun, R. Schoepfer, Identification of amino acid residues of the NR2A subunit that control glutamate potency in recombinant NR1/NR2A NMDA receptors, *J. Neurosci.*, 18 (1998) 581-589.

[160] T.L. Kalbaugh, H.M. VanDongen, A.M. VanDongen, Ligand-binding residues integrate affinity and efficacy in the NMDA receptor, *Mol. Pharmacol.*, 66 (2004) 209-219.

[161] P.E. Chen, M.T. Geballe, P.J. Stansfeld, A.R. Johnston, H. Yuan, A.L. Jacob, J.P. Snyder, S.F. Traynelis, D.J. Wyllie, Structural features of the glutamate binding site in recombinant NR1/NR2A *N*-methyl-D-aspartate receptors determined by site-directed mutagenesis and molecular modeling, *Mol. Pharmacol.*, 67 (2005) 1470-1484.

[162] L. Kinarsky, B. Feng, D.A. Skifter, R.M. Morley, S. Sherman, D.E. Jane, D.T. Monaghan, Identification of subunit- and antagonist-specific amino acid residues in the *N*-methyl-D-aspartate receptor glutamate-binding pocket, *J. Pharmacol. Exp. Ther.*, 313 (2005) 1066-1074.

[163] K.L. Strong, Y. Jing, A.R. Prosser, S.F. Traynelis, D.C. Liotta, NMDA receptor modulators: an updated patent review (2013-2014), *Expert Opin. Ther. Pat.*, 24 (2014) 1349-1366.

[164] K.B. Hansen, H. Furukawa, S.F. Traynelis, Control of assembly and function of glutamate receptors by the amino-terminal domain, *Mol. Pharmacol.*, 78 (2010) 535-549.

[165] A.I. Sobolevsky, M.P. Rosconi, E. Gouaux, X-ray structure, symmetry and mechanism of an AMPA-subtype glutamate receptor, *Nature*, 462 (2009) 745-756.

[166] M.L. Mayer, G.L. Westbrook, P.B. Guthrie, Voltage-dependent block by Mg²⁺ of NMDA responses in spinal cord neurones, *Nature*, 309 (1984) 261.

[167] S.F. Traynelis, L.P. Wollmuth, C.J. McBain, F.S. Menniti, K.M. Vance, K.K. Ogden, K.B. Hansen, H. Yuan, S.J. Myers, R. Dingledine, Glutamate receptor ion channels: structure, regulation, and function, *Pharmacol. Rev.*, 62 (2010) 405-496.

[168] H. Furukawa, S.K. Singh, R. Mancusso, E. Gouaux, Subunit arrangement and function in NMDA receptors, *Nature*, 438 (2005) 185-192.

[169] P. Paoletti, Molecular basis of NMDA receptor functional diversity, *Eur. J. Neurosci.*, 33 (2011) 1351-1365.

- [170] P. Paoletti, C. Bellone, Q. Zhou, NMDA receptor subunit diversity: impact on receptor properties, synaptic plasticity and disease, *Nat. Rev. Neurosci.*, 14 (2013) 383-400.
- [171] S.G. Cull-Candy, D.N. Leszkiewicz, Role of distinct NMDA receptor subtypes at central synapses, *Sci STKE*, 2004 (2004) 1-16.
- [172] S. Vicini, J.F. Wang, J.H. Li, W.J. Zhu, Y.H. Wang, J.H. Luo, B.B. Wolfe, D.R. Grayson, Functional and pharmacological differences between recombinant *N*-methyl-D-aspartate receptors, *J. Neurophysiol.*, 79 (1998) 555-566.
- [173] K. Erreger, S.M. Dravid, T.G. Banke, D.J. Wyllie, S.F. Traynelis, Subunit-specific gating controls rat NR1/NR2A and NR1/NR2B NMDA channel kinetics and synaptic signalling profiles, *J. Physiol.*, 563 (2005) 345-358.
- [174] B. Sieglér Retchless, W. Gao, J.W. Johnson, A single GluN2 subunit residue controls NMDA receptor channel properties via intersubunit interaction, *Nat. Neurosci.*, 15 (2012) 406-413.
- [175] J.E. Huettner, B.P. Bean, Block of *N*-methyl-D-aspartate-activated current by the anticonvulsant MK-801: selective binding to open channels, *Proc. Natl. Acad. Sci.*, 85 (1988) 1307-1311.
- [176] B. Reisberg, R. Doody, A. Stoffler, F. Schmitt, S. Ferris, H.J. Mobius, Memantine in moderate-to-severe Alzheimer's disease, *N. Engl. J. Med.*, 348 (2003) 1333-1341.
- [177] C.G. Parsons, W. Danysz, A. Dekundy, I. Pulte, Memantine and cholinesterase inhibitors: complementary mechanisms in the treatment of Alzheimer's disease, *Neurotox. Res.*, 24 (2013) 358-369.
- [178] S.M. Dravid, K. Erreger, H. Yuan, K. Nicholson, P. Le, P. Lyuboslavsky, A. Almonte, E. Murray, C. Mosely, J. Barber, A. French, R. Balster, T.F. Murray, S.F. Traynelis, Subunit-specific mechanisms and proton sensitivity of NMDA receptor channel block, *J. Physiol.*, 581 (2007) 107-128.
- [179] S.A. Lipton, Failures and successes of NMDA receptor antagonists: molecular basis for the use of open-channel blockers like memantine in the treatment of acute and chronic neurologic insults, *NeuroRx*, 1 (2004) 101-110.
- [180] K. Williams, Ifenprodil discriminates subtypes of the *N*-methyl-D-aspartate receptor: selectivity and mechanisms at recombinant heteromeric receptors, *Mol. Pharmacol.*, 44 (1993) 851-859.
- [181] B.L. Chenard, J. Bordner, T.W. Butler, L.K. Chambers, M.A. Collins, D.L. De Costa, M.F. Ducat, M.L. Dumont, C.B. Fox, (1*S*,2*S*)-1-(4-Hydroxyphenyl)-2-(4-hydroxy-4-phenylpiperidino)-1-propanol: A potent new neuroprotectant which blocks *N*-methyl-D-aspartate responses, *J. Med. Chem.*, 38 (1995) 3138-3145.

Chapter 2. Novel *N*-benzylpiperidine carboxamide derivatives as inhibitors of acetylcholinesterase

Contributions to this chapter

*All of the synthesis and compound characterization described in this chapter were performed by Mr DG van Greunen under the supervision of Dr DL Riley and Dr J-L Panayides. The synthetic work was undertaken in the Department of Chemistry at the University of Pretoria. The AChE and BuChE biological assays and statistical analysis described in this chapter were performed by Mr DG van Greunen under the supervision of Prof V Steenkamp and Dr J-L Panayides with assistance from Dr W Cordier and Ms M Nell. The cytotoxicity assays and statistical analysis were performed by Ms M Nell. The biological work was undertaken in the Department of Pharmacology at the University of Pretoria. This chapter was published in the European Journal of Medicinal Chemistry: D.G. van Greunen, C.J. van der Westhuizen, W. Cordier, M. Nell, A. Stander, V. Steenkamp, J.-L. Panayides, D.L. Riley, Novel *N*-benzylpiperidine carboxamide derivatives as potential cholinesterase inhibitors for the treatment of Alzheimer's disease, Eur. J. Med. Chem., 179 (2019) 680-693.*

Novel *N*-benzylpiperidine carboxamide derivatives as inhibitors of acetylcholinesterase

Divan G. van Greunen^a, Werner Cordier^b, Margo Nell^b, Vanessa Steenkamp^b, Jenny-Lee Panayides^c, Darren L. Riley^{a,*}

^a Department of Chemistry, Faculty of Natural and Agricultural Sciences, University of Pretoria, Lynnwood Road, Pretoria, South Africa

^b Department of Pharmacology, Faculty of Health Sciences, University of Pretoria, Bophelo Road, Pretoria, South Africa

^c Pioneering Health Sciences, CSIR Biosciences, Meiring Naudé Road, Pretoria, South Africa

* Corresponding author. E-mail address: darren.riley@up.ac.za (D.L. Riley)

ABSTRACT

A series of fifteen acetylcholinesterase inhibitors, based upon the skeleton of 5,6-dimethoxy-1-oxo-2,3-dihydro-1*H*-inden-2-yl 1-benzylpiperidine-4-carboxylate **8**, were synthesized and their activity evaluated against acetyl and butyrylcholinesterase. The most active analogues in this series, 1-benzyl-*N*-(1-methyl-3-oxo-2-phenyl-2,3-dihydro-1*H*-pyrazol-4-yl) piperidine-4-carboxamide **22** and 1-benzyl-*N*-(5,6-dimethoxy-8*H*-indeno[1,2-*d*]thiazol-2-yl)piperidine-4-carboxamide **30** afforded *in vitro* IC₅₀ values of 5.94 ± 1.08 μM and 0.41 ± 1.25 μM against acetylcholinesterase, respectively. Furthermore, 1-benzyl-*N*-(1-methyl-3-oxo-2-phenyl-2,3-dihydro-1*H*-pyrazol-4-yl) piperidine-4-carboxamide **22** showed no observable cytotoxicity *in vitro* against SH-SY5Y cells.

Key Words

Acetylcholinesterase, Alzheimer's disease, benzylpiperidine, butyrylcholinesterase, cytotoxicity, donepezil

2.1. INTRODUCTION

During the development of donepezil **1** (an FDA approved acetyl cholinesterase inhibitor used for the alleviation of the symptoms associated with Alzheimer's disease) (**Figure 2.1**), Sugimoto and co-workers noted that the *N*-benzylpiperidine moiety was important in small molecules, which functioned by the inhibition of acetylcholinesterase (AChE), as it facilitated binding to the catalytic anionic site (CAS) of AChE [1]. As part of the structure-activity relationship (SAR) studies undertaken by the researchers, the use of an indanone moiety was also identified, which allowed binding within the peripheral anionic site (PAS) of AChE by the interaction of amino acid residues with the carbonyl functional group [1-4].

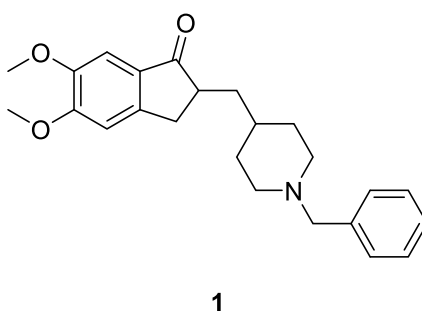


Figure 2.1. Donepezil **1**.

Subsequently, several SAR studies involving the exploration of chemical space surrounding donepezil **1** have been undertaken, and notably, in a few examples the indanone moiety has been replaced with other heterocycles such as indole (**Figure 2.2**) [5], pyridine [6], ebselen (**Figure 2.3**) [7], benzimidazole and benzofuran [8]. In the exploration of new AChE inhibitors, Samadi and co-workers substituted the indanone moiety with indole and pyridine derivatives which resulted in the synthesis of compounds **2** and **3** which had a potency of 0.23 μM and 0.023 μM for AChE, respectively (**Figure 2.2**) [5, 6].

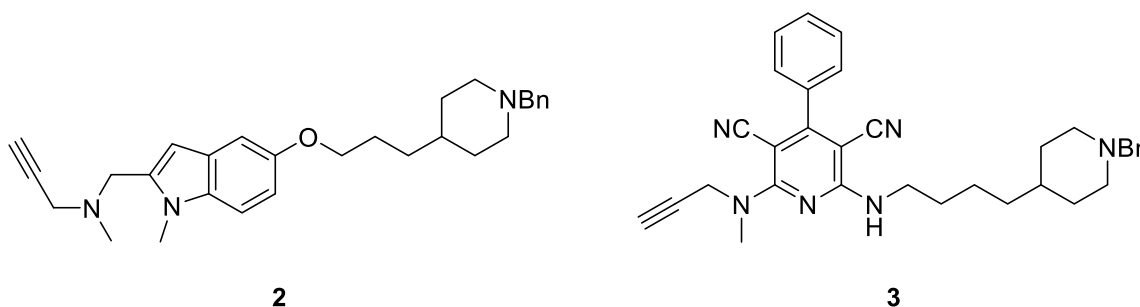


Figure 2.2. Indole-substituted compound **2** and bis-amino pyridine-substituted compound **3** [5, 6].

The Huang research group introduced selenium into the indanone moiety. In this research they used the antioxidant ebselen **4** (**Figure 2.3**) as a scaffold and fused it with the *N*-benzylpiperidine moiety of

donepezil **1**. This afforded the potent AChE inhibiting compound **5**, with an IC_{50} value of 42 nM (**Figure 2.3**) [7].

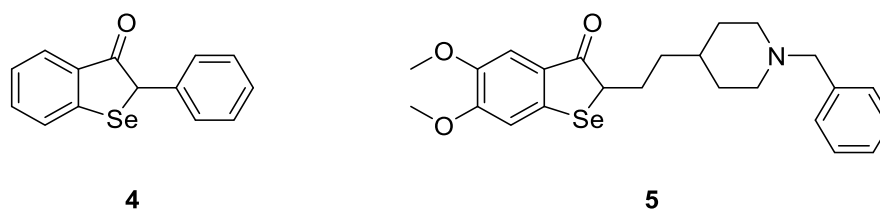


Figure 2.3. Ebselen **4** and ebselen-compound **5** [7].

Santos *et al.* found that the replacement of the indanone moiety with a benzimidazole or benzofuran moiety also produced AChE inhibitors. Shown in **Figure 2.4** are examples of a benzimidazole **6** (IC_{50} = 4.2 μ M) and benzofuran **7** (IC_{50} = 4.0 μ M) derivative that demonstrated inhibition of amyloid- β_{1-42} self-mediated aggregation of 36.3% and 19.0%, respectively [8].

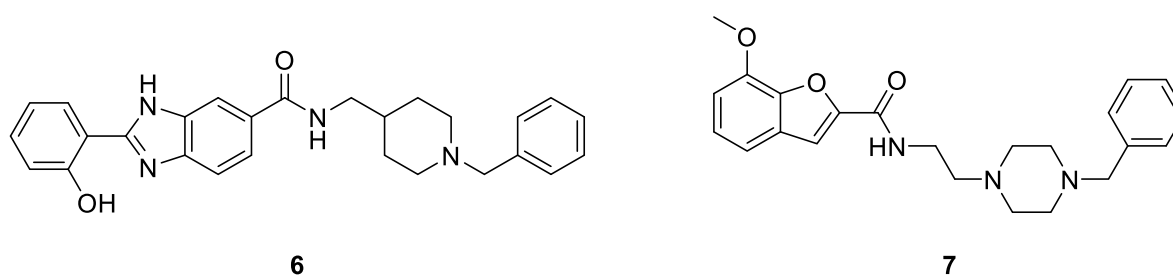


Figure 2.4. Benzimidazole derivative **6** and benzofuran derivative **7** [8].

The objectives of the aforementioned studies were to explore the chemical space around donepezil **1** and to improve activity against AChE. Subsequently it became evident that concomitant inhibition of amyloid- β ($A\beta$) aggregation was observed in systems where there was binding to the PAS of AChE [5, 6, 8, 9]. Additional exploration of the chemical space surrounding donepezil **1**, with the aim of improving the binding within the PAS sites, afforded the opportunity to identify potent inhibitors of AChE [10]. Previously, two replacements were investigated; namely i) the *N*-benzylpiperidine ring system of donepezil **1** was replaced with a range of different saturated *N*-benzylated ring systems, and ii) the methyl bridge between the indanone and the *N*-benzylpiperidine ring system was replaced with different linkers [10]. The SAR conducted identified compound **8** (**Figure 2.5**) as the most active species with an AChE IC_{50} of 0.03 ± 0.07 μ M with no observable cytotoxicity (IC_{50} of >100 μ M, SH-SY5Y cell line).

In the present study, compound **8** was further modified by replacing the ester linkage (Part B) with that of an amide linker, in order to reduce the metabolic liability associated with the ester.

Furthermore, in an effort to develop a potent inhibitor of AChE, the indanone moiety (Part A) was replaced with several heterocyclic and aryl systems, hoping that this would afford improved binding interactions with the PAS.

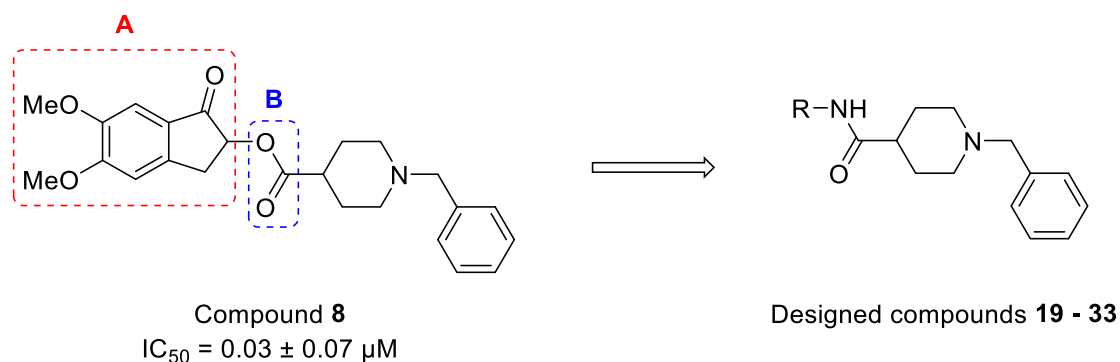
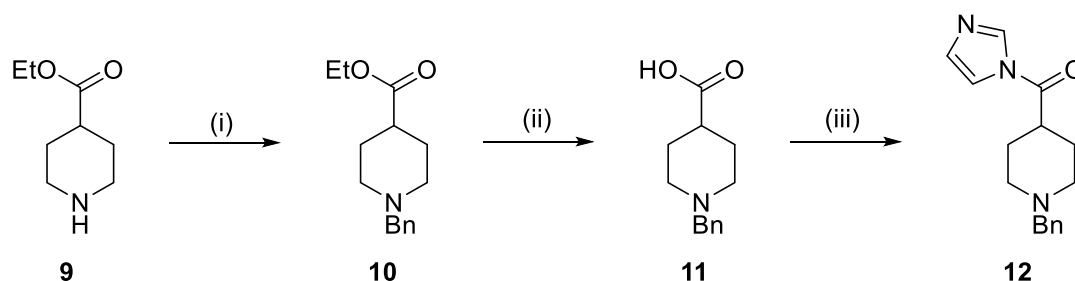


Figure 2.5. Design strategy of the targeted compounds **19 - 33** [10].

In this study, the synthesis of fifteen novel analogues of donepezil **1**, as well as *in vitro* biological evaluation targeted at the inhibition of AChE and butyrylcholinesterase (BuChE) binding to the active site of AChE and BuChE, were investigated. The cytotoxicity of these compounds was also assessed.

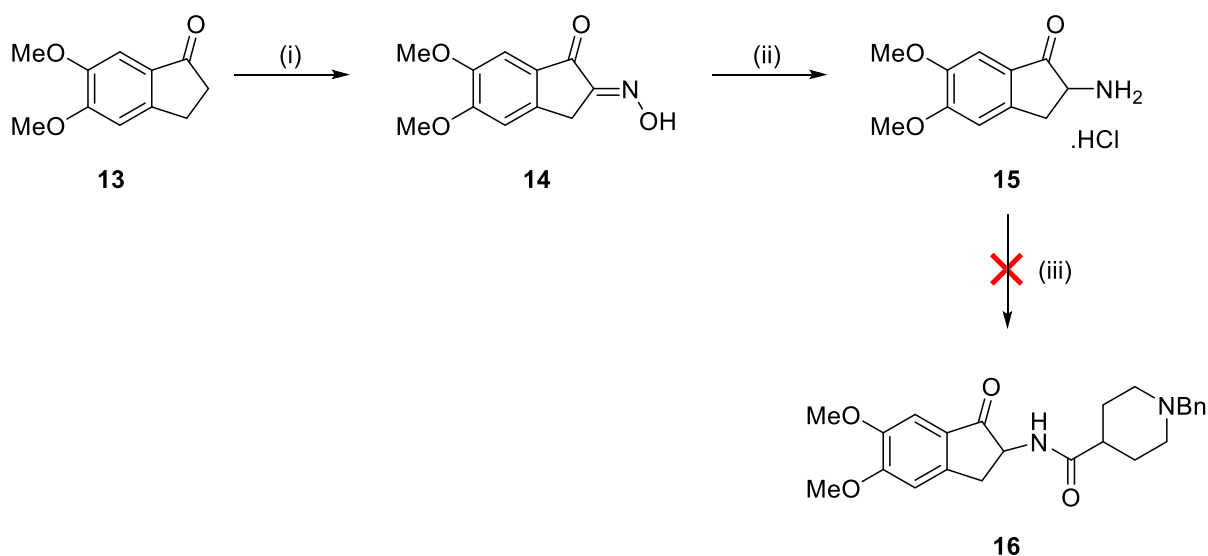
2.2. CHEMISTRY

The preparation of the desired carboxamide derivatives was envisaged using standard amide coupling chemistry to allow the coupling of imidazole **12** with various commercial and synthetic heterocyclic amines. The preparation of the *N*-benzylpiperidine imidazole derivative was achieved in three steps from ethyl isonipecotate **9** (**Scheme 2.1**) [11, 12]. The ethyl isonipecotate **9** was treated with benzyl chloride affording the *N*-benzylated ester **10**, followed by the ester hydrolysis in the presence of methanolic sodium hydroxide affording acid **11**. Subsequent treatment with carbonyl diimidazole (CDI) afforded the imidazole derivative **12** with a 71% yield over three steps.



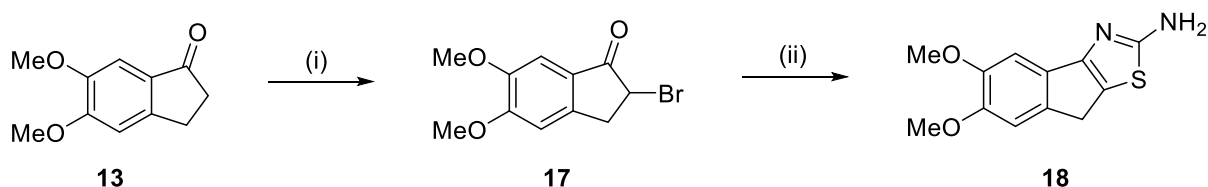
Scheme 2.1: (i) 1.05 eq. BnCl, 3 eq. Et₃N, ACN, reflux, 3h, 88%, (ii) 2 eq. NaOH, MeOH, reflux, 24h, 98%, (iii) 1.2 eq. CDI, DCM, 0°C, 2h, 82%.

Initially, it was envisaged to use this approach to access the amide analogue **16** of previously identified compound **8**. To access the required amine **15**, 5,6-dimethoxy-1-indanone **13** was treated with isopentyl nitrite in an acidic methanolic solution affording the oximino compound **14** as a precipitate in 81% yield (**Scheme 2.2**) [13]. Thereafter, catalytic reduction under acidic conditions afforded the amine as an ammonium salt **15** in 95% yield [14]. Unfortunately, the subsequent coupling attempts proved unsuccessful. This may be due to deprotonation of the amine not occurring.



Scheme 2.2: (i) 1 eq. isopentyl nitrite, conc. HCl, MeOH, 40 °C, 30 min, 81%, (ii) H₂, Pd/C, 1.5 eq. conc. HCl, EtOH, rt, 1 h, 95%, (iii) 6 eq. NaH, DMSO, rt, 3 h, 0%.

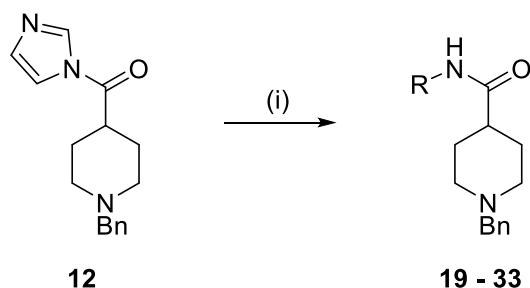
The synthesis of a substituted aminothiazole heterocycle **18** was achieved in two steps from 5,6-dimethoxy-1-indanone **13** (**Scheme 2.3**) [10, 15] by bromination, affording the α -brominated indanone **17**, followed by treatment with thiourea affording **18** in a 70% yield over two steps.



Scheme 2.3: (i) 1.05 eq. Br₂, MeOH, rt, 30 min, 84%, (ii) 1 eq. thiourea, 5 eq. 3M aq. NH₃, H₂O, rt-reflux, 12h, 83%.

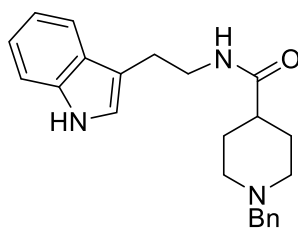
The carboxamide derivatives **19** - **33** were obtained through a standard amide coupling between imidazole derivative **12** (**Scheme 2.4**) and various primary amines in the presence of catalytic 4-dimethylaminopyridine (4-DMAP), affording the requisite amides **19** - **33** (**Table 2.1**) in low to good

yields [16]. In the case of amide **33**, the coupling initially required the deprotonation of amine **18** with sodium hydride, affording amide **33** in 12% yield when performed in the absence of 4-DMAP.



Scheme 2.4: 1 eq. R-NH₂, 0.6 eq. 4-DMAP, 1 eq. Et₃N, DCM, rt – reflux, 12 h, 12 – 99%.

Compound **19** (**Figure 2.6**) is used as a representative example to highlight the structure elucidation of the series. The desired compound **19** was identified by the disappearance of the imidazole peaks at 8.16, 7.46 and 7.09 in the proton NMR spectrum and the corresponding appearance of a singlet at 5.66 ppm integrating for 1H which was assigned to the amide proton. The presence of the heterocycle (indole) was evidenced by the appearance of a singlet at 8.45 ppm integrating for 1H in the ¹H NMR spectrum which is characteristic of the indole amine peak. The formation of **19** was further supported by the shift in the carbonyl peak in the ¹³C NMR spectrum from 171.9 to 175.0 ppm which was assigned to the new amide carbonyl. In addition, a new peak in the IR spectrum at 1630 cm⁻¹ was distinctive of an amide carbonyl stretch. Final confirmation was given by the presence of a peak assigned as [M + H]⁺ at 362.2209 in the high-resolution mass spectrometry (HRMS), with the [M + H]⁺ value calculated as 362.2227. The remaining compounds in the series were analysed in a similar manner, and the spectral assignments are provided in the experimental section.



19

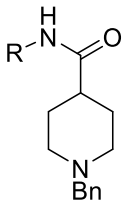
Figure 2.6. Compound **19**.

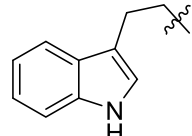
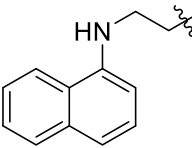
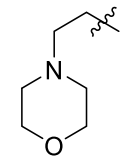
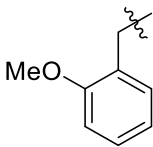
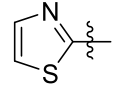
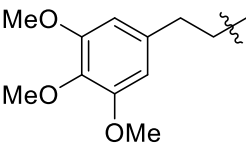
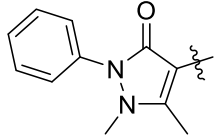
2.3. STRUCTURE-ACTIVITY RELATIONSHIP STUDY

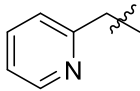
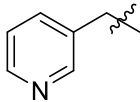
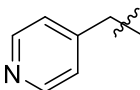
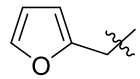
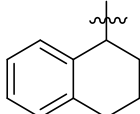
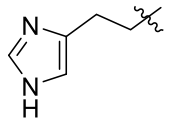
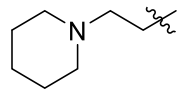
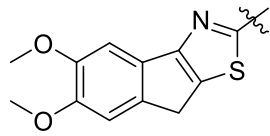
The inhibitory activity of all new synthetic compounds was assessed against *Electrophorus electricus* AChE (*EeAChE*) and BuChE from equine serum (eqBuChE) using Ellman's spectrophotometric method [17] with minor modifications [18]. Galantamine was used as a positive control. The anticholinesterase

activities for the synthesised compounds expressed as half-maximal inhibitory concentration (IC_{50}) values is provided in **Table 2.1**. In addition, selected compounds were assessed for cytotoxicity in the SH-SY5Y neuroblastoma cell line using the sulforhodamine B (SRB) staining assay as described by Vichai and Kirtikara [19].

Table 2.1. *In vitro* AChE, BuChE inhibitory activity and cytotoxicity results of compounds **1** and **19 - 33**.



| Compound | R | Yield % | <i>Ee</i> AChE $IC_{50} \pm SEM$ (μM) ^a | eqBuChE $IC_{50} \pm SEM$ (μM) ^a | Cytotoxicity $IC_{50} \pm SEM$ (μM) ^a |
|-----------|---|---------|---|--|---|
| 19 |  | 91 | 25.60 ± 1.10 | >100 | 40.48 ± 1.21 |
| 20 |  | 90 | 13.98 ± 1.16 | >100 | 13.57 ± 1.15 |
| 21 |  | 85 | >100 | >100 | 73.42 ± 1.35 |
| 22 |  | 99 | 44.39 ± 1.17 | >100 | 50.90 ± 1.58 |
| 23 |  | 59 | 51.10 ± 1.12 | >100 | 76.62 ± 1.11 |
| 24 |  | 93 | >100 | >100 | >100 |
| 25 |  | 34 | 5.94 ± 1.08 | >100 | >100 |

| | | | | | |
|--------------------|---|----|------------------|-----------------|------------------|
| 26 |  | 77 | 30.88 ± 1.19 | >100 | >100 |
| 27 |  | 59 | 58.89 ± 1.15 | >100 | >100 |
| 28 |  | 77 | 58.18 ± 1.14 | >100 | 3.37 ± 1.19 |
| 29 |  | 97 | >100 | >100 | >100 |
| 30 |  | 53 | >100 | >100 | 99.32 ± 1.04 |
| 31 |  | 38 | >100 | >100 | >100 |
| 32 |  | 59 | 82.10 ± 1.14 | >100 | >100 |
| 33 |  | 12 | 0.41 ± 1.25 | >100 | 31.31 ± 1.32 |
| Donepezil 1 | | - | 0.05 ± 1.27 | 5.20 ± 0.01 | 95.13 ± 1.30 |
| Galantamine | | - | 3.58 ± 1.24 | - | - |

^a Data are the mean \pm SEM of three independent experiments

From **Table 1**, it is evident that only two compounds contained an IC_{50} value below $10 \mu M$; compound **25** ($IC_{50} = 5.94 \mu M$) and **33** ($IC_{50} = 0.41 \mu M$). The heterocyclic systems for **25** and **33** were found to have a resemblance to the indanone moiety of donepezil **1** and compound **8**, which could have affected the inhibition of AChE, as they have a proton acceptor in a similar position as **1** and **8**. However, when comparing the heterocyclic structures of compounds **1**, **8**, **25** and **33** it is evident that when the carbonyl functionality is exchanged to that of an imine type (compound **33**) the cytotoxicity of the compounds increased.

It was also noted that the position of the nitrogen in the heterocycles has an effect on inhibition. When compounds **26** - **28** were compared, it was noted that by changing the nitrogen from an *ortho* to a

para-position, the inhibition of AChE decreased from 30.88 to 58.18 μM . Comparison of the two thiazole moieties of compounds **23** and **33**, which contained increased aromaticity to the thiazole core, indicated increased inhibition from 51.10 μM (compound **23**) to 0.41 μM (compound **33**). From these observations we can conclude that the replacement of carbonyl groups with that of imine, as well as by modifying the position of the nitrogen in the heterocycle, we will be able to design more sufficient inhibitors. The inhibitors synthesized that had activity, were selective towards AChE but not to BuChE, where no inhibition in activity was observed. A cytotoxicity selectivity index of 76 was obtained for the most active compounds **33**, while **25** displayed a selectivity index >16.84 as no cytotoxicity was apparent.

2.4. CONCLUSION

A small library of fifteen potential AChE inhibitors was designed and prepared based upon the molecular skeleton of a potent lead compound **8** (IC_{50} 0.03 μM) which was reported previously by this group. Analogues were prepared by changing the ester linker present in **8** to that of an amide linker to potentially reduce the metabolic liability associated with the ester functional group. Introduction of the amide linker appears to reduce activity, although it should be noted that the direct amide analogue **16** of compound **8** could not be accessed synthetically. That been said, two potential lead compounds were identified with AChE inhibitory IC_{50} activities below 10 μM , namely **23** (5.94 μM) and **33** (0.41 μM). The replacement of the carbonyl groups with that of an imine together with the alteration in the position of the nitrogen in the heterocycle, led to the synthesis of more potent inhibitors. These compounds demonstrated inhibition of AChE rather than BuChE. Further studies will be conducted with structural changes to increase the selectivity of inhibition.

2.5. EXPERIMENTAL

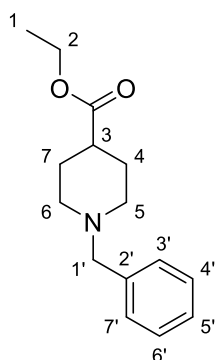
2.5.1. Chemistry

2.5.1.1. General methods

All solvents, chemicals, and reagents were obtained commercially and used without further purification. ^1H NMR (300 MHz) and ^{13}C NMR (75 MHz) spectra were recorded on Bruker AVANCE-III-300 instrument using CDCl_3 and $\text{DMSO}-d_6$. CDCl_3 contained tetramethylsilane as an internal standard. Chemical shifts, δ , are reported in parts per million (ppm), and splitting patterns are given as singlet (s), doublet (d), triplet (t), quartet (q), or multiplet (m). Coupling constants, J , are expressed in hertz (Hz). Mass spectra were recorded in electron spray ionisation (ESI) mode on a Waters Synapt G2 Mass Spectrometer at 70 eV and 200 mA. Samples were dissolved in acetonitrile (containing 0.1% formic acid) to an approximate concentration of 10 $\mu\text{g}/\text{mL}$. Infrared spectra were run on a Bruker ALPHA

Platinum ATR spectrometer. The absorptions are reported on the wavenumber (cm^{-1}) scale, in the range 400 - 4000 cm^{-1} . Abbreviations used in quoting spectra are: v = very, s = strong, m = medium, w = weak, str = stretch. Melting points were measured on a Stuart Melting Point SMP10. The retention factor (R_f) values denoted are for thin layer chromatography (TLC) on aluminium-backed Macherey-Nagel ALUGRAM Sil G/UV₂₅₄ plates pre-coated with 0.25 mm silica gel 60, spots were visualised with UV light and basic KMnO_4 spray reagent. Chromatographic separations were performed on Macherey-Nagel Silica gel 60 (particle size 0.063 – 0.200 mm). Yields refer to isolated pure products unless stated otherwise. Each compound is named either according to PerkinElmer's *ChemDraw Version 15.0.0.106* or according to common names. The numbering of compounds was not done according to priority, but rather to the author's convenience for characterization.

2.5.1.2. Ethyl 1-benzylpiperidine-4-carboxylate **10**

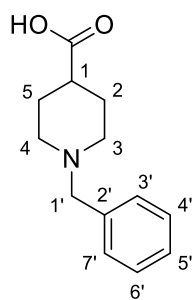


10

A mixture of ethyl isonipecotate **9** (10.00 g, 63.61 mmol, 1 eq.), benzyl chloride (7.7 mL, 67 mmol, 1.05 eq.) and triethylamine (26.5 mL, 191 mmol, 3 eq.) in anhydrous acetonitrile (100 mL) was refluxed for 3 h after which time the reaction mixture was left to cool to room temperature and the solvent was evaporated *in vacuo*. The obtained oil was diluted with ethyl acetate (100 mL) and washed with a 10% aqueous solution of sodium hydroxide (3 x 50 mL) and water (50 mL). The organic layer was dried over anhydrous sodium sulfate, filtered and the solvent evaporated *in vacuo* to afford the product. The product was used without any

further purification. (Yield 88%); Transparent orange oil; R_f 0.42 (1:3 ethyl acetate: hexane); ν_{max} (neat)/ cm^{-1} 2944 (C-H str, m), 2801 (C-H str, m), 2760 (C-H str, m), 1728 (C=O str, s), 1448 (C-C str, m), 1168 (C-O str, s), 1046 (C-N str, m), 736 (C-H "oop", s), 698 (C-H "oop", s); $^1\text{H NMR}$ (300 MHz, CDCl_3); δ 7.41 – 7.15 (5H, m, ArH's), 4.13 (2H, q, $J = 7.1$ Hz, H-2), 3.51 (2H, s, H-1'), 2.87 (2H, dt, $J = 11.4, 3.1$ Hz, *H-5a & H-6a), 2.30 (1H, tt, $J = 10.9, 4.2$ Hz, H-3), 2.05 (2H, td, $J = 11.3, 2.7$ Hz, *H-5b & H-6b), 1.95 – 1.71 (4H, m, H-4 & H-7), 1.26 (3H, t, $J = 7.1$ Hz, H-1); $^{13}\text{C NMR}$ (75 MHz, CDCl_3); δ 175.3 (C=O), 138.5 (C-2'), 129.2 (C-3' & C-7'), 128.3 (C-4' & C-6'), 127.1 (C-5'), 63.4 (C-1'), 60.3 (C-2), 53.0 (C-5 & C-6), 41.3 (C-3), 28.4 (C-4 & C-7), 14.3 (C-1); HRMS m/z (ESI) ($\text{C}_{15}\text{H}_{21}\text{NO}_2$) 248.1682 ($[\text{M} + \text{H}]^+$ requires 248.1645). *Assignments are interchangeable. Characterization of this compound compared well to literature [10].

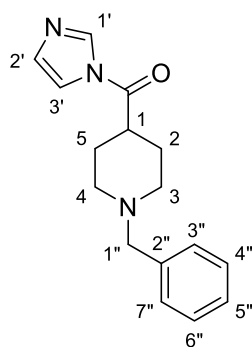
2.5.1.3. 1-Benzylpiperidine-4-carboxylic acid **11**



11

To a stirring solution of sodium hydroxide (3.44 g, 86.02 mmol, 2 eq.) in methanol (100 mL) at room temperature was added ethyl 1-benzylpiperidine-4-carboxylate **10** (10.01 g, 41.82 mmol, 1 eq.) in one portion. The resulting mixture was heated to reflux temperature and left to stir overnight. The resulting solution was cooled to room temperature and the solvent was evaporated *in vacuo* to afford a yellow solid. The solid was re-dissolved in distilled water (100 mL) and the pH was adjusted to pH 5.5. The solvent was removed *in vacuo* to afford a yellow solid. A pre-mixed solution of ethanol: chloroform (1:1, 200 mL) was added and the mixture was left to stir for 1 h after which time the solids were filtered off and washed with chloroform (10 mL). The filtrate was collected and the solvent was evaporated *in vacuo* to afford the product. The product was used without any purification. (Yield 98%); Off-white solid; R_f 0.07 (4:1 dichloromethane: methanol); **mp** 168 °C; ν_{\max} (neat)/ cm^{-1} 2969 (O-H str, m), 1602 (C=O str, s), 1448 (C-C str, m), 1382 (O-H bend, s), 921 (s), 756 (s), 702 (s), 659 (s); $^1\text{H NMR}$ (300 MHz, CDCl_3); δ 10.71 (1H, s, OH), 7.38 – 7.27 (5H, m, ArH's), 3.89 (2H, s, H-1'), 3.14 (2H, d, J = 11.2 Hz, *H-3a & H-4a), 2.46 (2H, t, J = 8.9 Hz, *H-3b & H-4b), 2.34 – 2.21 (1H, m, H-1), 2.07 – 1.82 (4H, m, 4H, H-2 & H-5); $^{13}\text{C NMR}$ (75 MHz, CDCl_3); δ 178.9 (C=O), 132.3 (C-2'), 130.8 (C-3' & C-7'), 128.7 (C-5' & C-4' & C-6'), 60.8 (C-1'), 51.5 (C-3 & C-4), 40.7 (C-1), 26.7 (C-2 & C-5); **HRMS** m/z (ESI) ($\text{C}_{13}\text{H}_{17}\text{NO}_2$) 220.1353 ([M + H]⁺ requires 220.1332). *Assignments are interchangeable. Characterization of this compound compared well to literature [10].

2.5.1.4. (1-Benzylpiperidin-4-yl)(1H-imidazol-1-yl)methanone **12**



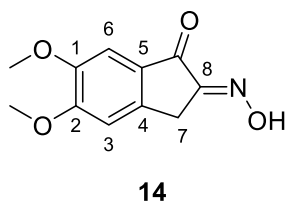
12

1-Benzylpiperidine-4-carboxylic acid **11** (6.24 g, 28.5 mmol, 1 eq.) in dry dichloromethane (100 mL) was cooled to 0 °C, and carbonyl diimidazole (5.57 g, 34.4 mmol, 1.2 eq.) was added portion-wise over 5 min. After 2 h, the mixture was diluted with dichloromethane (10 mL), and water (100 mL) was added carefully. The organic layer was washed with water (2 x 40 mL) and brine (30 mL), dried over anhydrous sodium sulfate and the solvent evaporated *in vacuo* to afford the product as solid. The product was used as is. (Yield 82%); Off-white solid; **mp** 119 - 121 °C; ν_{\max} (neat)/ cm^{-1} 2932 (CH_2 bend, m), 1604 (C=O & C=N str, s), 1447 (m), 1383 (m), 1065 (C-N str, m), 922 (s), 825 (m), 753 (m); $^1\text{H NMR}$ (300 MHz, CDCl_3); δ 8.16 (1H, s, H-1'), 7.46 (1H, s, H-3'), 7.37 – 7.23 (5H, m, ArH's), 7.09 (1H, s, H-2'), 3.58 (2H, s, H-1''), 3.00 (2H, d, J = 11.7 Hz, *H-3a & H-4a), 2.99 – 2.84 (1H, m, H-1), 2.27 – 2.09 (2H, m, *H-3b & H-4b), 2.08 – 1.91 (4H, m, H-2 & H-5); $^{13}\text{C NMR}$ (75 MHz, CDCl_3); δ 171.9 (C=O), 136.2 (C-1'), 131.3 (C-2'), 129.3 (C-2''), 128.5 (C-3'' & C-4'' & C-6'' & C-7''), 127.5 (C-5''), 116.2 (C-3'), 63.0 (C-1''), 52.4 (C-3 & C-

4), 41.7 (C-1), 28.5 (C-2 & C-5); **HRMS m/z (ESI)** ($C_{16}H_{19}N_3O$) 270.1707 ($[M + H]^+$ requires 270.1601).

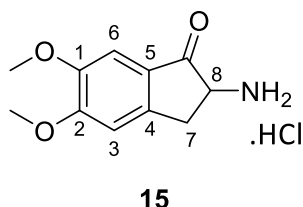
*Assignments are interchangeable.

2.5.1.5. 2-Oximino-5,6-dimethoxy-2,3-dihydro-1H-inden-1-one **14**



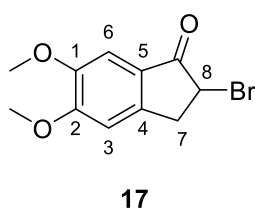
To a solution of 5,6-dimethoxy-1-indanone **13** (1.50 g, 7.82 mmol, 1.0 eq.) in methanol (25 mL) at 40°C was added 96% isopentyl nitrite (1.3 mL, 9.4 mmol, 1.2 eq.) followed by concentrated aqueous hydrochloric acid (0.78 mL, 9.40 mmol, 1.2 eq.). The solution was stirred for 30 min during which time a precipitate formed. The precipitate was collected and dried to yield the product a solid. The product was used as is without any further purification. (Yield 81%); Yellow solid; R_f 0.45 (3:1 ethyl acetate: hexane); **mp** 240 °C (literature [13] 227 - 228 °C); ν_{max} (neat)/ cm^{-1} 3189, 1694, 1579, 1498, 1449, 1304, 1233, 1119, 1029, 978, 915, 801, 746; **1H NMR (300 MHz, DMSO)**; δ 12.41 (1H, s, NOH), 7.17 (1H, s, ArH), 7.16 (1H, s, ArH), 3.89 (3H, s, OCH₃), 3.82 (3H, s, OCH₃), 3.64 (2H, s, H-7); **^{13}C NMR (75 MHz, DMSO)**; δ 187.6 (C=O), 156.0 (C-8), 154.7 (C-2), 149.3 (C-1), 142.5 (C-5), 130.5 (C-4), 108.6 (C-3), 104.5 (C-6), 56.2 (OCH₃), 55.7 (OCH₃), 27.6 (C-7); **HRMS m/z (ESI)** ($C_{11}H_{11}N_4O$) 292.1558 ($[M + H]^+$ requires 292.0761). Characterization of this compound compared well to literature [10].

2.5.1.6. 2-Amino-5,6-dimethoxy-2,3-dihydro-1H-inden-1-one hydrochloride **15**



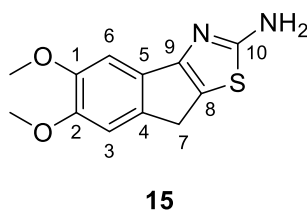
A suspension of 2-oximino-5,6-dimethoxy-2,3-dihydro-1H-inden-1-one **14** (0.21 g, 0.93 mmol, 1.0 eq.), concentrated aqueous hydrochloric acid (0.1 mL, 1.4 mmol, 1.5 eq.) and 10% palladium on carbon (0.05 g, 50 mg.mmol⁻¹) in ethanol (15 mL) was hydrogenated at atmospheric pressure and room temperature until the incorporation of the hydrogen was complete. The catalyst was then filtered off and washed with ethanol (3 x 25 mL). The solvent of the filtrate was then removed *in vacuo* to afford the product as a solid. The product was used as is without any further purification. (Yield 95%); Light yellow solid; R_f 0.54 (3:1 ethyl acetate: hexane); **mp** 240 °C decomposed (literature [14] 240 °C decomposed); ν_{max} (neat)/ cm^{-1} 2915, 1708, 1590, 1496, 1318, 1270, 1128, 1087, 1014, 801; **1H NMR (300 MHz, DMSO)**; δ 8.90 (3H, s, NH₃⁺), 7.20 (1H, s, ArH), 7.14 (1H, s, ArH), 4.17 (1H, s, H-8), 3.88 (3H, s, OCH₃), 3.81 (3H, s, OCH₃), 3.46 (1H, d, J = 7.9 Hz, H-7), 3.07 (1H, dd, J = 16.8, 4.6 Hz, H-7); **^{13}C NMR (75 MHz, DMSO)**; δ 198.5 (C=O), 156.3 (C-2), 149.7 (C-4), 147.2 (C-1), 126.4 (C-5), 108.4 (C-3), 104.3 (C-6), 56.2 (OCH₃), 55.8 (OCH₃), 53.3 (C-8), 31.0 (C-7); **HRMS m/z (ESI)** ($C_{11}H_{13}NO_3$) 208.1000 ($[M + H]^+$ requires 208.0968). Characterization of this compound compared well to literature [10].

2.5.1.7. 2-Bromo-5,6-dimethoxy-1-indanone **17**



To a stirring solution of 5,6-dimethoxy-1-indanone **13** (10.00 g, 52.03 mmol, 1 eq.) in methanol (100 mL), was added bromine (2.8 mL, 55 mmol, 1.1 eq.) drop-wise. After addition of bromine the product precipitated out of solution. The mixture was left to stir for 30 min after which time the precipitate was filtered off, washed with ice cold methanol (50 mL), and dried *in vacuo* to afford the product as a solid. The product was used without any further purification. (Yield 84%); Light yellow solid; R_f 0.72 (3:1 ethyl acetate: hexane); mp 162 - 163 °C [10]; ν_{\max} (neat)/ cm^{-1} 2959 (CH₂ bend, m), 1687 (C=O str, s), 1583 (s), 1497 (C-C str, m), 1309 (C-H wag (-CHBr), m), 1261 (s), 1218 (C-N str, m), 1107 (m), 1015 (m), 727 (s); $^1\text{H NMR}$ (300 MHz, CDCl₃); δ 7.19 (1H, s, H-6), 6.82 (1H, s, H-3), 4.61 (1H, dd, $J = 2.9$ & 7.3 Hz, H-8), 3.95 (3H, s, OCH₃), 3.88 (3H, s, OCH₃), 3.72 (1H, dd, $J = 7.2$ & 17.9 Hz, H-7), 3.30 (1H, dd, $J = 2.98$ & 17.9 Hz, H-7); $^{13}\text{C NMR}$ (75 MHz, CDCl₃); δ 198.2 (C=O), 156.8 (C-2), 150.2 (C-4), 146.7 (C-1), 126.4 (C-5), 107.3 (C-3), 105.2 (C-6), 56.5 (OCH₃), 56.3 (OCH₃), 44.7 (C-8), 37.9 (C-7). Characterization of this compound compared well to literature [10].

2.5.1.8. 5,6-Dimethoxy-8H-indeno[1,2-d]thiazol-2-amine **18**

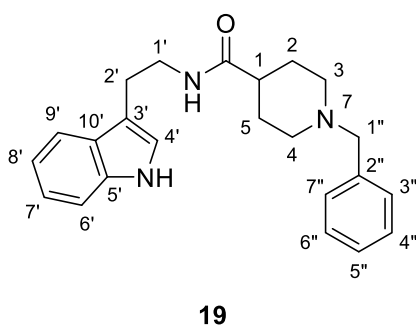


To a suspension of thiourea (1.97 g, 25.9 mmol, 1 eq.) in distilled water (100 mL) was added 2-bromo-5,6-dimethoxy-1-indanone **17** (7.00 g, 25.8 mmol, 1 eq.) in three portions over 30 min at room temperature. The resulting mixture was refluxed for 12 h. The solution was then cooled to room temperature and a 3 M ammonium hydroxide solution (64.6 mL, 129.1 mmol, 5 eq.) was added, which resulted in the precipitation of the product. The resulting mixture was left to stir for 30 min. The product was filtered off and washed with distilled water (100 mL) after which time it was dried *in vacuo*. The product was used without any further purification. (Yield 83%); Yellow solid; R_f 0.27 (3:1 ethyl acetate: hexane); mp 204 °C (decomp.); ν_{\max} (neat)/ cm^{-1} 3376 (N-H str, m), 3111 (m), 2933 (C-H str, m), 1524 (N-H bend, s), 1456 (C-C str, m), 1377 (C-H bend, s), 1271 (C-N str, s), 1203 (C-N str, m), 1148 (m), 1097 (s), 750 (C-H "oop", s); $^1\text{H NMR}$ (300 MHz, DMSO-*d*₆); δ 7.15 (1H, s, H-6), 7.08 (2H, s, NH₂), 6.98 (1H, s, H-3), 3.79 (3H, s, OCH₃), 3.76 (3H, s, OCH₃), 3.58 (2H, s, H-7); $^{13}\text{C NMR}$ (75 MHz, DMSO-*d*₆); δ 172.8 (C-10), 156.0 (C-2), 148.0 (C-9), 146.4 (C-1), 137.5 (C-5), 130.8 (C-4), 120.7 (C-8), 110.1 (C-3), 102.1 (C-6), 55.9 (OCH₃), 55.7 (OCH₃), 32.0 (C-7); HRMS m/z (ESI) (C₁₂H₁₂N₂O₂S) 249.0697 ([M + H]⁺ requires 249.0692).

2.5.1.9. General method for amide couplings

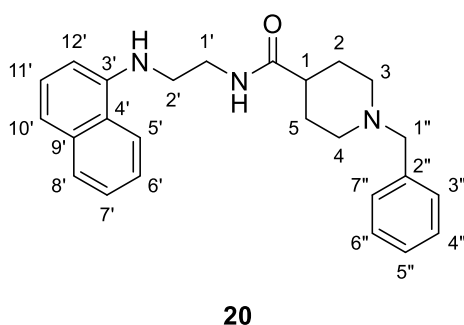
A mixture of amine (1.00 mmol, 1 eq.), (1-benzylpiperidin-4-yl)(1*H*-imidazol-1-yl) methanone **12** (1.11 mmol, 1.1 eq.), 4-dimethylaminopyridine (0.60 mmol, 0.6 eq.) and triethylamine (1.00 mmol, 1 eq.) in anhydrous dichloromethane (15 mL) was left to stir overnight at room temperature. The mixture was then refluxed for 2 h, after which time the mixture was left to cool to room temperature. A solution of 3 M aqueous sodium hydroxide (50 mL) was added to the reaction mixture. The organic layer was separated and the aqueous layer was washed with dichloromethane (2 x 30 mL). The organic layers were combined and washed with distilled water (30 mL). The organic layer was dried over anhydrous sodium sulfate, filtered and the solvent was evaporated *in vacuo*. The product was purified by column chromatography.

2.5.1.9.1. *N*-[2-(1*H*-indole-3-yl)ethyl]-1-benzylpiperidine-4-carboxamide **19**



(Yield 91%); Off-white solid; R_f 0.42 (9:1 dichloromethane:methanol); **mp** 144 - 145 °C; ν_{\max} (neat)/ cm^{-1} 3309 (N-H str, m), 2929 (C-H str, m), 2816 (m), 1630 (C=O str, s), 1532 (N-H bend, s), 1445 (C-C str, m), 1348 (C-H bend, m), 1294 (C-N str, m), 1207 (C-N str, m), 1105 (m), 1031 (m), 990 (m), 922 (m), 741 (C-H "oop", s), 702 (C-H "oop", s); $^1\text{H NMR}$ (300 MHz, CDCl_3); δ 8.45 (1H, s, indole NH), 7.59 (1H, d, $J = 7.8$ Hz, ArH), 7.39 – 7.24 (6H, m, H-4' & ArH's), 7.23 – 7.16 (1H, m, ArH), 7.15 – 7.08 (1H, m, ArH), 6.98 (1H, d, $J = 1.9$ Hz, ArH), 5.66 (1H, s, NH), 3.58 (2H, dd, $J = 15.0, 9.0$ Hz, H-1'), 3.51 (s, 2H, H-1''), 3.01 – 2.86 (4H, m, H-2' & *H-3a & *H-4a), 2.08 – 1.92 (3H, m, H-1 & *H-3b & *H-4b), 1.82 – 1.62 (m, 4H, H-2 & H-5); $^{13}\text{C NMR}$ (75 MHz, CDCl_3); δ 175.0 (C=O), 136.5 (C-5'), 129.4 (C-2''), 128.4 (C-3' & C-4' & C-6'' & C-7''), 127.4 (C-5''), 127.4 (C-10), 122.3 (C-4'), 122.2 (C-7'), 119.5 (C-8'), 118.8 (C-9'), 112.9 (C-3'), 111.5 (C-6'), 63.1 (C-1''), 52.9 (C-3 & C-4), 43.1 (C-1'), 39.6 (C-1), 28.7 (C-2 & C-5), 25.4 (C-2'); **HRMS m/z (ESI)** ($\text{C}_{23}\text{H}_{27}\text{N}_3\text{O}$) 362.2209 ([$M + H$] $^+$ requires 362.2227). *Assignments are interchangeable.

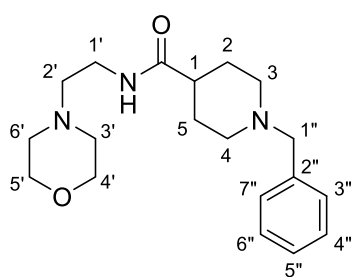
2.5.1.9.2. 1-Benzyl-*N*-[2-(naphthalen-1-ylamino)ethyl] piperidine-4-carboxamide **20**



(Yield 90%); Green solid; R_f 0.61 (9:1 dichloromethane:methanol); **mp** 120 - 121 °C; ν_{\max} (neat)/ cm^{-1} 3402 (N-H str, m), 3314 (N-H str, m), 2929 (C-H str, m), 1628 (C=O str, s), 1582 (N-H bend, m), 1538 (N-H bend, s), 1412 (C-C str, m), 1292 (C-N str, m), 1135 (s), 954 (m), 753 (C-H "oop", s), 689 (C-H "oop", s); $^1\text{H NMR}$ (300 MHz, CDCl_3); δ 7.89 – 7.82 (1H,

m, ArH), 7.81 – 7.74 (1H, m, ArH), 7.47 – 7.40 (2H, m, ArH's), 7.36 – 7.24 (6H, m, ArH's), 7.22 (1H, d, $J = 8.2$ Hz, ArH), 6.51 (1H, d, $J = 7.4$ Hz, ArH), 6.15 (1H, s, amide NH), 5.20 (1H, s, NH), 3.64 (2H, dd, $J = 12.0, 6.0$ Hz, H-1'), 3.47 (2H, s, 2H, H-1''), 3.36 (2H, t, $J = 5.4$ Hz, H-2'), 2.89 (2H, d, $J = 11.5$ Hz, *H-3a & *H-4a), 2.17 – 1.89 (3H, m, H-1 & *H-3b & *H-4b), 1.84 – 1.72 (4H, m, H-2 & H-5); $^{13}\text{C NMR}$ (75 MHz, CDCl_3); δ 176.8 (C=O), 143.7 (C-3'), 137.6 (C-2''), 134.4 (C-9'), 129.3 (C-3'' & C-7''), 128.6 (C-8'), 128.4 (C-4'' & C-6''), 127.3 (C-5''), 126.7 (C-11'), 125.9 (C-7'), 124.9 (C-6'), 123.4 (C-4'), 120.5 (C-5'), 117.2 (C-10'), 103.5 (C-12'), 63.0 (C-1''), 52.8 (C-3 & C-4), 45.4 (C-2'), 42.9 (C-1'), 38.9 (C-1), 28.7 (C-2 & C-5); **HRMS m/z (ESI)** ($\text{C}_{25}\text{H}_{29}\text{N}_3\text{O}$) 388.2424 ($[\text{M} + \text{H}]^+$ requires 388.2383). *Assignments are interchangeable.

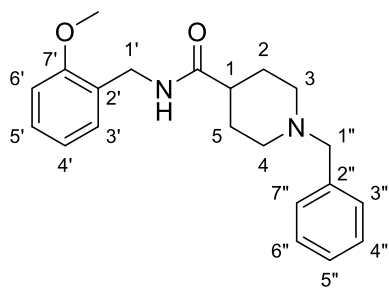
2.5.1.9.3. 1-Benzyl-N-(2-morpholinoethyl) piperidine-4-carboxamide **21**



21

(Yield 85%); Yellow solid; R_f 0.30 (9:1 dichloromethane: methanol); **mp** 89 - 90 °C; ν_{max} (neat)/ cm^{-1} 3266 (N-H str, m), 2928 (C-H str, m), 1638 (C=O str, s), 1540 (N-H bend, s), 1441 (C-C str, m), 1227 (C-N str, m), 1114 (s), 1002 (m), 913 (m), 863 (m), 732 (C-H "oop", s), 698 (C-H "oop", s); $^1\text{H NMR}$ (300 MHz, CDCl_3); δ 7.35 – 7.19 (5H, m, ArH's), 6.15 (1H, s, NH), 3.71 – 3.63 (4H, m, H-4' & H-5'), 3.52 (2H, s, H-1''), 3.32 (2H, dd, $J = 11.2, 5.7$ Hz, H-1'), 2.94 (2H, dd, $J = 11.6, 3.2$ Hz, H-2'), 2.49 – 2.38 (6H, m, H-3' & H-6' & *H-3a & *H-4a), 2.18 – 1.98 (3H, m, H-1 & *H-3b & *H-4b), 1.89 – 1.67 (4H, m, H-2 & H-5); $^{13}\text{C NMR}$ (75 MHz, CDCl_3); δ 175.1 (C=O), 137.7 (C-2''), 129.3 (C-3'' & C-7''), 128.3 (C-4'' & C-6''), 127.3 (C-5''), 67.0 (C-4' & C-5'), 63.1 (C-1''), 57.1 (C-2'), 53.4 (C-3' & C-6'), 53.0 (C-3 & C-4), 43.0 (C-1), 35.5 (C-1'), 28.8 (C-2 & C-5); **HRMS m/z (ESI)** ($\text{C}_{19}\text{H}_{29}\text{N}_3\text{O}_2$) 332.2341 ($[\text{M} + \text{H}]^+$ requires 332.2332). *Assignments are interchangeable.

2.5.1.9.4. 1-Benzyl-N-(2-methoxybenzyl) piperidine-4-carboxamide **22**

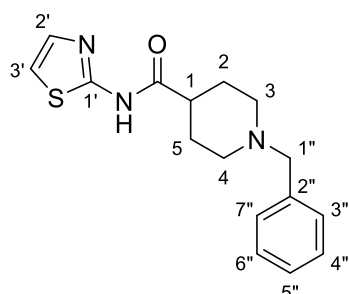


22

(Yield 99%); Yellow crystalline solid; R_f 0.50 (9:1 dichloromethane: methanol); **mp** 120 °C; ν_{max} (neat)/ cm^{-1} 3274 (N-H str, m), 2932 (C-H str, m), 1642 (C=O), 1546 (N-H bend, s), 1489 (m), 1445 (C-C str, m), 1236 (C-N str, m), 1114 (s), 1025 (m), 985 (m), 736 (C-H "oop", s), 696 (C-H "oop", s); $^1\text{H NMR}$ (300 MHz, CDCl_3); δ 7.34 – 7.20 (7H, m, ArH's), 6.94 – 6.84 (2H, m, ArH's), 6.06 (1H, s, NH), 4.43 (2H, d, $J = 5.7$ Hz, H-1'), 3.84 (3H, s, OCH_3), 3.50 (2H, s, H-1''), 2.93 (2H, d, $J = 11.7$ Hz, *H-3a & *H-4a), 2.18 – 1.93 (3H, m, H-1 & *H-3b & *H-4b), 1.90 – 1.67 (4H, m, H-2 & H-5); $^{13}\text{C NMR}$ (75 MHz, CDCl_3); δ 174.6 (C=O), 157.6 (C-7'), 138.0 (C-2''), 129.8 (C-3'), 129.3 (C-3'' & C-7''), 128.9 (C-5'), 128.3 (C-4'' & C-6''), 127.2 (C-5''), 126.4 (C-2'), 120.8 (C-4'), 110.4 (C-6'), 63.2 (C-1''), 55.4

(OCH₃), 53.1 (C-3 & C-4), 43.3 (C-1), 39.4 (C-1'), 28.9 (C-2 & C-5); **HRMS *m/z* (ESI)** (C₂₁H₂₆N₂O₂) 339.2069 ([M + H]⁺ requires 339.2067). *Assignments are interchangeable.

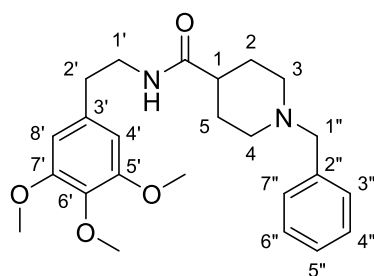
2.5.1.9.5. 1-Benzyl-N-(thiazol-2-yl) piperidine-4-carboxamide **23**



23

(Yield 59%); Off-white solid; **R_f** 0.50 (9:1 dichloromethane: methanol); **mp** 179 - 181 °C; **v_{max} (neat)/cm⁻¹** 3156 (N-H str, w), 2928 (C-H str, m), 1679 (C=O str, s), 1560 (N-H bend, s), 1494 (m), 1442 (C-C str, m), 1368 (C-H bend, s), 1329 (s), 1290 (m), 1267 (C-N str, m), 1186 (s), 1167 (C-N str, s), 1141 (C-N str, s), 1108 (m), 1075 (m), 1010 (m), 964 (C=C-H str, s), 799 (C=C-H str, s), 743 (C-H "oop", s), 726 (C-H "oop", s), 700 (C-H "oop", s); **¹H NMR (300 MHz, CDCl₃)**; δ 12.53 (1H, s, 1H, NH), 7.50 (1H, d, *J* = 3.6 Hz, H-2'), 7.38 – 7.23 (5H, m, ArH's), 7.02 (1H, d, *J* = 3.6 Hz, H-3'), 3.55 (2H, s, H-1''), 3.01 (2H, d, *J* = 11.0 Hz, *H-3a & *H-4a), 2.59 – 2.46 (1H, m, H-1), 2.16 – 1.84 (6H, m, *H-3b & *H-4b & H-2 & H-5); **¹³C NMR (75 MHz, CDCl₃)**; δ 173.7 (C=O), 160.5 (C-1'), 138.3 (C-2''), 136.2 (C-2'), 129.2 (C-3'' & C-7''), 128.4 (C-4'' & C-6''), 127.2 (C-5''), 113.7 (C-3'), 63.3 (C-1''), 53.1 (C-3 & C-4), 43.1 (C-1), 28.5 (C-2 & C-5); **HRMS *m/z* (ESI)** (C₁₆H₁₉N₃OS) 302.1362 ([M + H]⁺ requires 302.1322). *Assignments are interchangeable.

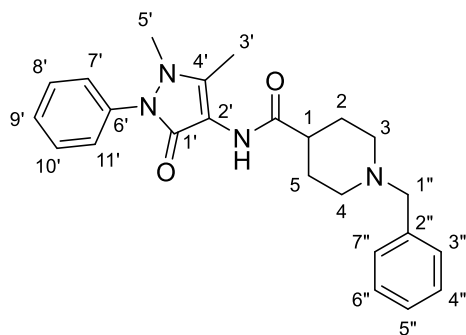
2.5.1.9.6. 1-Benzyl-N-(3,4,5-trimethoxyphenethyl)piperidine-4-carboxamide **24**



24

(Yield 93%); Light yellow solid; **R_f** 0.56 (9:1 dichloromethane: methanol); **mp** 119 - 121 °C; **v_{max} (neat)/cm⁻¹** 3327 (N-H str, m), 2926 (C-H str, m), 1635 (C=O str, s), 1589 (C=C str, m), 1547 (N-H bend, s), 1509 (m), 1454 (C-C str, m), 1435 (m), 1324 (C-H bend, m), 1245 (C-N str, s), 1128 (vs), 999 (s), 817 (m), 714 (C-H "oop", s), 676 (C-H "oop", s); **¹H NMR (300 MHz, CDCl₃)**; δ 7.32 – 7.20 (5H, m, ArH's), 6.38 (2H, s, ArH's), 5.69 (1H, s, 1H, NH), 3.82 (6H, s, OCH₃), 3.81 (3H, s, OCH₃), 3.53 – 3.44 (4H, m, H-1'' & H-1'), 2.91 (2H, d, *J* = 11.6 Hz, *H-3a & *H-4a), 2.73 (2H, t, *J* = 7.0 Hz, H-2'), 2.15 – 1.91 (3H, m, H-1 & *H-3b & *H-4b), 1.85 – 1.63 (4H, m, H-2 & H-5); **¹³C NMR (75 MHz, CDCl₃)**; δ 175.0 (C=O), 153.3 (C-5' C-7'), 137.7 (C-2''), 136.6 (C-6'), 134.7 (C-3'), 129.2 (C-3'' & C-7''), 128.3 (C-4'' & C-6''), 127.3 (C-5''), 105.6 (C-4' & C-8'), 63.1 (C-1''), 60.9 (OCH₃), 56.2 (OCH₃), 52.9 (C-3 & C-4), 43.1 (C-1), 40.5 (C-1'), 36.1 (C-2'), 28.8 (C-2 & C-5); **HRMS *m/z* (ESI)** (C₂₄H₃₂N₂O₄) 413.2458 ([M + H]⁺ requires 413.2453). *Assignments are interchangeable.

2.5.1.9.7. 1-Benzyl-N-(1-methyl-3-oxo-2-phenyl-2,3-dihydro-1H-pyrazol-4-yl) piperidine-4-carboxamide **25**

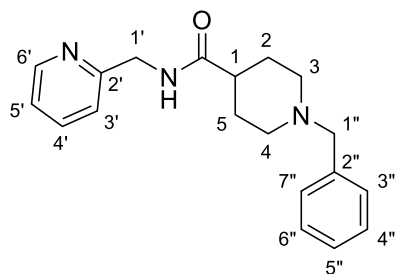


25

(Yield 34%); Off-white crystalline solid; R_f 0.33 (9:1 dichloromethane: methanol); **mp** 235 - 236 °C; ν_{\max} (**neat**)/ cm^{-1} 3228 (NH str, m), 3185 (m), 2925 (C-H str, m), 1684 (C=O str, m), 1612 (C=O str, s), 1587 (N-H bend, m), 1451 (C-C str, m), 1296 (C-N str, s), 1195 (m), 1109 (C-N str, m), 957 (m), 746 (C-H "oop", s), 692 (C-H "oop", s); $^1\text{H NMR}$ (**300 MHz, CDCl₃**); δ 8.33 (1H, s, NH), 7.49 – 7.19 (10H, m, ArH's), 3.51 (2H, s, H-1''), 3.04 (3H, d, $J = 0.8$ Hz, H-5'), 2.90

(2H, d, $J = 11.0$ Hz, *H-3a & *H-4a), 2.33 (1H, dt, $J = 14.4, 7.3$ Hz, H-1), 2.19 (3H, s, H-3'), 2.09 – 1.92 (2H, m, *H-3b & *H-4), 1.90 – 1.77 (4H, m, H-2 & H-5); $^{13}\text{C NMR}$ (**75 MHz, CDCl₃**); δ 174.7 (C=O), 161.9 (C-1'), 149.7 (C-6'), 138.0 (C-2''), 134.7 (C-4'), 129.4 (C-3'' & C-7''), 129.3 (C-8' & C-10'), 128.3 (C-4'' & C-6''), 127.2 (C-5''), 127.1 (C-9'), 124.3 (C-7' & C-11'), 109.0 (C-2'), 63.1 (C-1''), 52.8 (C-3 & C-4), 42.6 (C-1), 36.3 (C-5'), 28.8 (C-2 & C-5), 12.7 (C-3'); **HRMS m/z (ESI)** ($\text{C}_{24}\text{H}_{28}\text{N}_4\text{O}_2$) 405.2292 ([M + H]⁺ requires 405.2285). *Assignments are interchangeable.

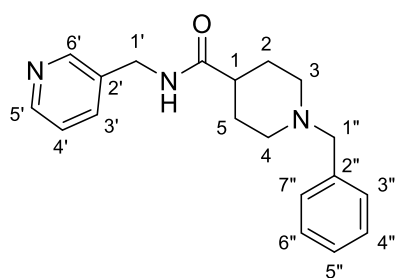
2.5.1.9.8. 1-Benzyl-N-(pyridine-2-ylmethyl) piperidine-4-carboxamide **26**



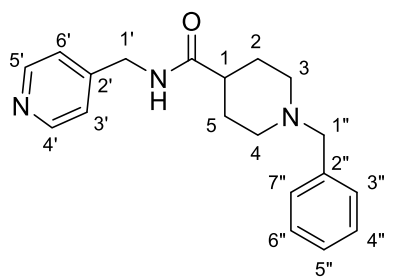
26

(Yield 77%); Yellow viscous oil; R_f 0.33 (9:1 dichloromethane: methanol); ν_{\max} (**neat**)/ cm^{-1} 3343 (N-H str, m), 2940 (C-H str, m), 1639 (C=O str, s), 1592 (C-N bend, m), 1537 (N-H bend, s), 1429 (C-C str, m), 1295 (C-O str, m), 1214 (m), 1133 (C-N str, m), 993 (m), 732 (C-H "oop", m); $^1\text{H NMR}$ (**300 MHz, CDCl₃**); δ 8.50 (1H, d, $J = 4.7$ Hz, ArH), 7.67 – 7.59 (1H, m, ArH), 7.36 – 7.13 (7H, m, ArH's), 6.97 (1H, s, NH), 4.53 (2H, d, $J = 4.8$ Hz, H-1'), 3.53 (2H, s, H-1''),

2.96 (2H, d, $J = 11.6$ Hz, *H-3a & H-4a), 2.30 – 2.16 (1H, m, H-1), 2.07 (2H, m, *H-3b & *H-4b), 1.96 – 1.74 (4H, m, H-2 & H-5); $^{13}\text{C NMR}$ (**75 MHz, CDCl₃**); δ 175.1 (C=O), 156.5 (C-2'), 149.0 (C-6'), 137.7 (C-2''), 136.9 (C-4'), 129.3 (C-3'' & C-7''), 128.4 (C-4'' & C-6''), 127.3 (C-5''), 122.4 (C-3'), 122.1 (C-5'), 63.1 (C-1''), 53.0 (C-3 & C-4), 44.3 (C-1'), 43.0 (C-1), 28.7 (C-2 & C-5); **HRMS m/z (ESI)** ($\text{C}_{19}\text{H}_{23}\text{N}_3\text{O}$) 310.1939 ([M + H]⁺ requires 310.1914). *Assignments are interchangeable.

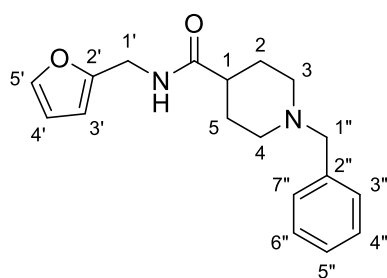
2.5.1.9.9. 1-Benzyl-N-(pyridine-3-ylmethyl) piperidine-4-carboxamide **27**

27

(Yield 59%); Yellow viscous oil; R_f 0.23 (9:1 dichloromethane:methanol); ν_{\max} (neat)/ cm^{-1} 3312 (N-H str, m), 2947 (C-H str, m), 2793 (C-H str, m), 1635 (C=O str, s), 1533 (N-H bend, s), 1430 (C-C str, m), 1296 (C-N str, m), 1218 (m), 1132 (m), 1020 (m), 978 (m), 704 (C-H "oop", s), 657 (C-H "oop", s); $^1\text{H NMR}$ (300 MHz, CDCl_3); δ 8.46 (1H, s, ArH), 8.45 (1H, s, ArH), 7.57 (1H, d, $J = 7.8$ Hz, ArH), 7.32 – 7.18 (6H, m, ArH's), 6.45 (1H, s, NH), 4.40 (2H, d, $J = 5.9$ Hz, H-1'), 3.49 (2H, s, H-1''), 2.92 (2H, d, $J = 11.7$ Hz, *H-3a & *H-4a), 2.22 – 2.09 (1H, m, H-1), 2.00 (2H, td, $J = 11.1, 3.5$ Hz, *H-3b & *H-4b), 1.87 – 1.69 (4H, m, H-2); $^{13}\text{C NMR}$ (75 MHz, CDCl_3); δ 175.3 (C=O), 149.1 (C-6'), 148.8 (C-5'), 137.9 (C-2''), 135.6 (C-2'), 134.4 (C-3'), 129.2 (C-3'' & C-7''), 128.3 (C-4'' & C-6''), 127.2 (C-5''), 123.7 (C-4'), 63.1 (C-1''), 53.0 (C-3 & C-4), 43.1 (C-1), 40.8 (C-1'), 28.8 (C-2 & C-5); **HRMS m/z (ESI)** ($\text{C}_{19}\text{H}_{23}\text{N}_3\text{O}$) 310.1939 ($[\text{M} + \text{H}]^+$ requires 310.1914). *Assignments are interchangeable.

 2.5.1.9.10. 1-Benzyl-N-(pyridine-4-ylmethyl) piperidine-4-carboxamide **28**

28

(Yield 77%); Yellow viscous oil; R_f 0.33 (9:1 dichloromethane:methanol); ν_{\max} (neat)/ cm^{-1} 3290 (N-H str, m), 2917 (C-H str, m), 1638 (C=O str, s), 1542 (N-H bend, s), 1428 (C-C str, m), 1374 (C-H bend, m), 1302 (m), 1073 (m), 990 (m), 795 (C-H "oop", m), 736 (C-H "oop", m), 693 (C-H "oop", s); $^1\text{H NMR}$ (300 MHz, CDCl_3); δ 8.48 (2H, d, $J = 4.8$ Hz, H-4' & H-5'), 7.35 – 7.20 (5H, m, ArH's), 7.12 (2H, d, $J = 5.0$ Hz, H-3' & H-6'), 6.48 (1H, s, NH), 4.41 (2H, d, $J = 5.9$ Hz, H-1'), 3.52 (2H, s, H-1''), 2.95 (2H, d, $J = 11.2$ Hz, *H-3a & H-4a), 2.21 (1H, m, H-1), 2.04 (2H, td, $J = 10.8, 2.6$ Hz, *H-3b & *H-4b), 1.90 – 1.73 (4H, m, H-2 & H-5); $^{13}\text{C NMR}$ (75 MHz, CDCl_3); δ 175.4 (C=O), 150.0 (C-4' & C-5'), 147.8 (C-2'), 137.7 (C-2''), 129.3 (C-3'' & C-7''), 128.4 (C-4'' & C-6''), 127.3 (C-5''), 122.3 (C-3' & C-6'), 63.1 (C-1''), 52.9 (C-3 & C-4), 43.0 (C-1), 42.2 (C-1'), 28.8 (C-2 & C-5); **HRMS m/z (ESI)** ($\text{C}_{19}\text{H}_{23}\text{N}_3\text{O}$) 310.1939 ($[\text{M} + \text{H}]^+$ requires 310.1914). *Assignments are interchangeable.

2.5.1.9.11. 1-Benzyl-N-(furan-2-ylmethyl) piperidine-4-carboxamide **29**

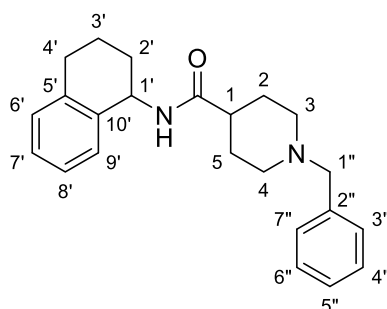


29

(Yield 97%); Off-white crystalline solid; R_f 0.46 (9:1 dichloromethane: methanol); **mp** 110 °C; ν_{\max} (neat)/ cm^{-1} 3308 (N-H str, m), 2939 (C-H str, m), 2922 (C-H str, m), 1639 (C=O str, s), 1535 (N-H bend, s), 1450 (C-C str, m), 1256 (C-N str, m), 1143 (s), 1109 (C-N str, m), 1076 (m), 1011 (s), 911 (C=C-H str, s), 822 (C=C-H str, m), 749 (C-H "oop", s), 697 (C-H "oop", s); $^1\text{H NMR}$ (300 MHz, CDCl_3); δ 7.36 – 7.20 (6H, m, ArH's & H-5'), 6.30 (1H, dd, $J = 3.1, 1.9$

Hz, H-4'), 6.19 (1H, d, $J = 2.9$ Hz, H-3'), 6.01 (1H, s, NH), 4.41 (2H, d, $J = 5.4$ Hz, H-1'), 3.51 (2H, s, H-1''), 2.94 (2H, d, $J = 11.7$ Hz, *H-3a & *H-4a), 2.20 – 1.95 (3H, m, H-1 & *H-3b & *H-4b), 1.89 – 1.68 (4H, m, H-2 & H-5); $^{13}\text{C NMR}$ (75 MHz, CDCl_3); δ 174.8 (C=O), 151.4 (C-2'), 142.2 (C-5'), 137.9 (C-2''), 129.3 (C-3'' & C-7''), 128.3 (C-4'' & C-6''), 127.3 (C-5''), 110.5 (C-4'), 107.5 (C-3'), 63.1 (C-1''), 53.0 (C-3 & C-4), 43.0 (C-1), 36.5 (C-1'), 28.8 (C-2 & C-5); **HRMS m/z (ESI)** ($\text{C}_{18}\text{H}_{22}\text{N}_2\text{O}_2$) 299.1740 ($[\text{M} + \text{H}]^+$ requires 299.1754). * Assignments are interchangeable.

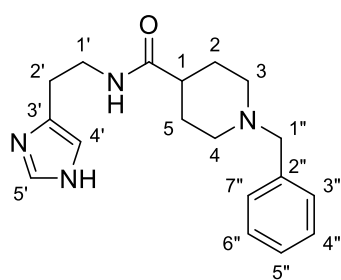
2.5.1.9.12. 1-Benzyl-N-(1,2,3,4-tetrahydro-naphthalen-1-yl) piperidine-4-carboxamide **30**



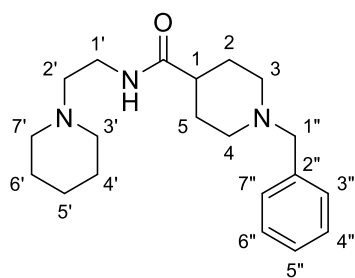
30

(Yield 53%); Pink crystalline solid; R_f 0.56 (9:1 dichloromethane: methanol); **mp** 135-136 °C; ν_{\max} (neat)/ cm^{-1} 3256 (N-H str, m), 2929 (C-H str, m), 1637 (C=O str, s), 1539 (N-H bend, s), 1446 (C-C str, m), 1223 (C-N str, m), 1119 (m), 963 (m), 737 (C-H "oop", s), 695 (C-H "oop", m); $^1\text{H NMR}$ (300 MHz, CDCl_3); δ 7.37 – 7.04 (9H, m, ArH's), 5.80 (1H, d, $J = 8.3$ Hz, NH), 5.22 – 5.12 (1H, m, H-1'), 3.52 (2H, s, H-1''), 2.95 (2H, d, $J = 11.6$ Hz, *H-3a & *H-4a), 2.85-2.68 (2H, m, H-4'), 2.19 – 1.96 (3H, m, H-1 & *H-3b & *H-4b), 1.92

– 1.71 (8H, m, H-2 & H-5 & H-2' & H-3'); $^{13}\text{C NMR}$ (75 MHz, CDCl_3); δ 174.3 (C=O), 137.7 (C-2''), 136.9 (C-5' & C-10'), 129.3 (C-3'' & C-7''), 128.6 (C-9'), 128.4 (C-4'' & C-6''), 127.3 (C-7' & C-8'), 127.2 (C-5''), 126.4 (C-6'), 63.2 (C-1''), 53.0 (C-3 & C-4), 47.2 (C-1'), 43.3 (C-1), 30.3 (C-2'), 29.3 (C-4'), 28.9 (C-2 & C-5), 20.1 (C-3'); **HRMS m/z (ESI)** ($\text{C}_{23}\text{H}_{28}\text{N}_2\text{O}$) 349.2260 ($[\text{M} + \text{H}]^+$ requires 349.2274). *Assignments are interchangeable.

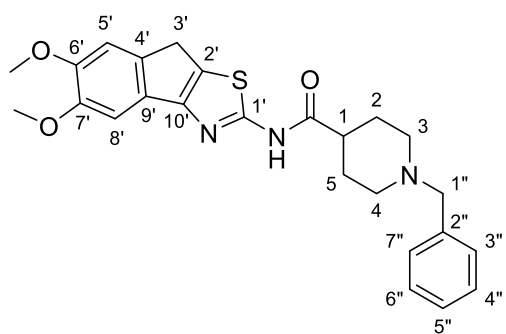
2.5.1.9.13. *N*-[2-(1*H*-imidazol-4-yl)ethyl]-1-benzylpiperidine-4-carboxamide **31**

31

(Yield 38%); Yellow viscous oil; R_f 0.13 (9:1 dichloromethane:methanol); ν_{\max} (neat)/ cm^{-1} 3246 (N-H str, m), 3084 (N-H str, m), 2938 (C-H str, m), 1632 (C=O str, s), 1555 (N-H bend, s), 1442 (C-C str, m), 1336 (C-H bend, m), 1226 (C-N str, m), 1104 (m), 931 (C=C-H str, m), 801 (C-H "oop", m), 728 (C-H "oop", s), 698 (C-H "oop", s); $^1\text{H NMR}$ (300 MHz, CDCl_3); δ 9.74 (1H, s, imidazole NH), 7.56 (1H, s, H-5'), 7.32 – 7.18 (5H, m, ArH's), 6.95 (1H, t, $J = 5.4$ Hz, NH), 6.77 (1H, s, H-4'), 3.53 – 3.44 (m, 4H, H-1' & H-1'), 2.90 (d, 2H, $J = 11.4$ Hz, *H-3a & *H-4a), 2.78 (2H, t, $J = 6.5$ Hz, H-2'), 2.17 – 2.04 (1H, m, H-1), 1.97 (td, 2H, $J = 11.1, 3.6$ Hz, *H-3b & *H-4b), 1.81 – 1.64 (4H, m, H-2 & H-5); $^{13}\text{C NMR}$ (75 MHz, CDCl_3); δ 175.7 (C=O), 138.0 (C-2''), 135.8 (C-5'), 134.9 (C-3'), 129.3 (C-3'' & C-7''), 128.3 (C-4'' & C-6''), 127.2 (C-5''), 116.4 (C-4'), 63.2 (C-1''), 53.1 (C-3 & C-4), 43.2 (C-1), 39.4 (C-1'), 28.9 (C-2 & C-5), 26.8 (C-2'); **HRMS m/z (ESI)** ($\text{C}_{18}\text{H}_{24}\text{N}_4\text{O}$) 313.2023 ([M + H]⁺ requires 313.2023). *Assignments are interchangeable.

 2.5.1.9.14. 1-Benzyl-*N*-(2-(piperidin-1-yl)ethyl)piperidine-4-carboxamide **32**

32

(Yield 59%); Yellow viscous oil; R_f 0.24 (9:1 dichloromethane:methanol); ν_{\max} (neat)/ cm^{-1} 3294 (N-H str, m), 2933 (C-H str, m), 2770 (C-H str, m), 1637 (C=O str, s), 1551 (N-H bend, s), 1443 (C-C str, m), 1300 (C-H bend, m), 1126 (m), 1038 (m), 785 (C-H "oop", m), 726 (C-H "oop", s), 687 (C-H "oop", s); $^1\text{H NMR}$ (300 MHz, CDCl_3); δ 7.33 – 7.21 (5H, m, ArH's), 6.46 (1H, s, NH), 3.50 (2H, s, H-1''), 3.35 (2H, dd, $J = 11.2, 5.6$ Hz, H-1'), 2.93 (2H, d, $J = 11.6$ Hz, *H-3a & *H-4a), 2.48 (6H, m, H-2' & H-3' & H-7'), 2.12 (1H, m H-1), 2.00 (2H, td, $J = 11.4, 2.8$ Hz, *H-3b & *H-4b), 1.88 – 1.70 (4H, m, H-2 & H-5), 1.61 (4H, dt, $J = 10.7, 5.5$ Hz, H-4' & H-6'), 1.51 – 1.41 (2H, m, H-5'); $^{13}\text{C NMR}$ (75 MHz, CDCl_3); δ 175.3 (C=O), 138.4 (C-2''), 129.2 (C-3'' & C-7''), 128.3 (C-4'' & C-6''), 127.1 (C-5''), 63.3 (C-1''), 57.2 (C-2'), 54.3 (C-3' & C-7'), 53.3 (C-3 & C-4), 43.4 (C-1), 35.7 (C-1'), 29.0 (C-2 & C-5), 25.7 (C-4' & C-6'), 24.8 (C-5'); **HRMS m/z (ESI)** ($\text{C}_{20}\text{H}_{31}\text{N}_3\text{O}$) 330.2541 ([M + H]⁺ requires 330.2540). *Assignments are interchangeable.

2.5.1.9.15. 1-Benzyl-N-(5,6-dimethoxy-8H-indeno[1,2-d]thiazol-2-yl)piperidine-4-carboxamide **33**



33

A mixture of 5,6-dimethoxy-8H-indeno[1,2-d]thiazole-2-amine **18** (0.25 g, 1.00 mmol, 1 eq.), (1-benzylpiperidin-4-yl)(1H-imidazol-1-yl) methanone **12** (0.30 g, 1.11 mmol, 1.1 eq.) and sodium hydride (0.08 g, 2.03 mmol, 2 eq., 60% in oil) in anhydrous tetrahydrofuran (15 mL) was refluxed overnight after which time the reaction mixture was left to cool down to room temperature. The reaction was quenched with the slow addition of a saturated

aqueous solution of sodium sulfate (1 mL). A solution of 3M aqueous sodium hydroxide (10 mL) was added and left to stir for 5 min. The organic layer was separated and the aqueous layer was washed with dichloromethane (2 x 30mL). The organic layers were combined, washed with distilled water (30 mL), dried (Na₂SO₄), filtered and evaporated *in vacuo*. The product was purified by column chromatography. (Yield 12%); Brown solid; **R_f** 0.55 (9:1 dichloromethane: methanol); **mp** 218 °C (decomp.); **v_{max} (neat)/cm⁻¹** 3420 (N-H str, m), 2932 (C-H str, m), 1687 (C=O str, m), 1536 (N-H bend, s), 1452 (C-C str, m), 1383 (C-H bend, s), 1272 (C-N str, s), 1208 (s), 1142 (s), 1070 (s), 989 (m), 846 (m), 738 (C-H "oop", s), 697 (C-H "oop", s); **¹H NMR (300 MHz, CDCl₃)**; δ 10.29 (1H, s, NH), 7.33 – 7.19 (5H, m, ArH's), 7.20 (1H, s, ArH), 7.13 (1H, s, ArH), 3.95 (3H, s, OCH₃), 3.91 (3H, s, OCH₃), 3.74 (2H, s, H-3'), 3.35 (2H, s, H-1''), 2.79 (2H, d, *J* = 11.3 Hz, *H-3a & *H-4a), 2.34 – 2.20 (1H, m, H-1), 1.89 – 1.56 (6H, m, *H-3b & *H-4b & H-2 & H-5); **¹³C NMR (75 MHz, CDCl₃)**; δ 172.9 (C=O), 162.3 (C-1'), 155.3 (C-6'), 148.8 (C-10'), 147.7 (C-7'), 138.3 (C-9'), 138.0 (C-2''), 129.9 (C-4'), 129.2 (C-3'' & C-7''), 129.1 (C-2'), 128.4 (C-4'' & C-6''), 127.2 (C-5''), 109.5 (C-5'), 102.4 (C-8'), 63.1 (C-1''), 56.5 (OCH₃), 56.4 (OCH₃), 52.5 (C-3 & C-4), 42.9 (C-1), 32.5 (C-3'), 28.5 (C-2 & C-5); **HRMS *m/z* (ESI)** (C₂₅H₂₇N₃O₃S) 450.1859 ([M + H]⁺ requires 450.1846). *Assignments are interchangeable.

2.5.2. Bioactivity screening

Prior to screening, all compounds were dissolved in dimethyl sulfoxide due to the compounds being insoluble in water at high concentrations (10 mM). The final concentration of dimethyl sulfoxide in the assay were below 1%.

2.5.2.1. Cholinesterase inhibitory activity

Cholinesterase inhibitory activity for *EeAChE* and *eqBuChE* were determined using the 5,5-dithiobis-2-nitrobenzoic acid (DTNB) assay as described by Ellman [17] and modified by Eldeen and co-workers [18]. Three buffers were prepared: Buffer A – 50 mM Tris-hydrochloride (pH 8); Buffer B - 50 mM Tris-

hydrochloride (pH 8), containing 0.1% bovine serum albumin; Buffer C - 50 mM Tris-hydrochloride (pH 8), fortified with 0.1 M sodium chloride and 0.02 M magnesium chloride. Into 96-well plates were pipetted: 25 mL acetylthiocholine iodide (15 mM in distilled water), 125 mL DTNB (3 mM in buffer C), 50 mL buffer B and either 25 mL buffer A (negative control), galantamine (positive control at 1 μ M) or compounds **1**, **19** - **33**. Absorbance was measured at 405 nm (four times) to account for baseline interference. An aliquot of 25 mL *EeAChE* (0.2 U/mL in buffer A) was pipetted into the plates and the absorbance measured every 45 s for fifteen cycles. *EeAChE* inhibition (%) was determined as the rate of the reaction (correcting for spontaneous colour changes) relative to the negative control. In the case of the *eqBuChE* inhibitory activity assay, *EeAChE* was replaced with *eqBuChE* (0.2 U/mL in buffer A) as well as acetylcholine iodide with butyrylcholine iodide (15 mM in distilled water) and the assay was incubated for 2 h instead of 5 min.

2.5.2.2. Cytotoxicity screening

Cytotoxicity was assessed using the SRB staining assay on the SH-SY5Y neuroblastoma cell line as described by Vichai and Kirtikara with minor modifications [19]. Although the SH-SY5Y cell line is cancerous in nature, it does present as a model of a neurological cellular environment. The SH-SY5Y cell line was cultured in DMEM/Ham's F12 nutrient, in a 1 to 1 ratio, medium supplemented with 10% foetal calf serum (FCS) in 75 mL flasks at 37 °C and 5% CO₂ in a humidified incubator. Culture flasks with confluent cells were rinsed with phosphate buffered saline and harvested using TrypLe™ Express to detach the cells. Detached cells were centrifuged (200 x *g*, 5 min), counted using the trypan blue exclusion assay (0.1%), and diluted to 1 x 10⁵ cells/ μ L in 10% FCS-fortified medium. The cell suspension (100 μ L) was seeded into sterile, clear 96-well plates, and incubated overnight to allow the cells to attach. Blank wells contained 200 μ L FCS (5%)-fortified media without cells to account for background noise and sterility. Attached cells were exposed to 100 μ L medium (negative control), compounds **1**, **19** - **33** (0.01 - 100 μ M) or saponin (1%; positive control) prepared in FCS negative medium for 72 h at 37 °C and 5% CO₂ in a humidified incubator. Cells were fixed in the wells by adding 50 μ L trichloroacetic acid (50%) and left overnight at 4 °C. Plates containing the fixed cells were washed three times with tap water and stained using 100 μ L SRB solution (0.057% in 1% acetic acid) for 30 min at room temperature in the dark. Stained cells were washed four times with 150 μ L acetic acid (1%) and air-dried. The bound dye was eluted using 200 μ L Tris-buffer (10 mM, pH 10.5) and the absorbance measured at 510 nm (reference 630 nm) using a ELx 800 microplate plate reader (Bio-Tek Instruments, Inc.). The blank value was subtracted from all the other values and the cell density was expressed relative to the negative control as a percentage.

2.5.2.3. Statistics

Assays were performed as three intra- as well as three inter-replicates. Statistical analyses were performed using Graph-Pad Prism 5.0 (GraphPad). The IC₅₀ values were determined using non-linear regression analysis (variable slope).

2.6. ACKNOWLEDGEMENTS

This work was supported by the National Research Foundation (NRF) of South Africa (Thuthuka grant number 87893), the University of Pretoria (University, Science Faculty Research Councils and Research and Development Program) and the Council for Scientific and Industrial Research (CSIR), South Africa. Opinions expressed in this publication and the conclusions arrived at, are those of the authors, and are not necessarily attributed to the NRF. The authors would like to gratefully acknowledge Ms Madelien Wooding (University of Pretoria) for LC-MS services.

2.7. CONFLICT OF INTEREST

The authors declare no conflict of interest.

2.8. APPENDIX A. SUPPLEMENTARY INFORMATION

Appendix A can be found as a separate document on the CD.

2.9. REFERENCES

- [1] H. Sugimoto, Y. Yamanishi, Y. Iimura, Y. Kawakami, Donepezil hydrochloride (E2020) and other acetylcholinesterase inhibitors, *Curr. Med. Chem.*, 7 (2000) 303-339.
- [2] H. Sugimoto, Y. Tsuchiya, H. Sugumi, K. Higurashi, N. Karibe, Y. Iimura, A. Sasaki, Y. Kawakami, T. Nakamura, Novel piperidine derivatives. Synthesis and anti-acetylcholinesterase activity of 1-benzyl-4-[2-(*N*-benzoylamino)ethyl]piperidine derivatives, *J. Med. Chem.*, 33 (1990) 1880-1887.
- [3] Y. Kawakami, A. Inoue, T. Kawai, M. Wakita, H. Sugimoto, A.J. Hopfinger, The rationale for E2020 as a potent acetylcholinesterase inhibitor, *Bioorg. Med. Chem.*, 4 (1996) 1429-1446.
- [4] H. Sugimoto, Y. Iimura, Y. Yamanishi, K. Yamatsu, Synthesis and structure-activity relationships of acetylcholinesterase inhibitors: 1-Benzyl-4-[(5,6-dimethoxy-1-oxoindan-2-yl)methyl]piperidine hydrochloride and related compounds, *J. Med. Chem.*, 38 (1995) 4821-4829.
- [5] I. Bolea, J. Juarez-Jimenez, C. de Los Rios, M. Chioua, R. Pouplana, F.J. Luque, M. Unzeta, J. Marco-Contelles, A. Samadi, Synthesis, biological evaluation, and molecular modeling of donepezil and *N*-[(5-(benzyloxy)-1-methyl-1*H*-indol-2-yl)methyl]-*N*-methylprop-2-yn-1-amine hybrids as new multipotent cholinesterase/monoamine oxidase inhibitors for the treatment of Alzheimer's disease, *J. Med. Chem.*, 54 (2011) 8251-8270.
- [6] A. Samadi, M. de la Fuente Revenga, C. Perez, I. Iriepa, I. Moraleda, M.I. Rodriguez-Franco, J. Marco-Contelles, Synthesis, pharmacological assessment, and molecular modeling of 6-chloropyridonepezils: new dual AChE inhibitors as potential drugs for the treatment of Alzheimer's disease, *Eur. J. Med. Chem.*, 67 (2013) 64-74.

- [7] Z. Luo, J. Sheng, Y. Sun, C. Lu, J. Yan, A. Liu, H.B. Luo, L. Huang, X. Li, Synthesis and evaluation of multi-target-directed ligands against Alzheimer's disease based on the fusion of donepezil and ebselen, *J. Med. Chem.*, 56 (2013) 9089-9099.
- [8] L. Piemontese, D. Tomas, A. Hiremathad, V. Capriati, E. Candeias, S.M. Cardoso, S. Chaves, M.A. Santos, Donepezil structure-based hybrids as potential multifunctional anti-Alzheimer's drug candidates, *J. Enzyme Inhib. Med. Chem.*, 33 (2018) 1212-1224.
- [9] H. Dong, C.M. Yuede, C.A. Coughlan, K.M. Murphy, J.G. Csernansky, Effects of donepezil on amyloid- β and synapse density in the Tg2576 mouse model of Alzheimer's disease, *Brain Res.*, 1303 (2009) 169-178.
- [10] D.G. van Greunen, W. Cordier, M. Nell, C. van der Westhuyzen, V. Steenkamp, J.-L. Panayides, D.L. Riley, Targeting Alzheimer's disease by investigating previously unexplored chemical space surrounding the cholinesterase inhibitor donepezil, *Eur. J. Med. Chem.*, 127 (2017) 671-690.
- [11] D. Manetti, L. Di Cesare Mannelli, S. Dei, N. Galeotti, C. Ghelardini, M.N. Romanelli, S. Scapecchi, E. Teodori, A. Pacini, A. Bartolini, F. Gualtieri, Design, synthesis, and preliminary pharmacological evaluation of a set of small molecules that directly activate Gi proteins, *J. Med. Chem.*, 48 (2005) 6491-6503.
- [12] Z.F. Tao, G. Li, Y. Tong, Z. Chen, P. Merta, P. Kovar, H. Zhang, S.H. Rosenberg, H.L. Sham, T.J. Sowin, N.H. Lin, Synthesis and biological evaluation of 4'-(6,7-disubstituted-2,4-dihydro-indeno[1,2-c]pyrazol-3-yl)-biphenyl-4-ol as potent Chk1 inhibitors, *Bioorg. Med. Chem. Lett.*, 17 (2007) 4308-4315.
- [13] S.R. Haadsma-Svensson, K.A. Cleek, D.M. Dinh, J.N. Duncan, C.L. Haber, R.M. Huff, M.E. Lajiness, N.F. Nichols, M.W. Smith, K.A. Svensson, M.J. Zaya, A. Carlsson, C.-H. Lin, Dopamine D3-receptor antagonists. 1. Synthesis and structure-activity relationships of 5,6-dimethoxy-*N*-alkyl- and *N*-alkylaryl-substituted 2-aminoindans, *J. Med. Chem.*, 44 (2001) 4716-4732.
- [14] R. Perrone, F. Berardi, G. Bettoni, V. Tortorella, V. Cuomo, G. Racagni, E. Juliano, A.C. Rovescalli, Monophenolic 2-amino-1-indanone and 2-amino-1-tetralone derivatives: synthesis and assessment of dopaminergic activity, *Eur. J. Med. Chem.*, 22 (1987) 417-419.
- [15] A.I. Vogel, A.R. Tatchell, B.S. Furnis, A.J. Hannaford, P.W.G. Smith, Vogel's textbook of practical organic chemistry (5th Edition), 5th ed., Pearson, 1996.
- [16] B. Morkunas, W.R. Galloway, M. Wright, B.M. Ibbeson, J.T. Hodgkinson, K.M. O'Connell, N. Bartolucci, M. Della Valle, M. Welch, D.R. Spring, Inhibition of the production of the *Pseudomonas aeruginosa* virulence factor pyocyanin in wild-type cells by quorum sensing autoinducer-mimics, *Org. Biomol. Chem.*, 10 (2012) 8452-8464.
- [17] G.L. Ellman, K.D. Courtney, V. Andres, R.M. Featherstone, A new and rapid colorimetric determination of acetylcholinesterase activity, *Biochem. Pharmacol.*, 7 (1961) 88-95.
- [18] I.M. Eldeen, E.E. Elgorashi, J. van Staden, Antibacterial, anti-inflammatory, anti-cholinesterase and mutagenic effects of extracts obtained from some trees used in South African traditional medicine, *J. Ethnopharmacol.*, 102 (2005) 457-464.
- [19] V. Vichai, K. Kirtikara, Sulforhodamine B colorimetric assay for cytotoxicity screening, *Nat. Protoc.*, 1 (2006) 1112-1116.

Chapter 3. Novel 1-(5,6-dimethoxy-8*H*-indeno[1,2-*d*]thiazol-2-yl)urea derivatives as potential dual acetylcholinesterase and glycogen synthase kinase 3 inhibitors for the potential treatment of Alzheimer's disease

Contributions to this chapter

All of the synthesis and compound characterization described in this chapter were performed by Mr DG van Greunen under the supervision of Dr DL Riley and Dr J-L Panayides. The synthetic work was undertaken in the Department of Chemistry at the University of Pretoria. Computational work was performed by Mr CJ van der Westhuizen, whereas the analysis of the results was performed by Mr DG van Greunen. All of the AChE biological assays and statistical analysis described in this chapter were performed by Mr DG van Greunen under the supervision of Prof V Steenkamp and Dr J-L Panayides, with assistance from Dr W Cordier and Ms M Nell. The cytotoxicity assays and statistical analysis performed by Ms M Nell. The biological work was undertaken in the Department of Pharmacology at the University of Pretoria.

Novel 1-(5,6-dimethoxy-8*H*-indeno[1,2-*d*]thiazol-2-yl)urea derivatives as potential dual acetylcholinesterase and glycogen synthase kinase 3 inhibitors for the potential treatment of Alzheimer's disease

Divan G. van Greunen^a, Werner Cordier^b, Margo Nell^b, C. Johan van der Westhuizen^a, Vanessa Steenkamp^b, Jenny-Lee Panayides^c, Darren L. Riley^{a,*}

^a Department of Chemistry, Faculty of Natural and Agricultural Sciences, University of Pretoria, Lynnwood Road, Pretoria, South Africa

^b Department of Pharmacology, Faculty of Health Sciences, University of Pretoria, Bophelo Road, Pretoria, South Africa

^c Pioneering Health Sciences, CSIR Biosciences, Meiring Naudé Road, Pretoria, South Africa

* Corresponding author. E-mail address: darren.riley@up.ac.za (D.L. Riley)

ABSTRACT

A series of thirty-five dual acetylcholinesterase and glycogen synthase kinase 3 inhibitors, as potential agents for the treatment of Alzheimer's disease, were designed and synthesized based upon the skeleton of 1-benzyl-*N*-(5,6-dimethoxy-8*H*-indeno[1,2-*d*]thiazol-2-yl)piperidine-4-carboxamide **4**, a compound synthesized previously, which was shown to possess an IC₅₀ value of 0.41 ± 1.25 μM against acetylcholinesterase (AChE) *in vitro*. The most active analogue, 1-(5,6-dimethoxy-8*H*-indeno[1,2-*d*]thiazol-2-yl)-3-(4-ethoxybenzyl)urea **35** afforded an AChE IC₅₀ value of 12.74 ± 2.33 μM. This compound was however found to be toxic to SH-SY5Y neuroblastoma cells (IC₅₀ of 2.78 ± 1.16 μM). In general, the compounds were found to be relatively cytotoxic.

Key Words

Acetylcholinesterase, Alzheimer's disease, cytotoxicity, glycogen synthase kinase 3, thiazole, urea

3.1. INTRODUCTION

Thiazole is a five-membered heterocyclic compound which possesses both an electron-accepting group (C=N) and an electron donating thiol group. It is considered aromatic due to the delocalization of the sulphur's lone pair electrons, thus completing Hückel's rule for aromaticity [1, 2]. Thiazole derivatives are typically accessed by one of three methods; the Hantzsch synthesis, the Gabriel synthesis or the Cook-Heilborn synthesis [3, 4].

The Hantzsch synthesis involves the condensation of haloketones with thioamides, followed by cyclization. The reaction proceeds with a nucleophilic attack of the sulphur atom of the thioamide on the α -carbon atom of α -haloketone producing an α -thioketone intermediate, followed by dehydration to afford the desired thiazole (**Figure 3.1**) [3, 4].

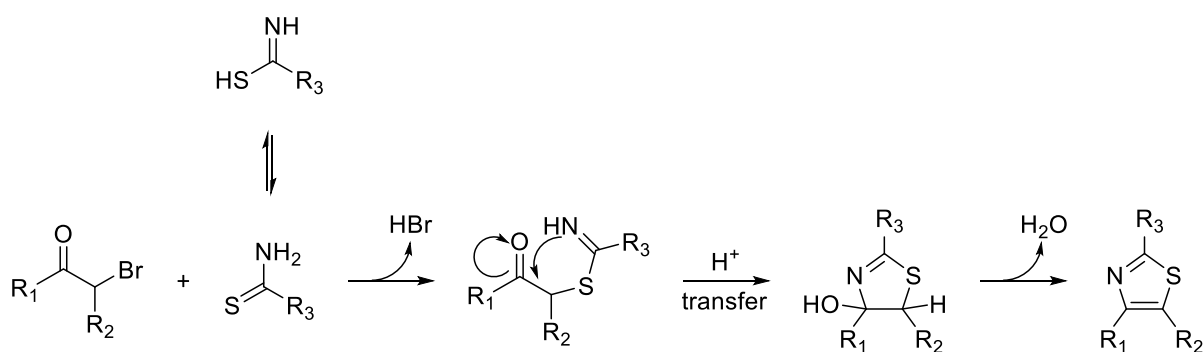


Figure 3.1. Hantzsch synthesis of thiazoles [3, 4].

Another approach, the Gabriel synthesis, is widely used to synthesize alkyl, aryl or alkoxy substituted thiazoles at the 2 or 5 or 2,5 positions. It involves the treatment of α -acylamino-ketones, which can be synthesized from the Dakin-West reaction, with a stoichiometric amount of phosphorous pentasulfide at high temperatures, followed by dehydration to afford the desired thiazole (**Figure 3.2**) [3].

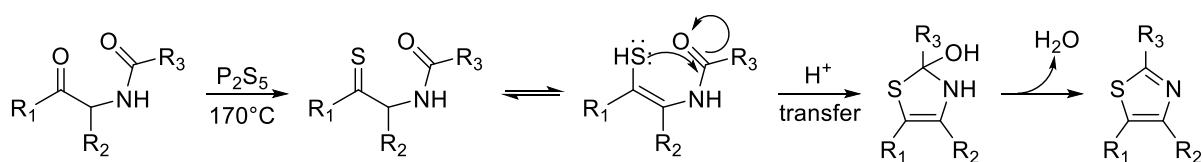


Figure 3.2. Gabriel synthesis of thiazoles [3].

The Cook-Heilborn's approach can be used for the synthesis of substituted aminothiazoles. It involves the reaction of α -aminonitriles with substrates such as: dithioacids, esters, carbonyl sulphide, isothiocyanates or carbon disulphide, forming a thioamide intermediate, followed by cyclisation under mild conditions resulting in the formation of substituted 5-aminothiazoles (**Figure 3.3**) [3].

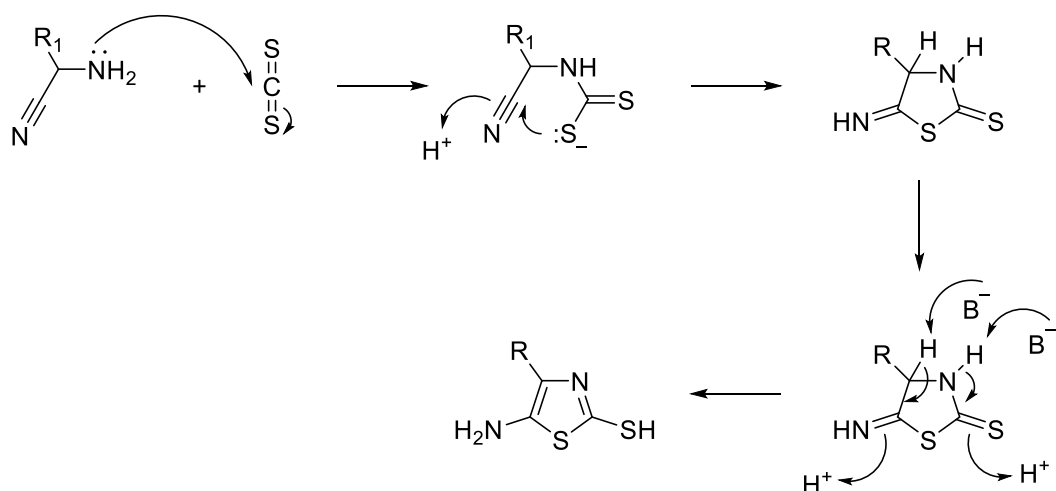


Figure 3.3. Cook-Heilborn synthesis of aminothiazoles [3].

Thiazole derivatives are known to be privileged structures with a wide range of pharmacological activities such as: antimicrobial [5-7], antiviral [8-10], anticancer [11, 12], anticonvulsant [13-15], anti-inflammatory [16-18], antioxidant [19-21], antidiabetic [22-24] and neuroprotective ability [25-27].

The derivatives of tri-substituted thiazole **1** [28], imidazo[1,2-*b*]thiazole **2** [29] and 2-aminothiazole **3** [30] have been reported to possess anti-cholinergic activities due to the ability of the thiazole moiety to i) form H-bonds with the peripheral anionic site (PAS) and catalytic anionic site (CAS) of acetylcholinesterase (AChE) [2, 31, 32] or ii) form π - π stacking interactions with the CAS [30] (**Figure 3.4**).

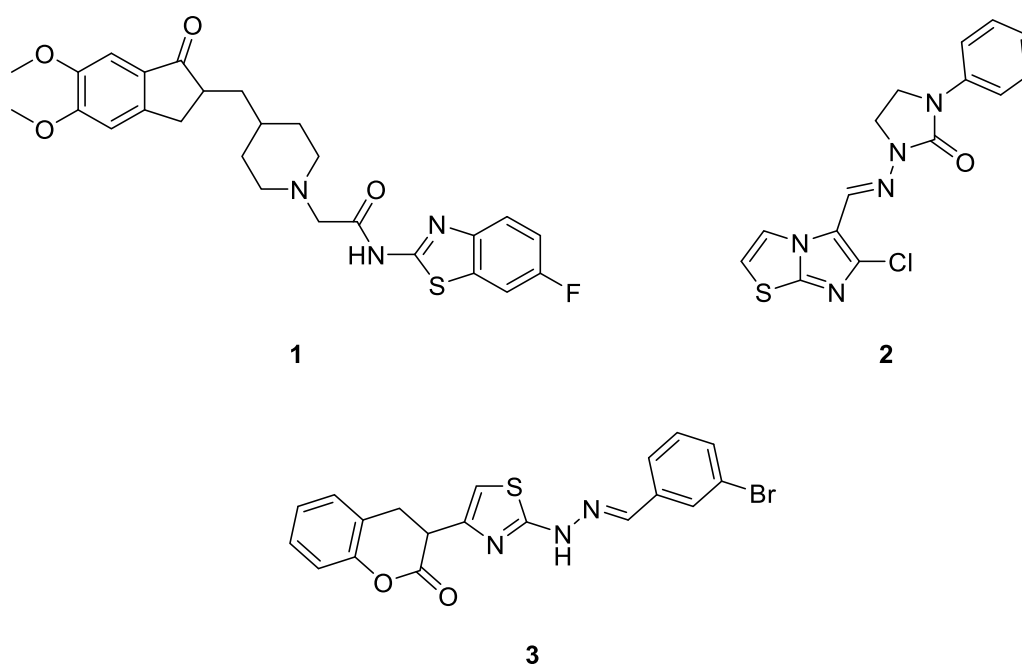


Figure 3.4. Structures of thiazole derivatives with AChE inhibition activity [28-30].

Previously, it was found that the introduction of a 5,6-dimethoxy-8*H*-indeno[1,2-*d*]thiazol-2-amine moiety through an amide coupling to a *N*-benzylpiperidine moiety, afforded an AChE inhibitor 1-benzyl-*N*-(5,6-dimethoxy-8*H*-indeno[1,2-*d*]thiazol-2-yl)piperidine-4-carboxamide **4** (Figure 3.5), also see Chapter 2) with a good inhibitory activity against AChE ($IC_{50} = 0.41 \pm 1.25 \mu\text{M}$). Compound **4** was seen as an attractive lead compound and was selected for further development.

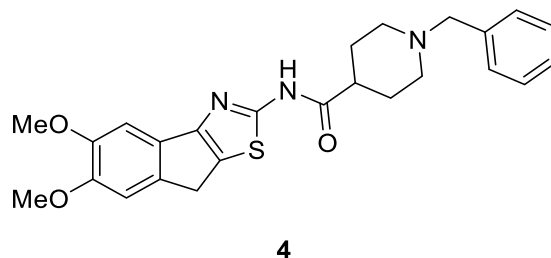


Figure 3.5. AChE inhibitor 1-benzyl-*N*-(5,6-dimethoxy-8*H*-indeno[1,2-*d*]thiazol-2-yl)piperidine-4-carboxamide **4**.

Several research groups have shown that the introduction of urea or amide groups led to an increase in cholinesterase inhibition due to these functionalities' ability to H-bond with a range of amino acid residues in both the PAS and CAS [2, 28, 31-36]. Furthermore, the introduction of a urea moiety linked to a 2-aminothiazole moiety was also shown to afford antioxidant activity in select examples [32, 35].

In the search for new AChE inhibitors, Sonmez and co-workers designed compound **5**, which contains a benzofuran moiety and was found to have an IC_{50} value of $3.85 \mu\text{M}$ against AChE (Figure 3.6) [32]. When using computational studies to rationalise the results obtained, it was found that the compound's thiazole ring played a critical role in the binding capacity to form an H-bond interaction through its nitrogen with Tyr121; in addition, the amidic moiety acted as a H-bond acceptor towards the hydroxyl group of Ser122. The authors also established that the phenyl moiety of compound **5** was directed at the PAS pocket which resulted in π - π -stacking with the phenolic side chain of Tyr84. Also, it was noted that the benzofuran moiety stacked between Tyr334 and Phe331, thereby stabilizing compound **5** at the entrance of the active binding site [32].

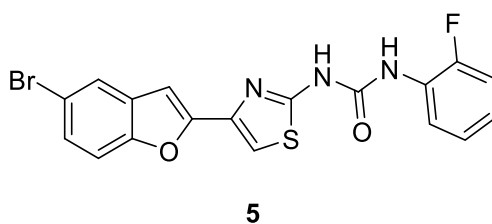


Figure 3.6. Sonmez compound **5** [32].

Interestingly, a literature overview of biologically active molecules containing thiazole moieties, revealed a potent glycogen synthase kinase 3 (GSK-3) inhibitor that had the same thiazole and urea structural features found in compound **5**. The inhibitor, known as AR-A014418 **6** (Figure 3.7) was developed by AstraZeneca and is both a selective and potent inhibitor (IC_{50} 3.85 μ M) of GSK-3 [37]. The compound acts by reducing tau phosphorylation and cell death, both of which have been directly linked to key neuropathological mechanisms associated with Alzheimer's disease [38-40].

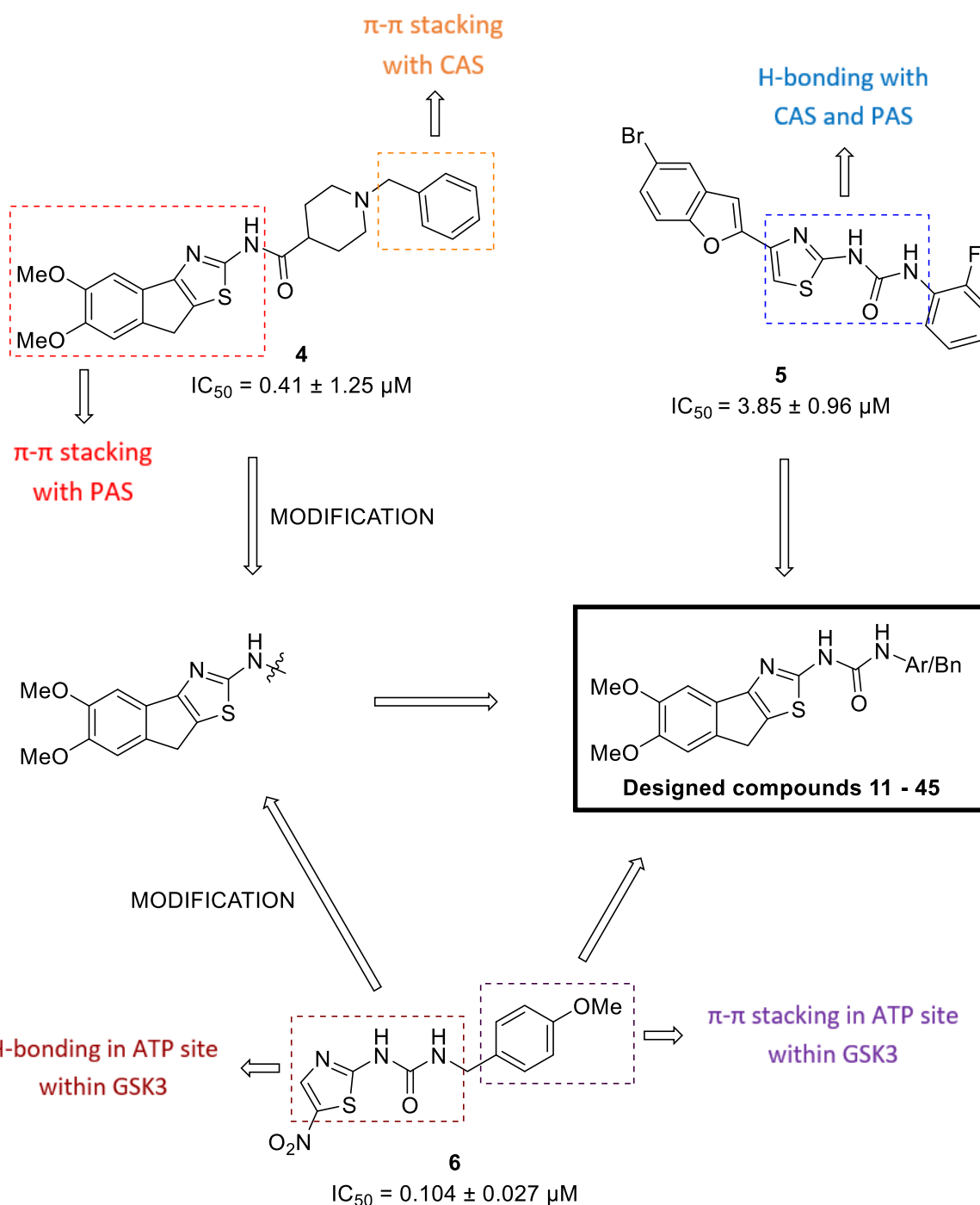


Figure 3.7. Design strategy of the targeted compound **11 - 45**.

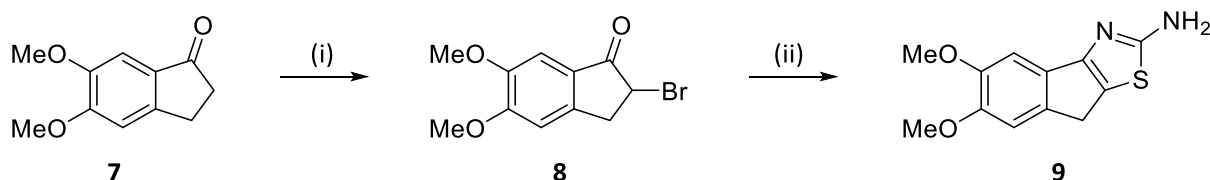
Further studies were conducted including solving the crystal structure of AR-A014418 **6** inside GSK-3 which revealed that the inhibitor binds within the adenosine triphosphate (ATP) site. More specifically, it binds along the hinge region of the ATP pocket in which three hydrogen bond interactions occur with the Val135 residue of the hinge and one of the nitro oxygen atoms occupies the inner part of the ATP pocket. The phenyl group of the inhibitor was also shown to have a stacking interaction with the guanidine group of the Arg141 residue.

These findings prompted the design of new inhibitors based on the 5,6-dimethoxy-8*H*-indeno[1,2-*d*]thiazol-2-amine moiety from the previous study conducted (Chapter 2), wherein the amide linker of **4** was substituted with that of a urea linker. The latter modification was based upon literature precedent which suggests that the urea moiety may afford better H-bonding with the active sites of both AChE and the ATP pocket of GSK-3 (**Figure 3.7**) [32, 35]. It was hypothesized that the 5,6-dimethoxy-8*H*-indeno[1,2-*d*]thiazol-2-amine heterocycle may show strong π - π stacking in the PAS and the aryl/benzyl groups may show moderate to strong π - π stacking in the CAS of AChE, whereas the thiazole moiety may show good H-bonding in the ATP pocket of GSK-3.

In this study, a series of thirty-five novel urea substituted 5,6-dimethoxy-8*H*-indeno[1,2-*d*]thiazol-2-amine derivatives (**11 - 45**) were synthesized and screened as potential inhibitors of AChE. The cytotoxicity of compounds indicating AChE inhibitory activity were also determined.

3.2. CHEMISTRY

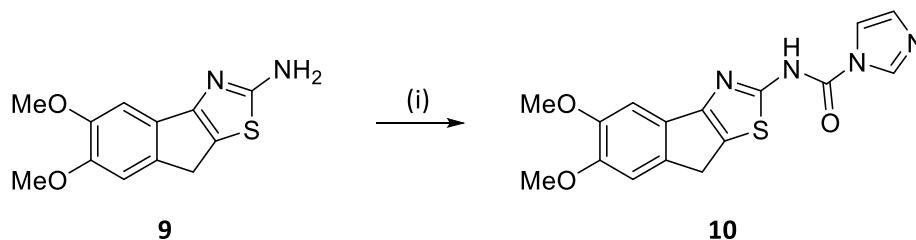
The preparation of the 2-aminothiazole heterocycle **9** was achieved in two steps by the bromination of commercially available 5,6-dimethoxy-1-indanone **7** (**Scheme 3.1**) [41] affording the α -brominated indanone **8**, followed by the Hantzsch-type thiazole synthesis [4] using thiourea, affording the desired heterocycle **9** in 70% across two steps.



Scheme 3.1: (i) 1.05 eq. Br₂, MeOH, rt, 30 min, 84%, (ii) 1 eq. thiourea, 5 eq. 3M aq. NH₃, H₂O, rt - reflux, 12h, 83%.

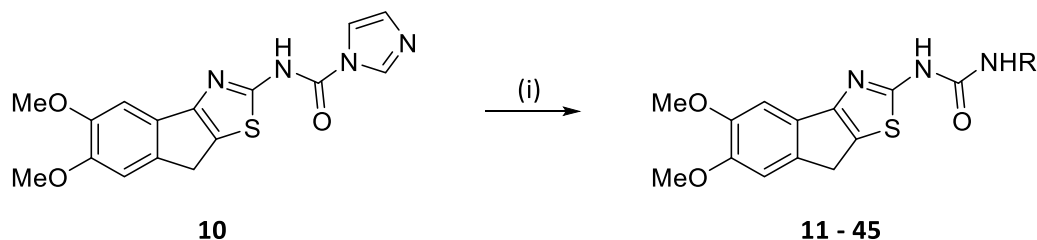
The synthesis of the substituted *N*-(5,6-dimethoxy-8*H*-indeno[1,2-*d*]thiazol-2-yl)-1*H*-imidazol-1-carboxamide **10** (**Scheme 3.2**) was then achieved in one step, where-by the thiazole heterocycle **9** was

left to react with carbonyl diimidazole (CDI) under inert conditions, affording the moisture sensitive intermediate **10** in 97% yield [27].



Scheme 3.2: (i) 1.2 eq. CDI, DCM, reflux, 24 h, 97%.

The urea derivatives **11 - 45** (**Scheme 3.3, Table 3.1**) were obtained through a standard amide coupling between the imidazole derivative **10** and various aryl- and benzyl amines, affording the desired substituted ureas **11 - 45** (**Table 3.1**) in good yields of 66 - 91% [27].



Scheme 3.3: (i) 1.1 eq. RNH₂, ACN, reflux, 20 h, 66 – 91%.

Compound **11** is used as a representative example to describe how the structures were elucidated using NMR, HRMS and IR spectroscopy. ¹H NMR spectroscopy showed the disappearance of one of the distinctive imidazole proton peaks at 7.86 ppm, as well as the appearance of one urea singlet peak (imidazole-NH-CO) integrating for 1H at 9.29 ppm whereas the other urea peak (Ph-NH-CO) could be found as part of a multiplet at 7.25- 7.00 ppm. The carbonyl carbon peak was observed by a shift from 155.98 to 154.00 ppm in the ¹³C NMR spectrum, whereas the distinctive thiazole carbon (N=C-S) peak shifted from 172.70 to 162.84 ppm. The formation of **11** was also supported by the disappearance of the imidazole carbon peaks at 137.98, 137.50 and 121.42 ppm. The formation of **11** was further supported by the appearance of an amide carbonyl peak in the IR spectrum at 1672 cm⁻¹ which is distinctive for an amide carbonyl stretch. Final confirmation was given by the presence of a peak assigned as [M + H]⁺ at 368.0997 in the HRMS, with the [M + H]⁺ value calculated as 368.1063. The remaining compounds in the series were analysed in a similar manner, and the spectral assignments are provided in the experimental section.

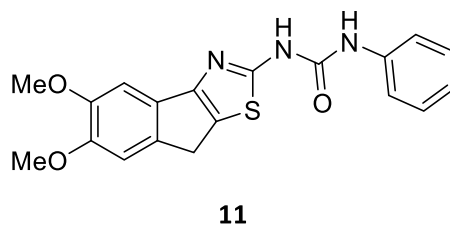


Figure 3.8. Compound **11**.

To support the hypothesis of dual inhibition of AChE and GSK-3, computational chemistry was employed as a predictive tool, where it was possible to dock compounds **4** (Figure 3.7), **11** (Figure 3.8) and **34** (Figure 3.9) into the active site of AChE and the ATP site of GSK-3, in order to predict possible interactions between the ligand and the amino acid residues of these enzymes.

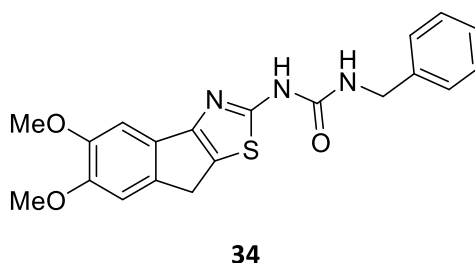


Figure 3.9. Compound **34**.

From the *in silico* results obtained, it was predicted that compound **34** would have a π - π stacking interaction in the PAS between Trp279 and the aryl group of the 5,6-dimethoxy-8H-indeno[1,2-d]thiazol-2-amine moiety of **34**, as well as π - π stacking interactions in the CAS between Trp84 and the aromatic benzyl group of **34** which is similar to the interactions which compound **4** had in the active site of AChE. However, it was predicted that compound **4** would have additional π -cation interactions between the protonated nitrogen of the piperidine moiety of **4** and the phenyl groups of Phe330 and Tyr334. In addition to these interactions, the nitrogen of the piperidine moiety also forms a water bridge between Tyr121 through HOH 1159 as depicted in Figure 3.10.

Although compound **11** does not have a similar π - π stacking interaction between Trp279 and the aryl group of the 5,6-dimethoxy-8H-indeno[1,2-d]thiazol-2-amine moiety of **11**, it has a different π - π stacking interaction between Tyr334 and the thiazole group of the 5,6-dimethoxy-8H-indeno[1,2-d]thiazol-2-amine moiety. It was also predicted that compound **11** would have similar π - π stacking interactions between Trp84 and the phenyl moiety to that of **4**.

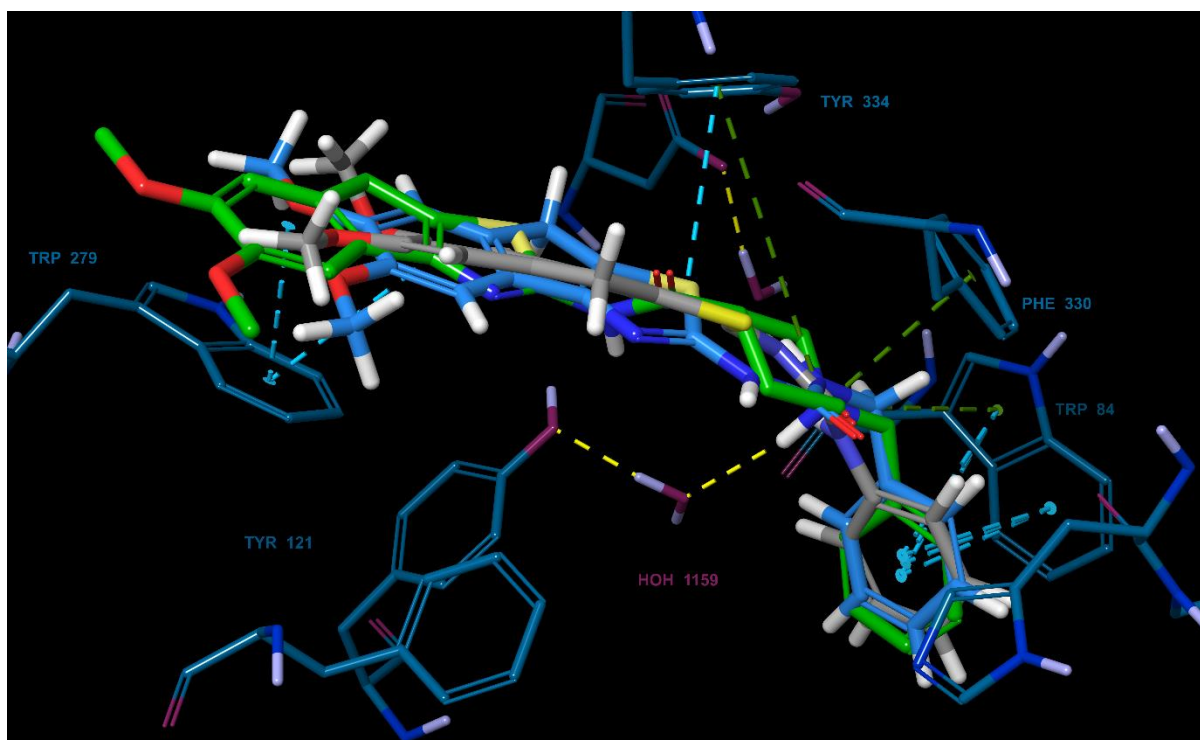


Figure 3.10. Docking poses of compounds **4** (green), **11** (grey) and **34** (blue) in the active site of torpedo eel AChE.

When compounds **11** and **34** were docked into the ATP pocket of GSK-3 together with compound **6** (**Figure 3.7**), it was predicted that compounds **11** and **34** would have only one H-bonding interaction with the carbonyl oxygen of Val135 through the urea NH closest to the thiazole moiety compared to the three H-bonding interactions of the urea NH's and the nitrogen of the thiazole ring of compound **6** (**Figure 3.11**). It was also predicted that although compounds **11** and **34** lost this H-bonding interaction, they would have individually gained a new H-bonding interaction through the urea NH furthest away from the thiazole moiety and the carbonyl oxygen of Pro136. In addition to new interactions formed, compounds **11** and **34** were also predicted to have an individual H-bonding interaction between Lys85 and the oxygen of the methoxy group of the 5,6-dimethoxy-8*H*-indeno[1,2-*d*]thiazol-2-amine moiety of **11** and **34** (**Figure 3.11**). It was also predicted that only compounds **6** and **11** would have a π -cation interaction between the nitrogen of the guanidine group of Arg141 and the phenyl groups compared to Arg141 and **34**.

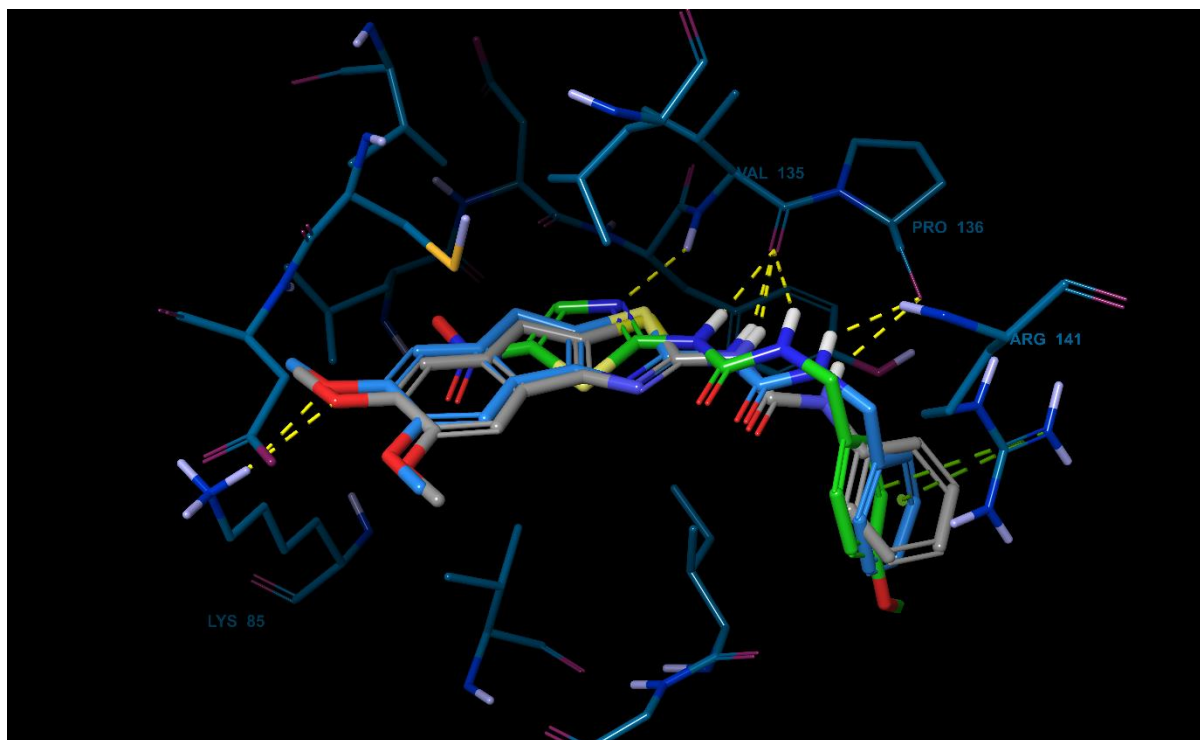
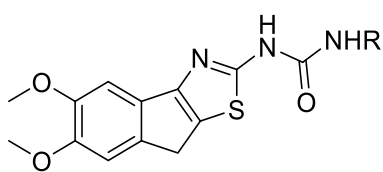


Figure 3.11. Docking poses of compounds **6** (green), **11** (grey) and **34** (blue) in the ATP active site of GSK-3.

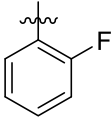
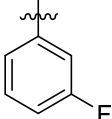
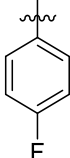
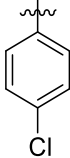
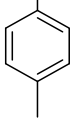
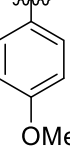
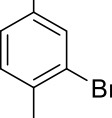
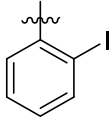
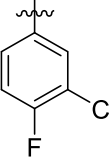
3.3. STRUCTURE ACTIVITY RELATIONSHIP STUDY

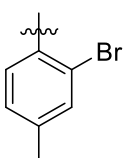
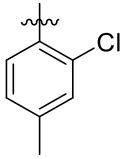
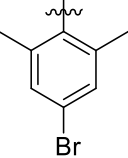
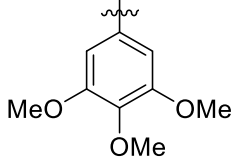
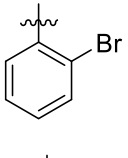
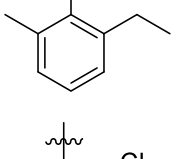
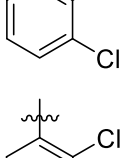
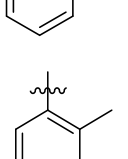
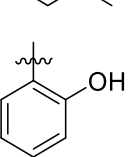
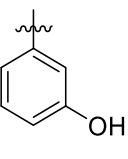
The inhibitory activity of all new synthetic compounds was assessed against *Electrophorus electricus* AChE (*EeAChE*) using Ellman's spectrophotometric method [42] with minor modifications [43]. Galantamine was used as positive control. The AChE inhibitory activities for the synthesized compounds, expressed as half-maximal inhibitory concentration (IC_{50}) values, is provided in **Table 3.1**. In addition, selected compounds were assessed for cytotoxicity in the SH-SY5Y neuroblastoma cell line using the sulforhodamine B (SRB) staining assay as described by Vichai and Kirtikara [44].

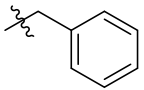
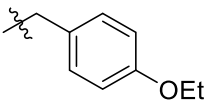
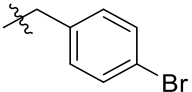
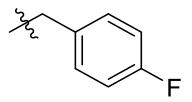
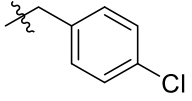
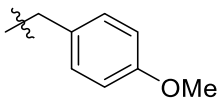
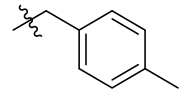
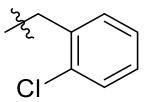
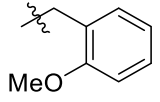
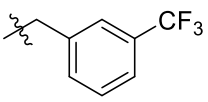
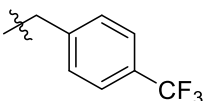
Table 3.1. *In vitro* AChE inhibitory activity and cytotoxicity of compounds **11** - **45**.

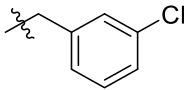


| Compound | R | Yield (%) | <i>EeAChE</i> $IC_{50} \pm SEM$ (μM) ^a | Cytotoxicity $IC_{50} \pm SEM$ (μM) ^a |
|-----------|---|-----------|---|--|
| 11 |  | 89 | 83.18 ± 3.65 | nd ^b |

| | | | | |
|----|---|----|------------------|-----------------|
| 12 |  | 75 | 77.45 ± 5.43 | nd ^b |
| 13 |  | 81 | 58.08 ± 3.28 | nd ^b |
| 14 |  | 76 | 83.56 ± 6.02 | nd ^b |
| 15 |  | 75 | >100 | nd ^c |
| 16 |  | 76 | >100 | nd ^c |
| 17 |  | 71 | >100 | nd ^c |
| 18 |  | 89 | >100 | nd ^c |
| 19 |  | 83 | >100 | nd ^c |
| 20 |  | 86 | >100 | nd ^c |
| 21 |  | 90 | 97.50 ± 5.37 | 5.70 ± 1.12 |

| | | | | |
|----|---|----|-------------------|------------------|
| 22 |  | 89 | 72.44 ± 0.84 | 18.92 ± 1.21 |
| 23 |  | 76 | 80.54 ± 8.71 | nd ^b |
| 24 |  | 83 | 85.90 ± 22.20 | nd ^b |
| 25 |  | 83 | 81.10 ± 3.37 | nd ^b |
| 26 |  | 70 | 82.60 ± 6.36 | nd ^b |
| 27 |  | 74 | 54.95 ± 3.44 | nd ^b |
| 28 |  | 73 | 96.83 ± 28.39 | nd ^b |
| 29 |  | 71 | >100 | nd ^c |
| 30 |  | 86 | >100 | nd ^c |
| 31 |  | 90 | 67.92 ± 2.30 | nd ^b |
| 32 |  | 89 | >100 | nd ^c |

| | | | | |
|----|---|----|------------------|------------------|
| 33 |  | 66 | 88.51 ± 4.32 | nd ^b |
| 34 |  | 74 | 72.28 ± 2.33 | 7.25 ± 1.12 |
| 35 |  | 79 | 12.74 ± 2.33 | 2.78 ± 1.16 |
| 36 |  | 79 | >100 | nd ^c |
| 37 |  | 75 | 73.45 ± 5.77 | 3.80 ± 1.18 |
| 38 |  | 79 | >100 | nd ^c |
| 39 |  | 74 | 75.86 ± 5.68 | 11.23 ± 1.19 |
| 40 |  | 76 | 82.41 ± 2.69 | 5.23 ± 1.14 |
| 41 |  | 91 | 43.65 ± 2.66 | 4.52 ± 1.17 |
| 42 |  | 73 | >100 | nd ^c |
| 43 |  | 87 | 73.79 ± 2.69 | 8.30 ± 1.13 |
| 44 |  | 76 | 86.70 ± 3.72 | 4.50 ± 1.48 |

| | | | | |
|--------------------|---|----|---------------|-------------|
| 45 |  | 74 | 48.42 ± 11.80 | 4.98 ± 1.16 |
| Galantamine | | - | 3.58 ± 1.24 | - |

^a Data are the mean ± SEM of three independent experiments

^b Not determined due to precipitation occurring

^c Not determined as AChE IC₅₀ inhibitory activity exceeded 100 μM

Only one compound was found to have an IC₅₀ value below 15 μM, namely compound **35** (IC₅₀ = 12.74 μM) (**Table 3.1**). When the *N*-benzylpiperidine ring of compound **4** (IC₅₀ = 0.24 μM) was replaced with aryl and benzyl groups, the inhibition of AChE was negatively affected. When comparing the aryl and benzyl group substitutions, it was evident that the benzyl derivatives provided better inhibitory activity than the aryl derivatives. Within the aryl group derivatives, only compounds **13** (IC₅₀ = 58.08 μM) and **27** (IC₅₀ = 54.95 μM) showed moderate inhibitory activity against *Ee*AChE compared to compounds **35** (IC₅₀ = 12.74 μM), **41** (IC₅₀ = 43.65 μM) and **45** (IC₅₀ = 48.42 μM). It would thus appear as if increased length in benzyl vs. aryl substituents on the respective *para*-position might be responsible for increased inhibitory activity.

With regard to the halogen substituted aryl groups, inhibitory values observed were suggestive that fluoro in the *para*-position (compound **14**, IC₅₀ = 83.56 μM) provides better results than chloro (compound **15**, IC₅₀ >100 μM) or bromo (compound **16**, IC₅₀ >100 μM) substituents. A similar pattern was observed for the benzyl group in which fluoro in the *para*-position (compound **37**, IC₅₀ = 73.45 μM) provided better inhibition than chloro (compound **38**, IC₅₀ >100 μM) or bromo (compound **36**, IC₅₀ >100 μM) substituents. When comparing the halogen substitution on the preferred *ortho*-position for aryl groups, a similar pattern was observed. However, when the substitution position of fluoro on the aryl groups was investigated, it is found that the preferred position is the *meta*-position (compound **13**, IC₅₀ = 58.08 μM). In general, mono-substituted chloro and bromo aryl groups indicated inactivity against AChE; however, the addition of an electron-donating group either in the *para*-position (compounds **22** and **23**) or the *ortho*-position (compound **24**) led to a modest increase in *Ee*AChE inhibitory activity.

The positioning of the benzyl group significantly affects activity where it is observed that subtle changes in the length of the alkoxy chain, for example compound **35** (IC₅₀ = 12.74 μM) and **39** (IC₅₀ = 75.86 μM), afforded dramatic differences. Interestingly, the *ortho* (compound **41**, IC₅₀ = 43.65 μM) and *meta* (compound **45**, IC₅₀ = 48.42 μM) chloro benzyl derivatives performed better than the *para* analogue (compound **38** IC₅₀ >100 μM). A similar trend was evident when comparing compounds **43**

(*meta*-CF₃, IC₅₀ = 73.79 μM) and **44** (*para*-CF₃, IC₅₀ = 86.70 μM). However, the opposite was noted for compounds **39** (*para*-OMe, IC₅₀ = 75.86 μM) and **42** (*ortho*-OMe, IC₅₀ > 100 μM). The cytotoxicity results indicated that the synthesized compounds were relatively cytotoxic with IC₅₀ values ranging from 2.78 – 18.92 μM.

3.4. CONCLUSION

Compound **35** was found to have the highest *EeAChE* inhibitory potential with an IC₅₀ value of 12.74 ± 2.33 μM. The benzyl group derivatives showed better inhibitory activity than the aryl group derivatives with substituents on the *para*-position. In the case of the halogen substituents of the aryl derivatives, fluorine substituents in the *ortho*-position showed better inhibitory activity. Elongated substituents on the benzyl derivatives is preferred with longer alkyl chains leading to increased inhibitory activity of *EeAChE* (compound **35** vs. compound **39**). The compounds were found to be relatively cytotoxic. It was predicted through molecular modelling that compounds **11** and **34** may have the capability to inhibit GSK-3. In order to validate this prediction, future research will include the determination of GSK-3 inhibition in which the compounds are to be evaluated as possible inhibitors. Further investigation will also be conducted in decreasing the cytotoxicity of these compounds without losing the inhibitory ability thereof.

3.5. EXPERIMENTAL

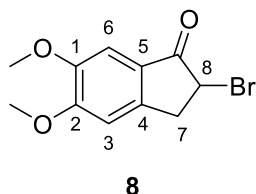
3.5.1. Chemistry

3.5.1.1. General methods

All solvents, chemicals, and reagents were obtained commercially and used without further purification. ¹H NMR (300 MHz) and ¹³C NMR (75 MHz) spectra were recorded on Bruker AVANCE-III-300 instrument using CDCl₃ and DMSO-*d*₆. CDCl₃ contained tetramethylsilane as an internal standard. Chemical shifts, δ, are reported in parts per million (ppm), and splitting patterns are given as singlet (s), doublet (d), triplet (t), quartet (q), or multiplet (m). Coupling constants, *J*, are expressed in hertz (Hz). Mass spectra were recorded in ESI mode on a Waters Synapt G2 Mass Spectrometer at 70 eV and 200 mA. Samples were dissolved in acetonitrile (containing 0.1% formic acid) to an approximate concentration of 10 μg/mL. Infrared spectra were run on a Bruker ALPHA Platinum ATR spectrometer. The absorptions are reported on the wavenumber (cm⁻¹) scale, in the range 400 - 4000 cm⁻¹. Abbreviations used in quoting spectra are: v = very, s = strong, m = medium, w = weak, str = stretch. Melting points were measured on a Stuart Melting Point SMP10 microscope. The retention factor (*R_f*) values denoted are for thin layer chromatography (TLC) on aluminium-backed Macherey-Nagel ALUGRAM Sil G/UV₂₅₄ plates pre-coated with 0.25 mm silica gel 60, spots were visualised with UV light

and basic KMnO_4 spray reagent. Yields refer to isolated pure products unless stated otherwise. Each compound is named either according to PerkinElmer's *ChemDraw Version 15.0.0.106* or according to common names. The numbering of compounds was not done according to priority, but rather to the author's convenience for characterization.

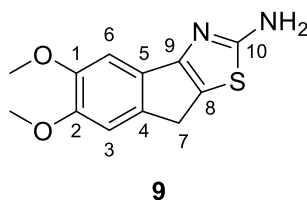
3.5.1.2. 2-Bromo-5,6-dimethoxy-1-indanone **8**



To a stirring solution of 5,6-dimethoxy-1-indanone **7** (10.00 g, 52.03 mmol, 1 eq.) in methanol (100 mL), was added bromine (2.8 mL, 55 mmol, 1.05 eq.) drop-wise. After addition of bromine the product precipitated out of solution.

The mixture was left to stir for 30 min, after which time the precipitate was filtered off, washed with ice cold methanol (50 mL), and dried *in vacuo* to afford the product as a solid. The product was used without any further purification. (Yield 84%); Light yellow solid; R_f 0.72 (3:1 ethyl acetate: hexane); mp 162 - 163 °C [45]; ν_{max} (neat)/ cm^{-1} 2959 (C-H str, m), 1687 (C=O str, s), 1583 (s), 1497 (C-C str, m), 1309 (C-H wag (-CHBr), m), 1261 (s), 1218 (C-N str, m), 1107 (m), 1015 (m), 727 (s); $^1\text{H NMR}$ (300 MHz, CDCl_3); δ 7.19 (1H, s, H-6), 6.82 (1H, s, H-3), 4.61 (1H, dd, $J = 2.9$ & 7.3 Hz, H-8), 3.95 (3H, s, OCH_3), 3.88 (3H, s, OCH_3), 3.72 (1H, dd, $J = 7.2$ & 17.9 Hz, H-7), 3.30 (1H, dd, $J = 3.0$ & 17.9 Hz, H-7); $^{13}\text{C NMR}$ (75 MHz, CDCl_3); δ 198.2 (C=O), 156.8 (C-2), 150.2 (C-4), 146.7 (C-1), 126.4 (C-5), 107.3 (C-3), 105.2 (C-6), 56.7 (OCH_3), 56.3 (OCH_3), 44.7 (C-8), 37.9 (C-7). Characterization of this compound compared well to literature [45].

3.5.1.3. 5,6-Dimethoxy-8H-indeno[1,2-d]thiazol-2-amine **9**

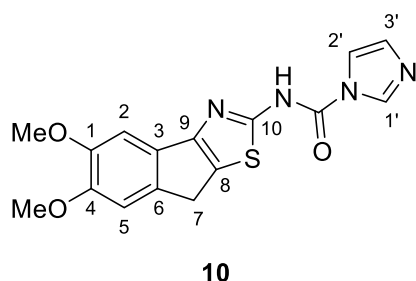


To a suspension of thiourea (1.97 g, 25.89 mmol, 1 eq.) in distilled water (100 mL) was added 2-bromo-5,6-dimethoxy-1-indanone **8** (7.00 g, 25.8 mmol, 1 eq.) in three portions over 30 min at room temperature. The resulting mixture was refluxed for 12 h. The solution was then cooled to

room temperature and a 3 M ammonium hydroxide solution (64.6 mL, 129 mmol, 5 eq.) was added, which resulted in the precipitation of the product. The resulting mixture was left to stir for 30 min. The product was filtered off and washed with distilled water (100 mL) after which time it was dried *in vacuo*. The product was used without any further purification. (Yield 83%); Yellow solid; R_f 0.27 (3:1 ethyl acetate: hexane); mp 204 °C (decomp.); ν_{max} (neat)/ cm^{-1} 3376 (N-H str, m), 3111 (m), 2933 (C-H str, m), 1524 (N-H bend, s), 1456 (C-C str, m), 1377 (C-H bend, s), 1271 (C-N str, s), 1203 (C-N str, m), 1148 (m), 1097 (C-N str, s), 750 (C-H "oop", s); $^1\text{H NMR}$ (300 MHz, $\text{DMSO}-d_6$); δ 7.16 (1H, s, H-6), 7.06 (2H, s, NH_2), 6.98 (1H, s, H-3), 3.79 (3H, s, OCH_3), 3.76 (3H, s, OCH_3), 3.58 (2H, s, H-7); $^{13}\text{C NMR}$ (75 MHz, $\text{DMSO}-d_6$); δ 172.6 (C-10), 156.0 (C-2), 148.1 (C-9), 146.4 (C-1), 137.5 (C-5), 130.8 (C-4), 120.7

(C-8), 110.1 (C-3), 102.1 (C-6), 56.0 (OCH₃), 55.7 (OCH₃), 32.0 (C-7); **HRMS *m/z* (ESI)** 249.0697 ([M + H]⁺ requires 249.0692). Characterization of this compound compared well to literature [45].

3.5.1.4. *N*-(5,6-Dimethoxy-8*H*-indeno[1,2-*d*]thiazol-2-yl)-1*H*-imidazol-1-carboxamide **10**

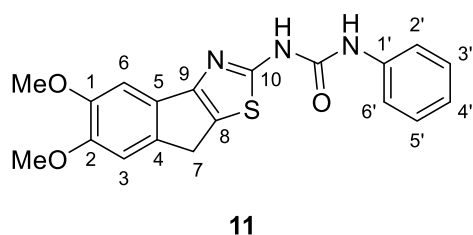


1,1'-Carbonyldiimidazole (3.64 g, 22.4 mmol, 1.2 eq.) was added to a mixture of 5,6-dimethoxy-8*H*-indeno[1,2-*d*]thiazol-2-amine **9** (4.60 g, 18.6 mmol, 1 eq.) in dry dichloromethane (100 ml) and the reaction was stirred for 24 h at reflux conditions. The reaction mixture was cooled down to 2 - 8 °C, filtered and washed with cold dichloromethane (30 ml). The product was collected and dried *in vacuo*. The product was used without any further purification. (Yield 97%); White solid; **R_f** 0.70 (ethyl acetate); **mp** 197 °C (decomp.); **v_{max} (neat)/cm⁻¹** 3159 (N-H str, w), 2827 (C-H str, w), 1648 (C=O str, m), 1563 (N-H bend, m), 1505 (C-C str (in-ring), m), 1377 (C-H bend, s), 1322 (s), 1210 (C-N str, m), 1057 (s), 861 (C-H "oop", m), 770 (C-H "oop", m); **¹H NMR (300 MHz, DMSO-*d*₆)**; δ 7.86 (1H, s, H-1'), 7.32 – 6.90 (4H, m, ArH's), 3.79 (3H, s, OCH₃), 3.76 (3H, s, OCH₃), 3.58 (2H, s, H-7); **¹³C NMR (75 MHz, DMSO-*d*₆)**; δ 172.7 (C-10), 156.0 (C=O), 148.2 (C-4), 148.1 (C-9), 146.4 (C-1), 138.0 (C-1'), 137.5 (C-2'), 135.1 (C-3), 130.8 (C-6), 121.4 (C-3'), 120.7 (C-7), 110.1 (C-5), 102.2 (C-2), 56.0 & 55.9 (OCH₃⁺), 55.8 & 55.6 (OCH₃⁺), 32.0 (C-7). *Doubling of carbon peaks due to rotamers.

3.5.1.5. General method for amide couplings

The appropriate amine (0.97 mmol, 1.1 eq.) was added to a suspension of *N*-(5,6-dimethoxy-8*H*-indeno[1,2-*d*]thiazol-2-yl)-1*H*-imidazol-1-carboxamide **10** (0.30 g, 0.88 mmol, 1 eq.) in dry acetonitrile (15 mL) and the reaction was stirred for 20 h at reflux conditions. The reaction was cooled down to room temperature, quenched with 1 M aqueous hydrochloric acid (15 mL) and the precipitate was filtered, washed with 3 M ammonium hydroxide (10 mL) followed by distilled water (10 mL) and collected, and dried *in vacuo* to afford the pure product. The product was used without any further purification.

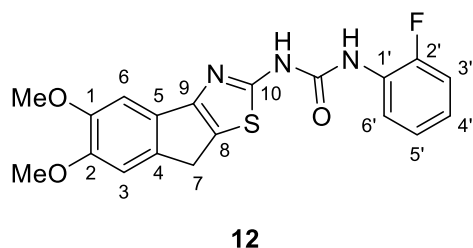
3.5.1.5.1. 1-(5,6-Dimethoxy-8*H*-indeno[1,2-*d*]thiazol-2-yl)-3-phenylurea **11**



(Yield 89%); Grey solid; **R_f** 0.38 (3:1 ethyl acetate: hexane); **mp** 130 °C (decomp.); **v_{max} (neat)/cm⁻¹** 2938 (C-H str, w), 1672 (C=O str, m), 1540 (N-H bend, s), 1496 (C-C str, m), 1384 (C-H bend, m), 1278 (C-N str, s), 1236 (C-N str, s), 1201 (C-N str, s), 750 (C-H "oop", s); **¹H NMR (300 MHz, DMSO-*d*₆)**; δ 9.29 (1H, s, NH), 7.55 (2H, d, *J* = 8.1 Hz, ArH's), 7.25 – 7.00 (4H, m, ArH's, NH), 6.89 (1H, s, H-3),

6.85–6.77 (1H, m, H-4'), 3.76 (3H, s, OCH₃), 3.62 (2H, s, H-7), 3.58 (3H, s, OCH₃); ¹³C NMR (75 MHz, DMSO-*d*₆); δ 162.8 (C-10), 154.0 (C=O), 151.5 (C-2), 148.2 (C-9), 147.0 (C-1), 138.7 (C-1'), 138.0 (C-5), 129.6 (C-4), 129.0 (C-3' & C-5'), 127.0 (C-8), 122.7 (C-2' & C-6'), 118.5 (C-4'), 110.1 (C-3), 102.4 (C-6), 55.9 (OCH₃), 55.8 & 55.7 (+OCH₃), 32.2 (C-7). HRMS *m/z* (ESI) (C₁₉H₁₇N₃O₃S) 368.0997 ([M + H]⁺ requires 368.1063). *Doubling of carbon peaks due to rotamers.

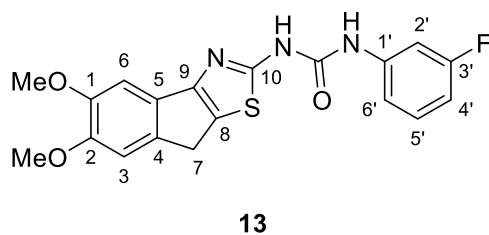
3.5.1.5.2. 1-(5,6-Dimethoxy-8H-indeno[1,2-d]thiazol-2-yl)-3-(2-fluorophenyl)urea **12**



(Yield 75%); White solid; *R_f* 0.36 (1:1 ethyl acetate: hexane); mp 244 °C (decomp.); *v*_{max} (neat)/cm⁻¹ 2952 (C-H str, m), 1685 (C=O str, s), 1620 (C=C str, m), 1517 (N-H bend, s), 1384 (C-H bend, m), 1326 (m), 1273 (C-N str, s), 1143 (m), 1074 (C-F str, m), 742 (C-H "oop", s); ¹H NMR (300 MHz,

DMSO-*d*₆); δ 10.80 (1H, s, NH), 9.10 (1H, s, NH), 8.16 (1H, t, *J* = 8.0 Hz, H-6'), 7.43–6.89 (5H, m, ArH's), 3.83 (3H, s, OCH₃), 3.78 (3H, s, OCH₃), 3.73 (2H, s, H-7); ¹³C NMR (75 MHz, DMSO-*d*₆); δ 162.5 (C-10), 154.5 (d, *J* = 87.8 Hz, +C-2'), 151.1 (C=O) 150.7 (C-2), 148.2 (C-9), 147.0 (C-1), 138.0 (C-5), 129.8 (C-4), 127.2 (C-8), 126.6 (d, *J* = 10.5 Hz, +C-5'), 124.7 (d, *J* = 2.6 Hz, +C-4'), 123.5 (d, *J* = 7.5 Hz, +C-6'), 120.8 (d, *J* = 0.7 Hz, +C-1'), 115.2 (d, *J* = 20.0 Hz, +C-3'), 110.0 (C-3), 102.3 (C-6), 55.8 (OCH₃), 55.7 (OCH₃), 32.2 (C-7). HRMS *m/z* (ESI) (C₁₉H₁₆FN₃O₃S) 386,0903 ([M + H]⁺ requires 386,0969). *Doubling of carbon peaks due to fluorine splitting.

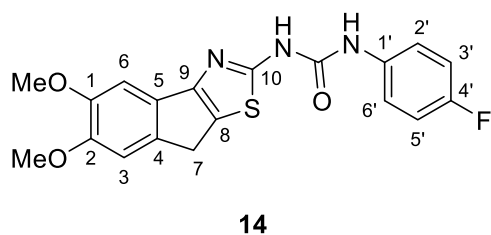
3.5.1.5.3. 1-(5,6-Dimethoxy-8H-indeno[1,2-d]thiazol-2-yl)-3-(3-fluorophenyl)urea **13**



(Yield 81%); Yellow solid; *R_f* 0.35 (3:1 ethyl acetate: hexane); mp 215 °C (decomp.); *v*_{max} (neat)/cm⁻¹ 2940 (C-H str, m), 1669 (C=O str, w), 1615 (C=C str, m), 1562 (N-H bend, s), 1387 (C-H bend, m), 1276 (C-N str, s), 1203 (C-N str, s), 1143 (s), 1077 (C-F str, m), 766 (C-H "oop", s); ¹H

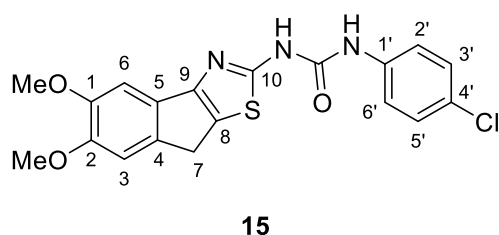
NMR (300 MHz, DMSO-*d*₆); δ 10.71 (1H, s, NH), 9.44 (1H, s, NH), 7.51 (1H, d, *J* = 11.3 Hz, H-2'), 7.40–7.30 (1H, m, H-5'), 7.25–7.17 (2H, m, ArH's), 7.13 (1H, s, H-6), 6.91–6.81 (1H, m, H-4'), 3.82 (3H, s, OCH₃), 3.78 (3H, s, OCH₃), 3.74 (2H, s, H-7); ¹³C NMR (75 MHz, DMSO-*d*₆); δ 162.7 (C-10), 162.4 (d, *J* = 241.1 Hz, #C-3), 154.5 (C=O), 151.5 (C-2), 148.2 (C-9), 147.0 (C-1), 140.6 (d, *J* = 11.4 Hz, #C-1'), 138.0 (C-5), 130.6 (d, *J* = 9.6 Hz, #C-5'), 129.7 (C-4), 127.2 (C-8), 114.4 (d, *J* = 2.1 Hz, #C-6'), 110.0 (C-3), 109.1 (d, *J* = 22.3 Hz, #C-2'), 105.3 (d, *J* = 25.5 Hz, #C-4'), 102.3 (C-6), 55.9 (OCH₃), 55.8 & 55.7 (+OCH₃), 32.1 (C-7). HRMS *m/z* (ESI) 386,0903 ([M + H]⁺ requires 386,0969). (C₁₉H₁₆FN₃O₃S) #Doubling of carbon peaks due to fluorine splitting. *Doubling of carbon peaks due to rotamers.

3.5.1.5.4. 1-(5,6-Dimethoxy-8H-indeno[1,2-d]thiazol-2-yl)-3-(4-fluorophenyl)urea **14**



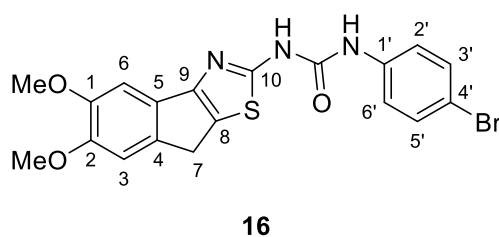
(Yield 78%); White solid; R_f 0.32 (3:1 ethyl acetate: hexane); mp 240 °C (decomp.); ν_{\max} (neat)/ cm^{-1} 2943 (C-H str, m), 1688 (C=O str, s), 1504 (N-H bend, s), 1382 (C-H bend, m), 1275 (C-N str, s), 1206 (C-N str, s), 1144 (s), 1076 (C-F str, m), 826 (C-H “oop”, s), 716 (C-H “oop”, s); $^1\text{H NMR}$ (300 MHz, DMSO- d_6); δ 10.57 (1H, s, NH), 9.08 (1H, s, NH), 7.52 (2H, dd, J = 8.6, 4.8 Hz, H-2 & H-6), 7.24 – 7.09 (4H, m, ArH's), 3.82 (3H, s, OCH₃), 3.78 (3H, s, OCH₃), 3.72 (2H, s, H-7); $^{13}\text{C NMR}$ (75 MHz, DMSO- d_6); δ 162.6 (d, J = 2.1 Hz, $^{\#}\text{C-4}'$), 159.5 (C-10), 156.3 (C=O), 151.6 (C-2), 148.2 (C-9), 147.0 (C-1), 138.0 (C-5), 135.0 (d, J = 2.3 Hz, C-1'), 129.8 (C-4), 127.1 (C-8), 120.7 (d, J = 7.7 Hz, $^{\#}\text{C-2}'$ & C-6'), 115.5 (d, J = 22.4 Hz, $^{\#}\text{C-3}'$ & C-5'), 110.0 (C-3), 102.3 (C-6), 55.9 & 55.8 ($^{\#}\text{OCH}_3$), 55.8 & 55.7 ($^{\#}\text{OCH}_3$), 32.1 (C-7). HRMS m/z (ESI) (C₁₉H₁₆FN₃O₃S) 386,0903 ([M + H]⁺ requires 386,0969). $^{\#}$ Doubling of carbon peaks due to fluorine splitting. † Doubling of carbon peaks due to rotamers.

3.5.1.5.5. 1-(4-Chlorophenyl)-3-(5,6-dimethoxy-8H-indeno[1,2-d]thiazol-2-yl)urea **15**



(Yield 75%); Light yellow solid; R_f 0.32 (3:1 ethyl acetate: hexane); mp 237 °C (decomp.); ν_{\max} (neat)/ cm^{-1} 2936 (C-H str, m), 1685 (C=O str, s), 1614 (C=C str, s), 1490 (N-H bend, s), 1384 (C-H bend, s), 1274 (C-N str, s), 1204 (C-N str, m), 1141 (m), 819 (C-Cl str, s), 734 (C-H “oop”, s); $^1\text{H NMR}$ (300 MHz, DMSO- d_6); δ 10.62 (1H, s, NH), 9.18 (1H, s, NH), 7.54 (2H, d, J = 8.2 Hz, H-2' & H-6'), 7.36 (2H, d, J = 8.2 Hz, H-3' & H-5'), 7.20 (1H, s, H-6), 7.12 (1H, s, H-3), 3.82 (3H, s, OCH₃), 3.78 (3H, s, OCH₃), 3.72 (2H, s, H-7); $^{13}\text{C NMR}$ (75 MHz, DMSO- d_6); δ 162.8 (C-10), 155.2 (C=O), 151.5 (C-2), 148.2 (C-9), 147.0 (C-1), 138.0 (C-5), 137.7 (C-1'), 129.8 (C-4), 128.8 (C-4'), 127.1 (C-8), 126.3 (C-3' & C-5'), 120.3 (C-2' & C-6'), 110.0 (C-3), 102.3 (C-6), 55.9 & 55.8 ($^{\#}\text{OCH}_3$), 55.7 (OCH₃), 32.1 (C-7). HRMS m/z (ESI) (C₁₉H₁₆ClN₃O₃S) 402.0627 ([M + H]⁺ requires 402.0674). † Doubling of carbon peaks due to rotamers.

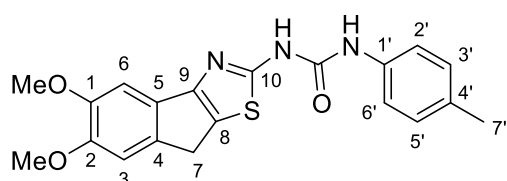
3.5.1.5.6. 1-(4-Bromophenyl)-3-(5,6-dimethoxy-8H-indeno[1,2-d]thiazol-2-yl)urea **16**



(Yield 76%); Light yellow solid; R_f 0.31 (3:1 ethyl acetate: hexane); mp 230 °C (decomp.); ν_{\max} (neat)/ cm^{-1} 2934 (C-H str, w), 1687 (C=O str, s), 1613 (C=C str, s), 1487 (N-H bend, s), 1274 (C-N str, s), 1144 (m), 823 (C-H “oop”, s), 737 (C-H “oop”, s); $^1\text{H NMR}$ (300 MHz, DMSO- d_6); δ 10.62

(1H, s, NH), 9.19 (1H, s, NH), 7.50 (4H, s, ArH's), 7.23 (1H, s, H-6), 7.13 (1H, s, H-3), 3.83 (3H, s, OCH₃), 3.79 (3H, s, OCH₃), 3.74 (2H, s, H-7); ¹³C NMR (75 MHz, DMSO-*d*₆); δ 162.8 (C-10), 154.9 (C=O), 151.5 (C-2), 148.2 (C-9), 146.9 (C-1), 138.1 (C-1'), 138.0 (C-5), 131.7 (C-3' & C-5'), 129.8 (C-4), 127.1 (C-8), 120.6 (C-2' & C-6'), 114.3 (C-4'), 110.0 (C-3), 102.3 (C-6), 55.9 & 55.8 (⁺OCH₃), 55.7 (OCH₃), 32.1 (C-7). **HRMS *m/z* (ESI)** (C₁₉H₁₆BrN₃O₃S) 446.0075 ([M + H]⁺ requires 446.0168). ⁺Doubling of carbon peaks due to rotamers.

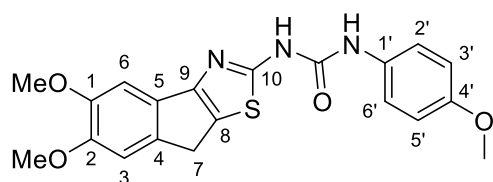
3.5.1.5.7. 1-(5,6-Dimethoxy-8H-indeno[1,2-*d*]thiazol-2-yl)-3-(*p*-tolyl)urea **17**



17

(Yield 71%); Light yellow solid; *R_f* 0.42 (3:1 ethyl acetate: hexane); **mp** 192 °C (decomp.); **v_{max} (neat)/cm⁻¹** 2935 (C-H str, m), 1681 (C=O str, s), 1616 (C=C str, s), 1510 (N-H bend, s), 1384 (C-H bend, s), 1262 (C-N str, s), 1143 (s), 814 (C-H "oop", s), 724 (C-H "oop", s); **¹H NMR (300 MHz, DMSO-*d*₆)**; δ 10.50 (1H, s, NH), 8.99 (1H, s, NH), 7.39 (2H, d, *J* = 7.3 Hz, H-2' & H-6'), 7.17 (4H, m, ArH's), 3.82 (3H, s, OCH₃), 3.78 (3H, s, OCH₃), 3.72 (2H, s, H-7), 2.26 (3H, s, H-7'); **¹³C NMR (75 MHz, DMSO-*d*₆)**; δ 162.9 (C-10), 154.7 (C=O), 151.4 (C-2), 148.2 (C-9), 146.9 (C-1), 138.0 (C-5), 136.1 (C-4'), 131.7 (C-1'), 129.9 (C-4), 129.4 (C-3' & C-5'), 127.0 (C-8), 118.7 (C-2' & C-6'), 110.1 (C-3), 102.3 (C-6), 55.9 & 55.8 (⁺OCH₃), 55.7 (OCH₃), 32.06 (C-7), 20.44 (C-7'). **HRMS *m/z* (ESI)** (C₂₀H₁₉N₃O₃S) 382.1179 ([M + H]⁺ requires 382.1220). ⁺Doubling of carbon peaks due to rotamers.

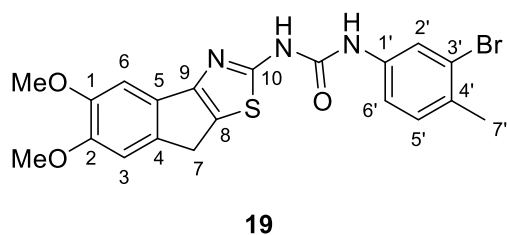
3.5.1.5.8. 1-(5,6-Dimethoxy-8H-indeno[1,2-*d*]thiazol-2-yl)-3-(4-methoxyphenyl)urea **18**



18

(Yield 89%); Light brown solid; *R_f* 0.33 (3:1 ethyl acetate: hexane); **mp** 211 °C (decomp.); **v_{max} (neat)/cm⁻¹** 3202 (N-H str, w), 2931 (C-H str, w), 1698 (C=O str, m), 1507 (N-H bend, s), 1383 (C-H bend, m), 1278 (C-N str, s), 1230 (C-N str, s), 1028 (m), 824 (C-H "oop", m); **¹H NMR (300 MHz, DMSO-*d*₆)**; δ 10.49 (1H, s, NH), 8.91 (1H, s, NH), 7.41 (2H, d, *J* = 7.5 Hz, H-2' & H-6'), 7.22 (1H, s, H-6), 7.13 (1H, s, H-3), 6.91 (2H, d, *J* = 7.3 Hz, H-3' & H-5'), 3.91 – 3.68 (11H, m, 3 x OCH₃, H-7); **¹³C NMR (75 MHz, DMSO-*d*₆)**; δ 163.0 (C-10), 155.1 (C-4'), 154.5 (C=O), 151.5 (C-2), 148.2 (C-9), 146.9 (C-1), 138.0 (C-5), 131.6 (C-1'), 129.8 (C-4), 126.9 (C-8), 120.5 (C-2' & C-6'), 114.1, (C-3' & C-5'), 110.1 (C-3), 102.3 (C-6), 55.9 (OCH₃), 55.8 (OCH₃), 55.2 (OCH₃), 32.1 (C-7). **HRMS *m/z* (ESI)** (C₂₀H₁₉N₃O₄S) 398.1133 ([M + H]⁺ requires 398.1169).

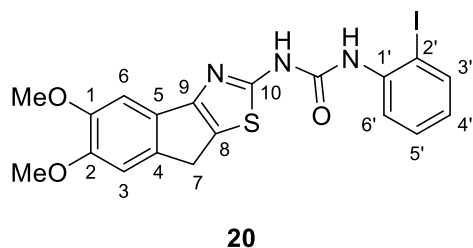
3.5.1.5.9. 1-(3-Bromo-4-methylphenyl)-3-(5,6-dimethoxy-8H-indeno[1,2-d]thiazol-2-yl)urea **19**



(Yield 83%); Light orange solid; R_f 0.36 (3:1 ethyl acetate: hexane); **mp** 198 °C (decomp.); ν_{\max} (neat)/ cm^{-1} 2940 (C-H str, w), 1683 (C=O str, m), 1534 (N-H bend, s), 1493 (C-C str, s), 1383 (C-H bend, s), 1277 (C-N str, s), 1239 (C-N str, s), 1202 (s), 678 (C-H “oop”, m); $^1\text{H NMR}$ (300 MHz, DMSO- d_6); δ 10.68 (1H, s, NH), 9.25 (1H, s, NH), 7.89 (1H, s, H-2'), 7.30 (2H, s, ArH'), 7.23 (1H, s, ArH), 7.12 (1H, s, ArH), 3.83 (3H, s, OCH₃), 3.78 (3H, s, OCH₃), 3.74 (2H, s, H-7), 2.29 (3H, s, H-7');

$^{13}\text{C NMR}$ (75 MHz, DMSO- d_6); δ 162.7 (C-10), 156.6 (C=O), 151.5 (C-2), 148.2 (C-9), 147.0 (C-1), 138.0 (C-5), 137.9 (C-1'), 131.1 (C-4'), 131.1 (C-5'), 129.8 (C-4), 127.1 (C-8), 124.0 (C-3'), 121.6 (C-2'), 118.0 (C-6'), 110.0 (C-3), 102.3 (C-6), 55.90 & 55.8 ($^+\text{OCH}_3$), 55.7 (OCH₃), 32.1 (C-7), 21.7 (C-7'). **HRMS m/z (ESI)** (C₂₀H₁₅BrN₃O₃S) 460.0277 ([M + H]⁺ requires 460.0325). *Doubling of carbon peaks due to rotamers.

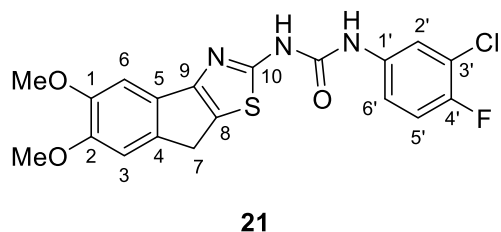
3.5.1.5.10. 1-(5,6-Dimethoxy-8H-indeno[1,2-d]thiazol-2-yl)-3-(2-iodophenyl)urea **20**



(Yield 86%); Light brown solid; R_f 0.36 (1:1 ethyl acetate: hexane); **mp** 211 °C (decomp.); ν_{\max} (neat)/ cm^{-1} 2933 (C-H str, w), 1682 (C=O str, s), 1580 (C-C str, s), 1515 (N-H bend, s), 1379 (C-H bend, s), 1270 (C-N str, s), 1201 (s), 1139 (C-N str, s), 703 (C-H “oop”, s); $^1\text{H NMR}$ (300 MHz, DMSO- d_6); δ 11.33 (1H, s, NH), 8.71 (1H, s, NH), 7.88 (2H, d, $J = 7.7$ Hz, H-3' & H-6'), 7.39 (1H, t, $J = 7.3$ Hz, H-5'), 7.22 (1H, s, H-6), 7.15 (1H, s, H-3), 6.91 (1H, t, $J = 6.2$ Hz, H-4'), 3.83 (3H, s, OCH₃), 3.78 (3H, s, OCH₃), 3.73 (2H, s, H-7); $^{13}\text{C NMR}$ (75 MHz, DMSO- d_6); δ 163.0 (C-10), 155.1 (C=O), 151.4 (C-2), 148.2 (C-9), 147.0 (C-1), 139.1 (C-1'), 137.9 (C-5), 129.8 (C-4), 128.8 (C-3'), 127.0 (C-5'), 126.9 (C-8), 125.9 (C-4'), 123.4 (C-6'), 110.0 (C-3), 102.3 (C-6), 91.8 (C-2'), 55.9 & 55.8 ($^+\text{OCH}_3$), 55.7 (OCH₃), 32.1 (C-7). **HRMS m/z (ESI)** (C₁₉H₁₆IN₃O₃S) 493.9964 ([M + H]⁺ requires 494.0030). *Doubling of carbon peaks due to rotamers.

$^{13}\text{C NMR}$ (75 MHz, DMSO- d_6); δ 163.0 (C-10), 155.1 (C=O), 151.4 (C-2), 148.2 (C-9), 147.0 (C-1), 139.1 (C-1'), 137.9 (C-5), 129.8 (C-4), 128.8 (C-3'), 127.0 (C-5'), 126.9 (C-8), 125.9 (C-4'), 123.4 (C-6'), 110.0 (C-3), 102.3 (C-6), 91.8 (C-2'), 55.9 & 55.8 ($^+\text{OCH}_3$), 55.7 (OCH₃), 32.1 (C-7). **HRMS m/z (ESI)** (C₁₉H₁₆IN₃O₃S) 493.9964 ([M + H]⁺ requires 494.0030). *Doubling of carbon peaks due to rotamers.

3.5.1.5.11. 1-(3-Chloro-4-fluorophenyl)-3-(5,6-dimethoxy-8H-indeno[1,2-d]thiazol-2-yl)urea **21**

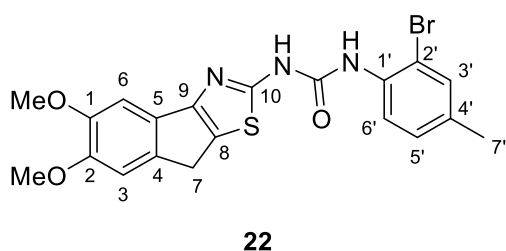


(Yield 90%); Off-white solid; R_f 0.22 (3:1 ethyl acetate: hexane); **mp** 238 °C (decomp.); ν_{\max} (neat)/ cm^{-1} 2956 (C-H str, m), 1686 (C=O str, s), 1499 (N-H bend, s), 1383 (C-H bend, m), 1250 (C-N str, s), 1207 (s), 1076 (C-F str, s), 803 (C-H “oop” s), 765 (C-Cl str, s), 708 (C-H “oop”, s); $^1\text{H NMR}$ (300 MHz, DMSO- d_6); δ 10.75 (1H, s, NH), 9.22 (1H, s, NH), 7.83 (1H, d, $J = 5.0$ Hz, H-2'), 7.37 (2H, d, J

$^{13}\text{C NMR}$ (75 MHz, DMSO- d_6); δ 10.75 (1H, s, NH), 9.22 (1H, s, NH), 7.83 (1H, d, $J = 5.0$ Hz, H-2'), 7.37 (2H, d, J

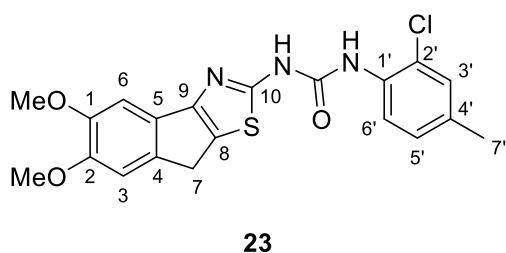
= 6.2 Hz, H-5' & H-6'), 7.21 (1H, s, H-6), 7.12 (1H, s, H-3), 3.82 (3H, s, OCH₃), 3.78 (3H, s, OCH₃), 3.72 (2H, s, H-7); ¹³C NMR (75 MHz, DMSO-*d*₆); δ 162.9 (C-10), 154.5 (C=O), 151.7 (d, *J* = 0.4 Hz, #C-4'), 151.3 (C-2), 148.2 (C-9), 147.0 (C-1), 138.0 (C-5), 136.0 (d, *J* = 2.9 Hz, #C-1'), 129.7 (C-4), 127.1 (C-8), 120.2 (d, *J* = 1.9 Hz, #C-6'), 119.5 (d, *J* = 0.5 Hz, #C-2'), 119.2 (d, *J* = 4.5 Hz, #C-3'), 117.0 (d, *J* = 22.1 Hz, #C-5'), 110.0 (C-3), 102.3 (C-6), 55.9 & 55.8 (+OCH₃), 55.72 (OCH₃), 32.11 (C-7). HRMS *m/z* (ESI) (C₁₉H₁₅ClF₃N₃O₃S) 420.0580 ([M + H]⁺ requires 420.0579). #Doubling of carbon peaks due to fluorine splitting. +Doubling of carbon peaks due to rotamers.

3.5.1.5.12. 1-(2-Bromo-4-methylphenyl)-3-(5,6-dimethoxy-8H-indeno[1,2-*d*]thiazol-2-yl)urea **22**



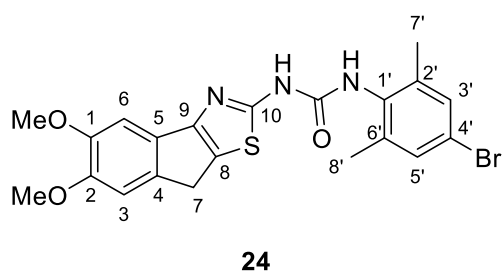
(Yield 89%); Light brown solid; *R_f* 0.40 (1:1 ethyl acetate: hexane); mp 180 °C (decomp.); *v*_{max} (neat)/cm⁻¹ 2940 (C-H str, w), 1682 (C=O str, m), 1520 (N-H bend, s), 1384 (C-H bend, s), 1274 (C-N str, s), 1143 (C-N str, s), 811 (C-H "oop", w), 721 (C-H "oop", w); ¹H NMR (300 MHz, DMSO-*d*₆); δ 11.29 (1H, s, NH), 8.88 (1H, s, NH), 7.94 (1H, d, *J* = 8.1 Hz, H-6'), 7.49 (1H, s, H-3'), 7.27 – 7.03 (3H, m, ArH's), 3.82 (3H, s, OCH₃), 3.78 (3H, s, OCH₃), 3.73 (2H, s, H-7), 2.27 (3H, s, H-7'); ¹³C NMR (75 MHz, DMSO-*d*₆); δ 163.0 (C-10), 155.0 (C=O), 151.3 (C-2), 148.2 (C-9), 147.0 (C-1), 137.9 (C-5), 134.7 (C-4'), 133.7 (C-3'), 132.7 (C-1'), 129.8 (C-4), 128.8 (C-5'), 127.0 (C-8), 122.5 (C-6'), 113.6 (C-2'), 110.0 (C-3), 102.2 (C-6), 55.9 & 55.8 (+OCH₃), 55.7 (OCH₃), 32.10 (C-7), 19.92 (C-7'). HRMS *m/z* (ESI) (C₂₀H₁₅BrN₃O₃S) 460.0277 ([M + H]⁺ requires 460.0325). +Doubling of carbon peaks due to rotamers.

3.5.1.5.13. 1-(2-Chloro-4-methylphenyl)-3-(5,6-dimethoxy-8H-indeno[1,2-*d*]thiazol-2-yl)urea **23**



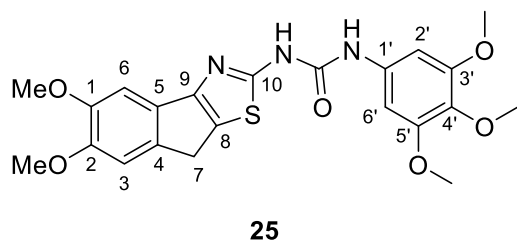
(Yield 76%); Off-white solid; *R_f* 0.42 (1:1 ethyl acetate: hexane); mp 220 °C (decomp.); *v*_{max} (neat)/cm⁻¹ 3348 (N-H str, m), 2913 (C-H str, m), 1673 (C=O str, s), 1528 (N-H bend, s), 1385 (C-H bend, s), 1260 (C-N str, s), 1204 (s), 811 (C-H "oop", m), 736 (C-Cl str, s), 640 (C-H "oop", m); ¹H NMR (300 MHz, DMSO-*d*₆); δ 11.17 (1H, s, NH), 8.97 (1H, s, NH), 8.05 (1H, d, *J* = 8.0 Hz, H-6), 7.31 (1H, s, H-3'), 7.21 (1H, s, H-6), 7.16 – 7.07 (2H, m, ArH's), 3.82 (3H, s, OCH₃), 3.78 (3H, s, OCH₃), 3.72 (2H, s, H-7), 2.26 (3H, s, H-7'); ¹³C NMR (75 MHz, DMSO-*d*₆); δ 162.9 (C-10), 155.1 (C=O), 151.2 (C-2), 148.2 (C-9), 147.0 (C-1), 137.9 (C-5), 133.9 (C-4'), 132.5 (C-1'), 129.8 (C-4), 129.5 (C-2'), 128.3 (C-3'), 127.0 (C-8), 122.3 (C-5'), 121.5 (C-6'), 110.0 (C-3), 102.2 (C-6), 55.9 & 55.8 (+OCH₃), 55.7 (OCH₃), 32.1 (C-7), 20.0 (C-7'). HRMS *m/z* (ESI) (C₂₀H₁₅ClN₃O₃S) 416.0834 ([M + H]⁺ requires 416.0830). +Doubling of carbon peaks due to rotamers.

3.5.1.5.14. 1-(4-Bromo-2,6-dimethylphenyl)-3-(5,6-dimethoxy-8H-indeno[1,2-d]thiazol-2-yl)urea **24**



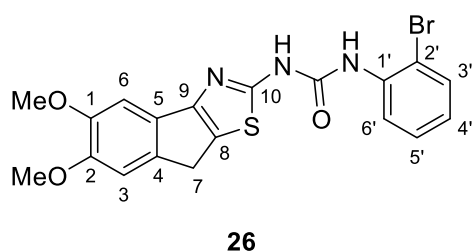
(Yield 83%); Light brown solid; R_f 0.47 (3:1 ethyl acetate: hexane); mp 203 °C (decomp.); ν_{\max} (neat)/ cm^{-1} 3401 (N-H str, w), 2954 (C-H str, m), 1694 (C=O str, s), 1546 (N-H bend, s), 1384 (C-H bend, s), 1276 (C-N str, s), 1211 (s), 1144 (m), 845 (C-H “oop”, m), 763 (C-H “oop”, m), 672 (C-H “oop”, m); $^1\text{H NMR}$ (300 MHz, $\text{DMSO-}d_6$); δ 10.85 (1H, s, NH), 8.43 (1H, s, NH), 7.34 (2H, s, H-3' & H-5'), 7.22 (1H, s, H-6), 7.13 (1H, s, H-3), 3.83 (3H, s, OCH_3), 3.79 (3H, s, OCH_3), 3.71 (2H, s, H-7), 2.21 (6H, s, H-7' & H-8'); $^{13}\text{C NMR}$ (75 MHz, $\text{DMSO-}d_6$); δ 163.4 (C-10), 154.8 (C=O), 151.9 (C-2), 148.2 (C-9), 146.9 (C-1), 138.4 (C-2' & C-6'), 137.9 (C-5), 134.1 (C-1'), 130.3 (C-3' & C-5'), 129.9 (C-4), 126.8 (C-8), 119.1 (C-4'), 110.1 (C-3), 102.3 (C-6), 55.9 (OCH_3), 55.8 & 55.7 ($^+\text{OCH}_3$), 32.1 (C-7), 18.0 & 17.9 (C-7' & C-8'). **HRMS m/z (ESI)** ($\text{C}_{21}\text{H}_{20}\text{BrN}_3\text{O}_3\text{S}$) 474.0462 ($[\text{M} + \text{H}]^+$ requires 474.0481). *Doubling up carbon peaks due to rotamers.

3.5.1.5.15. 1-(5,6-Dimethoxy-8H-indeno[1,2-d]thiazol-2-yl)-3-(3,4,5-trimethoxyphenyl)urea **25**



(Yield 83%); White solid; R_f 0.15 (3:1 ethyl acetate: hexane); mp 237 °C (decomp.); ν_{\max} (neat)/ cm^{-1} 2928 (C-H str, m), 1690 (C=O str, s), 1502 (N-H bend, s), 1457 (C-C str, s), 1421 (s), 1273 (C-N str, vs), 1123 (C-N str, m), 1077 (m), 1002 (m), 802 (C-H “oop”, s), 759 (C-H “oop”, s); $^1\text{H NMR}$ (300 MHz, $\text{DMSO-}d_6$); δ 10.50 (1H, s, NH), 9.01 (1H, s, NH), 7.21 (1H, s, H-6), 7.13 (1H, s, H-3), 6.84 (2H, s, H-2' & H-6'), 3.83 (3H, s, OCH_3), 3.78 (9H, s, 3 x OCH_3 's), 3.72 (2H, s, H-7), 3.63 (3H, s, OCH_3); $^{13}\text{C NMR}$ (75 MHz, $\text{DMSO-}d_6$); δ 162.8 (C-10), 154.9 (C=O), 153.0 (C-3' & C-5'), 151.4 (C-2), 148.2 (C-9), 147.0 (C-1), 138.0 (C-5), 134.7 (C-4'), 133.1 (C-1'), 129.8 (C-4), 127.0 (C-8), 110.0 (C-3), 102.3 (C-6), 96.5 (C-2' & C-6'), 60.2 & 60.1 ($^+\text{OCH}_3$), 55.9 & 55.8 ($^+\text{OCH}_3$), 55.70 (OCH_3), 32.1 (C-7). **HRMS m/z (ESI)** ($\text{C}_{22}\text{H}_{23}\text{N}_3\text{O}_6\text{S}$) 458.1371 ($[\text{M} + \text{H}]^+$ requires 458.1380). *Doubling up carbon peaks due to rotamers.

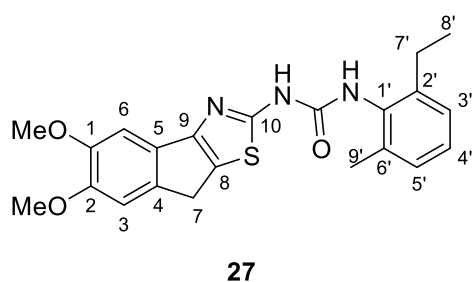
3.5.1.5.16. 1-(2-Bromophenyl)-3-(5,6-dimethoxy-8H-indeno[1,2-d]thiazol-2-yl)urea **26**



(Yield 70%); White solid; R_f 0.72 (3:1 ethyl acetate: hexane); mp 216 °C (decomp.); ν_{\max} (neat)/ cm^{-1} 2953 (C-H str, m), 1686 (C=O str, s), 1589 (C=C str, s), 1518 (N-H bend, s), 1382 (C-H bend, s), 1303 (s), 1272 (C-N str, vs), 1202 (s), 1142 (s), 733 (C-H “oop”, s); $^1\text{H NMR}$ (300 MHz, $\text{DMSO-}d_6$); δ 11.33

(1H, s, NH), 8.94 (1H, s, NH), 8.12 (1H, d, $J = 8.0$ Hz, H-3'), 7.66 (1H, d, $J = 7.9$ Hz, H-6'), 7.38 (1H, t, $J = 7.7$ Hz, H-5'), 7.21 (1H, s, H-6), 7.12 (1H, s, H-3), 7.04 (1H, t, $J = 7.4$ Hz, H-4'), 3.82 (3H, s, OCH₃), 3.78 (3H, s, OCH₃), 3.73 (2H, s, H-7); ¹³C NMR (75 MHz, DMSO-*d*₆); δ 162.9 (C-10), 155.1 (C=O), 151.2 (C-2), 148.2 (C-9), 147.0 (C-1), 137.9 (C-5), 136.3 (C-1'), 132.7 (C-4'), 129.8 (C-4), 128.3 (C-3'), 127.0 (C-8), 125.0 (C-5'), 122.4 (C-6'), 113.4 (C-2'), 110.0 (C-3), 102.2 (C-6), 55.9 & 55.8 (+OCH₃), 55.7 (OCH₃), 32.1 (C-7). HRMS m/z (ESI) (C₁₉H₁₆BrN₃O₃S) 446.0167 ([M + H]⁺ requires 446.0168). ⁺Doubling of carbon peaks due to rotamers.

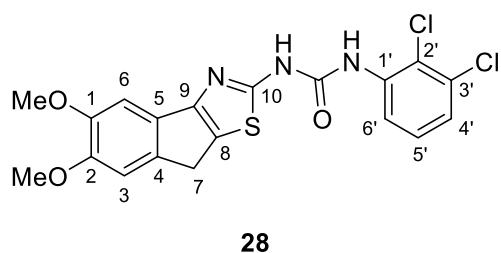
3.5.1.5.17. 1-(5,6-Dimethoxy-8H-indeno[1,2-d]thiazol-2-yl)-3-(2-ethyl-6-methylphenyl)urea **27**



(Yield 74%); Light orange solid; R_f 0.67 (3:1 ethyl acetate: hexane); mp 131 °C (decomp.); ν_{\max} (neat)/cm⁻¹ 3213 (N-H str, w), 2963 (C-H str, w), 1667 (C=O str, m), 1536 (N-H bend, s), 1464 (C-C str, s), 1385 (C-H bend, s), 1280 (C-N str, s), 1208 (s), 1145 (m), 776 (C-H "oop", m); ¹H NMR (300 MHz, DMSO-*d*₆); δ 10.88 (1H, s, NH), 8.57 (1H, s, NH), 7.25 – 7.07

(5H, m, ArH's), 3.82 (3H, s, OCH₃), 3.78 (3H, s, OCH₃), 3.70 (2H, s, H-7), 2.58 (2H, dd, $J = 14.5, 7.0$ Hz, H-7), 2.21 (3H, s, H-9), 1.12 (3H, t, $J = 7.1$ Hz, H-8); ¹³C NMR (75 MHz, DMSO-*d*₆); δ 163.5 (C-10), 154.9 (C=O), 152.4 (C-2), 148.2 (C-9), 146.9 (C-1), 141.4 (C-1'), 137.9 (C-5), 136.1 (C-2'), 133.8 (C-6'), 130.1 (C-5), 127.9 (C-5'), 126.9 (C-8), 126.7 (C-4'), 126.2 (C-3'), 110.1 (C-3), 102.3 (C-6), 55.8 (OCH₃), 55.7 (OCH₃), 32.02 (C-7), 24.59 (C-7'), 18.24 (C-9'), 14.75 (C-8'). HRMS m/z (ESI) (C₂₂H₂₃N₃O₃S) 410.1525 ([M + H]⁺ requires 410.1533).

3.5.1.5.18. 1-(2,3-Dichlorophenyl)-3-(5,6-dimethoxy-8H-indeno[1,2-d]thiazol-2-yl)urea **28**

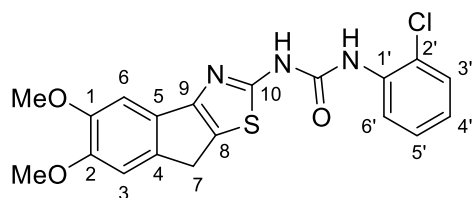


(Yield 73%); Grey solid; R_f 0.76 (3:1 ethyl acetate: hexane); mp 236 °C (decomp.); ν_{\max} (neat)/cm⁻¹ 3341 (N-H str, w), 2930 (C-H str, w), 1672 (C=O str, s), 1598 (C=C str, s), 1536 (N-H bend, s), 1456 (C-C str, s), 1383 (C-H bend, s), 1278 (C-N str, s), 1254 (C-N str, s), 1143 (s), 840

(C-H "oop", m), 772 (C-Cl str, s), 646 (C-H "oop", m); ¹H NMR (300 MHz, DMSO-*d*₆); δ 11.32 (1, s, NH), 9.16 (1H, br s, NH), 8.19 (1H, dd, $J = 5.6, 3.1$ Hz, H-6'), 7.43 – 7.27 (2H, m, H-4' & H-4'), 7.20 (1H, s, H-6), 7.11 (1H, s, H-3), 3.83 (3H, s, OCH₃), 3.78 (3H, s, OCH₃), 3.72 (2H, s, H-7); ¹³C NMR (75 MHz, DMSO-*d*₆); δ 162.6 (C-10), 155.1 (C=O), 151.1 (C-2), 148.2 (C-9), 147.0 (C-1), 137.9 (C-5), 137.2 (C-1'), 131.8 (C-3'), 129.7 (C-4), 128.4 (C-2'), 127.2 (C-8), 124.4 (C-4'), 120.8 (C-5'), 119.8 (C-6'), 110.0 (C-3), 102.3

(C-6), 55.9 (OCH₃), 55.8 (OCH₃), 32.08 (C-7). **HRMS *m/z* (ESI)** (C₁₉H₁₅Cl₂N₃O₃S) 436.0268 ([M + H]⁺ requires 436.0284).

3.5.1.5.19. 1-(2-Chlorophenyl)-3-(5,6-dimethoxy-8H-indeno[1,2-d]thiazol-2-yl)urea **29**

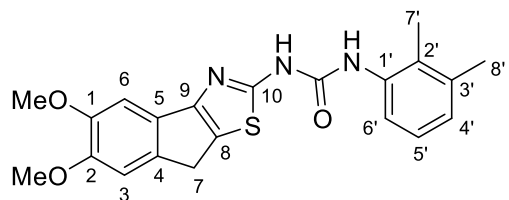


29

(Yield 71%); Off-white solid; **R_f** 0.76 (3:1 ethyl acetate: hexane); **mp** 228 °C (decomp.); **v_{max} (neat)/cm⁻¹** 2952 (C-H str, m), 1688 (C=O str, vs), 1596 (C=C str, s), 1517 (N-H bend, vs), 1384 (C-H bend, s), 1272 (C-N str, vs), 1142 (s), 838 (C-H “oop”, w), 738 (C-Cl str, vs), 669 (C-H “oop”, m); **¹H NMR (300 MHz, DMSO-*d*₆)**; δ 11.25 (1H, s, NH), 9.09 (1H, s, NH), 8.21 (1H, d, *J* = 8.2 Hz, H-6'), 7.50 (1H, d, *J* = 7.8 Hz, H-3'), 7.34 (1H, t, *J* = 7.7 Hz, H-5'), 7.21 (1H, s, H-6), 7.16 – 7.04 (2H, m, H-3 & H-4'), 3.82 (3H, s, OCH₃), 3.78 (3H, s, OCH₃), 3.73 (2H, s, H-7); **¹³C NMR (75 MHz, DMSO-*d*₆)**; δ 162.8 (C-10), 155.1 (C=O), 151.1 (C-2), 148.2 (C-9), 147.0 (C-1), 138.0 (C-5), 135.2 (C-1'), 129.8 (C-4), 129.4 (C-4'), 127.8 (C-3'), 127.1 (C-8), 124.2 (C-6'), 122.4 (C-2'), 121.4 (C-5'), 110.0 (C-3), 102.2 (C-6), 55.9 & 55.8 (⁺OCH₃), 55.7 (OCH₃), 32.10 (C-7). **HRMS *m/z* (ESI)** (C₁₉H₁₆ClN₃O₃S) 402.0627 ([M + H]⁺ requires 402.0674).

⁺Doubling of carbon peaks due to rotamers.

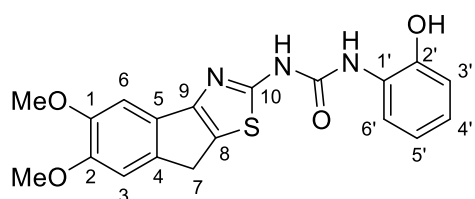
3.5.1.5.20. 1-(5,6-Dimethoxy-8H-indeno[1,2-d]thiazol-2-yl)-3-(2,3-dimethylphenyl)urea **30**



30

(Yield 86%); Off-white solid; **R_f** 0.59 (3:1 ethyl acetate: hexane); **mp** 235 °C (decomp.); **v_{max} (neat)/cm⁻¹** 3209 (N-H str, w), 2933 (C-H str, m), 1682 (C=O str, s), 1617 (C=C str, m), 1520 (N-H bend, s), 1463 (C-C str, s), 1381 (s), 1267 (C-N str, s), 1140 (m), 776 (C-H “oop”, m), 727 (C-H “oop”, m); **¹H NMR (300 MHz, DMSO-*d*₆)**; δ 10.83 (1H, s, NH), 8.59 (1H, s, NH), 7.61 (1H, d, *J* = 7.8 Hz, H-6'), 7.21 (1H, s, H-6), 7.11 (1H, s, H-3), 7.07 (1H, t, *J* = 7.8 Hz, H-5'), 6.95 (1H, d, *J* = 7.3 Hz, H-4'), 3.83 (3H, s, OCH₃), 3.78 (3H, s, OCH₃), 3.71 (2H, s, H-7), 2.26 (3H, s, H-8'), 2.17 (3H, s, H-7'); **¹³C NMR (75 MHz, DMSO-*d*₆)**; δ 163.3 (C-10), 155.0 (C=O), 151.7 (C-2), 148.2 (C-9), 147.0 (C-1), 138.0 (C-5), 136.9 (C-3'), 136.1 (C-1'), 129.9 (C-4), 127.7 (C-2'), 126.8 (C-8), 125.6 (C-4'), 125.5 (C-5'), 120.3 (C-6'), 110.1 (C-3), 102.2 (C-6), 55.9 & 55.8 (⁺OCH₃), 55.7 (OCH₃), 32.1 (C-7), 20.4 & 20.3 (C-8'), 13.6 (C-7'). **HRMS *m/z* (ESI)** (C₂₁H₂₁N₃O₃S) 396.1372 ([M + H]⁺ requires 396.1376). ⁺Doubling of carbon peaks due to rotamers.

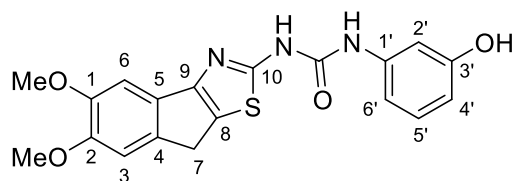
3.5.1.5.21. 1-(5,6-Dimethoxy-8H-indeno[1,2-d]thiazol-2-yl)-3-(2-hydroxyphenyl)urea **31**



31

(Yield 90%); Dark brown solid; R_f 0.28 (3:1 ethyl acetate: hexane); **mp** 158 °C (decomp.); ν_{\max} (neat)/ cm^{-1} 3257 (N-H str, m), 3195 (O-H str, m), 2939 (C-H str, m), 1676 (C=O str, m), 1540 (N-H bend, s), 1451 (C-C str, s), 1275 (C-N str, vs), 1198 (C-O str, s), 1143 (s), 745 (C-H “oop”, s); $^1\text{H NMR}$ (300 MHz, $\text{DMSO-}d_6$); δ 11.00 (1H, s, OH), 10.09 (1H, s, NH), 8.85 (1H, s, NH), 8.06 (1H, d, $J = 4.6$ Hz, H-6'), 7.22 (1H, s, H-6), 7.12 (1H, s, H-3), 6.94 – 6.75 (3H, m, ArH's), 3.83 (3H, s, OCH_3), 3.78 (3H, s, OCH_3), 3.73 (2H, s, H-7); $^{13}\text{C NMR}$ (75 MHz, $\text{DMSO-}d_6$); δ 163.0 (C-10), 155.0 (C=O), 151.3 (C-2), 148.2 (C-9), 146.9 (C-1), 146.1 (C-2'), 138.0 (C-5), 130.0 (C-4), 126.9 (C-8), 126.9 (C-1'), 122.8 (C-4'), 119.3 (C-5'), 119.0 (C-6'), 114.6 (C-3'), 110.1 (C-3), 102.3 (C-6), 55.9 (OCH_3), 55.8 (OCH_3), 32.1 (C-7). **HRMS m/z (ESI)** ($\text{C}_{19}\text{H}_{17}\text{N}_3\text{O}_4\text{S}$) 384.1016 ([M + H]⁺ requires 384.1012).

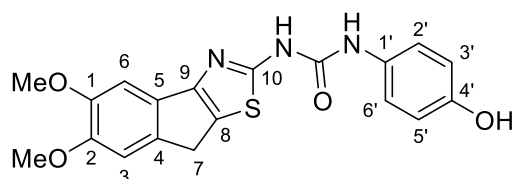
3.5.1.5.22. 1-(5,6-Dimethoxy-8H-indeno[1,2-d]thiazol-2-yl)-3-(3-hydroxyphenyl)urea **32**



32

(Yield 89%); Brown solid; R_f 0.20 (3:1 ethyl acetate: hexane); **mp** 158 °C (decomp.); ν_{\max} (neat)/ cm^{-1} 3210 (N-H str, m), 3157 (O-H str, m), 2936 (C-H str, m), 1717 (C=O str, m), 1609 (C=C str, m), 1544 (N-H bend, s), 1490 (C-C str, s), 1385 (C-H bend, m), 1270 (C-N str, s), 1202 (C-O str, vs), 771 (C-H “oop”, m), 684 (C-H “oop”, m); $^1\text{H NMR}$ (300 MHz, $\text{DMSO-}d_6$); δ 9.43 (1H, s, NH), 7.21 (1H, s, H-6), 7.17 – 7.05 (3H, m, ArH's), 6.85 (1H, d, $J = 7.9$ Hz, H-6'), 6.44 (1H, d, $J = 7.9$ Hz, H-4'), 5.11 (2H, br s, OH & NH), 3.82 (3H, s, OCH_3), 3.77 (3H, s, OCH_3), 3.72 (2H, s, H-7); $^{13}\text{C NMR}$ (75 MHz, $\text{DMSO-}d_6$); δ 162.8 (C-10), 158.0 (C-3'), 154.3 (C=O), 151.3 (C-2), 148.3 (C-9), 147.0 (C-1), 139.8 (C-1'), 138.0 (C-5), 129.8 (C-4), 129.7 (C-5'), 127.1 (C-8), 110.1 (C-3), 110.0 (C-4'), 109.2 (C-6'), 105.5 (C-2'), 102.4 (C-6), 55.88 (OCH_3), 55.80 (OCH_3), 32.17 (C-7). **HRMS m/z (ESI)** ($\text{C}_{19}\text{H}_{17}\text{N}_3\text{O}_4\text{S}$) 384.1016 ([M + H]⁺ requires 384.1012).

3.5.1.5.23. 1-(5,6-Dimethoxy-8H-indeno[1,2-d]thiazol-2-yl)-3-(4-hydroxyphenyl)urea **33**

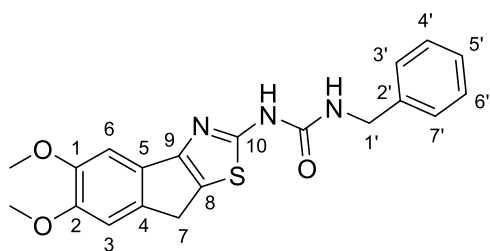


33

(Yield 66%); Grey solid; R_f 0.20 (3:1 ethyl acetate: hexane); **mp** 200 °C (decomp.); ν_{\max} (neat)/ cm^{-1} 3209 (N-H str, m), 2944 (C-H str, m), 1704 (C=O str, s), 1614 (C=C str, m), 1560 (C-C str (in-ring), s), 1509 (N-H bend, s), 1448 (C-C str, s), 1271 (C-N str, vs), 1199 (C-O str, s), 1073 (s), 826 (C-H “oop”, m), 766 (C-H “oop”, m); $^1\text{H NMR}$ (300 MHz, $\text{DMSO-}d_6$); δ 9.42 (1H, s, NH),

7.27 (2H, d, $J = 8.6$ Hz, H-2' & H-6'), 7.21 (1H, s, H-6), 7.16 (1H, s, H-3), 6.73 (2H, d, $J = 8.6$ Hz, H-3' & H-5'), 6.10 (2H, br s, OH & NH), 3.81 (3H, s, OCH₃), 3.77 (3H, s, OCH₃), 3.72 (2H, s, H-7); ¹³C NMR (75 MHz, DMSO-*d*₆); δ 163.2 (C-10), 153.6 (C-4'), 153.3 (C=O), 151.5 (C-2), 148.2 (C-9), 147.0 (C-1), 138.0 (C-5), 130.0 (C-1'), 129.5 (C-4), 126.8 (C-8), 120.7 (C-2' & C-6'), 115.4 (C-3' & C-5'), 110.0 (C-3), 102.4 (C-6), 55.88 (OCH₃), 55.8 (OCH₃), 32.24 (C-7). HRMS m/z (ESI) (C₁₉H₁₇N₃O₄S) 384.1016 ([M + H]⁺ requires 384.1012).

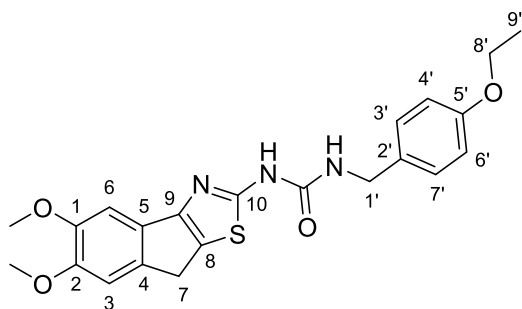
3.5.1.5.24. 1-Benzyl-(5,6-dimethoxy-8H-indeno[1,2-d]thiazol-2-yl)urea **34**



34

(Yield 74 %); Light orange solid; R_f 0.44 (3:1 ethyl acetate: hexane); mp 234 °C (decomp.); v_{max} (neat)/cm⁻¹ 3385 (N-H str, m), 2990 (C-H str, w), 1690 (C=O str, w), 1641 (C=C str, m), 1561 (N-H bend, s), 1384 (C-H str, m), 1277 (C-N str, s), 1207 (s), 1074 (m), 778 (C-H "oop", s), 724 (C-H "oop", s); ¹H NMR (300 MHz, DMSO-*d*₆); δ 10.59 (1H, s, NH), 7.40 – 7.17 (6H, m, ArH's & NH), 7.20 (1H, s, H-6), 7.08 (1H, s, H-3), 4.36 (2H, d, $J = 5.5$ Hz, H-1'), 3.81 (3H, s, OCH₃), 3.77 (3H, s, OCH₃), 3.69 (2H, s, H-7); ¹³C NMR (75 MHz, DMSO-*d*₆); δ 163.6 (C-10), 154.8 (C=O), 153.8 (C-2), 148.2 (C-9), 146.8 (C-1), 139.6 (C-2'), 137.9 (C-5), 130.1 (C-4), 128.4 (C-4' & C-6'), 127.3 (C-3' & C-7'), 127.0 (C-4), 126.5 (C-5), 110.1 (C-3), 102.2 (C-6), 55.9 (OCH₃), 55.7 (OCH₃), 42.93 (C-1'), 31.98 (C-7). HRMS m/z (ESI) (C₂₀H₁₉N₃O₃S) 382.1285 ([M + H]⁺ requires 382.1220).

3.5.1.5.25. 1-(5,6-Dimethoxy-8H-indeno[1,2-d]thiazol-2-yl)-3-(4-ethoxybenzyl)urea **35**

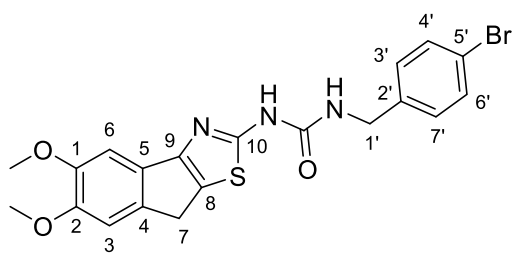


35

(Yield 79%); Light orange solid; R_f 0.44 (3:1 ethyl acetate: hexane); mp 195 °C (decomp.); v_{max} (neat)/cm⁻¹ 3370 (N-H str, w), 2973 (C-H str, w), 1701 (C=O str, m), 1674 (C=C str, m), 1550 (C-C str (in-ring), s), 1515 (N-H bend, s), 1389 (C-H str, s), 1278 (C-N str, s), 1245 (C-N str, s), 1210 (s), 776 (C-H "oop", s); ¹H NMR (300 MHz, DMSO-*d*₆); δ 10.47 (1H, s, NH), 7.25 (1H, s, H-6), 7.21 (2H, d, $J = 4.9$ Hz, H-3' & H-7'), 7.07 (2H, s, H-3 & NH), 6.89 (2H, d, $J = 8.5$ Hz, H-4' & H-6'), 4.27 (2H, d, $J = 5.6$ Hz, H-1'), 3.99 (2H, q, $J = 7.0$ Hz, H-8'), 3.81 (3H, s, OCH₃), 3.77 (3H, s, OCH₃), 3.69 (2H, s, H-7), 1.30 (3H, t, $J = 7.0$ Hz, H-9'); ¹³C NMR (75 MHz, DMSO-*d*₆); δ 163.6 (C-10), 157.6 (C-5'), 154.9 (C=O), 153.7 (C-2), 148.2 (C-9), 146.8 (C-1), 137.9 (C-5), 131.3 (C-2'), 130.1 (C-4), 128.7 (C-3' & C-7'), 126.5 (C-8), 114.3 (C-4' & C-6'), 110.1 (C-3), 102.2 (C-6), 63.0 (C-8'), 55.9 & 55.8 (⁺OCH₃), 55.7 (OCH₃), 42.4 (C-1'), 32.0 (C-7), 14.7 (C-9'). HRMS m/z (ESI) (C₂₂H₂₃N₃O₄S) 426.1528 ([M + H]⁺ requires 426.1482).

⁺Doubling of carbon peaks due to rotamers.

3.5.1.5.26. 1-(4-Bromobenzyl)-3-(5,6-dimethoxy-8H-indeno[1,2-d]thiazol-2-yl)urea **36**

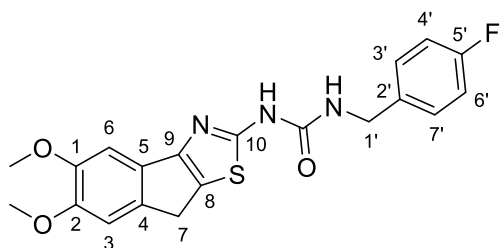


36

(Yield 79%); Light orange solid; R_f 0.37 (3:1 ethyl acetate: hexane); **mp** 221 °C (decomp.); ν_{\max} (neat)/ cm^{-1} 3230 (N-H str, w), 2897 (C-H str, m), 1676 (C=O str, s), 1558 (C-C str (in-ring), s), 1511 (N-H bend, s), 1381 (C-H bend, s), 1275 (C-N str, vs), 1203 (s), 1143 (s), 1070 (s), 762 (C-H “oop”, m), 653 (C-H “oop”, m); $^1\text{H NMR}$ (300 MHz,

DMSO- d_6); δ 10.63 (1H, s, NH), 7.54 (2H, d, $J = 8.3$ Hz, H-4' & H-6'), 7.28 (2H, d, $J = 8.3$ Hz, H-3' & H-7'), 7.25 – 7.17 (2H, m, NH & H-6), 7.08 (1H, s, H-3), 4.33 (2H, d, $J = 5.9$ Hz, H-1'), 3.81 (3H, s, OCH₃), 3.77 (3H, s, OCH₃), 3.69 (2H, s, H-7); $^{13}\text{C NMR}$ (75 MHz, **DMSO- d_6**); δ 163.5 (C-10), 154.8 (C=O), 153.9 (C-2), 148.2 (C-9), 146.9 (C-1), 139.2 (C-2'), 137.9 (C-5), 131.3 (C-4' & C-6'), 130.0 (C-4), 129.5 (C-3' & C-7'), 126.6 (C-8), 119.9 (C-5'), 110.1 (C-3), 102.2 (C-6), 55.9 (OCH₃), 55.8 & 55.7 ($^+\text{OCH}_3$), 42.3 (H-1'), 33.0 (H-7). **HRMS m/z (ESI)** (C₂₀H₁₈BrN₃O₃S) 460.0405 ([M + H]⁺ requires 460.0325). *Doubling of carbon peaks due to rotamers.

3.5.1.5.27. 1-(5,6-Dimethoxy-8H-indeno[1,2-d]thiazol-2-yl)-3-(4-fluorobenzyl)urea **37**



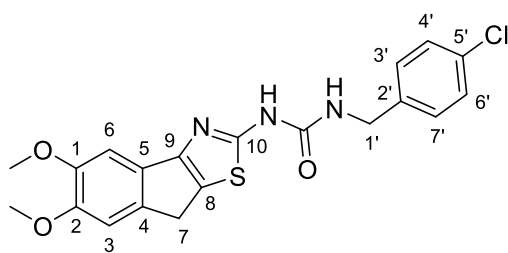
37

(Yield 75%); Light orange solid; R_f 0.37 (3:1 ethyl acetate: hexane); **mp** 206 °C (decomp.); ν_{\max} (neat)/ cm^{-1} 3277 (N-H str, w), 2938 (C-H str, w), 1667 (C=O str, m), 1552 (C-C str (in-ring), s), 1510 (N-H bend, s), 1384 (C-H bend, s), 1276 (C-N str, s), 1214 (s), 1149 (s), 831 (C-H “oop”, m), 773 (C-H “oop”, m); $^1\text{H NMR}$ (300 MHz, **DMSO- d_6**); δ

10.61 (1H, s, NH), 7.36 (2H, dd, $J = 8.4, 5.7$ Hz, H-3 & H-7), 7.26 – 7.12 (4H, m, ArH's & NH), 7.08 (1H, s, H-3), 4.34 (2H, d, $J = 5.7$ Hz, H-1'), 3.81 (3H, s, OCH₃), 3.77 (3H, s, OCH₃), 3.69 (2H, s, H-7); $^{13}\text{C NMR}$ (75 MHz, **DMSO- d_6**); δ 163.6 (C-10), 161.3 (d, $J = 242.2$ Hz, $^{\#}\text{C-5}'$), 154. (C=O), 153.8 (C-2), 148.2 (C-9), 146.9 (C-1), 137.9 (C-5), 135.9 (d, $J = 3.0$ Hz, $^{\#}\text{C-2}'$), 130.0 (C-4), 129.3 (d, $J = 242.2$ Hz, $^{\#}\text{C-3}'$ & C-7'), 126.6 (C-8), 115.2 (d, $J = 21.2$ Hz, $^{\#}\text{C-4}'$ & C-6'), 110.1 (C-3), 102.2 (C-6), 55.91 (OCH₃), 55.8 & 55.7 ($^+\text{OCH}_3$), 42.2 (C-1'), 32.0 (C-7). **HRMS m/z (ESI)** (C₂₀H₁₈FN₃O₃S) 400.1228 ([M + H]⁺ requires 400.1126).

$^{\#}$ Doubling of carbon peaks due to fluorine splitting. *Doubling of carbon peaks due to rotamers.

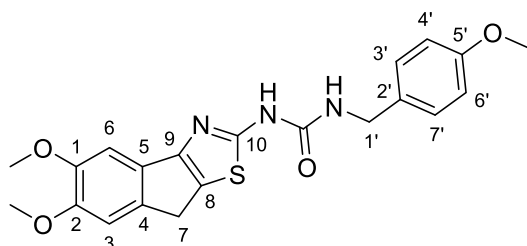
3.5.1.5.28. 1-(4-Chlorobenzyl)-3-(5,6-dimethoxy-8H-indeno[1,2-d]thiazol-2-yl)urea **38**



38

(Yield 79%); Light orange solid; R_f 0.37 (3:1 ethyl acetate: hexane); mp 207 °C (decomp.); ν_{max} (neat)/ cm^{-1} 3215 (N-H str, w), 2936 (C-H str, w), 1667 (C=O str, s), 1550, (C-C str (in-ring), s) 1384 (C-H bend, s), 1276 (C-N str, s), 1208 (s), 1146 (s), 773 (C-Cl str, m); 1H NMR (300 MHz, DMSO- d_6); δ 10.66 (1H, s, NH), 7.41 (2H, d, J = 8.5 Hz, H-3' & H-7'), 7.34 (2H, d, J = 8.5 Hz, H-4' & H-6'), 7.27 (1H, t, J = 5.8 Hz, NH), 7.21 (1H, s, H-6), 7.08 (1H, s, H-3), 4.35 (2H, d, J = 5.8 Hz, H-1'), 3.81 (3H, s, OCH₃), 3.77 (3H, s, OCH₃), 3.69 (2H, s, H-7); ^{13}C NMR (75 MHz, DMSO- d_6); δ 163.6 (C-10), 154.8 (C=O), 153.9 (C-2), 148.2 (C-9), 146.9 (C-1), 138.8 (C-2'), 137.9 (C-5), 131.5 (C-5'), 130.0 (C-4), 129.1 (C-3' & C-7'), 128.4 (C-4' & C-6'), 126.6 (C-8), 110.1 (C-3), 102.2 (C-6), 55.9 (OCH₃), 55.8 & 55.7 ($^+OCH_3$), 42.3 (C-1'), 32.0 (C-7). HRMS m/z (ESI) (C₂₀H₁₈ClN₃O₃S) 416.0860 ([M + H]⁺ requires 416.0830). *Doubling of carbon peaks due to rotamers.

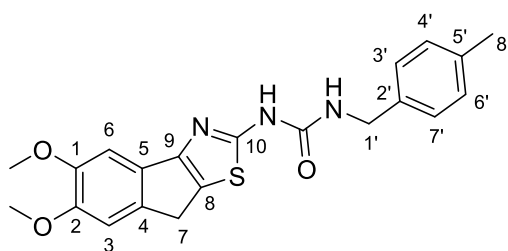
3.5.1.5.29. 1-(5,6-Dimethoxy-8H-indeno[1,2-d]thiazol-2-yl)-3-(4-methoxybenzyl)urea **39**



39

(Yield 74%); Orange solid; R_f 0.39 (3:1 ethyl acetate: hexane); mp 188 °C (decomp.); ν_{max} (neat)/ cm^{-1} 3211 (N-H str, m), 2933 (C-H str, m), 1665 (C=O str, s), 1547 (C-C str (in-ring), s), 1509 (N-H bend, s), 1383 (C-H bend, s), 1242 (C-N str, s), 1204 (s), 1143 (s), 1069 (m), 816 (C-H "oop", m), 771 (C-H "oop", m); 1H NMR (300 MHz, DMSO- d_6); δ 10.48 (1H, s, NH), 7.27 (1H, s, H-6), 7.22 (2H, d, J = 9.8 Hz, H-3' & H-7'), 7.14 – 7.04 (2H, m, NH & C-3), 6.91 (2H, d, J = 8.6 Hz, H-4' & H-6'), 4.28 (2H, d, J = 5.7 Hz, H-1'), 3.81 (3H, s, OCH₃), 3.77 (3H, s, CH₃), 3.73 (3H, s, OCH₃), 3.69 (2H, s, H-7); ^{13}C NMR (75 MHz, DMSO- d_6); δ 163.6 (C-10), 158.4 (C-5'), 154.8 (C=O), 153.7 (C-2), 148.2 (C-9), 146.8 (C-1), 137.9 (C-5), 131.5 (C-2'), 130.1 (C-4), 128.7 (C-3' & C-7'), 126.5 (C-8), 113.8 (C-4' & H-6'), 110.1 (C-3), 102.2 (C-6), 55.9 (OCH₃), 55.8 & 55.7 ($^+OCH_3$), 55.1 (OCH₃), 42.4 (C-1'), 32.0 (C-7). HRMS m/z (ESI) (C₂₁H₂₁N₃O₄S) 412.1391 ([M + H]⁺ requires 412.1325). *Doubling of carbon peaks due to rotamers.

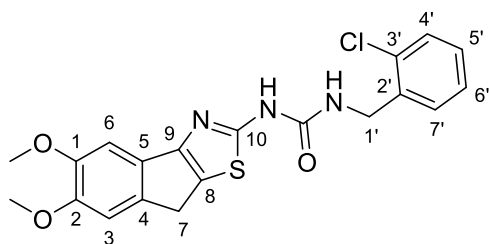
3.5.1.5.30. 1-(5,6-Dimethoxy-8H-indeno[1,2-d]thiazol-2-yl)-3-(4-methylbenzyl)urea **40**



40

(Yield 76%); Pink solid; R_f 0.46 (3:1 ethyl acetate: hexane); mp 99 °C (decomp.); ν_{max} (neat)/ cm^{-1} 3263 (N-H str, w), 2936 (C-H str, w), 1666 (C=O str, s), 1548 (C-C str (in-ring), s), 1385 (C-H bend, s), 1277 (C-N str, s), 1209 (s), 1147 (m), 1072 (m), 774 (C-H "oop", m); 1H NMR (300 MHz, DMSO- d_6); δ 10.54 (1H, s, NH), 7.25 – 7.11 (6H, m, ArH's & NH), 7.08 (1H, s, H-3), 4.31 (2H, d, J = 5.5 Hz, C-1'), 3.81 (3H, s, OCH₃), 3.77 (3H, s, OCH₃), 3.69 (2H, s, H-7), 2.28 (3H, s, H-8'); ^{13}C NMR (75 MHz, DMSO- d_6); δ 163.6 (C-10), 154.7 (C=O), 153.8 (C-2), 148.2 (C-9), 146.9 (C-1), 137.9 (C-5), 136.5 (C-5'), 136.1 (C-2'), 130.0 (C-4), 129.0 (C-4' & C-6'), 127.3 (C-3' & C-7'), 126.5 (C-8), 110.1 (C-3), 102.2 (C-6), 55.9 (OCH₃), 55.8 & 55.7 ($^+OCH_3$), 42.7 (C-1'), 32.0 (C-7), 20.7 (C-8'). HRMS m/z (ESI) (C₂₁H₂₁N₃O₃S) 396.1482 ([M + H]⁺ requires 396.1376). ⁺Doubling of carbon peaks due to rotamers.

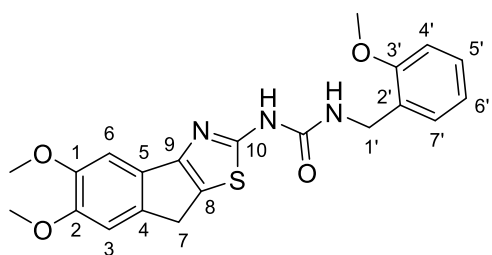
3.5.1.5.31. 1-(2-Chlorobenzyl)-3-(5,6-dimethoxy-8H-indeno[1,2-d]thiazol-2-yl)urea **41**



41

(Yield 91%); Yellow solid; R_f 0.50 (3:1 ethyl acetate: hexane); mp 195 °C (decomp.); ν_{max} (neat)/ cm^{-1} 3189 (N-H str, w), 2957 (C-H str, m), 1697 (C=O str, m), 1549 (C-C str (in-ring), s), 1463 (C-C str, m), 1387 (C-H bend, m), 1277 (C-N str, s), 1211 (s), 751 (C-Cl str, m); 1H NMR (300 MHz, DMSO- d_6); δ 10.76 (1H, s, NH), 7.53 – 7.26 (5H, m, ArH's & NH), 7.20 (1H, s, H-6), 7.10 (1H, s, H-3), 4.44 (2H, d, J = 5.5 Hz, H-1'), 3.81 (3H, s, OCH₃), 3.77 (3H, s, OCH₃), 3.69 (2H, s, H-7); ^{13}C NMR (75 MHz, DMSO- d_6); δ 163.5 (C-10), 154.8 (C=O), 153.9 (C-2), 148.2 (C-9), 146.9 (C-1), 137.9 (C-5), 136.6 (C-2'), 132.1 (C-3'), 130.0 (C-4), 129.3 (C-4'), 129.0 (C-7'), 128.9 (C-5'), 127.4 (C-6'), 126.6 (C-8), 110.1 (C-3), 102.3 (C-6), 55.9 (OCH₃), 55.8 & 55.7 ($^+OCH_3$), 41.0 (C-1'), 32.0 (C-7). HRMS m/z (ESI) (C₂₀H₁₈ClN₃O₃S) 416.0949 ([M + H]⁺ requires 416.0830). ⁺Doubling of carbon peaks due to rotamers.

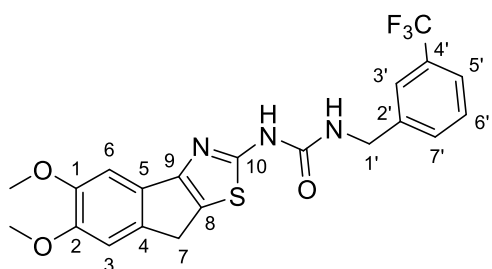
3.5.1.5.32. 1-(5,6-Dimethoxy-8H-indeno[1,2-d]thiazol-2-yl)-3-(2-methoxybenzyl)urea **42**



42

(Yield 73%); Pink solid; R_f 0.41 (3:1 ethyl acetate: hexane); **mp** 128 °C (decomp.); ν_{\max} (neat)/ cm^{-1} 3331 (N-H str, w), 2948 (C-H bend, w), 1672 (C=O str, s), 1552 (C-C str (in-ring), s), 1458 (C-C str, m), 1383 (C-H str, m), 1275 (C-N str, s), 1211 (s), 1070 (m), 992 (m), 855 (m), 755 (C-H "oop", s); $^1\text{H NMR}$ (300 MHz, $\text{DMSO-}d_6$); δ 10.50 (1H, s, NH), 7.33 – 7.18 (3H, m, ArH's), 7.11 – 6.99 (3H, m, ArH's), 6.97 -6.90 (1H, m, NH), 4.33 (2H, d, $J = 5.7$ Hz, H-1'), 3.85 (3H, s, OCH_3), 3.82 (3H, s, OCH_3), 3.78 (3H, s, OCH_3), 3.70 (2H, s, H-7); $^{13}\text{C NMR}$ (75 MHz, $\text{DMSO-}d_6$); δ 163.6 (C-10), 156.9 (C-3'), 154.9 (C=O), 153.7 (C-2), 148.2 (C-9), 146.8 (C-1), 137.9 (C-5), 130.1 (C-4), 128.5 (C-7'), 128.3 (C-5'), 126.8 (C-2'), 126.5 (C-8), 120.3 (C-6'), 110.7 (C-4'), 110.1 (C-3), 102.2 (C-6), 55.9 (OCH_3), 55.8 & 55.7 ($^+\text{OCH}_3$), 55.4 (OCH_3), 38.6 (C-1'), 32.0 (C-7). **HRMS m/z (ESI)** ($\text{C}_{21}\text{H}_{21}\text{N}_3\text{O}_4\text{S}$) 412.1391 ($[\text{M} + \text{H}]^+$ requires 412.1325). $^+$ Doubling of carbon peaks due to rotamers.

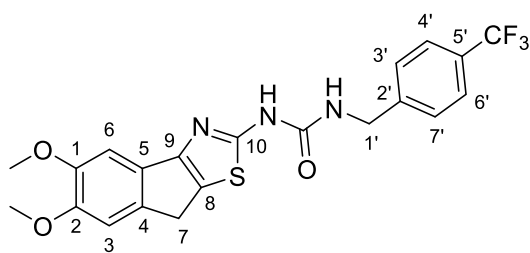
3.5.1.5.33. 1-(5,6-Dimethoxy-8H-indeno[1,2-d]thiazol-2-yl)-3-[3-(trifluoromethyl)benzyl]urea **43**



43

(Yield 87 %); Off-white solid; R_f 0.39 (3:1 ethyl acetate: hexane); **mp** 200 °C (decomp.); ν_{\max} (neat)/ cm^{-1} 3234 (N-H str, w), 2950 (C-H str, w), 2626 (m), 1725 (C=O str, s), 1547 (C-C str (in-ring), vs), 1329 (C-H bend, s), 1272 (C-N str, s), 1212 (s), 1155 (s), 1106 (C-F str, s), 1069 (s), 693 (C-H "oop", s); $^1\text{H NMR}$ (300 MHz, $\text{DMSO-}d_6$); δ 11.04 (1H, br s, NH), 7.76 (1H, t, $J = 5.6$ Hz, NH), 7.70 – 7.54 (4H, m, ArH's), 7.20 (1H, s, H-6), 7.13 (1H, s, H-3), 4.45 (2H, d, $J = 5.5$ Hz, H-1'), 3.80 (3H, s, OCH_3), 3.77 (3H, s, OCH_3), 3.69 (2H, s, H-7); $^{13}\text{C NMR}$ (75 MHz, $\text{DMSO-}d_6$); δ 163.8 (C-10), 154.0 (C=O), 152.9 (C-2), 148.2 (C-9), 147.1 (C-1), 141.3 (C-2'), 138.0 (C-5), 131.4 (C-4), 129.6 (C-4'), 129.4 (C-7'), 129.3 (C-6') 128.9 (C-3'), 126.5 (C-8), 123.7 (C-5'), 123.7 (ArCF₃), 110.1 (C-3), 102.4 (C-6), 56.0 & 55.9 ($^+\text{OCH}_3$), 55.8 & 55.7 ($^+\text{OCH}_3$), 42.5 (C-1'), 32.3 (C-7). **HRMS m/z (ESI)** ($\text{C}_{21}\text{H}_{18}\text{F}_3\text{N}_3\text{O}_3\text{S}$) 450.1161 ($[\text{M} + \text{H}]^+$ requires 450.1094). $^+$ Doubling of carbon peaks due to rotamers.

3.5.1.5.34. 1-(5,6-Dimethoxy-8H-indeno[1,2-d]thiazol-2-yl)-3-[4-(trifluoromethyl)benzyl]urea **44**

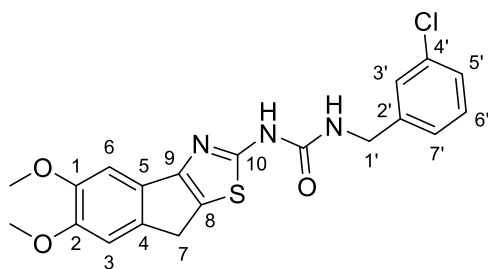


44

(Yield 76 %); Brown solid; R_f 0.37 (3:1 ethyl acetate: hexane); mp 170 °C (decomp.); ν_{max} (neat)/ cm^{-1} 3349 (N-H str, w), 2935 (C-H str, w), 1668 (C=O str, s), 1565 (C-C str (in-ring), s), 1517 (N-H bend, s), 1384 (C-H bend, m), 1324 (s), 1275 (C-N str, s), 1109 (C-F str, s), 1066 (s), 833 (C-H "oop", m), 772 (C-H "oop", m); 1H

NMR (300 MHz, DMSO- d_6); δ 10.70 (1H, s, NH), 7.72 (2H, d, J = 8.2 Hz, H-4' & H-6'), 7.54 (2H, d, J = 8.1 Hz, H-3' & H-7'), 7.33 (1H, t, J = 5.9 Hz, NH), 7.21 (1H, s, H-6), 7.09 (1H, s, H-3), 4.46 (2H, d, J = 5.8 Hz, H-1'), 3.81 (3H, s, OCH₃), 3.78 (3H, s, OCH₃), 3.69 (2H, s, H-7); ^{13}C **NMR (75 MHz, DMSO- d_6)**; δ 163.5 (C-10), 154.9 (C=O), 154.0 (C-2), 148.2 (C-9), 146.9 (C-1), 144.8 (C-2'), 137.9 (C-5), 130.1 (C-4), 127.8 (C-3' & C-7'), 127.4 (C-5'), 126.6 (C-8), 125.3 (H-4' & H-6'), 125.3 (ArCF₃) 110.1 (C-3), 102.2 (C-6), 55.91 (OCH₃), 55.8 & 55.7 (⁺OCH₃), 42.6 (C-1'), 32.0 (C-7). **HRMS m/z (ESI)** (C₂₁H₁₈F₃N₃O₃S) 450.1161 ([M + H]⁺ requires 450.1094). ⁺Doubling of carbon peaks due to rotomers.

3.5.1.5.35. 1-(3-Chlorobenzyl)-3-(5,6-dimethoxy-8H-indeno[1,2-d]thiazol-2-yl)urea **45**



45

(Yield 74 %); Pink solid; R_f 0.41 (3:1 ethyl acetate: hexane); mp 80 °C (decomp.); ν_{max} (neat)/ cm^{-1} 3271 (N-H str, w), 2938 (C-H str, w), 1667 (C=O str, m), 1550 (C-C str, s), 1384 (C-H bend, s), 1276 (C-N str, s), 1208 (s), 1146 (s), 1072 (s), 847 (C-H "oop", m), 774 (C-Cl str, m); 1H **NMR (300 MHz, DMSO- d_6)**; δ 10.66 (1H, s, NH), 7.42 – 7.23 (5H, m, ArH's & NH), 7.20 (1H, s, H-6), 7.08 (1H, s, H-3), 4.37 (2H, d, J = 5.4

Hz, H-1'), 3.81 (3H, s, OCH₃), 3.77 (3H, s, OCH₃), 3.69 (2H, s, H-7); ^{13}C **NMR (75 MHz, DMSO- d_6)**; δ 163.5 (C-10), 154.9 (C=O), 153.9 (C-2), 148.2 (C-9), 146.9 (C-1), 142.4 (C-2'), 137.9 (C-5), 133.1 (C-4'), 130.3 (C-7'), 130.1 (C-4), 127.0 (C-3'), 126.9 (C-5'), 126.6 (C-8), 125.9 (C-6'), 110.1 (C-3), 102.2 (C-6), 55.9 & 55.8 (⁺OCH₃), 55.7 (OCH₃), 42.4 (C-1'), 32.0 (C-7). **HRMS m/z (ESI)** (C₂₀H₁₈ClN₃O₃S) 416.0949 ([M + H]⁺ requires 416.0830). ⁺Doubling of carbon peaks due to rotomers.

3.5.2. Bioactivity screening

Prior to screening, all compounds were dissolved in dimethyl sulfoxide due to the compounds being insoluble in high concentrations of water (10 mM). The final concentration of dimethyl sulfoxide in the assay were below 1%.

3.5.2.1. *Acetylcholinesterase inhibitory activity*

Cholinesterase inhibitory activity for *EeAChE* was determined using the 5,5-dithiobis-2-nitrobenzoic acid (DTNB) assay as described by Ellman [42] and modified by Eldeen and co-workers [43]. Three buffers were prepared: Buffer A – 50 mM Tris-hydrochloride (pH 8); Buffer B - 50 mM Tris-hydrochloride (pH 8), containing 0.1% bovine serum albumin; Buffer C - 50 mM Tris-hydrochloride (pH 8), fortified with 0.1 M sodium chloride and 0.02 M magnesium chloride. Into 96-well plates were pipetted: 25 mL acetylthiocholine iodide (15 mM in distilled water), 125 mL DTNB (3 mM in buffer C), 50 mL buffer B and either 25 mL buffer A (negative control), galantamine (positive control at 1 μ M) or compounds **11** - **45**. Absorbance was measured at 405 nm (four times) to account for baseline interference. An aliquot of 25 mL *EeAChE* (0.2 U/mL in buffer A) was pipetted into the plates and the absorbance measured every 45 s for fifteen cycles. *EeAChE* inhibition (%) was determined as the rate of the reaction (correcting for spontaneous colour changes) relative to the negative control.

3.5.2.2. *Cytotoxicity screening*

Cytotoxicity was assessed using the SRB staining assay on the SH-SY5Y neuroblastoma cell line as described by Vichai and Kirtikara with minor modifications [44]. Although the SH-SY5Y cell line is cancerous in nature, it does present as a model of a neurological cellular environment. The SH-SY5Y cell line was cultured in DMEM/Ham's F12 nutrient, in a 1 to 1 ratio, medium supplemented with 10% foetal calf serum (FCS) in 75 mL flasks at 37 °C and 5% CO₂ in a humidified incubator. Culture flasks with confluent cells were rinsed with phosphate buffered saline and harvested using TrypLe™ Express to detach the cells. Detached cells were centrifuged (200 x *g*, 5 min), counted using the trypan blue exclusion assay (0.1%), and diluted to 1 x 10⁵ cells/ μ L in 10% FCS-fortified medium. The cell suspension (100 μ L) was seeded into sterile, clear 96-well plates, and incubated overnight to allow the cells to attach. Blank wells contained 200 μ L FCS (5%)-fortified media without cells to account for background noise and sterility. Attached cells were exposed to 100 μ L medium (negative control), compounds **11** - **45** (0.01 - 100 μ M) or saponin (1%; positive control) prepared in FCS negative medium for 72 h at 37 °C and 5% CO₂ in a humidified incubator. Cells were fixed in the wells by adding 50 μ L trichloroacetic acid (50%) and left overnight at 4 °C. Plates containing the fixed cells were washed three times with tap water and stained using 100 μ L SRB solution (0.057% in 1% acetic acid) for 30 min at room temperature in the dark. Stained cells were washed four times with 150 μ L acetic acid (1%) and air-dried. The bound dye was eluted using 200 μ L Tris-buffer (10 mM, pH 10.5) and the absorbance measured at 510 nm (reference 630 nm) using a ELx 800 microplate plate reader (Bio-Tek Instruments, Inc.). The blank value was subtracted from all the other values and the cell density was expressed relative to the negative control as a percentage.

3.5.2.3. Statistics

Assays were performed as three intra- as well as three inter-replicates. Statistical analyses were performed using Graph-Pad Prism 5.0 (GraphPad). The AChE IC₅₀ values were determined using non-linear regression analysis.

3.6. MOLECULAR MODELLING

Molecular docking for AChE was performed using the crystal structure of Torpedo eel acetylcholinesterase (PDB: 1EVE) [46] and Glide XP [47, 48] from the Schrödinger program suite. The binding pocket consists of the CAS containing Trp84 and Phe330 while the PAS consists mainly of Tyr70, Asp72, Try 121, Tyr334 and Trp279.

The crystal structure contains donepezil bound into the 20 Å deep gorge which is highly solvated, with the R-configuration of the alpha carbon of the indanone carbonyl being noted. Donepezil was docked back into the crystal structure and it was noted that several of the water molecules had to be included during the docking process to obtain the correct binding pose. This resulted in water-bridged interactions between the ligand and the residues within the binding pocket. However, this water bridge interaction was kept only with compound **4** as compounds **11** and **34** did not form this water bridge interaction with HOH1159 and Tyr121.

Molecular docking for GSK-3 was performed using the crystal structure of human GSK-3 (PDB: 1Q5K) [37] and Glide XP [47, 48] from the Schrödinger program suite. The crystal structure contains AR-A014418 **6** bound into the ATP active site of GSK-3. The ATP active site consists mainly of Arg141, Pro136, Val135 and Lys85. The docking protocol was confirmed by docking the crystallized ligand **6** back into the binding pocket and ensuring that the generated pose overlapped within a root-mean-square deviation (RMSD) of less than 2 Å. AR-A014418 **6** was found to form a H-bond with HOH626. HOH626 was removed so that the synthesized ligands may produce acceptable docking poses for GSK-3.

3.7. ACKNOWLEDGEMENTS

This work was supported by the National Research Foundation (NRF) of South Africa (Thuthuka grant number 87893), the University of Pretoria (University, Science Faculty Research Councils and Research and Development Program) and the Council for Scientific and Industrial Research (CSIR), South Africa. Opinions expressed in this publication and the conclusions arrived at, are those of the authors, and are not necessarily attributed to the NRF. The authors would like to gratefully acknowledge Ms Madelien Wooding (University of Pretoria) for LC-MS services.

3.8. CONFLICT OF INTEREST

The authors declare no conflict of interest.

3.9. APPENDIX B. SUPPLEMENTARY INFORMATION

Appendix B can be found as a separate document on the CD.

3.10. REFERENCES

- [1] C.B. Mishra, S. Kumari, M. Tiwari, Thiazole: a promising heterocycle for the development of potent CNS active agents, *Eur. J. Med. Chem.*, 92 (2015) 1-34.
- [2] D.-H. Shi, Z.-M. Tang, Y.-W. Liu, J.R. Harjani, H.-L. Zhu, X.-D. Ma, X.-K. Song, W.-W. Liu, C. Lu, W.-T. Yang, M.-Q. Song, Design, synthesis and biological evaluation of novel 2-phenylthiazole derivatives for the treatment of Alzheimer's disease, *ChemistrySelect*, 2 (2017) 10572-10579.
- [3] R.R. Gupta, M. Kumar, V. Gupta, *Heterocyclic chemistry: Volume II: Five-membered heterocycles*, Springer Berlin Heidelberg, 2013.
- [4] A.I. Vogel, A.R. Tatchell, B.S. Furnis, A.J. Hannaford, P.W.G. Smith, *Vogel's textbook of practical organic chemistry*, 5th ed., Pearson, 1996.
- [5] I. Singh, Synthesis, characterization and antimicrobial activity of some thiazole derivatives, *Chem. Sci. Trans.*, 4 (2015) 458-462.
- [6] B.K. Sarojini, B.G. Krishna, C.G. Darshanraj, B.R. Bharath, H. Manjunatha, Synthesis, characterization, *in vitro* and molecular docking studies of new 2,5-dichloro thienyl substituted thiazole derivatives for antimicrobial properties, *Eur. J. Med. Chem.*, 45 (2010) 3490-3496.
- [7] F. Chimenti, B. Bizzarri, A. Bolasco, D. Secci, P. Chimenti, A. Granese, S. Carradori, M. D'Ascenzio, D. Lilli, D. Rivanera, Synthesis and biological evaluation of novel 2,4-disubstituted-1,3-thiazoles as anti-*Candida spp.* agents, *Eur. J. Med. Chem.*, 46 (2011) 378-382.
- [8] Z. Xu, M. Ba, H. Zhou, Y. Cao, C. Tang, Y. Yang, R. He, Y. Liang, X. Zhang, Z. Li, L. Zhu, Y. Guo, C. Guo, 2,4,5-Trisubstituted thiazole derivatives: a novel and potent class of non-nucleoside inhibitors of wild type and mutant HIV-1 reverse transcriptase, *Eur. J. Med. Chem.*, 85 (2014) 27-42.
- [9] S. Tassini, L. Sun, K. Lanko, E. Crespan, E. Langron, F. Falchi, M. Kissova, J.I. Armijos-Rivera, L. Delang, C. Mirabelli, J. Neyts, M. Pieroni, A. Cavalli, G. Costantino, G. Maga, P. Vergani, P. Leyssen, M. Radi, Discovery of multitarget agents active as broad-spectrum antivirals and correctors of cystic fibrosis transmembrane conductance regulator for associated pulmonary diseases, *J. Med. Chem.*, 60 (2017) 1400-1416.
- [10] A.S. Mayhoub, M. Khaliq, R.J. Kuhn, M. Cushman, Design, synthesis, and biological evaluation of thiazoles targeting flavivirus envelope proteins, *J. Med. Chem.*, 54 (2011) 1704-1714.

- [11] H. Su, L. Yu, A. Nebbioso, V. Carafa, Y. Chen, L. Altucci, Q. You, Novel *N*-hydroxybenzamide-based HDAC inhibitors with branched CAP group, *Bioorg. Med. Chem. Lett.*, 19 (2009) 6284-6288.
- [12] S.M. El-Messery, G.S. Hassan, F.A. Al-Omary, H.I. El-Subbagh, Substituted thiazoles VI. Synthesis and antitumor activity of new 2-acetamido- and 2 or 3-propanamido-thiazole analogs, *Eur. J. Med. Chem.*, 54 (2012) 615-625.
- [13] N. Siddiqui, W. Ahsan, Triazole incorporated thiazoles as a new class of anticonvulsants: design, synthesis and *in vivo* screening, *Eur. J. Med. Chem.*, 45 (2010) 1536-1543.
- [14] N. Ahangar, A. Ayati, E. Alipour, A. Pashapour, A. Foroumadi, S. Emami, 1-[(2-Arylthiazol-4-yl)methyl]azoles as a new class of anticonvulsants: design, synthesis, *in vivo* screening, and *in silico* drug-like properties, *Chem. Biol. Drug. Des.*, 78 (2011) 844-852.
- [15] K.M. Amin, D.E. Rahman, Y.A. Al-Eryani, Synthesis and preliminary evaluation of some substituted coumarins as anticonvulsant agents, *Bioorg. Med. Chem.*, 16 (2008) 5377-5388.
- [16] C.B. Rodl, D. Vogt, S.B. Kretschmer, K. Ihlefeld, S. Barzen, A. Bruggerhoff, J. Achenbach, E. Proschak, D. Steinhilber, H. Stark, B. Hofmann, Multi-dimensional target profiling of *N*,4-diaryl-1,3-thiazole-2-amines as potent inhibitors of eicosanoid metabolism, *Eur. J. Med. Chem.*, 84 (2014) 302-311.
- [17] R.S. Giri, H.M. Thaker, T. Giordano, J. Williams, D. Rogers, V. Sudersanam, K.K. Vasu, Design, synthesis and characterization of novel 2-(2,4-disubstituted-thiazole-5-yl)-3-aryl-3*H*-quinazoline-4-one derivatives as inhibitors of NF- κ B and AP-1 mediated transcription activation and as potential anti-inflammatory agents, *Eur. J. Med. Chem.*, 44 (2009) 2184-2189.
- [18] R. Aggarwal, S. Kumar, P. Kaushik, D. Kaushik, G.K. Gupta, Synthesis and pharmacological evaluation of some novel 2-(5-hydroxy-5-trifluoromethyl-4,5-dihydropyrazol-1-yl)-4-(coumarin-3-yl)thiazoles, *Eur. J. Med. Chem.*, 62 (2013) 508-514.
- [19] M.R. Ali, S. Kumar, O. Afzal, N. Shalmali, M. Sharma, S. Bawa, Development of 2-(substituted benzylamino)-4-methyl-1,3-thiazole-5-carboxylic acid derivatives as xanthine oxidase inhibitors and free radical scavengers, *Chem. Biol. Drug. Des.*, 87 (2016) 508-516.
- [20] G.G. Mandawad, B.S. Dawane, S.D. Beedkar, C.N. Khobragade, O.S. Yemul, Trisubstituted thiophene analogues of 1-thiazolyl-2-pyrazoline, super oxidase inhibitors and free radical scavengers, *Bioorg. Med. Chem.*, 21 (2013) 365-372.
- [21] K.-M. Kim, K.-H. Kim, T.-C. Kang, W.-Y. Kim, M.-R. Lee, H.-J. Jung, I.K. Hwang, S.-B. Ko, J.-Y. Koh, M.H. Won, E.-G. Oh, I. Shin, Design and biological evaluation of novel antioxidants containing *N*-*t*-butyl-*N*-hydroxylaminophenyl moieties, *Bioorg. Med. Chem. Lett.*, 13 (2003) 2273-2275.
- [22] J.F. Cheng, C.C. Mak, Y. Huang, R. Penuliar, M. Nishimoto, L. Zhang, M. Chen, D. Wallace, T. Arrhenius, D. Chu, G. Yang, M. Barbosa, R. Barr, J.R. Dyck, G.D. Lopaschuk, A.M. Nadzan, Heteroaryl

substituted bis-trifluoromethyl carbinols as malonyl-CoA decarboxylase inhibitors, *Bioorg. Med. Chem. Lett.*, 16 (2006) 3484-3488.

[23] G. Mariappan, P. Prabhat, L. Sutharson, J. Banerjee, U. Patangia, S. Nath, Synthesis and antidiabetic evaluation of benzothiazole derivatives, *J. Korean Chem. Soc.*, 56 (2012) 251-256.

[24] C.S. Li, L. Belair, J. Guay, R. Murgasva, W. Sturkenboom, Y.K. Ramtohol, L. Zhang, Z. Huang, Thiazole analog as stearyl-CoA desaturase 1 inhibitor, *Bioorg. Med. Chem. Lett.*, 19 (2009) 5214-5217.

[25] G. Yan, L. Hao, Y. Niu, W. Huang, W. Wang, F. Xu, L. Liang, C. Wang, H. Jin, P. Xu, 2-Substituted-thio-*N*-(4-substituted-thiazol/1*H*-imidazol-2-yl)acetamides as BACE1 inhibitors: Synthesis, biological evaluation and docking studies, *Eur. J. Med. Chem.*, 137 (2017) 462-475.

[26] I. Lagoja, C. Pannecouque, G. Griffioen, S. Wera, V.M. Rojadelaparra, A. Van Aerschot, Substituted 2-aminothiazoles are exceptional inhibitors of neuronal degeneration in tau-driven models of Alzheimer's disease, *Eur. J. Pharm. Sci.*, 43 (2011) 386-392.

[27] L. Hroch, O. Benek, P. Guest, L. Aitken, O. Soukup, J. Janockova, K. Musil, V. Dohnal, R. Dolezal, K. Kuca, T.K. Smith, F. Gunn-Moore, K. Musilek, Design, synthesis and *in vitro* evaluation of benzothiazole-based ureas as potential ABAD/17 β -HSD10 modulators for Alzheimer's disease treatment, *Bioorg. Med. Chem. Lett.*, 26 (2016) 3675-3678.

[28] B.N. Sağlık, S. Ilgın, Y. Özkay, Synthesis of new donepezil analogues and investigation of their effects on cholinesterase enzymes, *Eur. J. Med. Chem.*, 124 (2016) 1026-1040.

[29] A. Andreani, S. Burnelli, M. Granaiola, M. Guardigli, A. Leoni, A. Locatelli, R. Morigi, M. Rambaldi, M. Rizzoli, L. Varoli, A. Roda, Chemiluminescent high-throughput microassay applied to imidazo[2,1-*b*]thiazole derivatives as potential acetylcholinesterase and butyrylcholinesterase inhibitors, *Eur. J. Med. Chem.*, 43 (2008) 657-661.

[30] R. Raza, A. Saeed, M. Arif, S. Mahmood, M. Muddassar, A. Raza, J. Iqbal, Synthesis and biological evaluation of 3-thiazolocoumarinyl Schiff-base derivatives as cholinesterase inhibitors, *Chem. Biol. Drug. Des.*, 80 (2012) 605-615.

[31] F. Sonmez, B. Zengin Kurt, I. Gazioglu, L. Basile, A. Dag, V. Cappello, T. Ginex, M. Kucukislamoglu, S. Guccione, Design, synthesis and docking study of novel coumarin ligands as potential selective acetylcholinesterase inhibitors, *J. Enzyme. Inhib. Med. Chem.*, 32 (2017) 285-297.

[32] B.Z. Kurt, I. Gazioglu, L. Basile, F. Sonmez, T. Ginex, M. Kucukislamoglu, S. Guccione, Potential of aryl-urea-benzofuranylthiazoles hybrids as multitasking agents in Alzheimer's disease, *Eur. J. Med. Chem.*, 102 (2015) 80-92.

[33] D. Knez, N. Coquelle, A. Pisljar, S. Zakelj, M. Jukic, M. Sova, J. Mravljak, F. Nachon, X. Brazzolotto, J. Kos, J.P. Colletier, S. Gobec, Multi-target-directed ligands for treating Alzheimer's disease:

Butyrylcholinesterase inhibitors displaying antioxidant and neuroprotective activities, *Eur. J. Med. Chem.*, 156 (2018) 598-617.

[34] Q. Li, H. Yang, Y. Chen, H. Sun, Recent progress in the identification of selective butyrylcholinesterase inhibitors for Alzheimer's disease, *Eur. J. Med. Chem.*, 132 (2017) 294-309.

[35] B.Z. Kurt, I. Gazioglu, F. Sonmez, M. Kucukislamoglu, Synthesis, antioxidant and anticholinesterase activities of novel coumarylthiazole derivatives, *Bioorg. Chem.*, 59 (2015) 80-90.

[36] B. Kaboudin, M. Arefi, S. Emadi, V. Sheikh-Hasani, Synthesis and inhibitory activity of ureidophosphonates, against acetylcholinesterase: pharmacological assay and molecular modeling, *Bioorg. Chem.*, 41-42 (2012) 22-27.

[37] R. Bhat, Y. Xue, S. Berg, S. Hellberg, M. Ormo, Y. Nilsson, A.C. Radesater, E. Jerning, P.O. Markgren, T. Borgegard, M. Nylof, A. Gimenez-Cassina, F. Hernandez, J.J. Lucas, J. Diaz-Nido, J. Avila, Structural insights and biological effects of glycogen synthase kinase 3-specific inhibitor AR-A014418, *J. Biol. Chem.*, 278 (2003) 45937-45945.

[38] J.-J. Pei, E. Braak, H. Braak, I. Grundke-Iqbal, K. Iqbal, B. Winblad, R.F. Cowburn, Distribution of active glycogen synthase kinase 3 β (GSK-3 β) in brains staged for Alzheimer disease neurofibrillary changes, *J. Neuropathol. Exp. Neurol.*, 58 (1999) 1010-1019.

[39] R.A. Shiurba, K. Ishiguro, M. Takahashi, K. Sato, E.T. Spooner, M. Mercken, R. Yoshida, T.R. Wheelock, H. Yanagawa, K. Imahori, R.A. Nixon, Immunocytochemistry of tau phosphoserine 413 and tau protein kinase I in Alzheimer pathology, *Brain Res.*, 737 (1996) 119-132.

[40] T. Jaworski, I. Dewachter, B. Lechat, M. Gees, A. Kremer, D. Demedts, P. Borghgraef, H. Devijver, S. Kugler, S. Patel, J.R. Woodgett, F. Van Leuven, GSK-3 α/β kinases and amyloid production *in vivo*, *Nature*, 480 (2011) 4-5.

[41] D.G. van Greunen, W. Cordier, M. Nell, C. van der Westhuyzen, V. Steenkamp, J.-L. Panayides, D.L. Riley, Targeting Alzheimer's disease by investigating previously unexplored chemical space surrounding the cholinesterase inhibitor donepezil, *Eur. J. Med. Chem.*, 127 (2017) 671-690.

[42] G.L. Ellman, K.D. Courtney, V. Andres, Jr., R.M. Feather-Stone, A new and rapid colorimetric determination of acetylcholinesterase activity, *Biochem. Pharmacol.*, 7 (1961) 88-95.

[43] I.M. Eldeen, E.E. Elgorashi, J. van Staden, Antibacterial, anti-inflammatory, anti-cholinesterase and mutagenic effects of extracts obtained from some trees used in South African traditional medicine, *J. Ethnopharmacol.*, 102 (2005) 457-464.

[44] V. Vichai, K. Kirtikara, Sulforhodamine B colorimetric assay for cytotoxicity screening, *Nat. Protoc.*, 1 (2006) 1112-1116.

- [45] D.G. van Greunen, C.J. van der Westhuizen, W. Cordier, M. Nell, A. Stander, V. Steenkamp, J.-L. Panayides, D.L. Riley, Novel *N*-benzylpiperidine carboxamide derivatives as potential cholinesterase inhibitors for the treatment of Alzheimer's disease, *Eur. J. Med. Chem.*, 179 (2019) 680-693.
- [46] G. Kryger, I. Silman, J.L. Sussman, Structure of acetylcholinesterase complexed with E2020 (Aricept®): implications for the design of new anti-Alzheimer drugs, *Structure*, 7 (1999) 297-307.
- [47] R.A. Friesner, J.L. Banks, R.B. Murphy, T.A. Halgren, J.J. Klicic, D.T. Mainz, M.P. Repasky, E.H. Knoll, M. Shelley, J.K. Perry, D.E. Shaw, P. Francis, P.S. Shenkin, Glide: a new approach for rapid, accurate docking and scoring. 1. Method and assessment of docking accuracy, *J. Med. Chem.*, 47 (2004) 1739-1749.
- [48] T.A. Halgren, R.B. Murphy, R.A. Friesner, H.S. Beard, L.L. Frye, W.T. Pollard, J.L. Banks, Glide: a new approach for rapid, accurate docking and scoring. 2. Enrichment factors in database screening, *J. Med. Chem.*, 47 (2004) 1750-1759.

Chapter 4. Novel 1-amino-3-(indeno[1,2-*b*]indol-5(10*H*)-yl)propan-2-ol derivatives as possible β -secretase inhibitors for the treatment of Alzheimer's disease

Contributions to this Chapter

All of the synthesis and compound characterization described in this chapter were performed by Mr DG van Greunen under the supervision of Dr DL Riley and Dr J-L Panayides. The synthetic work was undertaken in the Department of Chemistry at the University of Pretoria. All of the BACE1 biological assays and statistical analysis described in this chapter were performed by Mr DG van Greunen under the supervision of Prof V Steenkamp and Dr J-L Panayides, with assistance from Dr W Cordier and Ms M Nell. The cytotoxicity assays and statistical analysis performed by Ms M Nell. The biological work was undertaken in the Department of Pharmacology at the University of Pretoria.

Novel 1-amino-3-(indeno[1,2-*b*]indol-5(10*H*)-yl)propan-2-ol derivatives as possible β -secretase inhibitors for the treatment of Alzheimer's disease

Divan G. van Greunen^a, Werner Cordier^b, Margo Nell^b, Vanessa Steenkamp^b, Jenny-Lee Panayides^c, Darren L. Riley^{a,*}

^a Department of Chemistry, Faculty of Natural and Agricultural Sciences, University of Pretoria, Lynnwood Road, Pretoria, South Africa

^b Department of Pharmacology, Faculty of Health Sciences, University of Pretoria, Bophelo Road, Pretoria, South Africa

^c Pioneering Health Sciences, CSIR Biosciences, Meiring Naudé Road, Pretoria, South Africa

* Corresponding author. E-mail address: darren.riley@up.ac.za (D.L. Riley)

ABSTRACT

A series of seventeen β -secretase 1 inhibitors, as potential agents for the treatment of Alzheimer's disease, were designed and synthesized based on the skeleton of 1-(3,6-dichloro-9*H*-carbazol-9-yl)-3-(naphthalen-1-ylamino)propan-2-ol **5**, a compound previously synthesized by Macchia and co-workers, which has an *in vitro* IC₅₀ value of 0.50 μ M against β -secretase 1. The most active analogue, *rac*-1-[benzyl(methyl)amino]-3-(indeno[1,2-*b*]indol-5(10*H*)-yl)propan-2-ol **24** indicated an inhibition of 91% against β -secretase (human) with an observable cytotoxicity of IC₅₀ of 10.51 \pm 1.11 μ M against the SH-SY5Y cell line.

Key Words

Acetylcholinesterase, Alzheimer's disease, β -secretase 1, epoxide ring opening, indole

4.1. INTRODUCTION

Indole **1** is an electron rich benzopyrrole system in which a benzene ring is fused to a pyrrole ring at the 2-and 3-positions of the pyrrole (**Figure 4.1**) [1]. It is an aromatic molecule which satisfies Hückel's rule for aromaticity by having 10 π electrons (2 π electrons from the nitrogen lone pair and 8 π electrons from the double bonds). As with pyrrole, the π -excessive nature of the aromatic ring governs its reactivity and chemical properties [2]. It is classified as a weak base with a pK_a value of -3.5 and protonates only in the presence of strong acids as protonation of the nitrogen atom would disrupt the aromaticity of the five-membered ring [2, 3].

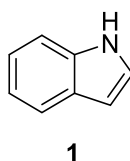
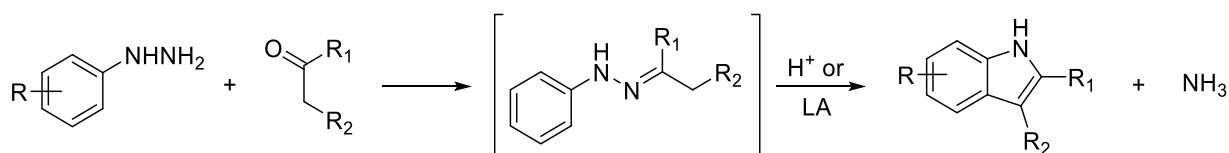


Figure 4.1. Indole.

Considered one of the most important heterocycles in heterocyclic chemistry, synthesis of substituted indoles has attracted a lot of attention in synthetic organic chemistry, and as such a great variety of synthetic methodologies and approaches have been devised [4, 5]. A few notable syntheses include the Fischer (**Scheme 4.1**), Bartoli (**Scheme 4.2**), Bischler-Möhlau (**Scheme 4.3**) and Madelung approaches (**Scheme 4.4**) [2].

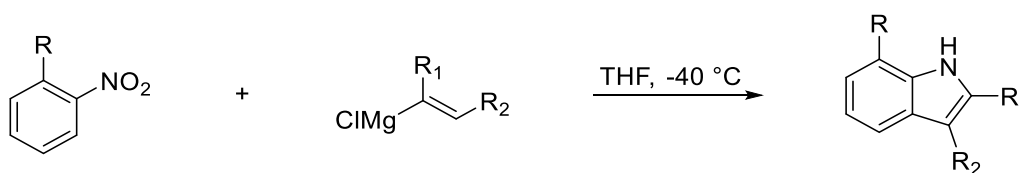
The Fischer indole synthesis (**Scheme 4.1**) is one of the most common ways to afford substituted indole derivatives. The methodology involves the heating of (un)substituted phenyl hydrazines with aldehydes or ketones in a suitable protic solvent to form a substituted phenyl hydrazone. This intermediate subsequently rearranges and liberates ammonia in the presence of a protic acid or a Lewis acid (LA) to afford the required substituted indole [6].



Scheme 4.1. Fischer indole synthesis [6].

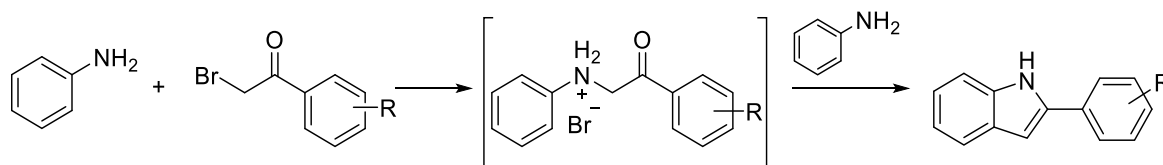
Bartoli and co-workers developed a method in which 7-substituted indoles are synthesized from *ortho*-substituted nitroarenes and vinyl Grignard reagents (**Scheme 4.2**). Due to the availability of the starting reagents and the simplicity of the reaction, it has become one of the most efficient methods

for the preparation of 7-substituted indoles. However, the limitation of this method is that an *ortho*-substituted nitroarene is required [7].



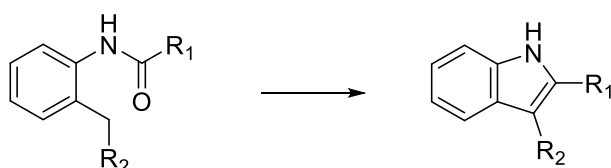
Scheme 4.2. Bartoli indole synthesis [7].

Cyclisation of α -(*N*-arylamino ketones) to afford 2-substituted indoles is known as the Bischler-Möhlau indole synthesis, or simply the Bischler synthesis. In this approach, the reaction of aniline and a substituted α -bromoacetophenone forms an α -(*N*-arylamino ketone) salt intermediate, which in turn reacts with another equivalent of aniline to afford the 2-substituted indole system (**Scheme 4.3**) [8].



Scheme 3. Bischler-Möhlau indole synthesis [8].

The Madelung indole synthesis (**Scheme 4.4**) produces either substituted or unsubstituted indoles by the intramolecular cyclization of *N*-phenylamides using strong bases like sodium amide or potassium *tert*-butoxide at high temperatures [9] or organolithium bases under milder conditions [9, 10].



Scheme 4.4. Madelung indole synthesis [11].

The indole core is widely present in natural products, as well as biological systems such as the essential amino acid tryptophan **2**, serotonin **3** (a neurotransmitter) and melatonin **4** (a hormone) (**Figure 4.2**) [4]. It has further gained popularity as a privileged pharmacophore, with antimicrobial [12-14], anticancer [15-17], antiviral [18-20], anti-inflammatory [21-23], antidepressant [24-26], antimigraine [27-29], anticholinergic [30-32] activities been previously reported.

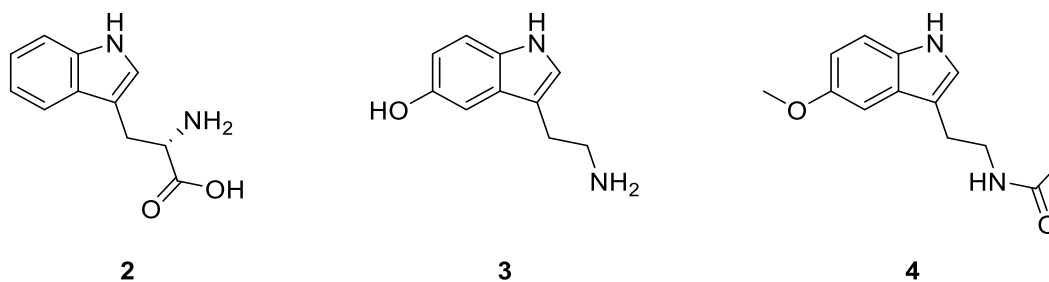


Figure 4.2. Tryptophan **2**, serotonin **3** and melatonin **4** [4].

In an effort to design compounds that combat Alzheimer's disease, Macchia and co-workers [33-35] as well as the Manetsch group [36] focussed their research on designing inhibitors of the β -secretase amyloid precursor protein cleaving enzyme 1 (BACE1) by modifying a carbazole moiety (a heterocycle based on indole) through the introduction of substituted hydroxyethylamine (HEA) linkers onto the carbazole. An example of such an inhibitor, compound **5** (**Figure 4.3**), synthesized by Macchia and co-workers, was found to have an IC_{50} value of 0.50 μ M against BACE1 [33].

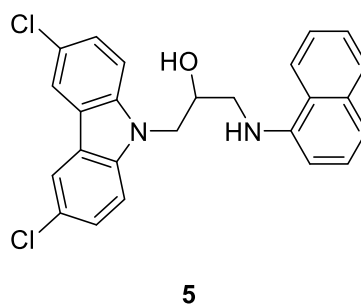


Figure 4.3. Carbazole based BACE1 inhibitor **5** [33].

Extensive molecular docking studies carried out on compound **5** (**Figure 4.4**) indicated that the hydroxy moiety has a key interaction with the Asp228 residue of BACE1, irrespective of chirality. It was also noted that the carbazole moiety allows hydrophobic interactions with both pockets S1 and S2, while the 1-naphthylamine moiety interacts in the S2' pocket through a hydrogen bond between the nitrogen and Tyr198 residue and van der Waals interactions. It was noted that bulky substituents on the carbazole moiety were not readily accommodated resulting in the disruption of the hydrogen bonding interactions with the Asp228 residue [33].

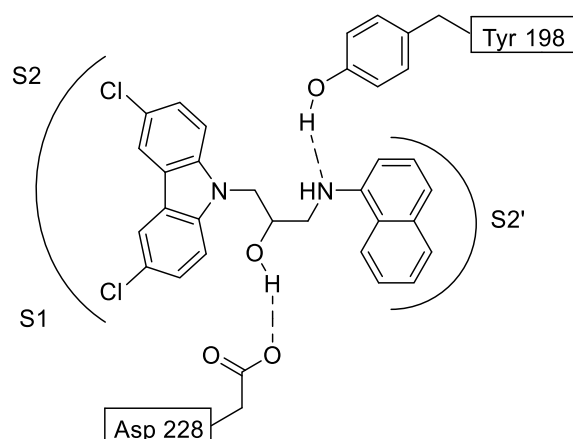


Figure 4.4. Schematic representation of the key interactions of compound **5** and the BACE 1 active site indicated by docking studies [33].

Through all of the structure activity relationship (SAR) studies done by the Macchia group, three key areas were identified where modification could occur: at the carbazole moiety (A), the HEA moiety (B) or the 1-naphthylamine moiety (C) (**Figure 4.5**) [33-35]. The HEA moiety and the 1-naphthylamine moieties have been extensively studied, wherein the HEA moiety has been replaced with different amine and hydroxyl derivatives [36] and the 1-naphthylamine moiety with sulphonamide or arylcarboxamide derivatives [34, 35]. In contrast, chemical space surrounding the carbazole moiety has remained largely unexplored, with only phenyl 2-substituted indoles having been previously reported [33]. In order to further explore the chemical space surrounding compound **5**, it was decided to replace the carbazole moiety with an indeno indole (keeping in mind the bulkiness factor) and the 1-naphthylamine moiety with various amines, while keeping the HEA moiety constant (**Figure 4.5**).

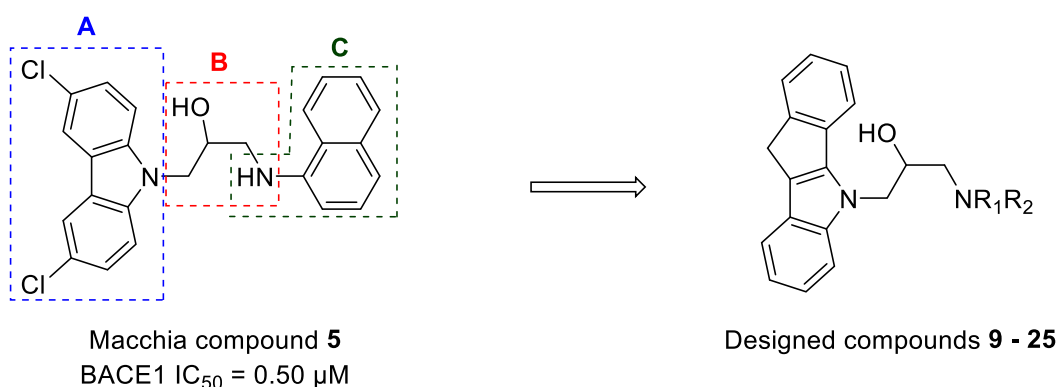


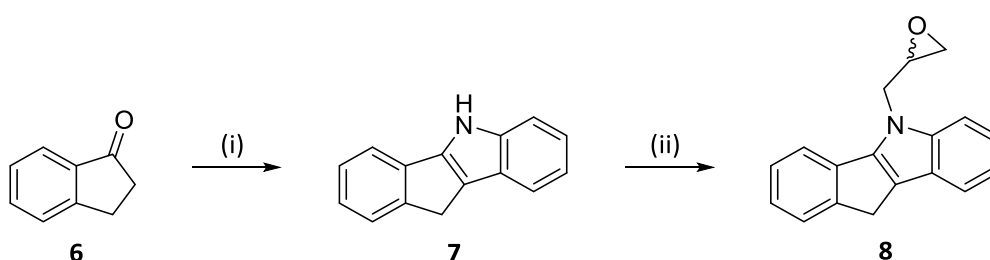
Figure 4.5. Design strategy of target compounds **9 - 25**.

In this study, the synthesis of 1-amino-3-(indeno[1,2-b]indol-5(10*H*)-yl)propan-2-ol derivatives (**9 - 25**) based on an indeno type scaffold, as well as the evaluation of these compounds as possible BACE-1

inhibitors for the treatment of Alzheimer's disease was undertaken. In addition, the acetylcholinesterase (AChE) inhibitory activity is also reported. The cytotoxicity of these compounds was also assessed.

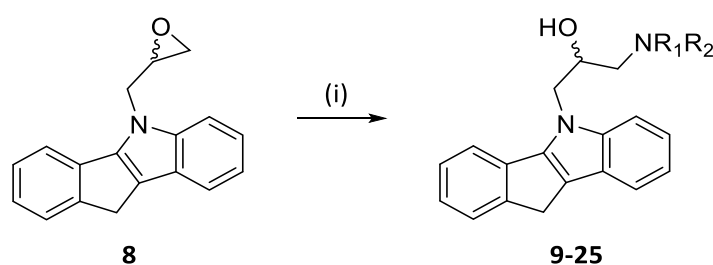
4.2. CHEMISTRY

The preparation of epoxide **8** (Scheme 4.5) was achieved in two steps by reacting commercially available 1-indanone **6** with phenyl hydrazine hydrochloride in the presence of Amberlyst-15 as a catalyst in a Fischer indole type reaction to afford indole **7** [37] which was subsequently reacted with excess (\pm)-epichlorohydrin (ECH) in the presence of base to afford epoxide **8** with an overall yield of 67% [38].



Scheme 4.5: (i) 1.2 eq. PhNHNH₂·HCl, cat. Amberlyst-15, EtOH, reflux, 12 h, 81%; (ii) 7 eq. (\pm)-ECH, 2.5 eq. KOH, THF, 85 °C, 10 h, 83%.

An epoxide ring opening reaction (Scheme 4.6), was then achieved by reacting various types of either primary or secondary amines with epoxide **8** which afforded the desired racemic HEA products **9 - 25** with moderate to high yields (42 - 98%) [39].



Scheme 4.6: (i) 2 eq. R₁R₂-NH, EtOH, reflux, 12 h, 42 – 98%.

Compound **9** is used as a representative example to describe the structure elucidation of the series of compounds. The desired compound **9** was identified by the disappearance of the racemic epoxide proton multiplet from 3.45 - 3.39 ppm and the appearance of a broad singlet at 2.32 ppm integrating for 2H which was assigned to the amine and hydroxyl proton, as well as the appearance of a multiplet at 4.19 – 4.07 ppm integrating for 1H in the ¹H NMR spectrum which is characteristic for the racemic

hydrogen peak to which the hydroxyl is bonded. The formation of **9** was further supported by the disappearance of the epoxide carbon peak at 51.10 and the appearance of a new peak in the ^{13}C NMR spectrum at 69.70 ppm which was assigned to the new hydroxyl carbon as well as the new peak benzylic carbon peak at 48.88 ppm. Two new peaks were observed in the IR spectrum at 3289 cm^{-1} and 3054 cm^{-1} , which are characteristic to an amine stretch and a hydroxyl stretch respectively. Final confirmation was given by the presence of a peak assigned as $[\text{M} + \text{H}]^+$ at 369.2119 in the HRMS, with the $[\text{M} + \text{H}]^+$ value calculated as 369.1961. The remaining compounds in the series were analysed in a similar manner, and the spectral assignments are provided in the experimental section.

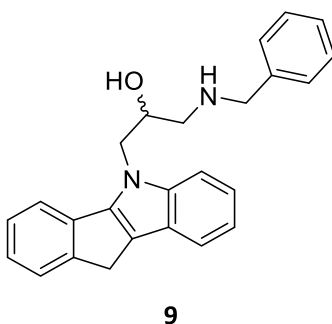
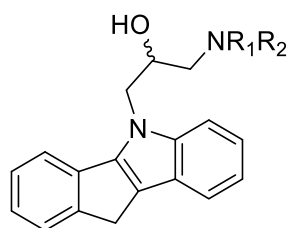
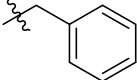
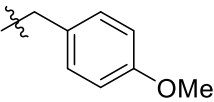
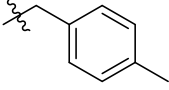
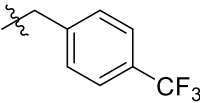
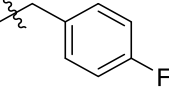
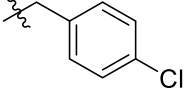
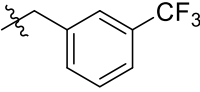
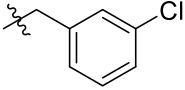
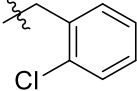
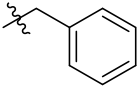
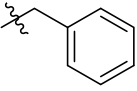


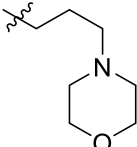
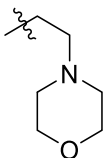
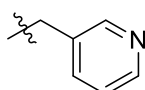
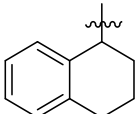
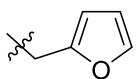
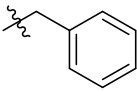
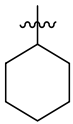
Figure 4.6: Compound **9**.

4.3. STRUCTURE ACTIVITY RELATIONSHIP STUDY

The AChE inhibitory activity of all new synthetic compounds was assessed against *Electrophorus electricus* AChE (*EeAChE*) using Ellman's spectrophotometric method [40] with minor modifications [41]. Galantamine was used as a positive control. The BACE1 inhibitory activity was assessed using a fluorescent BACE1 activity detection kit (Sigma-Aldrich, St. Louis, USA). The acetylcholinesterase inhibitory activities for the synthesized compounds, expressed as half-maximal inhibitory concentration (IC_{50}) values, and the BACE1 inhibitory activities, expressed as percentage at $10\ \mu\text{M}$, are presented in **Table 4.1**. Compounds were screened in both assays as racemic mixtures. In addition, selected compounds were assessed for cytotoxicity against SH-SY5Y neuroblastoma cells using the sulforhodamine B (SRB) staining assay as described by Vichai and Kirtikara [42].

Table 4.1. *In vitro* AChE, BACE-1 inhibitory activity and cytotoxicity results of compounds **9** - **25**.


| Compound | R ₁ | R ₂ | Yield % | <i>Ee</i> AChE IC ₅₀ ± SEM (μM) ^a | BACE-1 % Inhibition at 10 μM ^a | Cytotoxicity IC ₅₀ ± SEM (μM) ^a |
|-----------|---|---|---------|---|---|---|
| 9 |  | H | 42 | >100 | 42 | 4.00 ± 1.41 |
| 10 |  | H | 97 | 41.48 ± 1.51 | nd ^b | 3.37 ± 1.19 |
| 11 |  | H | 64 | >100 | nd ^b | 3.26 ± 2.52 |
| 12 |  | H | 82 | 35.04 ± 1.18 | 66 | nd ^c |
| 13 |  | H | 85 | >100 | 61 | nd ^c |
| 14 |  | H | 52 | 42.00 ± 1.17 | nd ^b | 2.98 ± 1.23 |
| 15 |  | H | 69 | >100 | 84 | nd ^c |
| 16 |  | H | 70 | >100 | 16 | nd ^c |
| 17 |  | H | 62 | >100 | nd ^b | 18.65 ± 1.08 |
| 18 |  |  | 46 | 72.06 ± 1.54 | nd ^b | >100 |

| | | | | | | |
|--------------------|---|-----------------|----|--------------|-----------------|-----------------|
| 19 |  | H | 91 | 82.75 ± 1.33 | nd ^b | 3.35 ± 1.10 |
| 20 |  | H | 85 | >100 | nd ^b | 55.92 ± 2.42 |
| 21 |  | H | 72 | 69.40 ± 1.73 | nd ^b | nd ^c |
| 22 |  | H | 98 | >100 | 71 | 2.55 ± 1.41 |
| 23 |  | H | 80 | >100 | 77 | 11.25 ± 1.04 |
| 24 |  | CH ₃ | 80 | 73.87 ± 1.22 | 91 | 10.51 ± 1.11 |
| 25 |  | CH ₃ | 80 | 13.50 ± 1.41 | 86 | 8.45 ± 1.17 |
| Galantamine | | | - | 3.58 ± 1.24 | - | - |

^a Data are the mean ± SEM of three independent experiments

^b No observable inhibition detected

^c Not determined due to precipitation occurring

Compound **25** was found to have an IC₅₀ value of 13.50 ± 1.41 μM when screened against *EeAChE*. In general, benzyl groups with bulky substituents on the *para*-position showed the highest inhibition, for example, compound **12** which contains a trifluoromethyl substituent (IC₅₀ = 35.04 μM), compound **10** which contains a methoxy substituent (41.48 μM) and compound **14** with a chloro substituent (42.00 μM). Compounds with substituents on the *ortho*- and *meta*-position had *EeAChE* IC₅₀ values higher than 100 μM.

Benzyl derivatives were found in general to be better inhibitors of BACE1 compared to heterocyclic aliphatic substituents such as compounds **19** and **20**. Addition of a methyl group to the benzyl nitrogen (compound **24**) afforded the compound with the highest inhibition (91%) compared to the addition of another benzyl group (compound **18**) which indicated no observable inhibition. The latter would imply

that derivatives with bulkier substituents may not act as inhibitors of BACE1. The substitution of the hydrogen on the benzyl nitrogen (compound **9**, 42%) for a methyl group (compound **24**, 91%) seems to be more favourable in terms of inhibition. The substitution of the planar aromatic benzyl group (compound **9**, 42%) with that of a cyclohexyl- and methyl group (compound **25**, 86%) or 1,2,3,4-tetrahydronaphthalene group (compound **22**, 71%) increased BACE1 inhibition substantially suggesting that cyclic aliphatic systems may be good substituents in the development of BACE1 inhibitors. Unfortunately, these inhibitors exhibited high cytotoxicity against the SH-SY5Y neuroblastoma cells with IC_{50} values of 2.98 – 55.92 μ M, in which accepted IC_{50} values needs to be less than 10 μ M [43]. It was noted that compound **25** inhibits both *EeAChE* ($13.50 \pm 1.41 \mu$ M) and BACE1 (86%), therefore showing the most promise as a dual inhibitor.

4.4. CONCLUSION

A series of seventeen novel 1-amino-3-(indeno[1,2-b]indol-5(10*H*)-yl)propan-2-ol derivatives were synthesized as possible BACE1 inhibitors, with compound **24** indicated the highest inhibitory activity (91%). Compound **25** had the best inhibitory activity against *EeAChE* with an IC_{50} value of $13.50 \pm 1.41 \mu$ M, as well as the second highest inhibition of BACE1 (86%), which shows promise for the development as a dual inhibitor. Although the compounds exhibit high cytotoxicity against the SH-SY5Y neuroblastoma cell line ($IC_{50} = 8.45 \pm 1.17 \mu$ M), future research will be done such as replacing the tetracyclic ring system with different substituted ring systems, in order to reduce the cytotoxicity while maintaining the current inhibition of AChE and BACE1. Further development of these compounds is also proposed in order to determine the effect of less bulky substituents on the inhibitory activity of BACE1.

4.5. EXPERIMENTAL

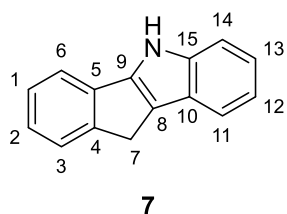
4.5.1. Chemistry

4.5.1.1. General methods

All solvents, chemicals, and reagents were obtained commercially and used without further purification. ^1H NMR (300 MHz) and ^{13}C NMR (75 MHz) spectra were recorded on Bruker AVANCE-III-300 instrument using CDCl_3 . CDCl_3 contained tetramethylsilane as an internal standard. Chemical shifts, δ , are reported in parts per million (ppm), and splitting patterns are given as singlet (s), doublet (d), triplet (t), quartet (q), or multiplet (m). Coupling constants, J , are expressed in hertz (Hz). Mass spectra were recorded in ESI mode on a Waters Synapt G2 Mass Spectrometer at 70 eV and 200 mA. Samples were dissolved in acetonitrile (containing 0.1% formic acid) to an approximate concentration of 10 μ g/mL. Infrared spectra were run on a Bruker ALPHA Platinum ATR spectrometer. The

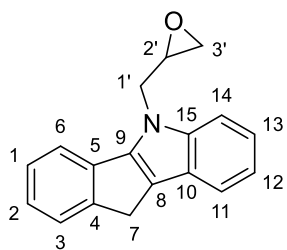
absorptions are reported on the wavenumber (cm^{-1}) scale, in the range 400 - 4000 cm^{-1} . The signals are reported: value (relative intensity, assignment if possible). Abbreviations used in quoting spectra are: v = very, s = strong, m = medium, w = weak, str = stretch. Melting points were measured on a Stuart Melting Point SMP10 microscope. The retention factor (R_f) values quoted are for thin layer chromatography (TLC) on aluminium-backed Macherey-Nagel ALUGRAM Sil G/UV₂₅₄ plates pre-coated with 0.25 mm silica gel 60, spots were visualised with UV light and basic KMnO_4 spray reagent. Chromatographic separations were performed on Macherey-Nagel Silica gel 60 (particle size 0.063 – 0.200 mm). Yields refer to isolated pure products unless stated otherwise. Each compound is named either according to PerkinElmer's *ChemDraw Version 15.0.0.106* or according to common names. The numbering of compounds was not done according to priority, but rather to the author's convenience for characterization.

4.5.1.2. 5,10-Dihydroindeno[1,2-b]indole **7**



A mixture of 1-indanone **6** (10.00 g, 75.68 mmol, 1 eq.), phenylhydrazine hydrochloride (13.14 g, 90.87 mmol, 1.2 eq.) and Amberlyst-15 (37.88 g, 0.5 g/mmol SM) was refluxed in absolute ethanol (250 mL) for 12 hours. The reaction was monitored by thin-layer chromatography, and upon completion, the mixture was cooled to room temperature, the catalyst filtered off, and the product was washed thoroughly with ethyl acetate (100 mL). The organic filtrate was collected, dried over sodium sulfate, filtered and the solvent was removed *in vacuo* to afford the product. The product was used without any further purification. (Yield 81%); Brown solid; R_f 0.48 (1:9 ethyl acetate: hexane); mp 202 °C (decomp., lit. 230 – 234 °C [44]); ν_{max} (neat)/ cm^{-1} 3404 (N-H str, m), 1405 (C-C str, m), 1303 (C-H bend, m), 1245 (C-N str, m), 736 (C-H "oop", vs), 719 (C-H "oop", vs), 520 (m), 429 (s); $^1\text{H NMR}$ (300 MHz, CDCl_3); δ 8.36 (1H, s, NH), 7.68 – 7.62 (1H, m, H-11), 7.55 (1H, d, J = 7.4 Hz, H-6), 7.50 – 7.41 (2H, m, H-14 & H-3), 7.37 - 7.29 (1H, m, H-2), 7.25 – 7.13 (3H, m, H-1 & H-12 & H-13), 3.74 (2H, s, H-7); $^{13}\text{C NMR}$ (75 MHz, CDCl_3); δ 148.0 (C-5), 143.5 (C-4), 140.8 (C-15), 135.2 (C-3), 126.7 (C-6), 125.6 (C-2), 124.9 (C-10), 124.8 (C-1), 121.9 (C-9), 121.8 (C-13), 120.4 (C-12), 119.1 (C-11), 117.5 (C-14), 112.2 (C-8), 30.5 (C-7). HRMS m/z (ESI) ($\text{C}_{15}\text{H}_{11}\text{N}$) 206.0952 ($[\text{M} + \text{H}]^+$ requires 206.0964). Characterization of this compound compared well to literature [44].

4.5.1.3. *rac*-5-(Oxiran-2-ylmethyl)-5,10-dihydroindeno[1,2-*b*]indole **8**



8

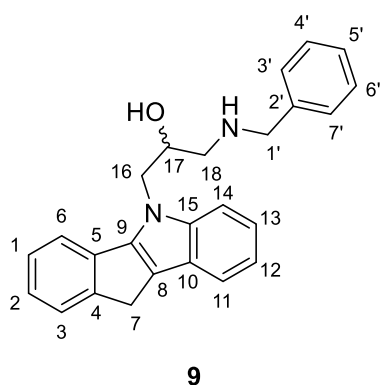
5,10-Dihydroindeno[1,2-*b*]indole **7** (8.00 g, 97.5 mmol, 1 eq.) was dissolved in dry tetrahydrofuran (100 mL), followed by the addition of (±)-epichlorohydrin (21.89 mL, 279.9 mmol, 7 eq.). Potassium hydroxide (5.47 g, 97.5 mmol, 2.5 eq.) was then added slowly and the reaction mixture was heated to 85 °C for 10 hours. The turbid reaction mixture was filtered to remove salts, and the salts mass was rinsed with acetone (20 cm³). The

solvent was then removed *in vacuo* and the solid obtained was dissolved in dichloromethane (100 mL) and washed with distilled water (100 mL). The organic layer was then dried over anhydrous sodium sulfate, filtered and the solvent was removed *in vacuo* to afford the crude product. The product was triturated from methanol. (Yield 83%); Light brown solid; **R_f** 0.33 (1:9 ethyl acetate: hexane); **mp** 121 - 122 °C; **v_{max} (neat)/cm⁻¹** 1459 (C-C str, m), 1439 (C-H str, m), 1345 (C-H bend, m), 837 (C-H “oop”, m), 736 (C-H “oop”, vs), 716 (C-H “oop”, s); **¹H NMR (300 MHz, CDCl₃)**; δ 7.67 – 7.62 (1H, m, ArH), 7.58 – 7.53 (1H, m, ArH), 7.45 – 7.40 (1H, m, ArH), 7.40 – 7.33 (1H, m, ArH), 7.28 – 7.15 (2H, m, ArH), 4.73 (1H, dd, *J* = 15.8, 3.4 Hz, H-1'), 4.58 (1H, dd, *J* = 15.7, 4.4 Hz, H-1'), 3.72 (2H, s, H-7), 3.45 – 3.39 (1H, m, H-2'), 2.82 – 2.77 (1H, m, H-3'), 2.57 (1H, dd, *J* = 4.7, 2.6 Hz, H-3'); **¹³C NMR (75 MHz, CDCl₃)**; δ 148.2 (C-5), 144.6 (C-15), 141.9 (C-4), 135.2 (C-3), 126.7 (C-10), 125.8 (C-2), 124.9 (C-1), 124.5 (C-6), 121.7 (C-13), 121.2 (C-12), 120.2 (C-11), 119.3 (C-14), 117.9 (C-8), 110.2 (C-9), 51.1 (C-2'), 45.9 (C-1'), 45.3 (C-3'), 30.3 (C-7). **HRMS *m/z* (ESI)** (C₁₈H₁₅NO) 262.1248 ([M + H]⁺ requires 262.1226).

4.5.1.4. General method for epoxide ring opening

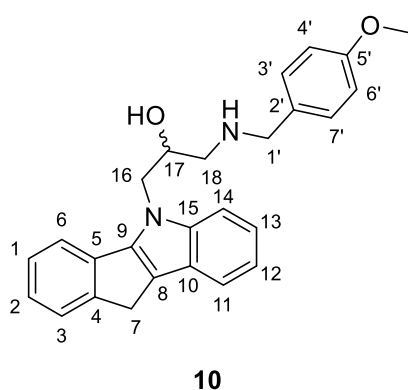
The appropriate amine (1.54 mmol, 2 eq.) was added to a solution of 5-(oxiran-2-ylmethyl)-5,10-dihydroindeno[1,2-*b*]indole **8** (0.20 g, 0.77 mmol, 1 eq.) in absolute ethanol (15 mL). The reaction mixture was heated at reflux for 12 h. The progress of the reaction was monitored by TLC. After reaction, the mixture was quenched with distilled water (30 mL) and extracted with ethyl acetate (3 x 20 mL). The organic phase was washed with water (3 x 20 mL) and brine (3 x 20 mL). The organic layer was then dried over anhydrous sodium sulfate, filtered and the solvent was removed *in vacuo* to afford the crude product. The obtained crude product was purified by either recrystallization from ethanol or column chromatography.

4.5.1.4.1. *rac*-1-(Benzylamino)-3-(indeno[1,2-*b*]indole-5(10*H*)-yl)propan-2-ol **9**



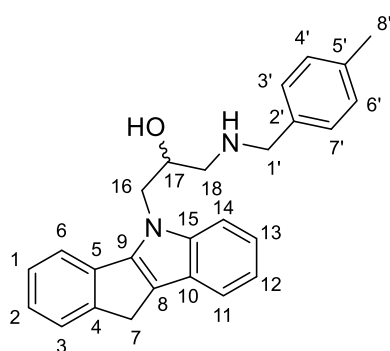
(Yield 42%); Off-white solid; R_f 0.24 (5% MeOH: DCM); mp 130 °C; ν_{\max} (neat)/ cm^{-1} 3289 (N-H str, w), 3054 (O-H str, w), 1495 (N-H bend, w), 1458 (C-C str, m), 1437 (O-H bend, m), 1342 (C-H bend, m), 1118 (C-N str, m), 1102 (C-O str, m), 879 (C-H “oop”, m), 732 (C-H “oop”, vs), 697 (C-H “oop”, s); $^1\text{H NMR}$ (300 MHz, CDCl_3); δ 7.66 – 7.58 (2H, m, ArH’s), 7.52 (1H, d, $J = 7.3$ Hz, ArH), 7.42 – 7.35 (1H, m, ArH), 7.34 – 7.10 (9H, m, ArH’s), 4.52 – 4.35 (2H, m, H-16), 4.19 – 4.07 (1H, m, H-17), 3.68 (2H, s, H-7), 3.68 – 3.54 (2H, m, H-1’), 2.75 (1H, dd, $J = 12.1, 3.7$ Hz, H-18), 2.62 (1H, dd, $J = 12.1, 8.3$ Hz, H-18), 2.32 (2H, br s, OH & NH); $^{13}\text{C NMR}$ (75 MHz, CDCl_3); δ 148.2 (C-4), 144.7 (C-5), 141.8 (C-15), 139.7 (C-2’), 135.4 (C-3), 128.6 (C-4’ & C-6’), 128.2 (C-3’ & C-7’), 127.3 (C-5’), 126.7 (C-2), 125.7 (C-10), 124.8 (C-1), 124.4 (C-6), 121.5 (C-13), 120.9 (C-12), 120.0 (C-11), 119.2 (C-14), 118.3 (C-8), 110.5 (C-9), 69.7 (C-17), 53.7 (C-16), 52.2 (C-18), 48.9 (C-1’), 30.2 (C-7). HRMS m/z (ESI) ($\text{C}_{25}\text{H}_{24}\text{N}_2\text{O}$) 369.1964 ([M + H]⁺ requires 369.1961).

4.5.1.4.2. *rac*-1-[Indeno[1,2-*b*]indole-5(10*H*)-yl]-3-[(4-methoxybenzyl)amino]propan-2-ol **10**



(Yield 97%); Yellow solid; R_f 0.26 (5% MeOH: DCM); mp 118 °C; ν_{\max} (neat)/ cm^{-1} 3268 (N-H str, m), 3053 (O-H str, m), 1608 (C-C str (in-ring), m), 1510 (N-H bend, s), 1437 (O-H bend, s), 1343 (C-H bend, s), 1246 (C-N str, vs), 1174 (C-N str, s), 1117 (C-O str, s), 1035 (s), 911 (s), 825 (C-H “oop”, s), 727 (C-H “oop”, vs); $^1\text{H NMR}$ (300 MHz, CDCl_3); δ 7.63 (2H, m, ArH’s), 7.54 (1H, d, $J = 7.3$ Hz, ArH), 7.40 (1H, d, $J = 7.3$ Hz, ArH), 7.33 (1H, dd, $J = 8.3, 7.5$ Hz, ArH), 7.25 – 7.12 (3H, m, ArH’s), 7.07 (2H, d, $J = 8.6$ Hz, H-3’ & H-7’), 6.79 (2H, d, $J = 8.6$ Hz, H-4’ & H-6’), 4.54 – 4.37 (2H, m, H-16), 4.22 – 4.10 (1H, m, H-17), 3.78 (3H, s, OCH₃), 3.70 (2H, s, H-7), 3.57 (2H, dd, $J = 18.0, 12.0$ Hz, H-1’), 2.81 – 2.57 (4H, m, OH & NH & H-18); $^{13}\text{C NMR}$ (75 MHz, CDCl_3); δ 158.9 (C-5’), 148.2 (C-4), 144.7 (C-5), 141.8 (C-15), 135.4 (C-3), 131.4 (C-2’), 129.5 (C-3’ & C-7’), 126.7 (C-2), 125.70(C-10), 124.8 (C-1), 124.4 (C-6), 121.5 (C-13), 121.0 (C-12), 120.0 (C-11), 119.2 (C-14), 118.3 (C-8), 114.0 (C-4’ & C-6’), 110.5 (C-9), 69.6 (C-17), 55.4 (OCH₃), 53.0 (C-16), 52.0 (C-18), 48.9 (C-1’), 30.2 (C-7). HRMS m/z (ESI) ($\text{C}_{26}\text{H}_{26}\text{N}_2\text{O}_2$) 399.2085 ([M + H]⁺ requires 399.2067).

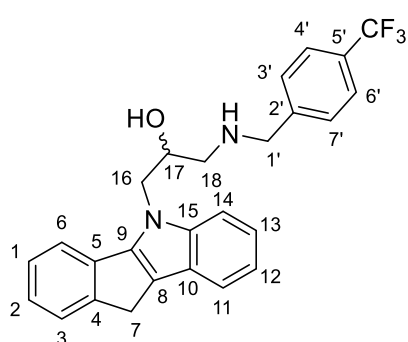
4.5.1.4.3. *rac*-1-[Indeno[1,2-*b*]indole-5(10*H*)-yl]-3-[(4-methylbenzyl)amino]propan-2-ol **11**



11

(Yield 64%); Yellow solid; R_f 0.20 (5% MeOH: DCM); mp 147 °C; ν_{\max} (neat)/ cm^{-1} 3293 (N-H str, w), 3050 (O-H str, w), 1493 (N-H bend, s), 1458 (C-C str, s), 1342 (C-H bend, s), 1120 (C-O str, s), 1097 (s), 908 (s), 881 (s), 812 (C-H “oop”, s), 733 (C-H “oop”, vs); $^1\text{H NMR}$ (300 MHz, CDCl_3); δ 7.69 – 7.61 (2H, m, ArH's), 7.55 (1H, d, $J = 7.3$ Hz, ArH), 7.41 (1H, d, $J = 7.3$ Hz, ArH), 7.34 (1H, td, $J = 7.5, 0.9$ Hz, ArH), 7.26 – 7.14 (3H, m, ArH's), 7.07 (4H, s, H-3' & H-4' & H-6' & H-7"), 4.54 – 4.36 (2H, m, H-16), 4.19 – 4.08 (1H, m, H-17), 3.71 (2H, s, H-7), 3.60 (2H, dd, $J = 18.0, 12.0$ Hz, H-1'), 2.76 (1H, dd, $J = 12.1, 3.7$ Hz, H-18), 2.64 (1H, dd, $J = 12.1, 8.3$ Hz, H-18), 2.33 (3H, s, H-8'); $^{13}\text{C NMR}$ (75 MHz, CDCl_3); δ 148.2 (C-4), 144.7 (C-5), 141.8 (C-15), 136.9 (C-2'), 136.7 (C-5'), 135.4 (C-3), 129.2 (C-3' & C-7'), 128.2 (C-4' & C-6'), 126.7 (C-2), 125.7 (C-10), 124.8 (C-1), 124.3 (C-6), 121.5 (C-13), 120.9 (C-12), 120.0 (C-11), 119.2 (C-14), 118.3 (C-8), 110.5 (C-9), 69.7 (C-17), 53.4 (C-16), 52.1 (C-18), 48.9 (C-1'), 30.2 (C-7), 21.2 (C-8'). HRMS m/z (ESI) ($\text{C}_{26}\text{H}_{26}\text{N}_2\text{O}$) 383.2137 ([M + H]⁺ requires 383.2118).

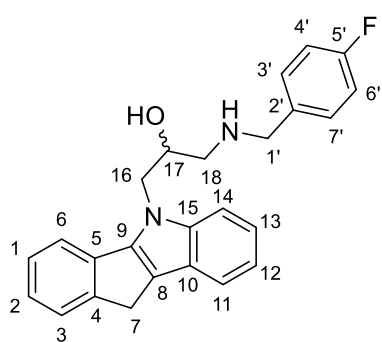
4.5.1.4.4. *rac*-1-[Indeno[1,2-*b*]indole-5(10*H*)-yl]-3-[(4-(trifluoromethyl)benzyl)amino]propan-2-ol **12**



12

(Yield 82%); Orange viscous oil; R_f 0.31 (EtOAc); ν_{\max} (neat)/ cm^{-1} 3057 (O-H str, w), 1460 (N-H bend, m), 1437 (O-H bend, m), 1323 (C-H bend, s), 1163 (C-N str, s), 1112 (C-O str, s), 1064 (s), 1016 (C-F str, s), 908 (s), 848 (C-H “oop”, m), 731 (C-H “oop”, vs), 634 (m); $^1\text{H NMR}$ (300 MHz, CDCl_3); δ 7.66 – 7.60 (2H, m, ArH's), 7.56 – 7.48 (3H, m, ArH's), 7.40 (1H, dd, $J = 6.9, 1.7$ Hz, ArH), 7.35 – 7.12 (6H, m, ArH's), 4.55 – 4.39 (2H, m, H-16), 4.25 – 4.14 (1H, m, H-17), 3.78 – 3.62 (4H, m, H-1' & H-7), 2.85 (2H, br s, OH & NH), 2.75 (1H, dd, $J = 12.2, 3.7$ Hz, H-18), 2.65 (1H, dd, $J = 12.1, 8.1$ Hz, H-18); $^{13}\text{C NMR}$ (75 MHz, CDCl_3); δ 148.2 (C-4), 144.6 (C-4), 143.1 (C-2'), 141.8 (C-15), 135.3 (C-3), 129.7 (q, $J = 32.3$ Hz, $^{\#}\text{C-3'}$ & C-7'), 128.5 (C-5'), 126.7 (C-2), 126.1 (CF_3), 125.8 (C-10), 125.5 (q, $J = 4.5$ Hz, $^{\#}\text{C-4'}$ & C-6'), 124.9 (C-1), 124.4 (C-6), 121.6 (C-13), 121.1 (C-12), 120.1 (C-11), 119.3 (C-14), 118.2 (C-8), 110.4 (C-9), 69.6 (C-17), 53.0 (C-16), 52.0 (C-18), 48.8 (C-1'), 30.2 (C-7). HRMS m/z (ESI) ($\text{C}_{26}\text{H}_{23}\text{F}_3\text{N}_2\text{O}$) 437.2012 ([M + H]⁺ requires 437.1835). $^{\#}$ Splitting of carbon peaks due to fluorine.

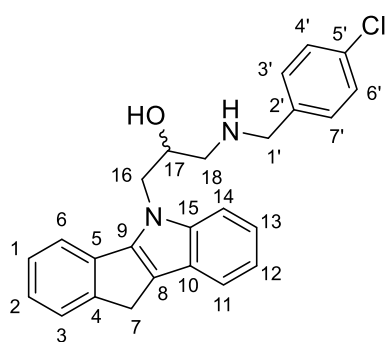
4.5.1.4.5. *rac*-1-[(4-Fluorobenzyl)amino]-3-(indeno[1,2-*b*]indole-5-(10*H*)-yl)propan-2-ol **13**



13

(Yield 85%); Orange viscous oil; R_f 0.15 (EtOAc); ν_{\max} (neat)/ cm^{-1} 3050 (O-H str, w), 2922 (C-H str, w), 1508 (N-H bend, s), 1459 (C-C str, s), 1344 (C-H bend, s), 1210 (C-N str, s), 1117 (C-O str, s), 1011 (C-F str, m), 823 (C-H “oop”, s), 737 (C-H “oop”, vs); $^1\text{H NMR}$ (300 MHz, CDCl_3); δ 7.62 (2H, d, $J = 6.9$ Hz, ArH's), 7.53 (1H, d, $J = 7.3$ Hz, ArH), 7.42 – 7.35 (1H, m, ArH), 7.31 (1H, td, $J = 7.7, 0.5$ Hz, ArH), 7.25 – 7.13 (3H, m, ArH's), 7.13 – 7.03 (2H, m, ArH's), 6.91 (2H, t, $J = 8.7$ Hz, ArH's), 4.51 – 4.34 (2H, m, H-16), 4.23 – 4.11 (1H, m, H-17), 3.68 (2H, s, H-7), 3.57 (2H, dd, $J = 18.0, 12.0$ Hz, H-1'), 3.40 (2H, br s, OH & NH), 2.71 (1H, dd, $J = 12.1, 3.6$ Hz, H-18), 2.61 (1H, dd, $J = 12.1, 8.4$ Hz, H-18); $^{13}\text{C NMR}$ (75 MHz, CDCl_3); δ 162.2 (d, $J = 245.4$ Hz, $^{\#}\text{C-5}'$), 148.2 (C-4), 144.6 (C-5), 141.7 (C-15), 135.3 (C-3), 134.3 (d, $J = 3.2$ Hz, $^{\#}\text{C-2}'$), 130.0 (d, $J = 8.0$ Hz, $^{\#}\text{C-3}'$ & C-7'), 126.7 (C-2), 125.7 (C-10), 124.9 (C-1), 124.4 (C-6), 121.6 (C-13), 121.0 (C-12), 120.1 (C-11), 119.3 (C-14), 118.2 (C-8), 115.4 (d, $J = 21.3$ Hz, $^{\#}\text{C-4}'$ & C-6'), 110.5 (C-9), 69.4 (C-17), 52.6 (C-16), 51.8 (C-18), 48.8 (d, $J = 2.3$ Hz, C-1'), 30.2 (C-7). **HRMS m/z (ESI)** ($\text{C}_{25}\text{H}_{23}\text{FN}_2\text{O}$) 387.1868 ($[\text{M} + \text{H}]^+$ requires 387.1867). $^{\#}$ Splitting of carbon peaks due to fluorine.

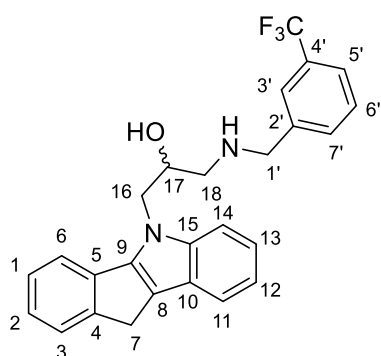
4.5.1.4.6. *rac*-1-[(4-Chlorobenzyl)amino]-3-(indeno[1,2-*b*]indole-5-(10*H*)-yl)propan-2-ol **14**



14

(Yield 52%); Off-white solid; R_f 0.29 (5% MeOH: DCM); **mp** 145 °C; ν_{\max} (neat)/ cm^{-1} 3293 (N-H str, w), 3052 (O-H str, w), 1493 (N-H bend, s), 1438 (O-H bend, m), 1342 (C-H bend, s), 1174 (C-N str, s), 1094 (s), 907 (s), 880 (s), 757 (C-Cl str, s), 731 (C-H “oop”, vs); $^1\text{H NMR}$ (300 MHz, CDCl_3); δ 7.67 – 7.60 (2H, m, ArH's), 7.54 (1H, d, $J = 7.3$ Hz, ArH), 7.40 (1H, dd, $J = 7.2, 1.3$ Hz, ArH), 7.32 (1H, td, $J = 7.5, 0.8$ Hz, ArH), 7.25 – 7.14 (5H, m, ArH's), 7.09 (2H, d, $J = 8.4$ Hz, ArH's), 4.55 – 4.38 (2H, m, H-16), 4.21 – 4.10 (1H, m, H-17), 3.70 (2H, s, H-7), 3.61 (2H, dd, $J = 18.9, 12.0$ Hz, H-1'), 2.74 (1H, dd, $J = 12.1, 3.7$ Hz, H-18), 2.62 (1H, dd, $J = 12.1, 8.1$ Hz, H-18), 2.24 (2H, br s, OH & NH); $^{13}\text{C NMR}$ (75 MHz, CDCl_3); δ 148.2 (C-4), 144.7 (C-5), 141.7 (C-15), 138.1 (C-2'), 135.4 (C-3), 133.0 (C-5'), 129.6 (C-3' & C-7'), 128.7 (C-4' & C-6'), 126.7 (C-2), 125.8 (C-10), 124.9 (C-1), 124.4 (C-6), 121.6 (C-13), 121.0 (C-12), 120.0 (C-11), 119.3 (C-14), 118.2 (C-8), 110.4 (C-9), 69.7 (C-17), 53.0 (C-16), 52.1 (C-18), 48.9 (C-1'), 30.2 (C-7). **HRMS m/z (ESI)** ($\text{C}_{25}\text{H}_{23}\text{ClN}_2\text{O}$) 403.1595 ($[\text{M} + \text{H}]^+$ requires 403.1572).

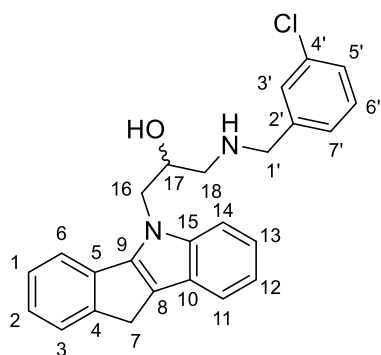
4.5.1.4.7. *rac*-1-[Indeno[1,2-*b*]indole-5(10*H*)-yl]-3-([3-(trifluoromethylbenzyl)amino]propan-2-ol) **15**



15

(Yield 69%); Yellow solid; R_f 0.39 (5% MeOH: DCM); mp 148 °C; ν_{\max} (neat)/ cm^{-1} 3289 (N-H str, w), 3054 (O-H str, w), 1494 (N-H bend, m), 1459 (C-C str, m), 1437 (O-H bend, m), 1328 (C-H bend, s), 1165 (C-N str, s), 1115 (C-O str, s), 1071 (C-F str, s), 917 (m), 803 (C-H "oop", m), 731 (C-H "oop", s), 703 (C-H "oop", s); $^1\text{H NMR}$ (300 MHz, CDCl_3); δ 7.67 – 7.60 (2H, m, ArH's), 7.57 – 7.47 (3H, m, ArH's), 7.43 – 7.35 (3H, m, ArH's), 7.32 (1H, td, $J = 7.6, 1.0$ Hz, ArH), 7.25 – 7.12 (3H, m, ArH's), 4.58 – 4.40 (2H, m, H-16), 4.25 – 4.12 (1H, m, H-17), 3.78 – 3.63 (4H, m, H-1' & H-7), 2.79 (1H, dd, $J = 12.1, 3.7$ Hz, H-18), 2.67 (1H, dd, $J = 12.1, 8.0$ Hz, H-18), 2.24 (2H, br s, OH & NH); $^{13}\text{C NMR}$ (75 MHz, CDCl_3); δ 148.2 (C-4), 144.7 (C-5), 141.7 (C-15), 140.7 (C-2'), 135.3 (C-3), 131.5 (C-7'), 131.1 (C-4'), 130.7 (C-6'), 129.0 (C-3'), 126.7 (C-2), 126.1 (CF₃), 125.8 (C-10), 124.9 (C-1), 124.4 (C-6), 124.2 (C-5'), 121.6 (C-13), 121.0 (C-12), 120.1 (C-11), 119.3 (C-14), 118.2 (C-8), 110.4 (C-9), 69.9 (C-17), 53.3 (C-16), 52.2 (C-18), 48.8 (C-1'), 30.2 (C-7). HRMS m/z (ESI) ($\text{C}_{26}\text{H}_{23}\text{F}_3\text{N}_2\text{O}$) 437.1878 ([M + H]⁺ requires 437.1835).

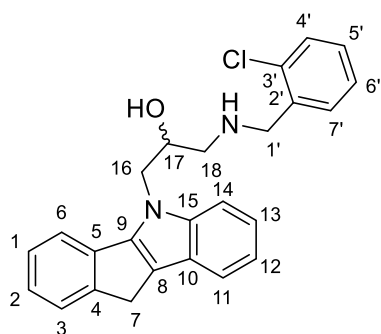
4.5.1.4.8. *rac*-1-[(3-Chlorobenzyl)amino]-3-(indeno[1,2-*b*]indole-5-(10*H*)-yl)propan-2-ol **16**



16

(Yield 70%); Off-white solid; R_f 0.37 (5% MeOH: DCM); mp 150 °C; ν_{\max} (neat)/ cm^{-1} 3278 (N-H str, m), 3051 (O-H str, w), 1495 (N-H bend, s), 1460 (C-C str, s), 1435 (O-H bend, s), 1343 (C-H bend, s), 1204 (C-N str, s), 1091 (s), 916 (s), 785 (C-Cl str, s), 733 (C-H "oop", vs), 704 (C-H "oop", s), 680 (C-H "oop", s); $^1\text{H NMR}$ (300 MHz, CDCl_3); δ 7.67 – 7.59 (2H, m, ArH's), 7.54 (1H, d, $J = 7.3$ Hz, ArH), 7.40 (1H, d, $J = 7.5$ Hz, ArH), 7.33 (1H, td, $J = 7.5, 0.7$ Hz, ArH), 7.25 – 7.11 (6H, m, ArH's), 7.05 (1H, d, $J = 6.7$ Hz, ArH), 4.55 – 4.39 (2H, m, H-16), 4.20 – 4.10 (1H, m, H-17), 3.71 (2H, s, H-7), 3.62 (2H, dd, $J = 18.0, 12.0$ Hz, H-1'), 2.76 (1H, dd, $J = 12.1, 3.7$ Hz, H-18), 2.64 (1H, dd, $J = 12.1, 8.1$ Hz, H-18), 2.25 (2H, br s, OH & NH); $^{13}\text{C NMR}$ (75 MHz, CDCl_3); δ 148.2 (C-4), 144.7 (C-5), 141.8 (C-2'), 141.7 (C-15), 135.3 (C-3), 134.4 (C-4'), 129.8 (C-3'), 128.3 (C-5'), 127.4 (C-6'), 126.7 (C-2), 126.3 (C-7'), 125.8 (C-10), 124.9 (C-1), 124.4 (C-6), 121.6 (C-13), 121.0 (C-12), 120.0 (C-11), 119.3 (C-14), 118.2 (C-8), 110.4 (C-9), 69.8 (C-17), 53.2 (C-16), 52.1 (C-18), 48.9 (C-1'), 30.2 (C-7). HRMS m/z (ESI) ($\text{C}_{25}\text{H}_{23}\text{ClN}_2\text{O}$) 403.1726 ([M + H]⁺ requires 403.1572).

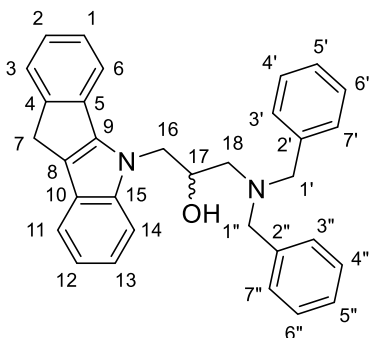
4.5.1.4.9. *rac*-1-[(2-Chlorobenzyl)amino]-3-(indeno[1,2-*b*]indole-5-(10*H*)-yl)propan-2-ol **17**



17

(Yield 62%); Off-white solid; R_f 0.39 (5% MeOH: DCM); mp 156 °C; ν_{\max} (neat)/ cm^{-1} 3269 (N-H str, m), 3055 (O-H str, w), 1497 (N-H bend, s), 1461 (C-C str, s), 1437 (O-H bend, s), 1345 (C-H bend, s), 1103 (C-O str, s), 911 (s), 756 (C-Cl str, s), 731 (C-H “oop”, vs); $^1\text{H NMR}$ (300 MHz, CDCl_3); δ 7.70 – 7.59 (2H, m, ArH’s), 7.54 (1H, d, $J = 7.3$ Hz, ArH), 7.42 (1H, d, $J = 7.5$ Hz, ArH), 7.37 – 7.28 (2H, m, ArH’s), 7.25 – 7.11 (6H, m, ArH’s), 4.57 – 4.42 (2H, m, H-16), 4.23 – 4.13 (1H, m, H-17), 3.86 – 3.74 (2H, m, H-1’), 3.71 (2H, s, H-7), 2.78 (1H, dd, $J = 12.2, 3.7$ Hz, H-18), 2.66 (1H, dd, $J = 12.2, 8.2$ Hz, H-18), 2.34 (2H, br s, OH & NH); $^{13}\text{C NMR}$ (75 MHz, CDCl_3); δ 148.2 (C-4), 144.7 (C-5), 141.8 (C-15), 137.0 (C-2’), 135.4 (C-3), 133.9 (C-3’), 130.3 (C-7’), 129.7 (C-4’), 128.7 (C-5’), 127.0 (C-6’), 126.7 (C-2), 125.7 (C-10), 124.8 (C-1), 124.4 (C-6), 121.5 (C-13), 121.0 (C-12), 120.0 (C-11), 119.2 (C-14), 118.3 (C-8), 110.5 (C-9), 69.7 (C-17), 55.0 (C-16), 51.2 (C-18), 48.8 (C-1’), 30.3 (C-7). HRMS m/z (ESI) ($\text{C}_{25}\text{H}_{23}\text{ClN}_2\text{O}$) 403.1577 ($[\text{M} + \text{H}]^+$ requires 403.1572).

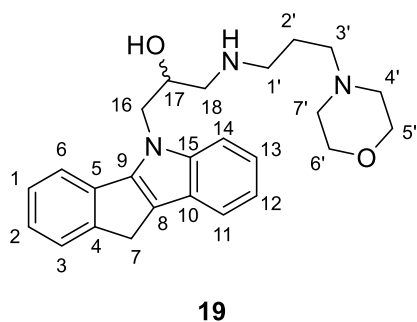
4.5.1.4.10. *rac*-1-(Dibenzylamino)-3-(indeno[1,2-*b*]indole-5-(10*H*)-yl)propan-2-ol **18**



18

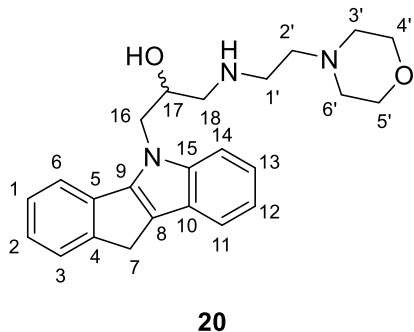
(Yield 46%); Orange viscous oil; R_f 0.39 (EtOAc); ν_{\max} (neat)/ cm^{-1} 3057 (O-H str, m), 1494 (N-H bend, s), 1456 (C-C str, s), 1440 (N-H bend, s), 1345 (C-H bend, s), 1025 (s), 734 (C-H “oop”, vs), 696 (C-H “oop”, vs); $^1\text{H NMR}$ (300 MHz, CDCl_3); δ 7.68 – 7.62 (1H, m, ArH), 7.54 (2H, t, $J = 7.4$ Hz, ArH’s), 7.40 – 7.14 (15H, m, ArH’s), 4.46 – 4.30 (2H, m, H-16), 4.26 – 4.16 (1H, m, H-17), 3.80 (2H, s, H-7), 3.73 (3H, t, $J = 6.7$ Hz, H-1’’ & OH), 3.43 (2H, d, $J = 13.4$ Hz, H-1’), 2.70 (1H, dd, $J = 12.7, 9.4$ Hz, H-18), 2.54 (1H, dd, $J = 12.7, 4.0$ Hz, H-18); $^{13}\text{C NMR}$ (75 MHz, CDCl_3); δ 148.2 (C-4), 144.6 (C-5), 141.7 (C-15), 138.2 (C-2’ & C-2’’), 135.4 (C-3), 129.2 (C-3’ & C-7’ & C-3’’ & C-7’’), 128.6 (C-4’ & C-6’ & C-4’’ & C-6’’), 127.5 (C-5’ & C-5’’), 126.7 (C-2), 125.7 (C-10), 124.7 (C-1), 124.3 (C-6), 121.4 (C-13), 120.9 (C-12), 119.9 (C-11), 119.2 (C-14), 118.3 (C-8), 110.4 (C-9), 67.5 (C-17), 58.6 (C-1’ & C-1’’), 53.2 (C-16), 49.0 (C-18), 30.2 (C-7). HRMS m/z (ESI) ($\text{C}_{32}\text{H}_{30}\text{N}_2\text{O}$) 459.2462 ($[\text{M} + \text{H}]^+$ requires 459.2431).

4.5.1.4.11. *rac*-1-(Indeno[1,2-*b*]indol-5(10*H*)-yl)-3-[(3-morpholinopropyl)amino]propan-2-ol **19**



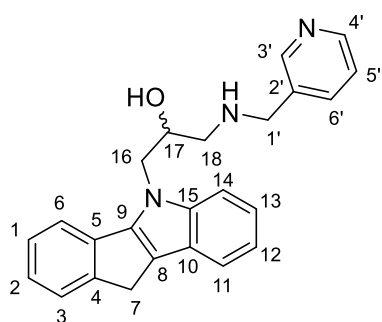
(Yield 91%); Orange viscous oil; R_f 0.27 (5% MeOH: DCM); ν_{\max} (**neat**)/ cm^{-1} 3053 (O-H str, w), 2810 (C-H str, s), 1608 (C-C str (in-ring), w), 1525 (N-H bend, m), 1460 (C-C str, s), 1439 (O-H bend, s), 1345 (C-H bend, s), 1114 (C-O str, vs), 861 (s), 735 (C-H "oop", vs); $^1\text{H NMR}$ (300 MHz, CDCl_3); δ 7.68 (1H, d, $J = 7.6$ Hz, ArH), 7.63 (1H, dd, $J = 7.1, 1.4$ Hz, ArH), 7.54 (1H, d, $J = 7.3$ Hz, ArH), 7.45 – 7.40 (1H, m, ArH), 7.34 (1H, td, $J = 7.5, 0.9$ Hz, ArH), 7.25 – 7.10 (3H, m, ArH's), 4.55 – 4.37 (2H, m, H-16), 4.19 – 4.08 (1H, m, H-17), 3.71 (2H, s, H-7), 3.69 – 3.60 (4H, m, H-5' & H-6'), 2.72 (1H, dd, $J = 12.2, 3.6$ Hz, H-18), 2.65 – 2.47 (3H, m, H-18 & H-1'), 2.41 – 2.23 (6H, m, H-3' & H-4' & H-7'), 1.62 – 1.47 (2H, m, H-2'); $^{13}\text{C NMR}$ (75 MHz, CDCl_3); δ 148.2 (C-4), 144.7 (C-5), 141.8 (C-15), 135.4 (C-3), 126.7 (C-2), 125.7 (C-10), 124.8 (C-1), 124.3 (C-6), 121.5 (C-13), 120.9 (C-12), 119.9 (C-11), 119.2 (C-14), 118.2 (C-8), 110.5 (C-9), 69.6 (C-17), 670.0 (C-5' & C-6'), 57.1 (C-16), 53.8 (C-4' & C-7'), 52.7 (C-18), 48.9 (C-3'), 48.1 (C-1'), 30.2 (C-7), 26.6 (C-2'). **HRMS m/z (ESI)** ($\text{C}_{25}\text{H}_{31}\text{N}_3\text{O}_2$) 406.2495 ($[\text{M} + \text{H}]^+$ requires 406.2489).

4.5.1.4.12. *rac*-1-(Indeno[1,2-*b*]indol-5(10*H*)-yl)-3-[(2-morpholinoethyl)amino]propan-2-ol **20**



(Yield 85%); Orange viscous oil; R_f 0.13 (EtOAc); ν_{\max} (**neat**)/ cm^{-1} 3053 (O-H str, w), 2811 (C-H str, m), 1496 (N-H bend, s), 1439 (O-H bend, s), 1345 (C-H bend, s), 1239 (C-N str, s), 1114 (C-O str, s), 1017 (m), 866 (C-H "oop", m), 736 (C-H "oop", vs); $^1\text{H NMR}$ (300 MHz, CDCl_3); δ 7.69 (1H, d, $J = 7.5$ Hz, ArH), 7.63 (1H, dd, $J = 7.0, 1.5$ Hz, ArH), 7.54 (1H, d, $J = 7.3$ Hz, ArH), 7.43 (1H, d, $J = 7.5$ Hz, ArH), 7.34 (1H, td, $J = 7.5, 0.9$ Hz, ArH), 7.25 – 7.11 (3H, m, ArH's), 4.56 – 4.38 (2H, m, H-16), 4.19 – 4.08 (1H, m, H-17), 3.71 (2H, s, H-7), 3.67 – 3.58 (4H, m, H-4' & H-5'), 2.72 (1H, dd, $J = 12.5, 3.5$ Hz, H-18), 2.65 – 2.53 (3H, m, H-18 & H-1'), 2.39 – 2.30 (6H, m, H-2' & H-3' & H-6'); $^{13}\text{C NMR}$ (75 MHz, CDCl_3); δ 148.1 (C-4), 144.6 (C-5), 141.7 (C-15), 135.3 (C-3), 126.8 (C-2), 125.7 (C-10), 124.9 (C-1), 124.3 (C-6), 121.6 (C-13), 120.9 (C-12), 120.0 (C-11), 119.2 (C-14), 118.3 (C-8), 110.5 (C-9), 68.8 (C-17), 66.8 (C-4' & C-5'), 56.6 (C-16), 53.4 (C-3' & C-6'), 52.1 (C-2'), 48.6 (C-18), 45.1 (C-1'), 30.2 (C-7). **HRMS m/z (ESI)** ($\text{C}_{24}\text{H}_{29}\text{N}_3\text{O}_2$) 392.2348 ($[\text{M} + \text{H}]^+$ requires 392.2332).

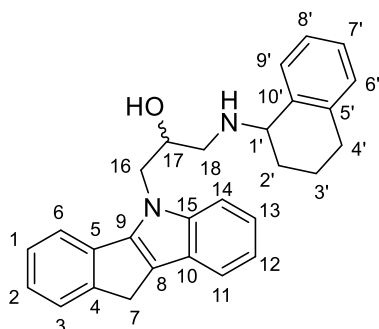
4.5.1.4.13. *rac-1-(Indeno[1,2-b]indole-5(10H)-yl)-3-[(pyridine-3-ylmethyl)amino]propan-2-ol 21*



21

(Yield 72%); Orange viscous oil; R_f 0.23 (5% MeOH: DCM); ν_{\max} (neat)/ cm^{-1} 3053 (O-H str, m), 2889 (C-H str, m), 1460 (N-H bend, s), 1439 (O-H bend, s), 1344 (C-H bend, s), 1123 (C-O str, s), 907 (m), 729 (C-H "oop"); $^1\text{H NMR}$ (300 MHz, CDCl_3); δ 8.44 – 8.37 (2H, m, H-3' & H-4'), 7.62 (2H, m, ArH'), 7.56 – 7.48 (2H, m, ArH's), 7.40 (1H, d, $J = 7.6$ Hz, ArH), 7.31 (1H, td, $J = 7.8, 0.6$ Hz, ArH), 7.24 – 7.11 (4H, m, ArH's), 4.57 – 4.40 (2H, m, H-16), 4.26 – 4.15 (1H, m, H-17), 3.75 – 3.58 (4H, m, H-1' & H-7), 2.79 (1H, dd, $J = 12.1, 3.7$ Hz, H-18), 2.67 (1H, dd, $J = 12.0, 7.9$ Hz, H-18), 2.47 (2H, s, OH & NH); $^{13}\text{C NMR}$ (75 MHz, CDCl_3); δ 149.6 (C-3'), 148.6 (C-4'), 148.2 (C-4), 144.7 (C-5), 141.8 (C-15), 135.9 (C-2'), 135.4 (C-3), 135.2 (C-6'), 126.7 (C-2), 125.7 (C-10), 124.9 (C-1), 124.4 (C-6), 123.5 (C-5'), 121.6 (C-13), 121.0 (C-12), 120.0 (C-11), 119.3 (C-14), 118.2 (C-8), 110.4 (C-9), 69.9 (C-17), 52.3 (C-16), 51.2 (C-1'), 48.9 (C-18), 30.2 (C-7). HRMS m/z (ESI) ($\text{C}_{24}\text{H}_{23}\text{N}_3\text{O}$) 370.1909 ($[\text{M} + \text{H}]^+$ requires 370.1914).

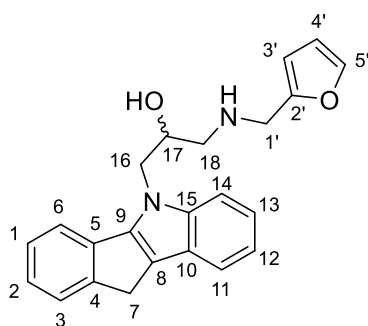
4.5.1.4.14. *rac-1-(Indeno[1,2-b]indol-5(10H)-yl)-3-[(1,2,3,4-tetrahydronaphthalen-1-yl)amino]propan-2-ol 22*



22

(Yield 98%); Orange viscous oil; R_f 0.31 (5% MeOH: DCM); ν_{\max} (neat)/ cm^{-1} 3055 (O-H str, m), 2927 (C-H str, s), 1488 (N-H bend, s), 1459 (C-C str, s), 1344 (C-H bend, m), 733 (C-H "oop", vs); $^1\text{H NMR}$ (300 MHz, CDCl_3); δ 7.71 (1H, d, $J = 7.5$ Hz, ArH), 7.65 (1H, d, $J = 6.9$ Hz, ArH), 7.55 (1H, d, $J = 7.3$ Hz, ArH), 7.46 (1H, d, $J = 7.6$ Hz, ArH), 7.39 – 7.04 (12H, m, ArH's), 4.61 – 4.45 (2H, m, H-16), 4.20 – 4.09 (1H, m, H-17), 3.91 (1H, t, $J = 5.6$ Hz, H-1'), 3.72 (2H, s, H-7), 3.70 (2H, s, OH & NH), 3.03 – 2.61 (6H, m, H-18 & H-4'), 2.05 – 1.58 (8H, m, *H-2' & *H-3'); $^{13}\text{C NMR}$ (75 MHz, CDCl_3); δ 148.22 (C-4), 144.7 (C-5), 141.8 & 141.1 (C-15), 138.7 & 138.6 (C-10'), 137.4 (C-5'), 135.40 (C-3), 129.2 & 129.1 (C-8'), 128.1 (C-7'), 127.0 & 126.7 (C-9'), 126.7 (C-2), 126.9 (C-6'), 125.7 (C-10), 124.8 (C-1), 124.3 (C-6), 121.5 (C-13), 120.9 (C-12), 119.9 (C-11), 119.2 (C-14), 118.3 (C-8), 110.5 (C-9), 70.2 & 69.8 (C-17), 55.9 & 55.1 (C-1), 50.6 & 50.1 (C-16), 49.4 & 49.3 & 48.9 & 48.8 (C-18), 33.4 (C-2'), 30.2 (C-7), 29.6 & 29.4 (C-4'), 19.6 & 19.0 & 18.9 (C-3'). HRMS m/z (ESI) ($\text{C}_{28}\text{H}_{28}\text{N}_2\text{O}$) 409.2291 ($[\text{M} + \text{H}]^+$ requires 409.2274).

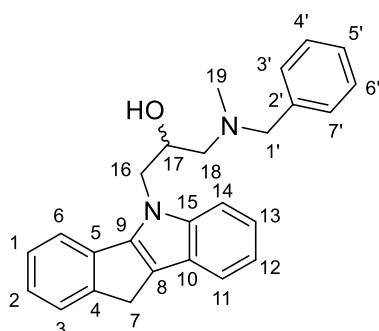
4.5.1.4.15. *rac-1-[(Furan-2-ylmethyl)amino]-3-(indeno[1,2-b]indol-5(10H)-yl)propan-2-ol* **23**



23

(Yield 80%); Orange solid; R_f 0.25 (EtOAc); mp 139 °C; ν_{max} (neat)/ cm^{-1} 2924 (C-H str, m), 2850 (C-H str, m), 1459 (C-C str, s), 1438 (O-H bend, s), 1343 (C-H bend, s), 1148 (C-O str, s), 1013 (s), 732 (C-H “oop”, vs); $^1\text{H NMR}$ (300 MHz, CDCl_3); δ 7.68 – 7.59 (2H, m, ArH's), 7.53 (1H, d, $J = 7.3$ Hz, ArH), 7.44 – 7.37 (1H, m, ArH), 7.32 (1H, td, $J = 7.4, 0.7$ Hz, ArH), 7.26 (1H, d, $J = 1.0$ Hz, H-5'), 7.25 – 7.11 (3H, m, ArH's), 6.24 (1H, dd, $J = 3.1, 1.9$ Hz, H-4'), 6.06 (1H, d, $J = 3.1$ Hz, H-3'), 4.52 – 4.37 (2H, m, H-16), 4.24 – 4.13 (1H, m, H-17), 3.70 (2H, s, H-7), 3.68 (2H, s, H-1'), 3.33 (2H, br s, OH & NH), 2.76 (dd, $J = 12.2, 3.6$ Hz, H-18), 2.66 (1H, dd, $J = 12.2, 8.4$ Hz, H-18); $^{13}\text{C NMR}$ (75 MHz, CDCl_3); δ 152.3 (C-2'), 148.2 (C-4), 144.6 (C-5), 142.3 (C-5'), 141.8 (C-15), 135.3 (C-3), 126.7 (C-2), 125.7 (C-10), 124.8 (C-1), 124.4 (C-6), 121.6 (C-13), 121.0 (C-12), 120.0 (C-11), 119.2 (C-14), 118.3 (C-8), 110.5 (C-9), 110.4 (C-4'), 108.0 & 107.9 (C-3'), 69.5 (C-17), 51.7 (C-16), 48.8 (C-1'), 45.6 (C-18), 30.2 (C-7). **HRMS m/z (ESI)** ($\text{C}_{23}\text{H}_{22}\text{N}_2\text{O}_2$) 359.1774 ([M + H]⁺ requires 359.1754).

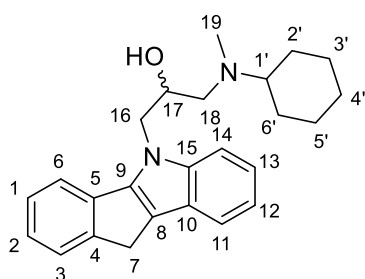
4.5.1.4.16. *rac-1-[Benzyl(methyl)amino]-3-(indeno[1,2-b]indol-5(10H)-yl)propan-2-ol* **24**



24

(Yield 80%); Orange viscous oil; R_f 0.41 (5% MeOH: DCM); ν_{max} (neat)/ cm^{-1} 3055 (O-H str, m), 2792 (C-H str, m), 1526 (C-C str (in-ring), m), 1495 (N-H bend, s), 1458 (C-C str, s), 1439 (O-H bend, s), 1345 (C-H bend, s), 1090 (m), 1018 (s), 734 (C-H “oop”, vs), 697 (C-H “oop”, vs); $^1\text{H NMR}$ (300 MHz, CDCl_3); δ 7.70 – 7.62 (2H, m, ArH's), 7.56 (1H, d, $J = 7.4$ Hz, ArH), 7.44 (1H, d, $J = 7.7$ Hz, ArH), 7.38 – 7.15 (9H, m, ArH's), 4.56 – 4.42 (2H, m, H-16), 4.28 – 4.18 (1H, m, H-17), 3.73 (2H, s, H-7), 3.62 (1H, d, $J = 13.0$ Hz, H-1'), 3.45 (1H, d, $J = 13.0$ Hz, H-1'), 2.63 (1H, dd, $J = 12.2, 9.8$ Hz, H-18), 2.46 (1H, dd, $J = 12.3, 4.1$ Hz, H-18), 2.43 (1H, s, OH), 2.20 (3H, s, H-19); $^{13}\text{C NMR}$ (75 MHz, CDCl_3); δ 148.3 (C-4), 144.7 (C-5), 141.9 (C-15), 138.2 (C-2'), 135.5 (C-3), 129.1 (C-3' & C-7'), 128.5 (C-4' & C-6'), 127.4 (C-5'), 126.7 (C-2), 125.7 (C-10), 124.7 (C-1), 124.4 (C-6), 121.5 (C-13), 120.9 (C-12), 119.9 (C-11), 119.2 (C-14), 118.3 (C-8), 110.5 (C-9), 67.6 (C-17), 62.5 (C-1'), 60.9 (C-18), 49.0 (C-16), 42.3 & 42.2 (C-19), 30.3 (C-7). **HRMS m/z (ESI)** ($\text{C}_{26}\text{H}_{26}\text{N}_2\text{O}$) 383.2142 ([M + H]⁺ requires 383.2118).

4.5.1.4.17. *rac*-1-[Hexyl(methyl)amino]-3-(indeno[1,2-*b*]indol-5(10*H*)-yl)propan-2-ol **25**



25

(Yield 80%); Orange viscous oil; R_f 0.41 (5% MeOH: DCM); ν_{\max} (neat)/ cm^{-1} 3157 (N-H str, m), 3048 (O-H str, m), 2926 (C-H str, s), 2850 (C-H str, s), 1498 (N-H bend, s), 1458 (C-C str, s), 1439 (O-H bend, s), 1342 (C-H bend, s), 1104 (C-O str, s), 1013 (s), 735 (C-H "oop", vs), 717 (C-H "oop", vs); $^1\text{H NMR}$ (300 MHz, CDCl_3); δ 7.73 (1H, d, $J = 7.6$ Hz, ArH), 7.64 (1H, d, $J = 7.7$ Hz, ArH), 7.55 (1H, d, $J = 7.4$ Hz, ArH), 7.46 (1H, d, $J = 7.9$ Hz, ArH), 7.36 (1H, td, $J = 7.6, 0.6$

Hz, ArH), 7.28 – 7.13 (3H, m, ArH's), 4.58 – 4.41 (2H, m, H-16), 4.18 – 4.06 (1H, m, H-17), 3.73 (2H, s, H-7), 2.62 – 2.50 (2H, m, H-18), 2.43 – 2.29 (1H, m, H-1'), 2.20 (3H, s, H-19), 1.83 – 1.57 (5H, m, H-2' & H-6' & H-4'), 1.32 – 1.00 (5H, m, H-3' & H-5' & H-4'); $^{13}\text{C NMR}$ (75 MHz, CDCl_3); δ 148.3 (C-4), 144.8 (C-5), 141.9 (C-15), 135.6 (C-3), 126.6 (C-2), 125.7 (C-10), 124.7 (C-1), 124.3 (C-6), 121.4 (C-13), 120.9 (C-12), 119.8 (C-11), 119.2 (C-14), 118.3 (C-8), 110.5 (C-9), 67.3 (C-17), 63.6 (C-1'), 57.6 (C-18), 49.20 (C-16), 30.3 (C-7), 29.2 (C-19), 28.6 (C-2' & C-6'), 26.3 (C-4'), 26.0 (C-3' & C-5'). **HRMS m/z (ESI)** ($\text{C}_{25}\text{H}_{30}\text{N}_2\text{O}$) 375.2448 ($[\text{M} + \text{H}]^+$ requires 375.2431).

4.5.2. Bioactivity screening

Prior to screening, all compounds were dissolved in dimethyl sulfoxide due to the compounds being insoluble in water at high concentrations (10 mM). The final concentration of dimethyl sulfoxide in the assay were below 1%.

4.5.2.1. Acetylcholinesterase inhibitory activity

Cholinesterase inhibitory activity for *EeAChE* was determined using the 5,5-dithiobis-2-nitrobenzoic acid (DTNB) assay as described by Ellman [40] and modified by Eldeen and co-workers [41]. Three buffers were prepared: Buffer A – 50 mM Tris-hydrochloride (pH 8); Buffer B - 50 mM Tris-hydrochloride (pH 8), containing 0.1% bovine serum albumin; Buffer C - 50 mM Tris-hydrochloride (pH 8), fortified with 0.1 M sodium chloride and 0.02 M magnesium chloride. Into 96-well plates were pipetted: 25 mL acetylthiocholine iodide (15 mM in distilled water), 125 mL DTNB (3 mM in buffer C), 50 ml buffer B and either 25 mL buffer A (negative control), galantamine (positive control at 1 μM) or compounds **9** - **25**. Absorbance was measured at 405 nm (four times) to account for baseline interference. An aliquot of 25 mL *EeAChE* (0.2 U/mL in buffer A) was pipetted into the plates and the absorbance measured every 45 s for fifteen cycles. *EeAChE* inhibition (%) was determined as the rate of the reaction (correcting for spontaneous colour changes) relative to the negative control.

4.5.2.2. β -Secretase cleaving enzyme 1 inhibitory activity

BACE 1 inhibitory activity was determined for compounds **9 - 25** using a purchased fluorescent BACE1 activity detection kit according to the manufacture's introductions (Sigma-Aldrich, St. Louis, USA). Two solutions were prepared: BACE1 substrate stock solution – 0.05 mM in supplied fluorescent assay buffer; BACE1 enzyme solution – 0.3 U/mL, containing supplied fluorescent assay buffer. Into 96-well plates were pipetted: 68 μ L supplied fluorescent assay buffer (to samples), 20 μ L BACE1 substrate solution (0.05 mM in supplied fluorescence assay buffer), 80 μ L fluorescence assay buffer (negative control), 2 μ L BACE1 enzyme solution (0.3 U/mL in supplied fluorescent assay buffer) or 2 μ L compounds **9 – 25** (0.5 mM in distilled water). Plates were incubated for 2 h. BACE1 inhibition (%) was determined using a Synergy 2 fluorimeter (Bio-Tek Instruments, Inc.) with excitation set at 340 nm and emission at 450 nm.

4.5.2.3. Cytotoxicity screening

Cytotoxicity was assessed using the SRB staining assay on the SH-SY5Y neuroblastoma cell line as described by Vichai and Kirtikara with minor modifications [42]. Although the SH-SY5Y cell line is cancerous in nature, it does present as a model of a neurological cellular environment. The SH-SY5Y cell line was cultured in DMEM/Ham's F12 nutrient, in a 1 to 1 ratio, medium supplemented with 10% foetal calf serum (FCS) in 75 mL flasks at 37 °C and 5% CO₂ in a humidified incubator. Culture flasks with confluent cells were rinsed with phosphate buffered saline and harvested using TrypLe™ Express to detach the cells. Detached cells were centrifuged (200 x g, 5 min), counted using the trypan blue exclusion assay (0.1%), and diluted to 1 x 10⁵ cells/ μ L in 10% FCS-fortified medium. The cell suspension (100 μ L) was seeded into sterile, clear 96-well plates, and incubated overnight to allow the cells to attach. Blank wells contained 200 μ L FCS (5%)-fortified media without cells to account for background noise and sterility. Attached cells were exposed to 100 μ L medium (negative control), compounds **9 - 25** (0.01 - 100 μ M) or saponin (1%; positive control) prepared in FCS negative medium for 72 h at 37 °C and 5% CO₂ in a humidified incubator. Cells were fixed in the wells by adding 50 μ L trichloroacetic acid (50%) and left overnight at 4 °C. Plates containing the fixed cells were washed three times with tap water and stained using 100 μ L SRB solution (0.057% in 1% acetic acid) for 30 min at room temperature in the dark. Stained cells were washed four times with 150 μ L acetic acid (1%) and air-dried. The bound dye was eluted using 200 μ L Tris-buffer (10 mM, pH 10.5) and the absorbance measured at 510 nm (reference 630 nm) using a ELx 800 microplate plate reader (Bio-Tek Instruments, Inc.). The blank value was subtracted from all the other values and the cell density was expressed relative to the negative control as a percentage.

4.5.2.4. Statistics

Assays were performed as three intra- as well as three inter-replicates. Statistical analyses were performed using Graph-Pad Prism 5.0 (GraphPad). The IC₅₀ values were determined using non-linear regression analysis (variable slope) for AChE. BACE1 percentage inhibition was determined using linear regression analysis.

4.6. ACKNOWLEDGEMENTS

This work was supported by the National Research Foundation (NRF) of South Africa (Thuthuka grant number 87893), the University of Pretoria (University, Science Faculty Research Councils and Research and Development Program) and the Council for Scientific and Industrial Research (CSIR), South Africa. Opinions expressed in this publication and the conclusions arrived at, are those of the authors, and are not necessarily attributed to the NRF. The authors would like to gratefully acknowledge Ms Madelien Wooding (University of Pretoria) for LC-MS services.

4.7. CONFLICT OF INTEREST

The authors declare no conflict of interest.

4.8. APPENDIX C. SUPPLEMENTARY INFORMATION

Appendix C can be found as a separate document on the CD.

4.9. REFERENCES

- [1] A. Baeyer, A. Emmerling, Synthese des indols, Ber. Dtsch. Chem. Ges., 2 (1869) 679-682.
- [2] J. Barluenga, C. Valdés, Five-membered heterocycles: indole and related systems, in: Modern heterocyclic chemistry, Wiley-VCH Verlag GmbH & Co. KGaA, Wiley-VCH Verlag GmbH & Co. KGaA, 2011, pp. 377-531.
- [3] R.J. Sundberg, Indoles, Academic Press London, 1996.
- [4] N. Chadha, O. Silakari, Indoles as therapeutics of interest in medicinal chemistry: Bird's eye view, Eur. J. Med. Chem., 134 (2017) 159-184.
- [5] D.F. Taber, P.K. Tirunahari, Indole synthesis: a review and proposed classification, Tetrahedron, 67 (2011) 7195-7210.
- [6] B. Robinson, Studies on the Fischer indole synthesis, Chem. Rev., 69 (1969) 227-250.
- [7] G. Bartoli, G. Palmieri, M. Bosco, R. Dalpozzo, The reaction of vinyl Grignard reagents with 2-substituted nitroarenes: a new approach to the synthesis of 7-substituted indoles, Tetrahedron Lett., 30 (1989) 2129-2132.

- [8] M. Inman, C.J. Moody, Indole synthesis – something old, something new, *Chem. Sci.*, 4 (2013) 29-41.
- [9] W.J. Houlihan, V.A. Parrino, Y. Uike, Lithiation of *N*-(2-alkylphenyl) alkanamides and related compounds. A modified Madelung indole synthesis, *J. Org. Chem.*, 46 (1981) 4511-4515.
- [10] G. Spadoni, B. Stankov, A. Duranti, G. Biella, V. Lucini, A. Salvatori, F. Fraschini, 2-Substituted 5-methoxy-*N*-acyltryptamines: Synthesis, binding affinity for the melatonin receptor, and evaluation of the biological activity, *J. Med. Chem.*, 36 (1993) 4069-4074.
- [11] C.F.H. Allen, J. VanAllan, 2-Methylindole, *Org. Synth.*, 22 (1942) 94.
- [12] L. Liu, Y.Y. Chen, X.J. Qin, B. Wang, Q. Jin, Y.P. Liu, X.D. Luo, Antibacterial monoterpene indole alkaloids from *Alstonia scholaris* cultivated in temperate zone, *Fitoterapia*, 105 (2015) 160-164.
- [13] N.C. Desai, H. Somani, A. Trivedi, K. Bhatt, L. Nawale, V.M. Khedkar, P.C. Jha, D. Sarkar, Synthesis, biological evaluation and molecular docking study of some novel indole and pyridine based 1,3,4-oxadiazole derivatives as potential antitubercular agents, *Bioorg. Med. Chem. Lett.*, 26 (2016) 1776-1783.
- [14] M. Mielczarek, R.V. Thomas, C. Ma, H. Kandemir, X. Yang, M. Bhadbhade, D.S. Black, R. Griffith, P.J. Lewis, N. Kumar, Synthesis and biological activity of novel mono-indole and mono-benzofuran inhibitors of bacterial transcription initiation complex formation, *Bioorg. Med. Chem.*, 23 (2015) 1763-1775.
- [15] S. Cai, S. Sun, J. Peng, X. Kong, H. Zhou, T. Zhu, Q. Gu, D. Li, Okaramines S–U, three new indole diketopiperazine alkaloids from *Aspergillus taichungensis* ZHN-7-07, *Tetrahedron*, 71 (2015) 3715-3719.
- [16] S.L. Greig, Osimertinib: first global approval, *Drugs*, 76 (2016) 263-273.
- [17] H.M. Prince, M.J. Bishton, R.W. Johnstone, Panobinostat (LBH589): A potent pan-deacetylase inhibitor with promising activity against hematologic and solid tumors, *Future Oncol.*, 5 (2009) 601-612.
- [18] P. Bag, D. Ojha, H. Mukherjee, U.C. Halder, S. Mondal, A. Biswas, A. Sharon, L. Van Kaer, S. Chakrabarty, G. Das, D. Mitra, D. Chattopadhyay, A dihydro-pyrindo-indole potently inhibits HSV-1 infection by interfering the viral immediate early transcriptional events, *Antiviral Res.*, 105 (2014) 126-134.
- [19] S. Castellino, M.R. Groseclose, J. Sigafos, D. Wagner, M. de Serres, J.W. Polli, E. Romach, J. Myer, B. Hamilton, Central nervous system disposition and metabolism of Fosdevirine (GSK2248761), a non-nucleoside reverse transcriptase inhibitor: an LC-MS and matrix-assisted laser desorption/ionization imaging MS investigation into central nervous system toxicity, *Chem. Res. Toxicol.*, 26 (2013) 241-251.

- [20] F. Narjes, B. Crescenzi, M. Ferrara, J. Habermann, S. Colarusso, R. Ferreira Mdel, I. Stansfield, A.C. Mackay, I. Conte, C. Ercolani, S. Zaramella, M.C. Palumbi, P. Meuleman, G. Leroux-Roels, C. Giuliano, F. Fiore, S. Di Marco, P. Baiocco, U. Koch, G. Migliaccio, S. Altamura, R. Laufer, R. De Francesco, M. Rowley, Discovery of (7*R*)-14-cyclohexyl-7-[[2-(dimethylamino)ethyl](methyl) amino]-7,8-dihydro-6*H*-indolo[1,2-*e*][1,5]benzoxazocine-11-carboxylic acid (MK-3281), a potent and orally bioavailable finger-loop inhibitor of the hepatitis C virus NS5B polymerase, *J. Med. Chem.*, 54 (2011) 289-301.
- [21] C. Lee, J.H. Sohn, J.H. Jang, J.S. Ahn, H. Oh, J. Baltrusaitis, I.H. Hwang, J.B. Gloer, Cycloexpansamines A and B: spiroindolinone alkaloids from a marine isolate of *Penicillium sp.* (SF-5292), *J. Antibiot.*, 68 (2015) 715-718.
- [22] S.K. Bhati, A. Kumar, Synthesis of new substituted azetidinoyl and thiazolidinoyl-1,3,4-thiadiazino [6,5-*b*]indoles as promising anti-inflammatory agents, *Eur. J. Med. Chem.*, 43 (2008) 2323-2330.
- [23] P. Singh, P. Prasher, P. Dhillon, R. Bhatti, Indole based peptidomimetics as anti-inflammatory and anti-hyperalgesic agents: Dual inhibition of 5-LOX and COX-2 enzymes, *Eur. J. Med. Chem.*, 97 (2015) 104-123.
- [24] S. Bulling, K. Schicker, Y.W. Zhang, T. Steinkellner, T. Stockner, C.W. Gruber, S. Boehm, M. Freissmuth, G. Rudnick, H.H. Sitte, W. Sandtner, The mechanistic basis for noncompetitive ibogaine inhibition of serotonin and dopamine transporters, *J. Biol. Chem.*, 287 (2012) 18524-18534.
- [25] J.A. Diers, K.D. Ivey, A. El-Alfy, J. Shaikh, J. Wang, A.J. Kochanowska, J.F. Stoker, M.T. Hamann, R.R. Matsumoto, Identification of antidepressant drug leads through the evaluation of marine natural products with neuropsychiatric pharmacophores, *Pharmacol. Biochem. Behav.*, 89 (2008) 46-53.
- [26] J. Baird-Lambert, P.A. Davis, K.M. Taylor, Methylaplysinopsin: a natural product of marine origin with effects on serotonergic neurotransmission, *Clin. Exp. Pharmacol. Physiol.*, 9 (1982) 203-212.
- [27] J.E. Macor, D. Gurley, T. Lanthorn, J. Loch, R.A. Mack, G. Mullen, O. Tran, N. Wright, J.C. Gordon, The 5-HT₃ antagonist tropisetron (ICS 205-930) is a potent and selective $\alpha 7$ nicotinic receptor partial agonist, *Bioorg. Med. Chem. Lett.*, 11 (2001) 319-321.
- [28] M.F. Hibert, R. Hoffmann, R.C. Miller, A.A. Carr, Conformation-activity relationship study of 5-HT₃ receptor antagonists and a definition of a model for this receptor site, *J. Med. Chem.*, 33 (1990) 1594-1600.
- [29] P.R. Brodfuehrer, B.-C. Chen, T.R. Sattelberg, P.R. Smith, J.P. Reddy, D.R. Stark, S.L. Quinlan, J.G. Reid, J.K. Thottathil, S. Wang, An efficient Fischer indole synthesis of Avitriptan, a potent 5-HT_{1D} receptor agonist, *J. Org. Chem.*, 62 (1997) 9192-9202.
- [30] M. Fadaeinasab, A. Basiri, Y. Kia, H. Karimian, H.M. Ali, V. Murugaiyah, New indole alkaloids from the bark of *Rauvolfia reflexa* and their cholinesterase inhibitory activity, *Cell. Physiol. Biochem.*, 37 (2015) 1997-2011.

- [31] M.T. Andrade, J.A. Lima, A.C. Pinto, C.M. Rezende, M.P. Carvalho, R.A. Epifanio, Indole alkaloids from *Tabernaemontana australis* (Muell. Arg) Miens that inhibit acetylcholinesterase enzyme, *Bioorg. Med. Chem.*, 13 (2005) 4092-4095.
- [32] L.K. Kinthada, S.R. Medisetty, A. Parida, K.N. Babu, A. Bisai, FeCl₃-Catalyzed allylation reactions onto 3-hydroxy-2-oxindoles: Formal total syntheses of bis-cyclotryptamine alkaloids, (+/-)-Chimonanthine, and (+/-)-Folicanthine, *J. Org. Chem.*, 82 (2017) 8548-8567.
- [33] V. Asso, E. Ghilardi, S. Bertini, M. Digiaco, C. Granchi, F. Minutolo, S. Rapposelli, A. Bortolato, S. Moro, M. Macchia, α -Naphthylaminopropan-2-ol derivatives as BACE1 inhibitors, *ChemMedChem*, 3 (2008) 1530-1534.
- [34] S. Bertini, V. Asso, E. Ghilardi, C. Granchi, C. Manera, F. Minutolo, G. Saccomanni, A. Bortolato, J. Mason, S. Moro, M. Macchia, Carbazole-containing arylcarboxamides as BACE1 inhibitors, *Bioorg. Med. Chem. Lett.*, 21 (2011) 6657-6661.
- [35] S. Bertini, E. Ghilardi, V. Asso, F. Minutolo, S. Rapposelli, M. Digiaco, G. Saccomanni, V. Salmaso, M. Sturlese, S. Moro, M. Macchia, C. Manera, Sulfonamido-derivatives of unsubstituted carbazoles as BACE1 inhibitors, *Bioorg. Med. Chem. Lett.*, 27 (2017) 4812-4816.
- [36] A.B. Kumar, J.M. Anderson, A.L. Melendez, R. Manetsch, Synthesis and structure-activity relationship studies of 1,3-disubstituted 2-propanols as BACE-1 inhibitors, *Bioorg. Med. Chem. Lett.*, 22 (2012) 4740-4744.
- [37] S. Chandrasekhar, S. Mukherjee, A convenient modification of the Fischer indole synthesis with a solid acid, *Synth. Commun.*, 45 (2015) 1018-1022.
- [38] L. Zhang, J. Zhou, L. Zhang, Effect of temperature on the fluorescence emission of carbazole-substituted methylcellulose in dilute aqueous solutions, *Cellulose*, 20 (2013) 105-114.
- [39] W. Wang, X. Sun, D. Sun, S. Li, Y. Yu, T. Yang, J. Yao, Z. Chen, L. Duan, Carbazole aminoalcohols induce antiproliferation and apoptosis of human tumor cells by inhibiting topoisomerase I, *ChemMedChem*, 11 (2016) 2675-2681.
- [40] G.L. Ellman, K.D. Courtney, V. Andres, R.M. Featherstone, A new and rapid colorimetric determination of acetylcholinesterase activity, *Biochem. Pharmacol.*, 7 (1961) 88-95.
- [41] I.M. Eldeen, E.E. Elgorashi, J. van Staden, Antibacterial, anti-inflammatory, anti-cholinesterase and mutagenic effects of extracts obtained from some trees used in South African traditional medicine, *J. Ethnopharmacol.*, 102 (2005) 457-464.
- [42] V. Vichai, K. Kirtikara, Sulforhodamine B colorimetric assay for cytotoxicity screening, *Nat. Protoc.*, 1 (2006) 1112-1116.

[43] P. Wiji Prasetyaningrum, A. Bahtiar, H. Hayun, Synthesis and cytotoxicity evaluation of novel asymmetrical mono-carbonyl analogs of curcumin (AMACs) against Vero, HeLa, and MCF7 cell lines, *Sci. Pharm.*, 86 (2018) 1-13.

[44] L.A. Crawford, N.C. Clemence, H. McNab, R.G. Tyas, Isoindolo[2,1-*a*]indol-6-one-a new pyrolytic synthesis and some unexpected chemical properties, *Org. Biomol. Chem.*, 6 (2008) 2334-2339.

Chapter 5. Synthesis of novel 6,7-dimethoxy-1-phenyl-1,4-dihydroindeno[1,2-c]pyrazole-3-carboxamide derivatives as potential *N*-methyl-D-aspartate receptor antagonists for the treatment of Alzheimer's disease

Contributions to this chapter

All of the synthesis and compound characterization described in this chapter were performed by Mr DG van Greunen under the supervision of Dr DL Riley and Dr J-L Panayides. The synthetic work was undertaken in the Department of Chemistry at the University of Pretoria. All of the AChE biological assays and statistical analysis described in this chapter were performed by Mr DG van Greunen under the supervision of Prof V Steenkamp and Dr J-L Panayides, with assistance from Dr W Cordier and Ms M Nell. The biological work was undertaken in the Department of Pharmacology at the University of Pretoria.

Synthesis of novel 6,7-dimethoxy-1-phenyl-1,4-dihydroindeno[1,2-c]pyrazole-3-carboxamide derivatives as potential *N*-methyl-D-aspartate receptor antagonists for the treatment of Alzheimer's disease

Divan G. van Greunen^a, Werner Cordier^b, Margo Nell^b, Vanessa Steenkamp^b, Jenny-Lee Panayides^c, Darren L. Riley^{a,*}

^a Department of Chemistry, Faculty of Natural and Agricultural Sciences, University of Pretoria, Lynnwood Road, Pretoria, South Africa

^b Department of Pharmacology, Faculty of Health Sciences, University of Pretoria, Bophelo Road, Pretoria, South Africa

^c Pioneering Health Sciences, CSIR Biosciences, Meiring Naudé Road, Pretoria, South Africa

* Corresponding author. E-mail address: darren.riley@up.ac.za (D.L. Riley)

ABSTRACT

A series of twenty-four *N*-methyl-D-aspartate receptor antagonists, as potential agents for the treatment of Alzheimer's disease, were designed and synthesized based upon the molecular skeletons of previously designed *N*-methyl-D-aspartate receptor antagonists. 6,7-Dimethoxy-*N*,1-diphenyl-1,4-dihydroindeno[1,2-c]pyrazole-3-carboxamide **9** was afforded with the highest yield (68%). The synthesized compounds were found not to be selective towards AChE, therefore excluding them as possible AChE inhibitors for the treatment of Alzheimer's disease.

Key Words

Acetylcholinesterase, Alzheimer's disease, *N*-Methyl-D-aspartate receptor antagonist, pyrazole

5.1. INTRODUCTION

Pyrazole **1** is an aromatic five-membered heterocyclic system belonging to the azole class of compounds containing two adjacent nitrogen atoms in the ring (**Figure 5.1**) [1, 2]. It is a π -excessive heterocycle, containing a pyrrole-type nitrogen (position 1) with unshared electrons that are conjugated with the aromatic ring and a pyridine-type nitrogen (position 2) in which the unshared electrons are not compromised with resonance [3]. Pyrazole **1** reacts differently with acids and bases in that the pyrrole-type nitrogen can form an anion, unlike the pyridine-type nitrogen which can form a cation, making it a very useful heterocyclic building block (**Figure 5.1**) [2, 3].

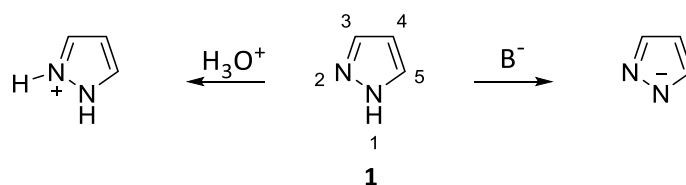
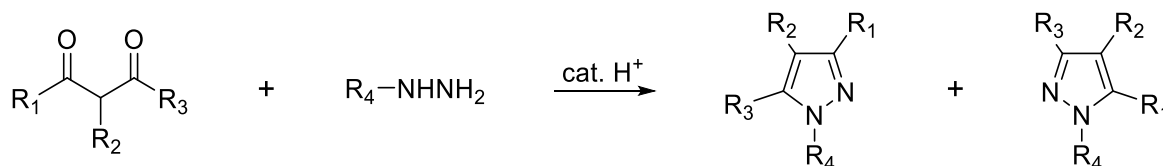


Figure 5.1: Neutral pyrazole (centre) with cationic (left) and anionic (right) forms [3].

Although there are a number of approaches which can be followed for the synthesis of substituted pyrazoles [4-10], three classical methods are commonly used. These methods are based either on the cyclocondensation of hydrazines with carbonyl systems, 1,3-dipolar cycloadditions or multicomponent reactions [11].

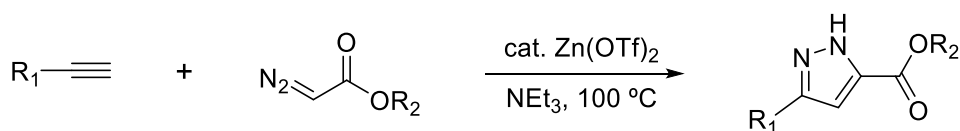
The most common approach for obtaining substituted pyrazoles is *via* the cyclocondensation reaction between appropriate hydrazines and various carbonyl systems such as the 1,3-dicarbonyl system or the α,β -unsaturated carbonyl system [2, 12-14]. The Knorr pyrazole synthesis is a simple and rapid approach to obtain substituted pyrazole systems where a substituted 1,3-dicarbonyl system reacts with an appropriate hydrazine derivative to afford two regioisomers (**Scheme 5.1**) [11].



Scheme 5.1. Knorr pyrazole synthesis [11].

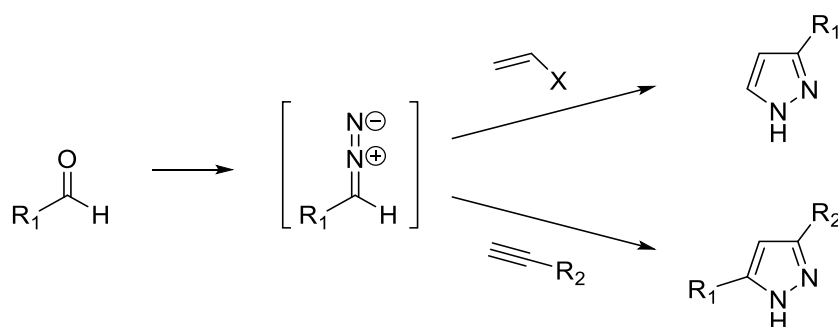
1,3-Dipolar cycloadditions to access pyrazoles depend on [3 + 2] cycloaddition reactions between an alkyne or an olefin and 1,3-dipolar compounds such as diazo compounds, sydnone or nitrimines. The Liang research group developed a method using zinc triflate as catalyst in the 1,3-dipolar cycloaddition between diazocarbonyl compounds and terminal alkynes in the presence of triethylamine to afford

the desired pyrazoles (**Scheme 5.2**) [15]. This is one of many examples which allow one to access pyrazoles via the 1,3-dipolar cycloaddition approach [16-19].



Scheme 5.2. 1,3-Dipolar cycloaddition between diazocarbonyl compounds and terminal alkynes [15].

Multicomponent reactions are a versatile way of synthesizing pyrazoles in that one of the starting materials may be light or moisture sensitive and as such this approach may be seen as a one pot synthesis of pyrazoles. Due to the possible sensitivities it may therefore require the *in situ* formation of carbonyl [20-22], β -aminoenones [23], hydrazones [24-27] or diazo derivatives [28]. Aggarwal *et al.* developed a multicomponent process in which they generated diazo derivatives *in situ* and reacted them with various terminal alkynes and olefin derivatives to afford regioselective pyrazoles (**Scheme 5.3**) [28].



Scheme 5.3. Multicomponent reactions of the synthesis of pyrazoles via *in situ* diazo derivatives [28].

Pyrazole derivatives have been reported with biological activities against a range of different disease classes including antimicrobial [29-31], anticancer [32-34], anti-inflammatory and analgesic [35-37] or antiviral properties [38, 39]. In addition, the scaffold has also been used in the development of neuroprotective compounds [40-47].

The exploration of pyrazole and pyrazoline as pharmacophores for *N*-methyl-D-aspartate (NMDA) receptor antagonists has been explored by several research groups [48-53]. The work done by Liotta and co-workers [48, 49], as well as Kawai *et al.* [50], is of interest due to the selectivity that these antagonists show towards the different subunits of NMDA (**Figure 5.2**). Thus, it was of interest to develop a hybridized molecule based on compounds **2** and **3**.

Liotta *et al.*, designed the selective GluN2C and GluN2D subunit NMDA antagonist, compound **2** (**Figure 5.2**) which was found to have IC_{50} values of 0.22 μM and 0.17 μM against the subunits respectively. However, during their assessment of the physicochemical properties and pharmacokinetics of the inhibitor and its racemate, it was discovered that the compounds had a high topological polar surface area ($TPSA > 90 \text{ \AA}^2$), being outside the optimal range for blood-brain barrier (BBB) penetration [54], as well as poor P-glycoprotein (P-gp) penetration *in vitro* [49]. No literature could be found for the physicochemical properties and pharmacokinetics of Kawai compound **3** [50].

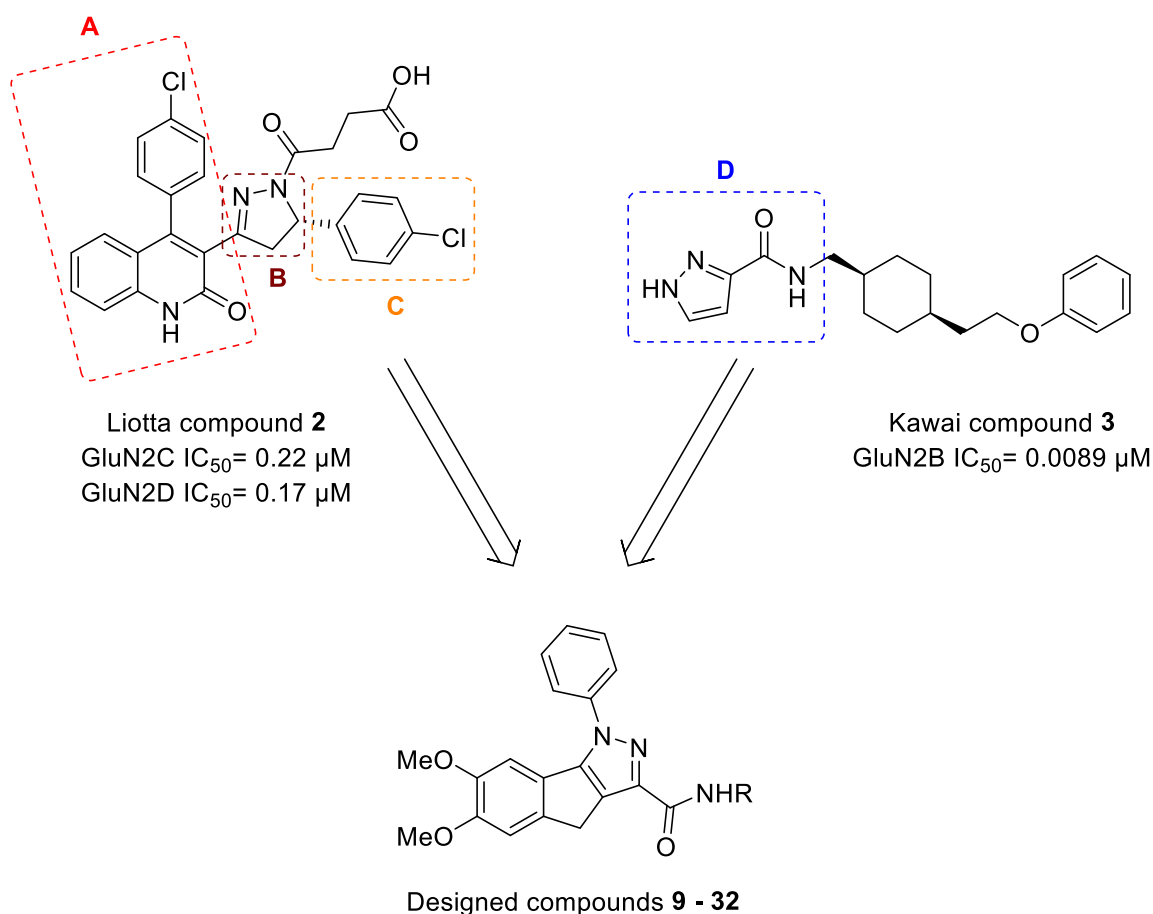


Figure 5.2. Design strategy of target compounds **9 - 32**.

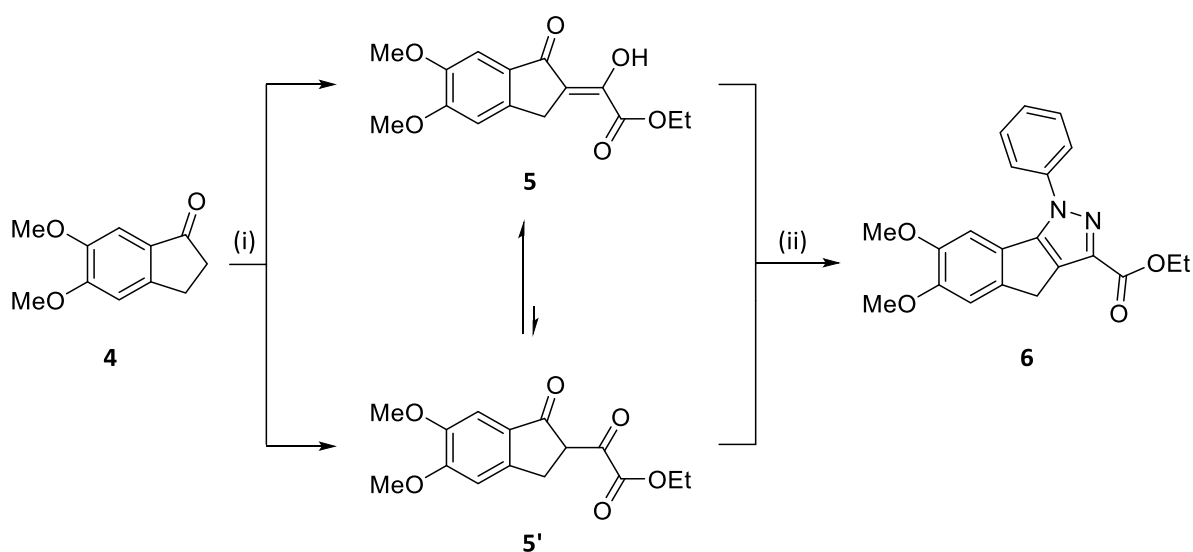
As such, in this study (**Figure 5.2**), the synthesis of hybrid compounds was proposed that combine the affinity for not only one but three of the four subunits of the NMDA receptor. As part of the design process, the rotatable substituted quinolone moiety (Part A) and pyrazoline moiety (Part B) of compound **2** were fused and the pyrazoline moiety was replaced with a pyrazole moiety to afford a simpler and more rigid system. Liotta and co-workers found that the aryl substituent on the quinolone moiety plays a role in the antagonism of NMDA, and to maintain this, an unsubstituted aryl moiety was introduced onto the pyrazole moiety, as an initial starting point in the design. In addition, as

heterocyclic amides have been shown to strongly antagonise the GluN2B receptor subunit [50], the aryl and pyrazoline moieties (Part B & C) of compound **2** were replaced with the amide moiety (Part D) of compound **3** and thereafter using different substituted aryl and benzyl groups as amide substituents.

In this study, the synthesis of novel 6,7-dimethoxy-1-phenyl-1,4-dihydroindeno[1,2-c]pyrazole-3-carboxamide derivatives (**9 - 32**), and their acetylcholinesterase (AChE) inhibitory activity is reported.

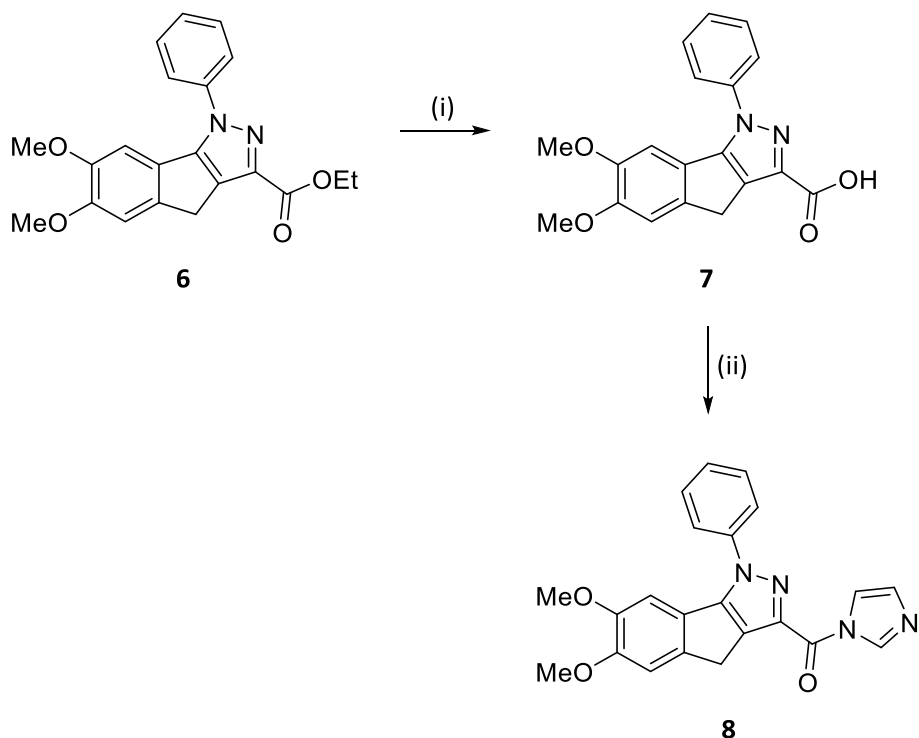
5.2. CHEMISTRY

The preparation of the trisubstituted pyrazole **6** was achieved in two steps by the condensation of commercially available 5,6-dimethoxy-1-indanone **4** (**Scheme 5.4**) with diethyl oxalate to afford the 1,3-diketoester **5'**; however, a tautomeric equilibrium was observed with the alkenylidene compound **5** being solely isolated without detection of the 1,3-diketoester **5'** [55, 56]. This was then followed by the Knorr pyrazole synthesis using phenylhydrazine hydrochloride to afford pyrazole **6** in a yield of 81% over the two steps [56].



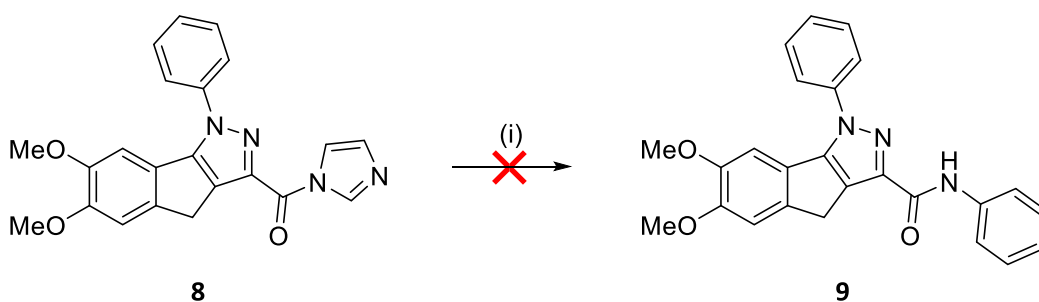
Scheme 5.4: (i) 2.2 eq. NaOEt, 1 eq. (CO₂Et)₂, EtOH, rt, 12 h, 86%; (ii) 1 eq. PhNHNH₂.HCl, EtOH, reflux, 18 h, 94%

The synthesis of the imidazole derivative **8** (**Scheme 5.5**) was achieved in two steps. The pyrazole ester **6** was hydrolysed to afford carboxylic acid **7**, which in turn was left to react under inert conditions with carbonyl diimidazole to afford the imidazole derivative **8** with a yield of 79% yield over two steps [57]. Interestingly, although imidazole derivatives of carboxylic acids are generally unstable in the presence of moisture, compound **8** proved to be moisture stable and once prepared could be readily stored for extended periods of time.



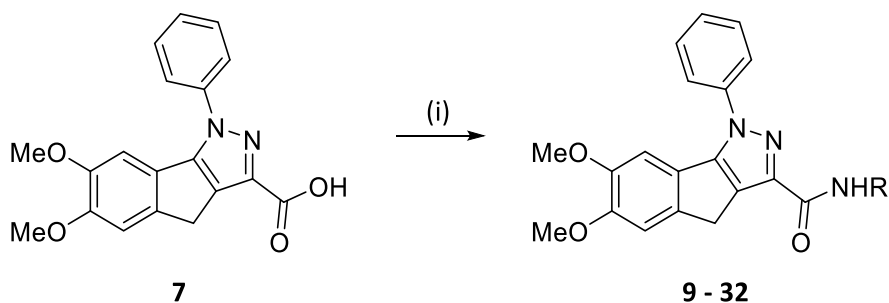
Scheme 5.5: (i) 2 eq. KOH, MeOH, reflux, 12 h, 95%; (ii) 1.2 eq. CDI, DCM, 0 °C, 2 h, 83%.

The imidazole intermediate **8** (Scheme 5.6) was left to react with aniline for 48 hours at which time the formation of the desired amide **9** could not be detected [57]. The imidazole intermediate **8** was subsequently abandoned as it was confirmed that the amide coupling would not occur with imidazole as leaving group. This surprising lack of reactivity may be due to the highly conjugated nature of the system affording a very stable compound, which is unreactive towards nucleophilic substitution. As a result, the use of an acid chloride was investigated as an alternative to compound **8**.



Scheme 5.6: (i) 1.1 eq. PhNH₂, ACN, reflux, 48 h, 0%.

Oxalyl chloride was used as chlorinating agent to facilitate the *in situ* formation of the acid chloride of **7**, which, was in turn reacted with various anilines and benzylamines under inert conditions in a classic amide coupling reaction to afford amides **9** - **32** with yields of 39 – 68% (Scheme 5.7).



Scheme 5.7: (i) 1.2 eq. (COCl)₂, 2.5 eq. Et₃N; (ii) 1.2 eq. R-NH₂, ACN, rt, 12 h, 39 – 68%.

Compound **9** (Figure 5.3) is used as a representative example to describe how the structures were elucidated using NMR, HRMS and IR spectroscopy. The synthesis of **9** was evident by the disappearance of the carboxylic acid proton singlet peak at 12.98 ppm and the presence of the new characteristic amide proton singlet peak integrating for 1H at 8.81 ppm. The carbonyl carbon peak was observed to have shifted from 163.18 to 160.19 ppm in the ¹³C NMR spectrum, whereas the distinctive pyrazole carbon (N=C-CO) peak was observed to have shifted from 141.86 to 142.96 ppm. HRMS also confirmed the formation of **9**, with a [M + H]⁺ peak observed at 412.1689 which corresponded to the calculated [M + H]⁺ value of 412.1689. The formation of **9** was further supported by the appearance of an amide carbonyl peak in the IR spectrum at 1691 cm⁻¹, which is indicative of an amide carbonyl stretch. The remaining compounds in the series were analysed in a similar manner, and the spectral assignments are provided in the experimental section.

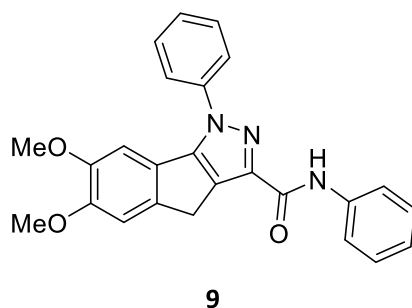


Figure 5.3. Compound **9**.

In order to correlate the correct regiochemistry of the phenyl-substituted pyrazole, the crystal structure of the precursor ester compound **6** was solved using x-ray diffraction (XRD) crystallography as indicated by the *MERCURY* diagram (indicating atoms at 50% probability) in Figure 5.4.

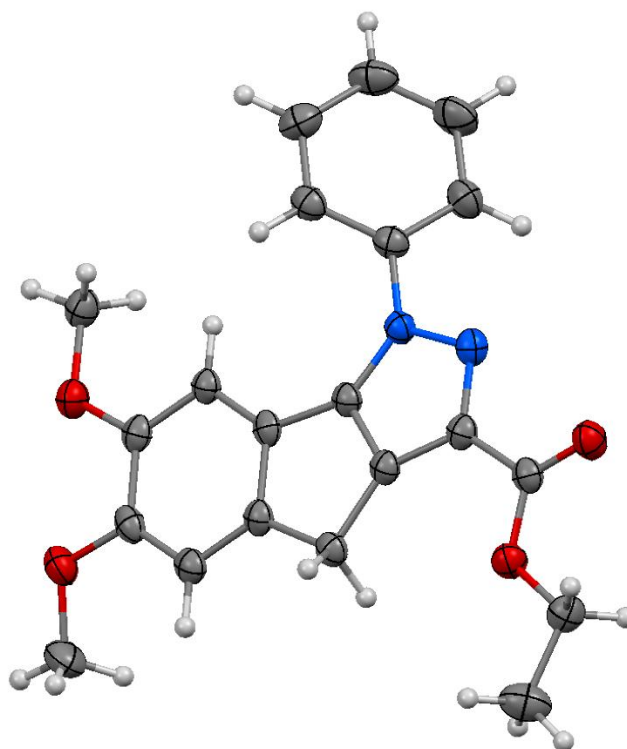


Figure 5.4. *MERCURY* diagram of ester precursor **6** (showing the 50% probability thermal ellipsoids for all non-hydrogen atoms).

When developing new drugs for medicinal use, certain guidelines need to be adhered to such as Lipinski's rule of five (RoF). The RoF serves as a guideline to assess drug-likeness or whether the chemical entity possesses certain pharmacological properties that would make it an orally active drug. One must, however, keep in mind that these rules do not predict whether a compound would be pharmacologically active or not. To adhere to Lipinski's RoF the following is required: (i) the compound must not have more than five H-bond donors (N and O atoms); (ii) the compound must not have more than ten H-bond acceptors (N & O atoms); (iii) the compound must have a molar mass <than 500 $\text{g}\cdot\text{mol}^{-1}$ and (iv) the compound must have a $\log P$ value less than 5 (or Morgushi $\log P$, denoted Mlog P , value less than 4.15) [58]. It was decided to assess and contrast the proposed compounds **9** and **21** (**Table 5.1**) against the Liotta **2** and Kawai **3** (**Figure 5.5**) compounds using the SwissADME web tool which uses *in silico* methods to assess physiochemical and pharmacokinetic properties [59]. Compounds **9** and **21** (**Figure 5.5**) were selected as representative examples of the aryl and benzyl derivatives. The parameters evaluated are provided in **Table 5.1**.

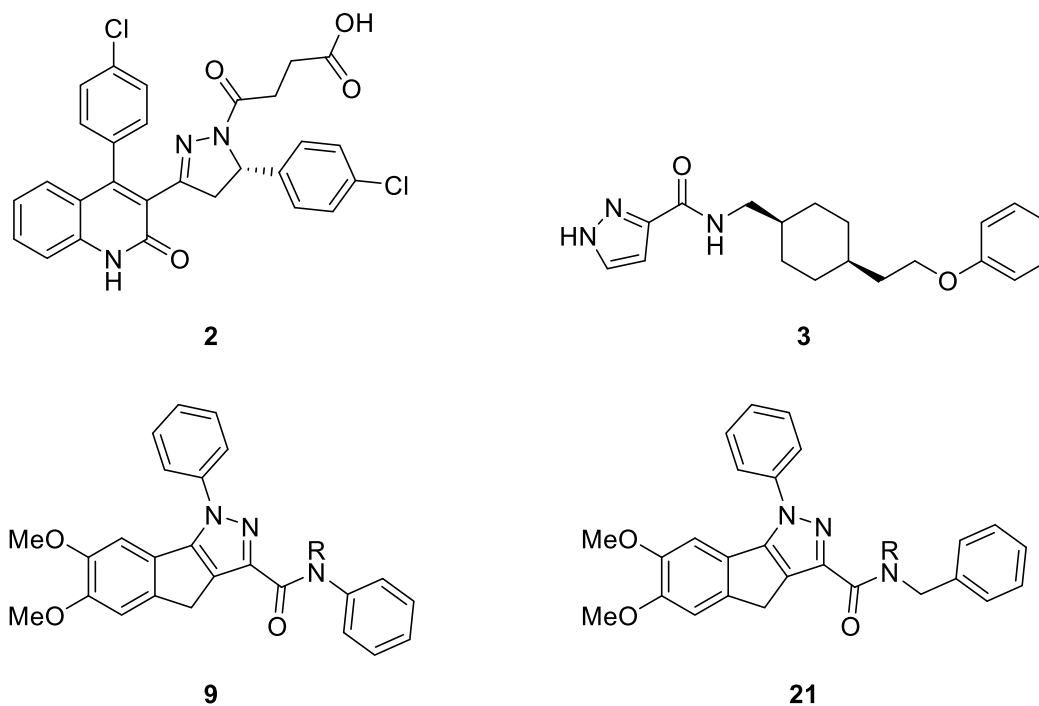


Figure 5.5. Compounds 2, 3, 9 and 21 used for *in silico* assessment.

Table 5.1. *In silico* assessment of compounds 2, 3, 9 and 21.

| Compounds | | | | |
|-----------------------------|--------|--------|--------|--------|
| Parameter | 2 | 3 | 9 | 21 |
| Molecular weight (g/mol) | 534.39 | 327.42 | 411.45 | 425.48 |
| Number of H-bond donors | 2 | 2 | 1 | 1 |
| Number of H-bond acceptors | 5 | 3 | 4 | 4 |
| TPSA (Å ²) | 102.83 | 67.01 | 65.38 | 65.38 |
| M log P | 4.32 | 2.39 | 3.24 | 3.18 |
| BBB permeability | No | Yes | Yes | Yes |
| P-gp | No | Yes | Yes | Yes |
| Gastrointestinal absorption | High | High | High | High |

| Bioavailability score | 0.56 | 0.55 | 0.55 | 0.55 |
|-----------------------|------|------|------|------|
|-----------------------|------|------|------|------|

TPSA = Topological polar surface area

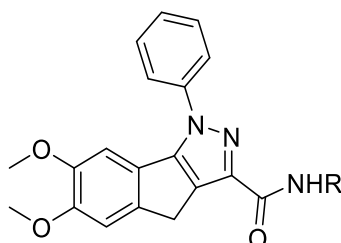
BBB = Blood-brain barrier

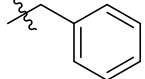
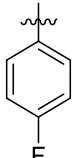
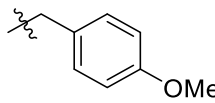
The prediction was found to correlate well with the experimental data obtained by the Liotta group for compound **2**. Compounds **3**, **9** and **21** all obeyed Lipinski's RoF, including the requirement that the TPSA should be smaller than 90\AA^2 . Therefore, *in silico* analysis predicted that compounds **3**, **9** and **21** may be better pharmacological drugs for antagonising the NMDA receptor.

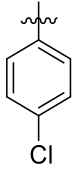
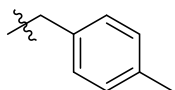
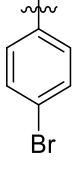
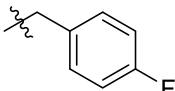
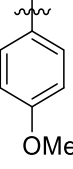
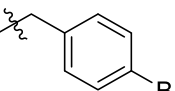
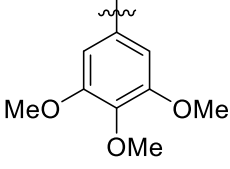
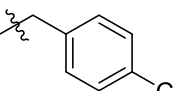
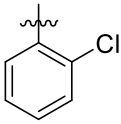
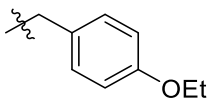
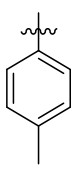
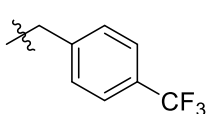
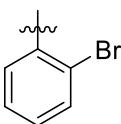
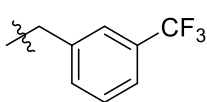
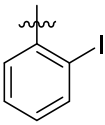
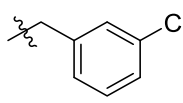
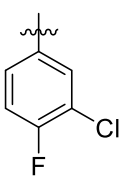
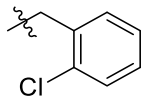
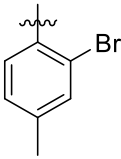
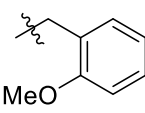
5.3. STRUCTURE ACTIVITY RELATIONSHIP STUDY

It should be noted that although the compounds were not designed as acetylcholinesterase (AChE) inhibitors, all synthesized compound were evaluated as part as a routine screening process against AChE as a possibility for the downstream development of dual inhibitors. The inhibitory activity of the newly synthesized compounds was assessed against *Electrophorus electricus* AChE (*EeAChE*) using Ellman's spectrophotometric method [60] with minor modifications [61] and galantamine was used as a positive control. The AChE inhibitory activities for the synthesized compounds are expressed as half-maximal inhibitory concentration (IC_{50}) values as provided in **Table 5.2**.

Table 5.2. *In vitro* AChE inhibitory activity of compounds **9** - **32**.



| Compound | R | <i>EeAChE</i> $IC_{50} \pm SEM$ (μM) ^a | Compound | R | <i>EeAChE</i> $IC_{50} \pm SEM$ (μM) ^a |
|-----------|---|--|-----------|---|--|
| 9 |  | >100 | 21 |  | nd ^b |
| 10 |  | >100 | 22 |  | 86.10 ± 3.25 |

| | | | | | |
|--------------------|---|---------------|----|---|---------------|
| 11 |  | >100 | 23 |  | 87.90 ± 2.42 |
| 12 |  | >100 | 24 |  | >100 |
| 13 |  | >100 | 25 |  | 95.06 ± 15.76 |
| 14 |  | >100 | 26 |  | 91.20 ± 5.70 |
| 15 |  | 78.34 ± 13.14 | 27 |  | >100 |
| 16 |  | 66.53 ± 14.35 | 28 |  | >100 |
| 17 |  | 52.12 ± 5.79 | 29 |  | >100 |
| 18 |  | 89.33 ± 28.90 | 30 |  | 98.17 ± 5.65 |
| 19 |  | 81.10 ± 2.60 | 31 |  | >100 |
| 20 |  | >100 | 32 |  | >100 |
| Galantamine | | 3.58 ± 1.24 | | | |

^a Data are the mean ± SEM of three independent experiments

^b Not determined due to precipitation occurring

The synthesized compounds showed no or negligible inhibitory activity against *EeAChE*, with no IC_{50} values below 10 μM . Compound **17** afforded the highest inhibitory activity against *EeAChE* with an IC_{50} value of $52.12 \pm 5.79 \mu\text{M}$. The inhibition of *EeAChE* was found to decrease when substituting the bromo-substituent (compound **17**, $52.12 \mu\text{M}$) with a chloro- (compound **15**, $78.34 \mu\text{M}$) or iodo-substituent (compound **18**, $89.33 \mu\text{M}$) in the *ortho*-position for aryl substitutions. A comparison of the aryl groups suggests that inhibition of *EeAChE* was preferred when a halogen is mono-substituted in the *ortho*-position.

A comparison of the aryl group substitutions, suggest that substitutions on the *para*-position of the benzyl group provides compounds with better *EeAChE* inhibitory activity. In addition, when assessing the substitution on the *para*-position for the benzyl groups, it seems that smaller groups such as chloro (compound **26**, $91.20 \mu\text{M}$), bromo (compound **25**, $95.06 \mu\text{M}$) and methyl (compound **23**, $97.90 \mu\text{M}$) substituents are more preferential. Thus, the substituted aryl groups were found to have a better inhibitory activity than the substituted benzyl groups. Unfortunately, the use of these compounds as potential dual AChE NMDA inhibitors is unfeasible as the AChE inhibition is limited at best.

5.4. CONCLUSION

A series of twenty-four novel 6,7-dimethoxy-1-phenyl-1,4-dihydroindeno[1,2-*c*]pyrazole-3-carboxamide derivatives were synthesized with yields ranging from 39 – 68%. The designed compounds were predicted to be within the boundaries as proposed by Lipinski's RoF guidelines in terms of drug-like properties. In an effort to identify dual inhibitors, the compounds were evaluated against *EeAChE*. Compound **17** afforded the highest inhibitory activity against *EeAChE* with an IC_{50} value of $52.12 \pm 5.79 \mu\text{M}$. The overall trend observed regarding *EeAChE* inhibition suggested that the identification of a potential dual inhibitor scaffold was unsuccessful. Thus, this series is not suitable for the development of AChE inhibitors and by default as dual inhibitors. Assessment of the antagonistic properties of these compounds against NMDA will be completed as part of future work linked to this project.

5.5. EXPERIMENTAL

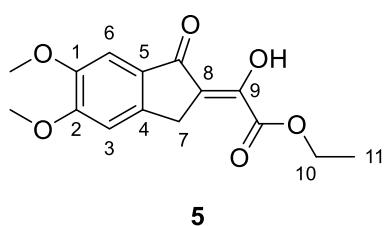
5.5.1. Chemistry

5.5.1.1. General methods

All solvents, chemicals, and reagents were obtained commercially and used without further purification. ^1H NMR (300 MHz) and ^{13}C NMR (75 MHz) spectra were recorded on Bruker AVANCE-III-300 instrument using CDCl_3 and $\text{DMSO-}d_6$. CDCl_3 contained tetramethylsilane as an internal standard.

Chemical shifts, δ , are reported in parts per million (ppm), and splitting patterns are given as singlet (s), doublet (d), triplet (t), quartet (q), or multiplet (m). Coupling constants, J , are expressed in hertz (Hz). Mass spectra were recorded in ESI mode on a Waters Synapt G2 Mass Spectrometer at 70 eV and 200 mA. Samples were dissolved in acetonitrile (containing 0.1% formic acid) to an approximate concentration of 10 $\mu\text{g}/\text{mL}$. Infrared spectra were run on a Bruker ALPHA Platinum ATR spectrometer. The absorptions are reported on the wavenumber (cm^{-1}) scale, in the range 400 - 4000 cm^{-1} . Abbreviations used in quoting spectra are: v = very, s = strong, m = medium, w = weak, str = stretch. Melting points were measured on a Stuart Melting Point SMP10 microscope. The retention factor (R_f) values denoted are for thin layer chromatography (TLC) on aluminium-backed Macherey-Nagel ALUGRAM Sil G/UV₂₅₄ plates pre-coated with 0.25 mm silica gel 60, spots were visualised with UV light and basic KMnO_4 spray reagent. Yields refer to isolated pure products unless stated otherwise. Crystal structure intensity data were collected on a Bruker APEX II-CCD area diffractometer with graphite monochromated $\text{Mo } K\alpha$ radiation ($\lambda = 0.71073 \text{ \AA}$). The collection method involved ω -scans of width 0.3°. The crystal structure was solved by direct methods using *SHELXTL* [62]. Non-hydrogen atoms were first refined isotropically followed by anisotropic refinement by full matrix least-squares calculations based on F_2 using *SHELXTL* [62]. Hydrogen atoms were first located in the difference map then positioned geometrically and allowed to ride on their respective parent atoms. Diagrams and publication material were generated using *MERCURY CSD 2.0* [63]. Each compound is named either according to PerkinElmer's *ChemDraw Version 15.0.0.106* or according to common names. The numbering of compounds was not done according to priority, but rather to the author's convenience for characterization.

5.5.1.2. Ethyl (Z)-2-(5,6-dimethoxy-1-oxo-1,3-dihydro-2H-inden-2-ylidene)-2-hydroxyacetate **5**

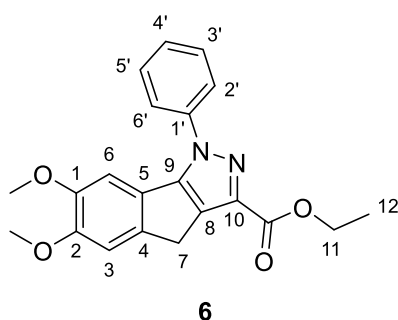


Sodium metal (2.64 g, 114 mmol, 2.2 eq.) was added to absolute ethanol (150 mL) at 0 °C. After all the sodium reacted the mixture was left to warm up to room temperature and diethyl oxalate (7.1 mL, 52 mmol, 1 eq.) was added. 5,6-Dimethoxy-1-indanone **4** (10.00 g, 52.04 mmol, 1 eq.) was then added in small portions.

After complete addition, the reaction was left to stir at room temperature overnight. The mixture was then neutralized by 1 M hydrochloric acid (100 mL), and the resulting precipitate was filtered off, washed with ice-cold ethanol (20 mL), collected and dried *in vacuo* to afford the product. The product was used without any further purification. (Yield 86%); Yellow solid; R_f 0.66 (1:1 ethyl acetate: hexane); mp 165 - 167 °C (lit. 158 – 162 °C [64]); ν_{max} (neat)/ cm^{-1} 3255 (O-H str, w), 1724 (C=O ester str, m), 1655 (C=O str, m), 1604 (C-C str (in-ring), m), 1500 (O-H bend, m), 1290 (C-O str, s); 1245 (C-O str, s), 1185 (C-O str, s), 1014, 806 (C-H "oop", m), 586 (C-H "oop", m); $^1\text{H NMR}$ (300 MHz, CDCl_3); δ 13.13

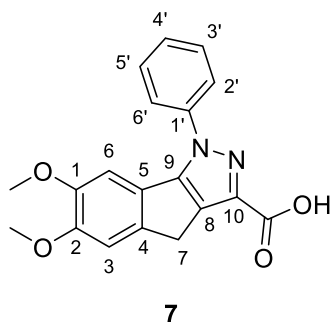
(1H, br s, OH), 7.23 (1H, s, H-6), 6.94 (1H, s, H-3), 4.38 (2H, q, $J = 7.1$ Hz, OCH_2CH_3), 3.98 (3H, s, OCH_3), 3.92 (3H, s, OCH_3), 3.86 (2H, s, H-7), 1.41 (3H, t, $J = 7.1$ Hz, OCH_2CH_3); ^{13}C NMR (75 MHz, CDCl_3); δ 197.7 (C=O, ketone), 163.0 (C=O, ester), 156.2 (C-9), 151.6 (C-2), 149.8 (C-1), 146.5 (C-5), 130.1 (C-4), 117.4 (C-8), 107.3 (C-3), 104.5 (C-3), 62.2 (C-10), 56.5 (OCH_3), 56.2 (OCH_3), 31.3 (C-7), 14.3 (C-11). HRMS m/z (ESI) ($\text{C}_{15}\text{H}_{16}\text{O}_6$) 293.1041 ($[\text{M} + \text{H}]^+$ requires 293.1020). Characterization of this compound compared well to literature [64].

5.5.1.3. Ethyl 6,7-dimethoxy-1-phenyl-1,4-dihydroindeno[1,2-*c*]pyrazole-3-carboxylate **6**



To a suspension of ethyl (*Z*)-2-(5,6-dimethoxy-1-oxo-1*H*-indeno-2(3*H*)ylidene)-2-hydroxyacetate **5** (17.50 g, 59.88 mmol, 1 eq.) in absolute ethanol (250 mL), was added phenylhydrazine hydrochloride (8.66 g, 59.9 mmol, 1 eq.). The resulting mixture was heated to reflux temperature for 18 h. The reaction mixture was then cooled down to room temperature and the crystalline product was filtered off and washed with absolute ethanol (20 mL). The product was collected and dried *in vacuo*. The product was used without any further purification. (Yield 94%); Light yellow crystalline solid; R_f 0.60 (1:1 ethyl acetate: hexane); mp 177 °C; ν_{max} (neat)/ cm^{-1} 1728 (C=O str, s), 1486 (C=N str, m), 1369 (C-H bend, m), 1255 (C-N str, s), 1196 (s), 1111 (C-O str, s), 1018 (s), 844 (C-H “oop”, s), 804 (C-H “oop”, s), 770 (C-H “oop”, s); ^1H NMR (300 MHz, CDCl_3); δ 7.79 – 7.72 (2H, m, H-2' & H-6'), 7.60 – 7.52 (2H, m, H-3' & H-5'), 7.50 – 7.41 (1H, m, H-4'), 7.12 (1 H, s, H-6), 6.98 (1H, s, H-3), 4.46 (2H, q, $J = 7.1$ Hz, OCH_2CH_3), 3.94 (3H, s, OCH_3), 3.79 (3H, s, OCH_3), 3.75 (2H, s, H-7), 1.44 (3H, t, $J = 7.1$ Hz, OCH_2CH_3); ^{13}C NMR (75 MHz, CDCl_3); δ 162.7 (C=O), 149.6 (C-2), 148.9 (C-9), 148.3 (C-1), 142.4 (C-10), 139.9 (C-1'), 138.8 (C-5), 130.5 (C-4), 129.4 (C-3' & C-5'), 128.6 (C-4'), 124.4 (C-8), 123.8 (C-2' & C-6'), 109.9 (C-3), 103.5 (C-6), 61.1 (C-11), 56.3 (OCH_3), 56.2 (OCH_3), 29.7 (C-7), 14.5 (C-12). HRMS m/z (ESI) ($\text{C}_{21}\text{H}_{20}\text{N}_2\text{O}_4$) 365.1523 ($[\text{M} + \text{H}]^+$ requires 365.1496). *Doubling up of carbon peaks due to rotomers.

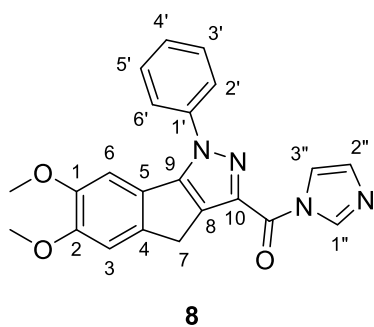
5.5.1.4. 6,7-Dimethoxy-1-phenyl-1,4-dihydroindeno[1,2-*c*]pyrazole-3-carboxylic acid **7**



To a stirring solution of potassium hydroxide (6.18 g, 110 mmol, 2 eq.) in methanol (250 mL) was added ethyl 6,7-dimethoxy-1-phenyl-1,4-dihydroindeno[1,2-*c*]pyrazole-3-carboxylate **6** (19.95 g, 54.75 mmol, 1 eq.) at room temperature. The resulting mixture was heated to reflux temperature overnight after which time the mixture was cooled to 0 °C. Concentrated hydrochloric acid (16.1 mL, 164 mmol, 3 eq.) was added slowly which caused the product to precipitate out of solution. The

product was filtered off and washed with ice-cold methanol (20 mL). The product was collected and dried *in vacuo*. The product was used without any further purification. (Yield 95%); White solid; **mp** 233 °C; ν_{\max} (**neat**)/ cm^{-1} 3320 (O-H str, m), 1727 (C=O str, s), 1475 (C=N str, m), 1259 (C-N str, m), 1190 (m), 1115 (m), 841 (C-H “oop”, s), 806 (C-H “oop”, s), 774 (C-H “oop”, s); $^1\text{H NMR}$ (**300 MHz, DMSO-*d*₆**); δ 12.98 (1H, s, OH), 7.75 (2H, d, $J = 7.7$ Hz, H-2' & H-6), 7.66 (2H, td, $J = 7.8, 1.6$ Hz, H-3' & H-5'), 7.53 (1H, dd, $J = 8.1, 6.3$ Hz, H-4'), 7.24 (1H, s, H-6), 6.90 (1H, s, H-3), 3.79 (3H, s, OCH₃), 3.67 (3H, s, OCH₃), 3.63 (2H, s, 2H, H-7); $^{13}\text{C NMR}$ (**75 MHz, DMSO-*d*₆**); δ 163.2 (C=O), 148.7 (C-2), 148.5 (C-9), 147.7 (C-1), 141.9 (C-10), 139.3 (C-1'), 138.9 (C-5), 130.0 (C-4), 129.7 (C-3' & C-5'), 128.5 (C-4'), 123.3 (C-8), 123.0 (C-2' & C-6'), 110.4 (C-3), 103.1 (C-6), 55.7 (OCH₃), 55.4 (OCH₃), 29.1 (C-7).

5.5.1.5. (6,7-Dimethoxy-1-phenyl-1,4-dihydroindeno[1,2-*c*]pyrazol-3-yl)(1H-imidazol-1-yl)methanone **8**



6,7-Dimethoxy-1-phenyl-1,4-dihydroindeno[1,2-*c*]pyrazole-3-carboxylic acid **7** (0.45 g, 1.3 mmol, 1 eq.) in dry dichloromethane (25 mL) was cooled to 0 °C, and carbonyl diimidazole (0.26 g, 1.6 mmol, 1.2 eq.) was added portion-wise over 5 min. After 2 h, the mixture was diluted with dichloromethane (10 mL), and water (20 mL) was added carefully. The organic layer was washed with water (20 mL) and brine (20 mL), dried over anhydrous sodium sulfate, and

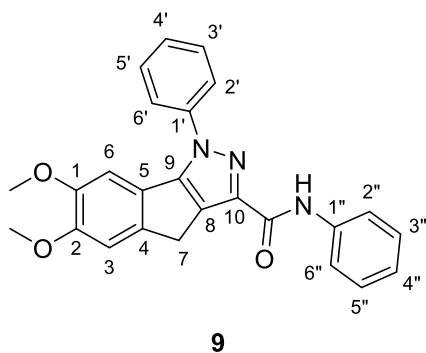
the solvent was evaporated to afford the product. The product was used without any further purification. (Yield 83%); Light yellow solid; **R_f** 0.24 (1:1 ethyl acetate: hexane); **mp** 244 °C; ν_{\max} (**neat**)/ cm^{-1} 1688 (C=O str, s), 1432 (C=N str, s), 1403 (s), 1320 (C-H bend, s), 1290 (C-N str, s), 1219 (s), 1205 (s), 1056 (s), 910 (m), 805 (C-H “oop”, s), 776 (C-H “oop”, s), 640 (C-H “oop”, s); $^1\text{H NMR}$ (**300 MHz, CDCl₃**); δ 9.10 (1H, s, H-1''), 8.06 – 8.03 (1H, m, H-3''), 7.80 – 7.73 (2H, m, H-2' & H-6'), 7.65 – 7.57 (2H, m, H-3' & H-5'), 7.56 – 7.48 (1H, m, H-4'), 7.11 (2H, s, H-2'' & H-6), 7.01 (1, s, H-3), 3.93 (3H, s, OCH₃), 3.80 (5H, s, OCH₃ & H-7); $^{13}\text{C NMR}$ (**75 MHz, CDCl₃**); δ 158.8 (C=O), 149.9 (C-1), 149.2 (C-9), 148.3 (C-2), 142.5 (C-10), 139.6 (C-1'), 139.4 (C-1''), 139.2 (C-5), 133.1 (C-2''), 130.3 (C-4), 129.7 (C-3' & C-5'), 129.0 (C-4'), 123.6 (C-8), 123.3 (C-2' & C-6'), 117.8 (C-3''), 109.7 (C-3), 103.4 (C-6), 56.3 (OCH₃), 56.2 (OCH₃), 29.9 (C-7). **HRMS *m/z* (ESI)** (C₂₂H₁₈N₄O₃) 387.1522 ([M + H]⁺ requires 387.1452).

5.5.1.6. General method for amide couplings

Oxalyl chloride (0.09 mL, 1.1 mmol, 1.2 eq.) was added to a mixture of 6,7-dimethoxy-1-phenyl-1,4-dihydroindeno[1,2-*c*]pyrazole-3-carboxylic acid **7** (0.30 g, 0.89 mmol, 1 eq.) and triethylamine (0.31 mL, 2.23 mmol, 2.5 eq.) in dry acetonitrile (15 mL) at room temperature. The resulting mixture was left to stir for 30 min after which time the appropriate aniline/benzylamine (1.1 mmol, 1.2 eq.)

derivative was added and the resulting mixture was left to stir for 12 h at room temperature. Distilled water (30 mL) was added carefully and the precipitate was filtered off and washed with ice-cold acetonitrile (10 mL). The precipitate was collected and dried *in vacuo*. The product was used without any further purification.

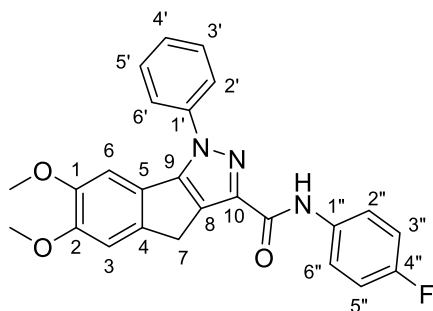
5.5.1.6.1. *6,7-Dimethoxy-N,1-diphenyl-1,4-dihydroindeno[1,2-c]pyrazole-3-carboxamide 9*



9

(Yield 68%); Yellow solid; R_f 0.67 (1:1 ethyl acetate: hexane); **mp** 193-194 °C; ν_{\max} (neat)/ cm^{-1} 3382 (N-H str, w), 1691 (C=O str, m), 1596 (C=C str, m), 1497 (C=N str, s), 1436 (C-C str, s), 1263 (C-N str, s), 1212 (s), 1110 (m), 755 (C-H "oop", s), 693 (C-H "oop", s); $^1\text{H NMR}$ (300 MHz, CDCl_3); δ 8.81 (1H, s, NH), 7.82 – 7.47 (7H, m, ArH's), 7.41 – 7.32 (2H, m, ArH's), 7.13 (2H, s, H-6 & ArH), 6.99 (1H, s, H-3), 3.95 (3H, s, OCH_3), 3.85 (3H, s, OCH_3), 3.81 (2H, s, H-7); $^{13}\text{C NMR}$ (75 MHz, CDCl_3); δ 160.2 (C=O), 150.5 (C-2), 148.9 (C-9), 148.1 (C-1), 143.0 (C-10), 141.4 (C-1'), 139.8 (C-5), 138.0 (C-1''), 129.6 (C-4), 129.4 (C-4''), 129.1 (C-3' & C-5'), 129.1 (C-3'' & C-5''), 128.6 (C-4'), 124.2 (C-2' & C-6'), 123.5 (C-8), 119.7 (C-2'' & C-6''), 109.9 (C-3), 103.4 (C-6), 56.3 (OCH_3), 56.2 (OCH_3), 29.6 (C-7). **HRMS m/z (ESI)** ($\text{C}_{25}\text{H}_{21}\text{N}_3\text{O}_3$) 412.1689 ([M + H]⁺ requires 412.1689).

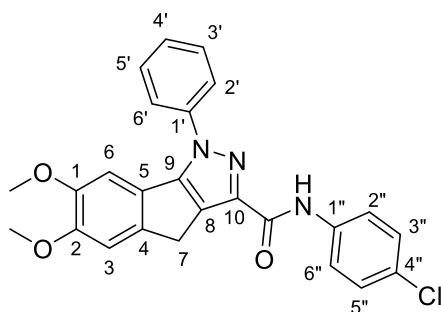
5.5.1.6.2. *N-(4-Fluorophenyl)-6,7-dimethoxy-1-phenyl-1,4-dihydroindeno[1,2-c]pyrazole-3-carboxamide 10*



10

(Yield 51%); Yellow solid; R_f 0.67 (1:1 ethyl acetate: hexane); **mp** 192 °C; ν_{\max} (neat)/ cm^{-1} 3394 (N-H str, w), 1686 (C=O str, m), 1607 (C=C str, s), 1556 (C-C str (in-ring), s), 1509 (s), 1406 (C=N str, m), 1259 (C-N str, s), 1208 (s), 1120 (s), 1065 (C-F str, s) 830 (C-H "oop", s), 805 (C-H "oop", s); $^1\text{H NMR}$ (300 MHz, CDCl_3); δ 8.80 (1H, s, NH), 7.76 (2H, d, $J = 7.5$ Hz, H-2' & H-6'), 7.68 (2H, dd, $J = 7.1, 4.3$ Hz, H-2'' & H-6''), 7.61 (2H, dd, $J = 7.5, 7.0$ Hz, H-3' & H-5'), 7.55 – 7.47 (1H, m, H-4'), 7.12 (1H, s, H-6), 7.05 (2H, dd, $J = 13.3, 6.2$ Hz, H-3'' & H-5''), 6.98 (1H, s, H-3), 3.94 (3H, s, OCH_3), 3.82 (2H, s, H-7), 3.80 (3H, s, OCH_3); $^{13}\text{C NMR}$ (75 MHz, CDCl_3); δ 160.2 (C=O), 156.6 (d, $J = 169.0$ Hz, #C-4''), 150.5 (C-2), 149.0 (C-9), 148.2 (C-1), 142.9 (C-10), 141.2 (C-1'), 139.8 (C-5), 134.1 (d, $J = 2.7$ Hz, #C-1''), 129.6 (C-3' & C-5'), 129.1 (C-4), 128.7 (C-4'), 124.1 (C-2' & C-6'), 123.5 (C-8), 121.4 (d, $J = 7.6$ Hz, #C-2'' & #C-6''), 115.8 (d, $J = 22.4$ Hz, #C-3'' & #C-5''), 109.9 (C-3), 103.4 (C-6), 56.3 (OCH_3), 56.2 (OCH_3), 29.6 (C-7). **HRMS m/z (ESI)** ($\text{C}_{25}\text{H}_{20}\text{FN}_3\text{O}_3$) 430.1602 ([M + H]⁺ requires 430.1561). #Splitting of carbon peaks due to fluorine.

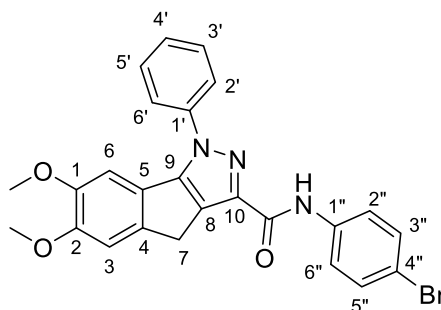
5.5.1.6.3. *N*-(4-Chlorophenyl)-6,7-dimethoxy-1-phenyl-1,4-dihydroindeno[1,2-*c*]pyrazole-3-carboxamide **11**



11

(Yield 44%); Yellow solid; R_f 0.67 (1:1 ethyl acetate: hexane); **mp** 193 °C; ν_{\max} (neat)/ cm^{-1} 3393 (N-H str, w), 1687 (C=O str, m), 1593 (C-C str (in-ring), s), 1489 (C=N str, s), 1399 (s), 1305 (s), 1260 (C-N str, s), 1118 (s), 850 (C-H “oop”, s), 825 (C-H “oop”, s), 804 (C-H “oop”, s), 759 (C-Cl str, s); $^1\text{H NMR}$ (300 MHz, CDCl_3); δ 8.81 (1H, s, NH), 7.78 (2H, d, J = 6.6 Hz, H-2'' & H-6''), 7.70 (2H, d, J = 7.4 Hz, H-2' & H-6'), 7.62 (2H, t, J = 7.0 Hz, H-3' & H-5'), 7.58 – 7.48 (1H, m, H-4'), 7.40 – 7.30 (2H, m, H-3'' & H-5''), 7.15 (1H, s, H-6), 7.00 (1H, s, H-3), 3.96 (3H, s, OCH_3), 3.85 (2H, s, H-7), 3.81 (3H, s, OCH_3); $^{13}\text{C NMR}$ (75 MHz, CDCl_3); δ 160.2 (C=O), 150.6 (C-2), 149.0 (C-9), 148.2 (C-1), 142.9 (C-10), 141.1 (C-1'), 139.8 (C-5), 136.6 (C-1''), 129.7 (C-3' & C-5'), 129.2 (C-3'' & C-5''), 129.1 (C-4''), 129.04 (C-4), 128.7 (C-4'), 124.1 (C-8), 123.5 (C-2' & C-6'), 120.9 (C-2'' & C-6''), 109.9 (C-3), 103.4 (C-6), 56.3 (OCH_3), 56.2 (OCH_3), 29.6 (C-7). **HRMS m/z (ESI)** ($\text{C}_{25}\text{H}_{20}\text{ClN}_3\text{O}_3$) 446.1336 ([M + H]⁺ requires 446.1266).

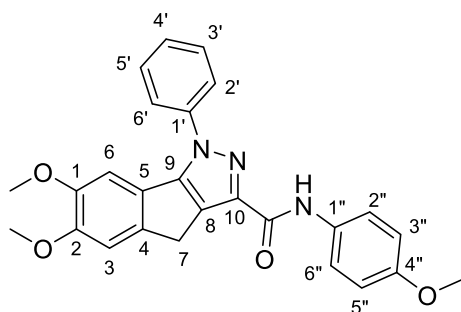
5.5.1.6.4. *N*-(4-Bromophenyl)-6,7-dimethoxy-1-phenyl-1,4-dihydroindeno[1,2-*c*]pyrazole-3-carboxamide **12**



12

(Yield 44%); Yellow solid; R_f 0.69 (1:1 ethyl acetate: hexane); **mp** 182 °C; ν_{\max} (neat)/ cm^{-1} 3390 (N-H str, w), 1687 (C=O str, s), 1588 (C-C str (in-ring), s), 1488 (C=N str, s), 1393 (s), 1259 (C-N str, s), 1117 (s), 1066 (s), 849 (C-H “oop”, s), 822 (C-H “oop”, s), 758 (C-H “oop”, s), 505 (C-Br str, s); $^1\text{H NMR}$ (300 MHz, CDCl_3); δ 8.80 (1H, s, NH), 7.76 (2H, d, J = 7.6 Hz, H-2'' & H-6''), 7.66 – 7.56 (4 H, m, ArH's), 7.56 – 7.39 (3H, m, ArH's), 7.12 (1H, s, H-6), 6.98 (1H, s, H-3), 3.94 (3H, s, OCH_3), 3.82 (2H, s, H-7), 3.80 (3H, s, OCH_3); $^{13}\text{C NMR}$ (75 MHz, CDCl_3); δ 160.2 (C=O), 150.6 (C-2), 149.0 (C-9), 148.2 (C-1), 142.9 (C-10), 141.1 (C-1'), 139.7 (C-5), 137.1 (C-1''), 132.1 (C-3'' & C-5''), 129.7 (C-3' & C-5'), 129.1 (C-4), 128.7 (C-4'), 124.1 (C-8), 123.5 (C-2' & C-6'), 121.2 (C-2'' & C-6''), 116.6 (C-4''), 109.9 (C-3), 103.4 (C-6), 56.3 (OCH_3), 56.2 (OCH_3), 29.6 (C-7). **HRMS m/z (ESI)** ($\text{C}_{25}\text{H}_{20}\text{BrN}_3\text{O}_3$) 490.0789 ([M + H]⁺ requires 490.0761).

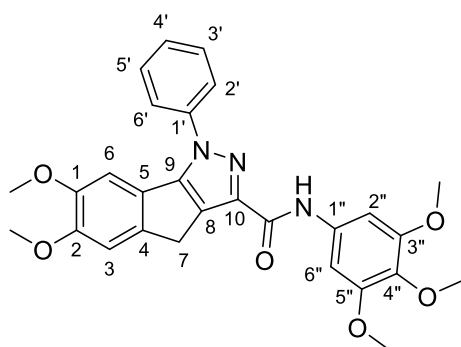
5.5.1.6.5. 6,7-Dimethoxy-N-(4-methoxyphenyl)-1-phenyl-1,4-dihydroindeno[1,2-c]pyrazole-3-carboxamide **13**



13

(Yield 63%); Yellow solid; R_f 0.50 (1:1 ethyl acetate: hexane); **mp** 141 °C; ν_{\max} (neat)/ cm^{-1} 3289 (N-H str, w), 1655 (C=O str, s), 1509 (C=N str, vs), 1214 (C-N str, s), 1176 (s), 1124 (s), 1029 (s), 825 (C-H "oop", s), 804 (C-H "oop", s), 769 (C-H "oop", s); $^1\text{H NMR}$ (300 MHz, CDCl_3); δ 8.72 (1H, s, NH), 7.84 – 7.74 (2H, m, H-2'' & H-6''), 7.70 – 7.57 (4H, m, ArH's), 7.56 – 7.46 (1H, m, H-4'), 7.15 (1H, s, H-6), 7.01 (1H, s, H-3), 6.96 – 6.87 (2H, m, H-3'' & H-5''), 3.96 (3H, s, OCH_3), 3.86 (2H, s, H-7), 3.82 (6 H, s, 2 x OCH_3); $^{13}\text{C NMR}$ (75 MHz, CDCl_3); δ 160.0 (C=O), 156.3 (C-4''), 150.4 (C-2), 148.9 (C-9), 148.1 (C-1), 143.0 (C-10), 141.5 (C-1'), 139.9 (C-5), 131.2 (C-1''), 129.6 (C-3' & C-5'), 129.1 (C-4), 128.6 (C-4'), 124.2 (C-8), 123.5 (C-2' & C-6'), 121.4 (C-2'' & C-6''), 114.3 (C-3'' & C-5''), 109.9 (C-3), 103.4 (C-6), 56.3 (2 x OCH_3), 55.6 (OCH_3), 29.7 (C-7). **HRMS m/z (ESI)** ($\text{C}_{26}\text{H}_{23}\text{N}_3\text{O}_4$) 442.1761 ($[\text{M} + \text{H}]^+$ requires 442.1750).

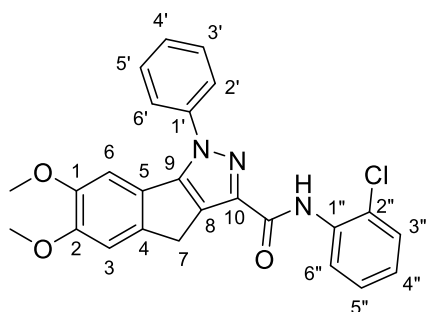
5.5.1.6.6. 6,7-Dimethoxy-1-phenyl-N-(3,4,5-trimethoxyphenyl)-1,4-dihydroindeno[1,2-c]pyrazole-3-carboxamide **14**



14

(Yield 43%); Yellow solid; R_f 0.32 (1:1 ethyl acetate: hexane); **mp** 213 °C; ν_{\max} (neat)/ cm^{-1} 3365 (N-H str, w), 1667 (C=O str, s), 1604 (C-C str (in-ring), s), 1506 (C=N str, vs), 1457 (C-C str, s), 1233 (C-N str, s), 1116 (s), 1004 (s), 769 (C-H "oop", s), 604 (C-H "oop", s); $^1\text{H NMR}$ (300 MHz, CDCl_3); δ 8.77 (1H, s, NH), 7.78 (2H, d, $J = 7.8$ Hz, H-2' & H-6'), 7.62 (2H, t, $J = 7.6$ Hz, H-3' & H-5'), 7.51 (1H, t, $J = 7.3$ Hz, H-4'), 7.12 (1H, s, H-6), 7.06 (2H, s, H-2'' & H-6''), 6.98 (1H, s, H-3), 3.94 (3H, s, OCH_3), 3.89 (6H, s, 2 x OCH_3), 3.84 (5H, s, OCH_3 & H-7), 3.80 (3H, s, OCH_3); $^{13}\text{C NMR}$ (75 MHz, CDCl_3); δ 160.1 (C=O), 153.5 (C-3'' & C-5''), 150.6 (C-2), 149.0 (C-9), 148.2 (C-1), 142.9 (C-10), 141.3 (C-1'), 139.8 (C-5), 134.5 (C-4''), 134.3 (C-1''), 129.7 (C-3' & C-5'), 128.9 (C-4), 128.7 (C-4'), 124.1 (C-8), 123.6 (C-2' & C-6'), 109.9 (C-3), 103.4 (C-6), 97.1 (C-2'' & C-6''), 61.2 (OCH_3), 61.1 (OCH_3), 56.3 (OCH_3), 56.2 (OCH_3), 56.2 (OCH_3), 29.6 (C-7). **HRMS m/z (ESI)** ($\text{C}_{28}\text{H}_{27}\text{N}_3\text{O}_6$) 502.1973 ($[\text{M} + \text{H}]^+$ requires 502.2023).

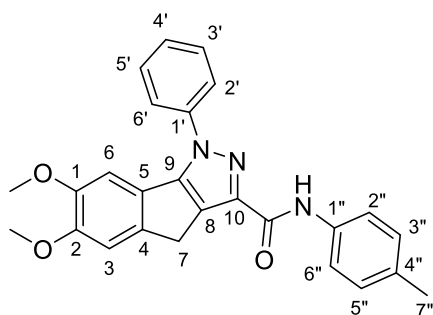
5.5.1.6.7. *N*-(2-Chlorophenyl)-6,7-dimethoxy-1-phenyl-1,4-dihydroindeno[1,2-*c*]pyrazole-3-carboxamide **15**



15

(Yield 43%); Yellow solid; R_f 0.67 (1:1 ethyl acetate: hexane); **mp** 189 °C; ν_{\max} (neat)/ cm^{-1} 3361 (N-H str, w), 1689 (C=O str, m), 1594 (C-C str, s), 1526 (C=N str, s), 1505 (s), 1437 (C-C str, s), 1305 (s), 1258 (C-N str, s), 1181 (s), 1066 (s), 804 (C-H "oop", s), 747 (C-Cl str, s), 703 (C-H "oop", s); $^1\text{H NMR}$ (300 MHz, CDCl_3); δ 9.46 (1H, s, NH), 8.60 (1H, d, $J = 8.0$ Hz, H-6''), 7.79 (2H, d, $J = 7.8$ Hz, H-2' & H-6'), 7.60 (2H, t, $J = 7.6$ Hz, H-3' & H-5'), 7.49 (1H, t, $J = 7.3$ Hz, H-4'), 7.39 (1H, d, $J = 8.0$ Hz, H-3''), 7.30 (1H, t, $J = 7.8$ Hz, H-5), 7.12 (1H, s, H-6), 7.08 – 6.99 (2H, m, H-3 & H-4'), 3.94 (3H, s, OCH_3), 3.83 (2H, s, H-7), 3.81 (3H, s, OCH_3); $^{13}\text{C NMR}$ (75 MHz, CDCl_3); δ 160.2 (C=O), 150.4 (C-2), 149.0 (C-9), 148.2 (C-1), 142.9 (C-10), 141.2 (C-1'), 139.9 (C-5), 135.0 (C-1''), 129.6 (C-3' & C-5'), 129.2 (C-3''), 129.1 (C-4), 128.5 (C-4'), 127.8 (C-4''), 124.4 (C-6''), 124.2 (C-8), 123.4 (C-2' & C-6'), 123.0 (C-2''), 121.2 (C-5''), 109.9 (C-3), 103.5 (C-6), 56.3 (OCH_3), 56.2 (OCH_3), 29.6 (C-7). **HRMS m/z (ESI)** ($\text{C}_{25}\text{H}_{20}\text{ClN}_3\text{O}_3$) 446.1336 ($[\text{M} + \text{H}]^+$ requires 446.1266).

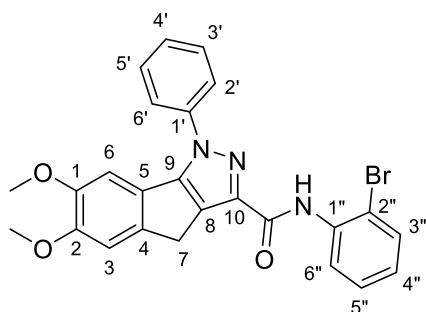
5.5.1.6.8. 6,7-Dimethoxy-1-phenyl-*N*-(*p*-tolyl)-1,4-dihydroindeno[1,2-*c*]pyrazole-3-carboxamide **16**



16

(Yield 57%); Yellow solid; R_f 0.62 (1:1 ethyl acetate: hexane); **mp** 149 °C; ν_{\max} (neat)/ cm^{-1} 3529 (N-H str, w), 1679 (C=O str, m), 1642 (C=C str, m), 1595 (C-C str (in-ring), m), 1518 (s), 1490 (C=N str, m), 1313 (s), 1256 (C-N str, m), 1114 (s), 803 (C-H "oop", vs), 754 (C-H "oop", s); $^1\text{H NMR}$ (300 MHz, CDCl_3); δ 8.77 (1H, s, NH), 7.78 (1H, d, $J = 6.9$ Hz, H-2' & H-6'), 7.62 (4H, m, ArH's), 7.54 – 7.46 (1H, m, H-4'), 7.22 – 7.09 (3H, m, H-6' & H-3' & H-5''), 6.99 (1H, s, H-3), 3.94 (3H, s, OCH_3), 3.84 (2H, s, H-7), 3.80 (3H, s, OCH_3), 2.34 (3H, s, H-7''); $^{13}\text{C NMR}$ (75 MHz, CDCl_3); δ 160.1 (C=O), 150.4 (C-2), 149.0 (C-9), 148.2 (C-1), 143.0 (C-10), 141.5 (C-1'), 139.9 (C-5), 135.5 (C-4''), 133.8 (C-1''), 129.6 (C-3' & C-5' & C-3' & C-5''), 129.1 (C-4), 128.6 (C-4'), 124.2 (C-8), 123.5 (C-2' & C-6'), 119.8 (C-2'' & C-6''), 109.9 (C-3), 103.4 (C-6), 56.3 (OCH_3), 56.2 (OCH_3), 29.6 (C-7), 21.1 (C-7''). **HRMS m/z (ESI)** ($\text{C}_{26}\text{H}_{23}\text{N}_3\text{O}_3$) 426.1830 ($[\text{M} + \text{H}]^+$ requires 426.1812).

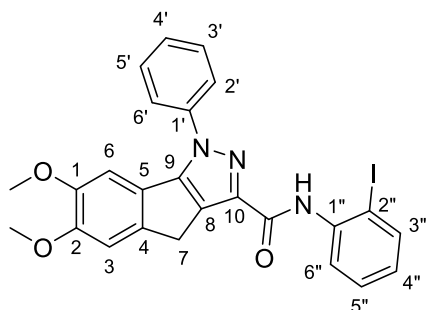
5.5.1.6.9. *N*-(2-Bromophenyl)-6,7-dimethoxy-1-phenyl-1,4-dihydroindeno[1,2-*c*]pyrazole-3-carboxamide **17**



17

(Yield 56%); Yellow solid; R_f 0.66 (1:1 ethyl acetate: hexane); mp 187 °C (decomp.); ν_{\max} (neat)/ cm^{-1} 3349 (N-H str, w), 1688 (C=O str, m), 1580 (C-C str (in-ring), s), 1493 (C=N str, s), 1434 (C-C str, s), 1258 (C-N str, s), 1212 (s), 1124 (s), 805 (C-H “oop”, s), 748 (C-H “oop”, s), 699 (C-H “oop”, s), 504 (C-Br str, m); $^1\text{H NMR}$ (300 MHz, CDCl_3); δ 9.48 (1H, s, NH), 8.59 (1H, d, $J = 8.4$ Hz, H-3’), 7.80 (2H, d, $J = 7.7$ Hz, H-2’ & H-6’), 7.66 – 7.45 (4H, m, ArH’s), 7.35 (1H, td, $J = 8.2, 0.8$ Hz, H-5’), 7.13 (1H, s, H-6), 7.04 (1H, s, H-3), 7.02 – 6.94 (1H, m, H-4’), 3.94 (3H, s, OCH_3), 3.83 (2H, s, H-7), 3.81 (3H, s, OCH_3); $^{13}\text{C NMR}$ (75 MHz, CDCl_3); δ 160.3 (C=O), 150.4 (C-2), 149.0 (C-9), 148.2 (C-1), 142.9 (C-10), 141.2 (C-1’), 139.9 (C-5), 136.1 (C-1’), 132.5 (C-4’), 132.5 (C-3’), 129.6 (C-3’ & C-5’), 129.2 (C-4), 128.4 (C-4’), 124.9 (C-5’), 124.2 (C-8), 123.3 (C-2’ & C-6’), 121.5 (C-6’), 113.5 (C-2’), 109.9 (C-3), 103.6 (C-6), 56.3 (OCH_3), 56.2 (OCH_3), 29.6 (C-7). HRMS m/z (ESI) ($\text{C}_{25}\text{H}_{20}\text{BrN}_3\text{O}_3$) 490.0886 ([M + H]⁺ requires 490.0761).

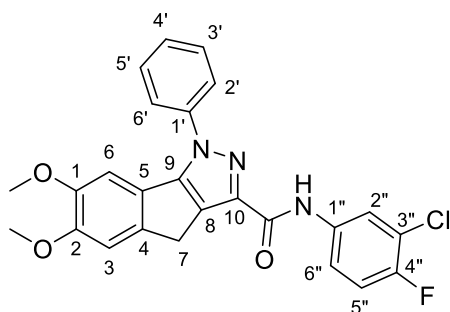
5.5.1.6.10. *N*-(2-Iodophenyl)-6,7-dimethoxy-1-phenyl-1,4-dihydroindeno[1,2-*c*]pyrazole-3-carboxamide **18**



18

(Yield 51%); Yellow solid; R_f 0.65 (1:1 ethyl acetate: hexane); mp 130 °C; ν_{\max} (neat)/ cm^{-1} 3324 (N-H str, w), 1690 (C=O str, m), 1576 (C-C str (in-ring), s), 1522 (s), 1502 (C=N str, s), 1431 (C-C str, s), 1296 (s), 1259 (C-N str, s), 1122 (s), 1066 (s), 803 (C-H “oop”, s), 746 (C-H “oop”, s); $^1\text{H NMR}$ (300 MHz, CDCl_3); δ 9.35 (1H, s, NH), 8.49 (1H, $J = 8.2$ Hz, H-6’), 7.82 (3H, d, $J = 7.4$ Hz, H-3’ & H-2’ H-6’), 7.64 – 7.56 (2H, m, H-3’ & H-5’), 7.50 (1H, d, $J = 7.0$ Hz, H-4’), 7.38 (1H, td, $J = 8.0, 0.6$ Hz, H-5’), 7.14 (1H, s, H-6), 7.06 (1H, s, H-3), 6.85 (1H, td, $J = 7.8, 0.7$ Hz, H-4’), 3.95 (3H, s, OCH_3), 3.84 (2H, s, H-7), 3.83 (3H, s, OCH_3); $^{13}\text{C NMR}$ (75 MHz, CDCl_3); δ 160.4 (C=O), 150.4 (C-2), 148.9 (C-9), 148.2 (C-1), 142.9 (C-10), 141.1 (C-1’), 140.0 (C-5), 139.1 (C-1’), 138.7 (C-3’), 129.6 (C-3’ & C-5’), 129.3 (C-5’), 129.2 (C-4), 128.4 (C-4’), 125.7 (C-4’), 124.3 (C-8), 123.3 (C-2’ & C-6’), 121.5 (C-6’), 109.9 (C-3), 103.5 (C-6), 89.6 (C-2’), 56.3 (OCH_3), 56.3 (OCH_3), 29.6 (C-7). HRMS m/z (ESI) ($\text{C}_{25}\text{H}_{20}\text{IN}_3\text{O}_3$) 538.0622 ([M + H]⁺ requires 538.0622).

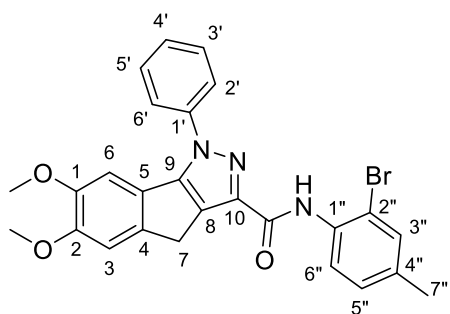
5.5.1.6.11. *N*-(3-Chloro-4-fluorophenyl)-6,7-dimethoxy-1-phenyl-1,4-dihydroindeno[1,2-*c*]pyrazole-3-carboxamide **19**



19

(Yield 47%); Yellow solid; R_f 0.65 (1:1 ethyl acetate: hexane); **mp** 209 °C; ν_{\max} (neat)/ cm^{-1} 3390 (N-H str, w), 1682 (C=O str, s), 1554 (C-C str (in-ring), s), 1489 (C=N str, s), 1259 (C-N str, s), 1207 (s), 1118 (s), 1066 (C-F str, m), 806 (C-H "oop", s), 759 (C-Cl str, s), 677 (C-H "oop", s); $^1\text{H NMR}$ (300 MHz, CDCl_3); δ 8.79 (1H, s, NH), 7.96 (1H, dd, $J = 6.6, 2.6$ Hz, H-2''), 7.79–7.72 (2H, m, H-2' & H-6'), 7.65–7.57 (2H, m, H-3' & H-5'), 7.52–7.44 (2H, m, H-4' & H-6''), 7.14–7.06 (2H, m, H-5'' & H-6), 6.97 (1H, s, H-3), 3.94 (3H, s, OCH_3), 3.80 (2H, s, H-7), 3.80 (3H, s, OCH_3); $^{13}\text{C NMR}$ (75 MHz, CDCl_3); δ 160.2 (C=O), 154.7 (d, $J = 245.8$ Hz, $^{\#}\text{C-4}''$), 150.6 (C-2), 149.1 (C-9), 148.2 (C-1), 142.9 (C-10), 140.8 (C-1'), 139.7 (C-5), 134.7 (d, $J = 3.4$ Hz, $^{\#}\text{C-1}''$), 129.7 (C-3' & C-5'), 129.1 (C-4), 128.8 (C-4'), 124.0 (C-8), 123.5 (C-2' & C-6'), 121.8 (d, $J = 2.4$ Hz, $^{\#}\text{C-6}''$), 121.3 (d, $J = 18.5$ Hz, $^{\#}\text{C-2}''$), 119.2 (d, $J = 6.6$ Hz, $^{\#}\text{C-3}''$), 116.7 (d, $J = 21.9$ Hz, $^{\#}\text{C-5}''$), 109.9 (C-3), 103.4 (C-6), 56.29 (OCH_3), 56.2 (OCH_3), 29.6 (C-7). **HRMS m/z (ESI)** ($\text{C}_{25}\text{H}_{19}\text{ClFN}_3\text{O}_3$) 464.1188 ($[\text{M} + \text{H}]^+$ requires 464.1172). $^{\#}$ Splitting of carbon peaks due to fluorine.

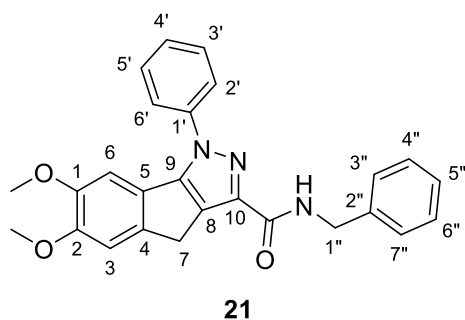
5.5.1.6.12. *N*-(2-Bromo-4-methylphenyl)-6,7-dimethoxy-1-phenyl-1,4-dihydroindeno[1,2-*c*]pyrazole-3-carboxamide **20**



20

(Yield 53%); Yellow solid; R_f 0.66 (1:1 ethyl acetate: hexane); **mp** 196 °C; ν_{\max} (neat)/ cm^{-1} 3340 (N-H str, w), 1688 (C=O str, m), 1579 (C-C str (in-ring), m), 1507 (C=N str, s), 1302 (s), 1260 (C-N str, s), 1116 (s), 1066 (s), 806 (C-H "oop", s), 762 (C-H "oop", s), 50 (C-Br str, m); $^1\text{H NMR}$ (300 MHz, CDCl_3); δ 9.39 (1H, s, NH), 8.44 (1H, d, $J = 8.4$ Hz, H-6''), 7.80 (2H, d, $J = 7.8$ Hz, H-2' & H-6'), 7.60 (2H, t, $J = 7.7$ Hz, H-3' & H-5'), 7.49 (1H, t, $J = 7.4$ Hz, H-4'), 7.39 (1H, d, $J = 1.1$ Hz, H-5''), 7.18–7.10 (2H, m, H-6 & H-3''), 7.04 (1H, s, H-3), 3.94 (3H, s, OCH_3), 3.83 (2H, s, H-7), 3.82 (3H, s, OCH_3), 2.32 (3H, s, H-7''); $^{13}\text{C NMR}$ (75 MHz, CDCl_3); δ 160.2 (C=O), 150.3 (C-2), 148.9 (C-9), 148.1 (C-1), 142.9 (C-10), 141.2 (C-1'), 139.9 (C-5), 135.0 (C-4''), 133.5 (C-3''), 132.7 (C-1''), 129.6 (C-3' & C-5'), 129.1 (C-5''), 129.1 (C-4), 128.4 (C-4'), 124.3 (C-8), 123.3 (C-2' & C-6'), 121.3 (C-6''), 113.4 (C-2''), 109.9 (C-3), 103.5 (C-6), 56.3 (OCH_3), 56.2 (OCH_3), 29.6 (C-7), 20.7 (C-7'). **HRMS m/z (ESI)** ($\text{C}_{26}\text{H}_{22}\text{BrN}_3\text{O}_3$) 504.0934 ($[\text{M} + \text{H}]^+$ requires 504.0917).

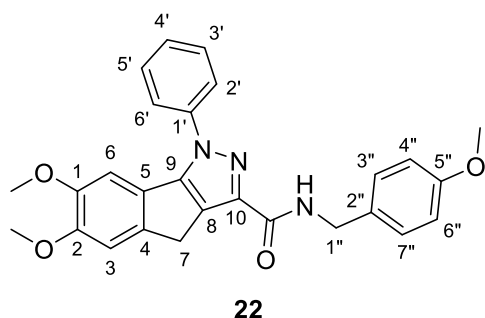
5.5.1.6.13. *N*-Benzyl-6,7-dimethoxy-1-phenyl-1,4-dihydroindeno[1,2-*c*]pyrazole-3-carboxamide **21**



(Yield 51%); Yellow solid; R_f 0.42 (1:1 ethyl acetate: hexane); **mp** 178 °C; ν_{\max} (neat)/ cm^{-1} 3418 (N-H str, w), 1677 (C=O str, s), 1488 (C=N str, s), 1256 (C-N str, s), 1212 (s), 1118 (s), 1073 (s), 804 (C-H "oop", s), 702 (C-H "oop", s); $^1\text{H NMR}$ (300 MHz, CDCl_3); δ 7.72 (2H, d, $J = 7.6$ Hz, H-2' & H-6'), 7.56 (2H, td, $J = 7.6, 0.6$ Hz, H-3' & H-5'), 7.47 (1H, d, $J = 7.3$ Hz, H-4'), 7.42 – 7.26 (5H, m, ArH's), 7.13 (1H, s, H-6), 6.99 (1H, s, H-3), 4.66

(2H, d, $J = 6.0$ Hz, H-1''), 3.95 (3H, s, OCH_3), 3.83 (2H, s, H-7), 3.80 (3H, s, OCH_3); $^{13}\text{C NMR}$ (75 MHz, CDCl_3); δ 162.2 (C=O), 150.0 (C-2), 148.8 (C-9), 148.1 (C-1), 143.0 (C-10), 141.2 (C-1'), 139.9 (C-5), 138.5 (C-2''), 129.5 (C-3' & C-5'), 129.0 (C-4), 128.8 (C-3'' & C-5''), 128.4 (C-4'), 128.1 (C-2'' & C-6''), 127.6 (C-4''), 124.3 (C-8), 123.4 (C-2'' & C-6''), 109.9 (C-3), 103.4 (C-6), 56.3 (OCH_3), 56.2 (OCH_3), 43.2 (C-1''), 29.6 (C-7). **HRMS m/z (ESI)** ($\text{C}_{26}\text{H}_{23}\text{N}_3\text{O}_3$) 426.1830 ($[\text{M} + \text{H}]^+$ requires 426.1812).

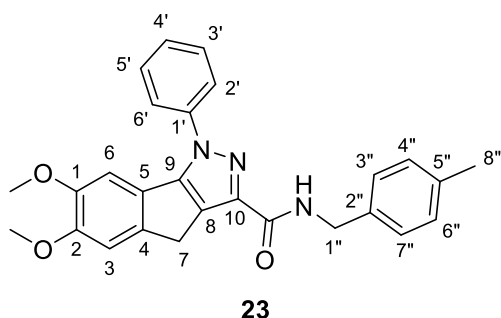
5.5.1.6.14. 6,7-Dimethoxy-*N*-(4-methoxybenzyl)-1-phenyl-1,4-dihydroindeno[1,2-*c*]pyrazole-3-carboxamide **22**



(Yield 53%); Yellow solid; R_f 0.32 (1:1 ethyl acetate: hexane); **mp** 169 °C; ν_{\max} (neat)/ cm^{-1} 3435 (N-H str, w), 1668 (C=O str, m), 1509 (C=N str, s), 1254 (C-N str, s), 1211 (m), 1115 (m), 1071 (m), 1021 (m), 850 (C-H "oop", m), 803 (C-H "oop", s), 760 (C-H "oop", m), 707 (C-H "oop" m); $^1\text{H NMR}$ (300 MHz, CDCl_3); δ 7.71 (2H, d, $J = 7.7$ Hz, H-2' & H-6'), 7.56 (2H, td, $J = 7.6, 0.6$ Hz, H-3' & H-5'), 7.49 – 7.41

(1H, m, H-4'), 7.31 (3H, d, $J = 8.6$ Hz, H-3'' & H-7'' & NH), 7.13 (1H, s, H-6), 6.98 (1H, s, H-3), 6.87 (2H, d, $J = 8.6$ Hz, H-4'' & H-6''), 4.58 (2H, d, $J = 5.9$ Hz, H-1''), 3.94 (3H, s, OCH_3), 3.82 (2H, s, H-7), 3.80 (3H, s, OCH_3), 3.79 (3H, s, OCH_3); $^{13}\text{C NMR}$ (75 MHz, CDCl_3); δ 162.1 (C=O), 159.08 (C-5''), 150.0 (C-2), 148.8 (C-9), 148.1 (C-1), 143.0 (C-10), 141.3 (C-1'), 139.9 (C-5), 130.6 (C-2''), 129.5 (C-3' & C-5'), 129.5 (C-3'' & C-7''), 128.9 (C-4), 128.4 (C-4'), 124.3 (C-8), 123.4 (C-2' & C-6'), 114.1 (C-4'' & C-6''), 109.9 (C-3), 103.4 (C-6), 56.3 (OCH_3), 56.2 (OCH_3), 55.4 (OCH_3), 42.7 (C-1''), 29.6 (C-7). **HRMS m/z (ESI)** ($\text{C}_{27}\text{H}_{26}\text{N}_3\text{O}_4$) 456.1914 ($[\text{M} + \text{H}]^+$ requires 456.1918).

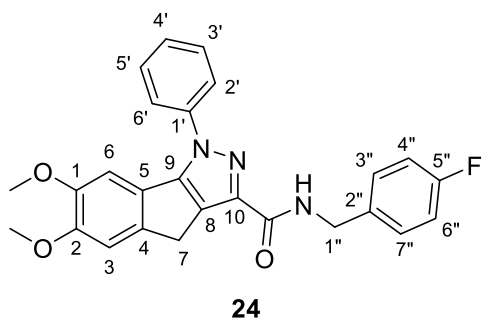
5.5.1.6.15. 6,7-Dimethoxy-N-(4-methylbenzyl)-1-phenyl-1,4-dihydroindeno[1,2-c]pyrazole-3-carboxamide **23**



(Yield 48%); Yellow solid; R_f 0.42 (1:1 ethyl acetate: hexane); mp 163 °C; ν_{max} (neat)/ cm^{-1} 3422 (N-H str, w), 1682 (C=O str, s), 1563 (C-C str (in-ring), m), 1490 (C=N str, s), 1344 (C-H bend, m), 1256 (C-N str, s), 1215 (s), 1118 (s), 1074 (m), 848 (C-H "oop", m), 803 (C-H "oop", s), 772 (C-H "oop", s), 705 (C-H "oop", s); 1H NMR (300 MHz, $CDCl_3$); δ 7.71 (2H, d, J = 7.6 Hz, H-2' & H-6'), 7.56

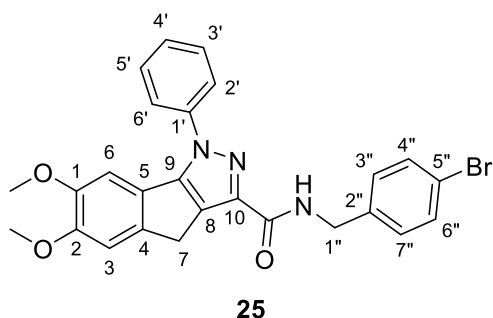
(2H, td, J = 7.6, 0.6 Hz, H-3' & H-5'), 7.49 – 7.41 (1H, m, H-4'), 7.28 (3H, d, J = 8.0 Hz, H-2'' & H-6'' & NH), 7.15 (3H, d, J = 8.7 Hz, H-3'' & H-5'' & H-6), 6.99 (1H, s, H-3), 4.61 (2H, d, J = 5.9 Hz, H-1''), 3.95 (3H, s, OCH_3), 3.82 (2H, s, H-7), 3.80 (3H, s, OCH_3), 2.33 (3H, s, H-8''); ^{13}C NMR (75 MHz, $CDCl_3$); δ 162.2 (C=O), 150.0 (C-2), 148.8 (C-9), 148.1 (C-1), 143.0 (C-10), 141.3 (C-1'), 139.9 (C-5), 137.2 (C-5''), 135.4 (C-2''), 129.5 (C-3' & C-5'), 129.4 (C-4' & C-6''), 128.9 (C-4), 128.4 (C-4'), 128.1 (C-3' & C-7''), 124.3 (C-8), 123.4 (C-2' & C-6'), 109.9 (C-3), 103.4 (C-6), 56.3 (OCH_3), 56.2 (OCH_3), 43.0 (C-1''), 29.6 (C-7), 21.2 (C-8''). HRMS m/z (ESI) ($C_{27}H_{26}N_3O_3$) 440.2022 ([M + H]⁺ requires 440.1969).

5.5.1.6.16. N-(4-Fluorobenzyl)-6,7-dimethoxy-1-phenyl-1,4-dihydroindeno[1,2-c]pyrazole-3-carboxamide **24**



(Yield 51%); White solid; R_f 0.39 (1:1 ethyl acetate: hexane); mp 174 °C; ν_{max} (neat)/ cm^{-1} 3422 (N-H str, w), 1684 (C=O str, s), 1562 (C-C str (in-ring), m), 1490 (C=N str, vs), 1256 (C-N str, s), 1217 (s), 1119 (s), 1073 (C-F str, m), 848 (C-H "oop", s), 804 (C-H "oop", s), 774 (C-H "oop", s), 707 (C-H "oop", s); 1H NMR (300 MHz, $CDCl_3$); δ 7.71 (2H, d, J = 7.8 Hz, H-2' & H-6'), 7.56 (2H, td, J = 7.6, 0.6 Hz, H-3' & H-5'), 7.49 – 7.40 (1H, m, H-4'), 7.35 (3H, dd, J = 8.6, 5.3 Hz, H-3'' & H-7'' & NH), 7.13 (1H, s, H-6), 7.06 – 6.96 (3H, m, H-4'' & H-6'' & H-3), 4.61 (2H, d, J = 6.1 Hz, H-1''), 3.94 (3H, s, OCH_3), 3.82 (2H, s, H-7), 3.80 (3H, s, OCH_3); ^{13}C NMR (75 MHz, $CDCl_3$); δ 162.3 (d, J = 245.4 Hz, ^{13}C -5''), 162.3 (C=O), 150.1 (C-2), 148.9 (C-9), 148.1 (C-1), 142.9 (C-10), 141.1 (C-1'), 139.9 (C-5), 134.3 (d, J = 3.2 Hz, ^{13}C -2''), 129.7 (d, J = 8.2 Hz, ^{13}C -3' & C-7''), 129.6 (C-3' & C-5'), 128.9 (C-4), 128.5 (C-4'), 124.2 (C-8), 123.4 (C-2' & C-6'), 115.6 (d, J = 21.4 Hz, ^{13}C -4'' & C-6''), 109.9 (C-3), 103.4 (C-6), 56.3 (OCH_3), 56.2 (OCH_3), 42.5 (C-1'), 29.6 (C-7). HRMS m/z (ESI) ($C_{26}H_{22}FN_3O_3$) 444.1797 ([M + H]⁺ requires 444.1718). #Splitting of carbon peaks due to fluorine.

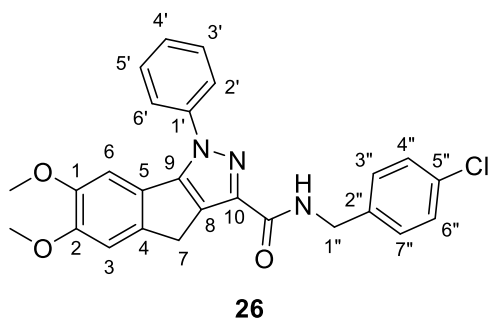
5.5.1.6.17. *N*-(4-Bromobenzyl)-6,7-dimethoxy-1-phenyl-1,4-dihydroindeno[1,2-*c*]pyrazole-3-carboxamide **25**.



(Yield 55%); White solid; R_f 0.41 (1:1 ethyl acetate: hexane); mp 188 °C; ν_{max} (neat)/ cm^{-1} 3302 (N-H str, w), 1643 (C=O str, s), 1554 (C-C str (in-ring), s), 1488 (C=N str, vs), 1251 (C-N str, s), 1215 (s), 1195 (s), 1115 (s), 840 (C-H "oop", s), 802 (C-H "oop", vs), 724 (C-H "oop", s), 512 (C-Br str, s); 1H NMR (300 MHz, $CDCl_3$); δ 7.71 (2H, d, J = 7.9 Hz, H-2' & H-6'), 7.57 (2H, td, J = 7.6, 0.6 Hz, H-3' & H-5'),

7.50 – 7.42 (3H, m, H-4' & H-4'' & H-6''), 7.38 (1H, t, J = 6.0 Hz, NH), 7.26 (2H, d, J = 8.4 Hz, H-3'' & H-7''), 7.13 (1H, s, H-6), 6.98 (1H, s, H-3), 4.59 (2H, d, J = 6.2 Hz, H-1''), 3.94 (3H, s, OCH₃), 3.81 (2H, s, H-7), 3.80 (3H, s, OCH₃); ^{13}C NMR (75 MHz, $CDCl_3$); δ 162.3 (C=O), 150.1 (C-2), 148.9 (C-9), 148.1 (C-1), 142.9 (C-10), 141.0 (C-1'), 139.9 (C-5), 137.3 (C-2''), 131.8 (C-4'' & C-6''), 129.7 (C-3' & C-7''), 129.6 (C-3' & C-5'), 128.9 (C-4), 128.5 (C-4'), 124.2 (C-8), 123.4 (C-2' & C-6'), 121.4 (C-5''), 109.9 (C-3), 103.4 (C-6), 56.3 (OCH₃), 56.2 (OCH₃), 42.6 (C-1''), 29.6 (C-7). HRMS m/z (ESI) (C₂₆H₂₂BrN₃O₃) 504.1033 ([M + H]⁺ requires 504.0917).

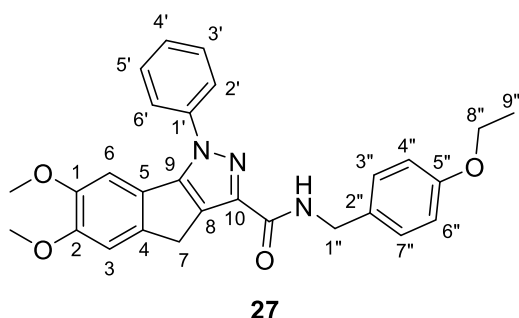
5.5.1.6.18. *N*-(4-Chlorobenzyl)-6,7-dimethoxy-1-phenyl-1,4-dihydroindeno[1,2-*c*]pyrazole-3-carboxamide **26**



(Yield 53%); White solid; R_f 0.41 (1:1 ethyl acetate: hexane); mp 182 °C; ν_{max} (neat)/ cm^{-1} 3303 (N-H str, w), 1643 (C=O str, s), 1555 (C-C str (in-ring), s), 1489 (C=N str, vs), 1252 (C-N str, s), 1195 (s), 1114 (s), 841 (C-H "oop", s), 804 (C-H "oop", s), 761 (C-Cl str, s), 699 (C-H "oop", s); 1H NMR (300 MHz, $CDCl_3$); δ 7.71 (2H, d, J = 7.8 Hz, H-2' & H-6'), 7.57 (2H, td, J = 7.6, 0.6 Hz, H-3' & H-5'), 7.48 – 7.41

(1H, m, H-4), 7.38 (1H, t, J = 6.1 Hz, NH), 7.34 – 7.26 (4H, m, H-3'' & H-4'' & H-6'' & H-7''), 7.13 (1H, s, H-6), 6.98 (1H, s, H-3), 4.61 (2H, d, J = 6.1 Hz, H-1''), 3.94 (3H, s, OCH₃), 3.81 (2H, s, H-7), 3.80 (3H, s, OCH₃); ^{13}C NMR (75 MHz, $CDCl_3$); δ 162.3 (C=O), 150.1 (C-2), 148.9 (C-9), 148.1 (C-1), 142.9 (C-10), 141.1 (C-1'), 139.9 (C-5), 137.1 (C-2''), 133.3 (C-5''), 129.6 (C-3' & C-5'), 129.4 (C-3'' & C-7''), 128.9 (C-4), 128.9 (C-4'' & C-6''), 128.5 (C-4'), 124.2 (C-8), 123.4 (C-2' & C-6'), 109.9 (C-3), 103.4 (C-6), 56.3 (OCH₃), 56.2 (OCH₃), 42.5 (C-1''), 29.6 (C-7). HRMS m/z (ESI) (C₂₆H₂₂ClN₃O₃) 460.1559 ([M + H]⁺ requires 460.1422).

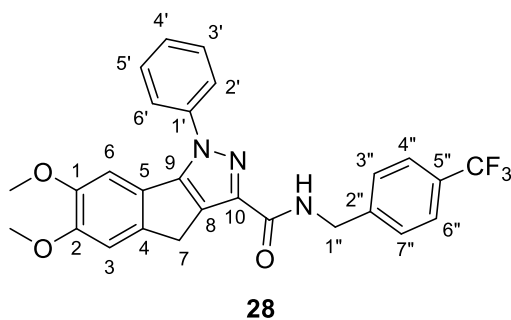
5.5.1.6.19. *N*-(4-Ethoxybenzyl)-6,7-dimethoxy-1-phenyl-1,4-dihydroindeno[1,2-*c*]pyrazole-3-carboxamide **27**



(Yield 39%); Off-white solid; R_f 0.35 (1:1 ethyl acetate: hexane); mp 144 °C; ν_{max} (neat)/ cm^{-1} 3422 (N-H str, w), 1682 (C=O str, s), 1491 (C=N str, s), 1251 (C-N str, s), 1215 (s), 1116 (s), 1045 (s), 846 (C-H “oop”, s), 804 (C-H “oop”, s), 705 (C-H “oop”, s); 1H NMR (300 MHz, $CDCl_3$); δ 7.71 (2H, d, J = 7.3 Hz, H-2' & H-6'), 7.56 (2H, td, J = 7.6, 0.6 Hz, H-3' & H-5'), 7.47 – 7.40 (1H, m, H-4'), 7.30

(3H, d, J = 8.4 Hz, H-3'' & H-7'' & NH), 7.13 (1H, s, H-6), 6.99 (1H, s, H-3), 6.86 (2H, d, J = 8.6 Hz, H-4' & H-6''), 4.58 (2H, d, J = 5.9 Hz, H-1''), 4.01 (2H, dd, J = 14.0, 7.0 Hz, H-8''), 3.94 (3H, s, OCH_3), 3.82 (2H, s, H-7), 3.80 (3H, s, OCH_3), 1.40 (3H, t, J = 7.0 Hz, H-9''); ^{13}C NMR (75 MHz, $CDCl_3$); δ 162.1 (C=O), 158.5 (C-5''), 150.0 (C-2), 148.8 (C-9), 148.1 (C-1), 143.0 (C-10), 141.3 (C-1'), 139.9 (C-5), 130.4 (C-2''), 129.5 (C-3' & C-5'), 129.5 (C-3'' & C-7''), 128.9 (C-4), 128.4 (C-4'), 124.3 (C-8), 123.4 (C-2' & C-6'), 114.7 (C-4'' & C-6''), 109.9 (C-3), 103.4 (C-6), 63.6 (C-8''), 56.3 (OCH_3), 56.2 (OCH_3), 42.7 (C-1''), 29.6 (C-7), 14.9 (C-9''). **HRMS m/z (ESI)** ($C_{28}H_{27}N_3O_4$) 470.2181 ($[M + H]^+$ requires 470.2074).

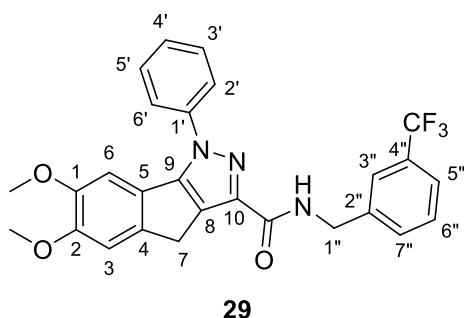
5.5.1.6.20. 6,7-Dimethoxy-1-phenyl-*N*-[4-(trifluoromethyl)benzyl]-1,4-dihydroindeno[1,2-*c*]pyrazole-3-carboxamide **28**



(Yield 54%); Light yellow solid; R_f 0.61 (1:1 ethyl acetate: hexane); mp 158 °C; ν_{max} (neat)/ cm^{-1} 3426 (N-H str, w), 1686 (C=O str, s), 1493 (C=N str, s), 1323 (C-H bend, vs), 1258 (C-N str, s), 1172 (s), 1115 (C-F str, vs), 1066 (s), 1016 (m), 805 (C-H “oop”, s), 775 (C-H “oop”, s); 1H NMR (300 MHz, $CDCl_3$); δ 7.72 (2H, d, J = 7.9 Hz, H-2' & H-6'), 7.57 (4H, m, ArH's), 7.52 – 7.42 (4H, m, ArH's) & NH),

7.13 (1H, s, H-6), 6.99 (1H, s, H-3), 4.70 (2H, d, J = 6.1 Hz, H-1''), 3.94 (3H, s, OCH_3), 3.80 (5H, s, OCH_3 & H-7); ^{13}C NMR (75 MHz, $CDCl_3$); δ 162.5 (C=O), 150.2 (C-2), 148.9 (C-9), 148.2 (C-1), 142.9 (C-10), 142.7 (d, J = 1.3 Hz, ^{13}C -2''), 140.9 (C-1'), 139.8 (C-5), 129.6 (C-3' & C-5'), 128.9 (C-4), 128.5 (C-4'), 128.1 (d, J = 0.5 Hz, ^{13}C -3'' & ^{13}C -7''), 125.7 (d, J = 3.6 Hz, ^{13}C -4'' & ^{13}C -6''), 125.6 (d, J = 1.2 Hz, ^{13}C -5''), 124.2 (C-8), 123.4 (C-2' & C-6'), 122.5 (CF_3), 109.9 (C-3), 103.4 (C-6), 56.3 (OCH_3), 56.2 (OCH_3), 42.7 (C-1''), 29.6 (C-7). **HRMS m/z (ESI)** ($C_{27}H_{22}F_3N_3O_3$) 494.1683 ($[M + H]^+$ requires 494.1686). #Splitting of carbon peaks due to fluorine.

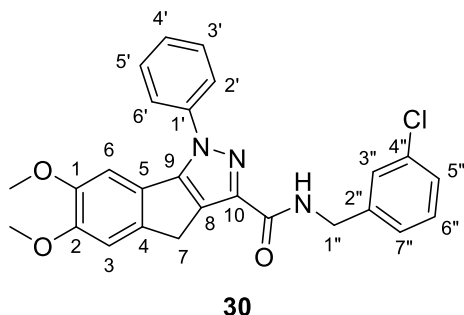
5.5.1.6.21. 6,7-Dimethoxy-1-phenyl-*N*-[3-(trifluoromethyl)benzyl]-1,4-dihydroindeno[1,2-*c*]pyrazole-3-carboxamide **29**



(Yield 47%); Light yellow solid; R_f 0.52 (1:1 ethyl acetate: hexane); mp 147 °C; ν_{\max} (neat)/ cm^{-1} 3421 (N-H str, w), 1684 (C=O str, s), 1489 (C=N str, s), 1329 (C-H bend, s), 1260 (C-N str, s), 1157 (s), 1116 (C-F str, vs), 1073 (vs), 848 (C-H “oop”, s), 804 (C-H “oop”, s), 704 (C-H “oop”, s); $^1\text{H NMR}$ (300 MHz, CDCl_3); δ 7.72 (2H, d, $J = 7.7$ Hz, H-2' & H-6'), 7.64 – 7.51 (5H, m, ArH's), 7.50 – 7.40 (3H, m, ArH's & NH), 7.13 (1H, s, H-6),

6.99 (1H, s, H-3), 4.70 (2H, d, $J = 6.2$ Hz, H-1''), 3.95 (3H, s, OCH_3), 3.82 (2H, s, H-7), 3.80 (3H, s, OCH_3); $^{13}\text{C NMR}$ (75 MHz, CDCl_3); δ 162.4 (C=O), 150.2 (C-2), 148.9 (C-9), 148.2 (C-1), 142.9 (C-10), 141.0 (C-1'), 139.9 (C-5), 139.6 (C-2''), 131.4 (d, $J = 1.3$ Hz, $^{\#}\text{C-4}''$), 131.3 (C-7''), 130.9 (C-6''), 129.6 (C-3' & C-5'), 129.3 (CF_3), 129.0 (C-4), 128.5 (C-4'), 124.7 (C-2''), 124.4 (C-5''), 124.2 (C-8), 123.5 (C-2' & C-6'), 109.9 (C-3), 103.4 (C-6), 56.3 (OCH_3), 56.2 (OCH_3), 42.7 (C-1''), 29.6 (C-7). HRMS m/z (ESI) ($\text{C}_{27}\text{H}_{22}\text{F}_3\text{N}_3\text{O}_3$) 494.1780 ($[\text{M} + \text{H}]^+$ requires 494.1686). $^{\#}$ Splitting of carbon peaks due to fluorine.

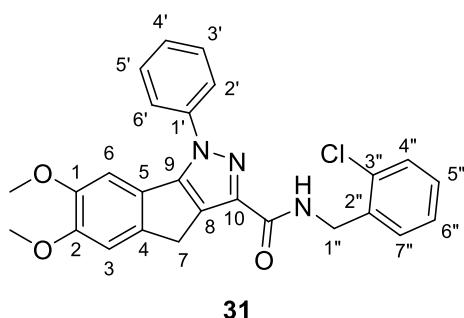
5.5.1.6.22. *N*-(3-Chlorobenzyl)-6,7-dimethoxy-1-phenyl-1,4-dihydroindeno[1,2-*c*]pyrazole-3-carboxamide **30**



(Yield 52%); Off-white solid; R_f 0.42 (1:1 ethyl acetate: hexane); mp 165 °C; ν_{\max} (neat)/ cm^{-1} 3418 (N-H str, w), 1685 (C=O str, s), 1489 (C=N str, vs), 1344 (C-H bend, s), 1258 (C-N str, s), 1215 (s), 1119 (s), 1074 (s), 990 (m), 805 (C-H “oop”, s), 772 (C-Cl str, vs), 705 (C-H “oop”, s); $^1\text{H NMR}$ (300 MHz, CDCl_3); δ 7.72 (2H, d, $J = 7.7$ Hz, H-2' & H-6'), 7.57 (2H, td, $J = 7.7, 0.7$ Hz, H-3' & H-5'), 7.49 – 7.42 (1H, m, H), 7.43 – 7.34

(2H, m, NH & H-3''), 7.29 – 7.22 (3H, m, H-5'' & H-6'' & H-7''), 7.13 (1H, s, H-6), 6.99 (1H, s, H-3), 4.62 (2H, d, $J = 6.2$ Hz, H-1''), 3.94 (3H, s, OCH_3), 3.81 (2H, s, H-7), 3.80 (3H, s, OCH_3); $^{13}\text{C NMR}$ (75 MHz, CDCl_3); δ 162.3 (C=O), 150.1 (C-2), 148.9 (C-9), 148.1 (C-1), 142.9 (C-10), 141.0 (C-1'), 140.6 (C-2''), 139.9 (C-5), 134.6 (C-4''), 130.0 (C-3''), 129.6 (C-3' & C-5'), 129.0 (C-4), 128.5 (C-4'), 128.0 (C-7''), 127.7 (C-5''), 126.1 (C-6''), 124.3 (C-8), 123.5 (C-2' & C-6'), 109.9 (C-3), 103.4 (C-6), 56.3 (OCH_3), 56.2 (OCH_3), 42.6 (C-1''), 29.6 (C-7). HRMS m/z (ESI) ($\text{C}_{26}\text{H}_{22}\text{ClN}_3\text{O}_3$) 460.1559 ($[\text{M} + \text{H}]^+$ requires 460.1422).

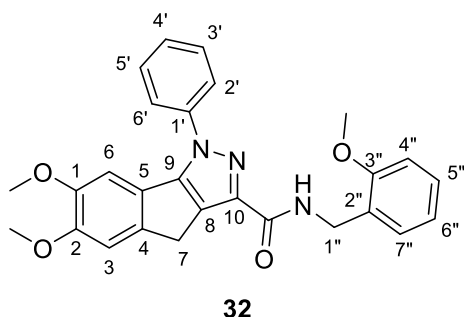
5.5.1.6.23. *N*-(2-Chlorobenzyl)-6,7-dimethoxy-1-phenyl-1,4-dihydroindeno[1,2-*c*]pyrazole-3-carboxamide **31**



(Yield 49%); Off-white solid; R_f 0.46 (1:1 ethyl acetate: hexane); mp 152 °C; ν_{\max} (neat)/ cm^{-1} 3414 (N-H str, w), 1683 (C=O str, vs), 1488 (C=N str, vs), 1257 (C-N str, s), 1215 (s), 1119 (s), 1074 (s), 804 (C-H “oop”, s), 756 (C-Cl str, s), 704 (C-H “oop”, s); $^1\text{H NMR}$ (300 MHz, CDCl_3); δ 7.73 (2H, d, $J = 7.7$ Hz, H-2' & H-6'), 7.57 (2H, td, $J = 7.6, 6.0$ Hz, H-3' & H-5'), 7.53 – 7.41 (3H, m, ArH's), 7.40 – 7.33 (1H, m, NH), 7.23 (2H,

dd, $J = 6.5, 2.9$ Hz, ArH's), 7.12 (1H, s, H-6), 6.99 (1H, s, H-3), 4.75 (2H, d, $J = 6.2$ Hz, H-1''), 3.94 (3H, s, OCH_3), 3.81 (2H, s, H-7), 3.80 (3H, s, OCH_3); $^{13}\text{C NMR}$ (75 MHz, CDCl_3); δ 162.3 (C=O), 150.1 (C-2), 148.9 (C-9), 148.1 (C-1), 143.0 (C-10), 141.1 (C-1'), 139.9 (C-5), 135.9 (C-2''), 133.8 (C-3''), 130.2 (C-4''), 129.6 (C-7''), 129.6 (C-3' & C-5'), 129.0 (C-4), 128.9 (C-5''), 128.4 (C-4'), 127.2 (C-6''), 124.3 (C-8), 123.5 (C-2' & C-6'), 109.9 (C-3), 103.4 (C-6), 56.3 (OCH_3), 56.2 (OCH_3), 41.1 (C-1''), 29.6 (C-7). HRMS m/z (ESI) ($\text{C}_{26}\text{H}_{22}\text{ClN}_3\text{O}_3$) 460.1559 ($[\text{M} + \text{H}]^+$ requires 460.1422).

5.5.1.6.24. 6,7-Dimethoxy-*N*-(2-methoxybenzyl)-1-phenyl-1,4-dihydroindeno[1,2-*c*]pyrazole-3-carboxamide **32**



(Yield 53%); Off-white solid; R_f 0.35 (1:1 ethyl acetate: hexane); mp 157 °C; ν_{\max} (neat)/ cm^{-1} 1660 (C=O str, m), 1489 (C=N str, vs), 1258 (C-N str, s), 1238 (s), 1121 (s), 1025 (s), 805 (C-H “oop”, s), 752 (C-H “oop”, s), 704 (C-H “oop”, s); $^1\text{H NMR}$ (300 MHz, CDCl_3); δ 7.72 (2H, d, $J = 7.8$ Hz, H-2' & H-6'), 7.57 (2H, td, $J = 7.7, 0.7$ Hz, H-3' & H-5'), 7.50 – 7.36 (3H, m, ArH's & NH), 7.29 – 7.21 (1H, m, H-4''), 7.12 (1H, s, H-6),

6.98 (1H, s, H-3), 6.91 (2H, dd, $J = 16.8, 8.0$ Hz, H-5'' & H-6''), 4.66 (2H, d, $J = 6.1$ Hz, H-1''), 3.94 (3H, s, OCH_3), 3.88 (3H, s, OCH_3), 3.81 (2H, s, H-7), 3.80 (3H, s, OCH_3); $^{13}\text{C NMR}$ (75 MHz, CDCl_3); δ 162.1 (C=O), 157.71 (C-3''), 149.9 (C-2), 148.8 (C-9), 148.1 (C-1), 143.0 (C-10), 141.5 (C-1'), 140.0 (C-5), 129.9 (C-7''), 129.5 (C-3' & C-5'), 129.0 (C-4), 128.8 (C-5''), 128.3 (C-4'), 126.5 (C-2''), 124.4 (C-8), 123.4 (C-2' & C-6'), 120.7 (C-6''), 110.4 (C-4''), 109.9 (C-3), 103.4 (C-6), 56.3 (OCH_3), 56.2 (OCH_3), 55.5 & 55.4 ($^+\text{OCH}_3$), 38.7 (C-1''), 29.6 (C-7). HRMS m/z (ESI) ($\text{C}_{27}\text{H}_{25}\text{N}_3\text{O}_4$) 456.2007 ($[\text{M} + \text{H}]^+$ requires 456.1918). *Doubling of carbon peaks due to rotomers.

5.5.2. Bioactivity screening

Prior to screening, all compounds were dissolved in dimethyl sulfoxide due to the compounds being insoluble in high concentrations of water (10 mM). The final concentration of dimethyl sulfoxide in the assay were below 1%.

5.5.2.1. *Acetylcholinesterase inhibitory activity*

Cholinesterase inhibitory activity for *EeAChE* was determined using the 5,5-dithiobis-2-nitrobenzoic acid (DTNB) assay as described by Ellman [60] and modified by Eldeen and co-workers [61]. Three buffers were prepared: Buffer A – 50 mM Tris-hydrochloride (pH 8); Buffer B - 50 mM Tris-hydrochloride (pH 8), containing 0.1% bovine serum albumin; Buffer C - 50 mM Tris-hydrochloride (pH 8), fortified with 0.1 M sodium chloride and 0.02 M magnesium chloride. Into 96-well plates were pipetted: 25 mL acetylthiocholine iodide (15 mM in distilled water), 125 mL DTNB (3 mM in buffer C), 50 mL buffer B and either 25 mL buffer A (negative control), galantamine (positive control at 1 μ M) or compounds **11** - **45**. Absorbance was measured at 405 nm (four times) to account for baseline interference. An aliquot of 25 mL *EeAChE* (0.2 U/mL in buffer A) was pipetted into the plates and the absorbance measured every 45 s for fifteen cycles. *EeAChE* inhibition (%) was determined as the rate of the reaction (correcting for spontaneous colour changes) relative to the negative control.

5.5.2.2. *Statistics*

Assays were performed as three intra- as well as three inter-replicates. Statistical analyses were performed using Graph-Pad Prism 5.0 (GraphPad). The AChE IC_{50} values were determined using non-linear regression analysis.

5.6. ACKNOWLEDGEMENTS

This work was supported by the National Research Foundation (NRF) of South Africa (Thuthuka grant number 87893), the University of Pretoria (University, Science Faculty Research Councils and Research and Development Program) and the Council for Scientific and Industrial Research (CSIR), South Africa. Opinions expressed in this publication and the conclusions arrived at, are those of the authors, and are not necessarily attributed to the NRF. The authors would like to gratefully acknowledge Ms Madelien Wooding (University of Pretoria) for LC-MS services and Dr Frederick Malan for XRD services.

5.7. CONFLICT OF INTEREST

The authors declare no conflict of interest.

5.8. APPENDIX D. SUPPLEMENTARY INFORMATION

Appendix D can be found as a separate document on the CD.

5.9. REFERENCES

- [1] J.V. Faria, P.F. Vegi, A.G.C. Miguita, M.S. Dos Santos, N. Boechat, A.M.R. Bernardino, Recently reported biological activities of pyrazole compounds, *Bioorg. Med. Chem.*, 25 (2017) 5891-5903.
- [2] Neha, A.R. Dwivedi, R. Kumar, V. Kumar, Recent synthetic strategies for monocyclicazole nucleus and its role in drug discovery and development, *Curr. Org. Synth.*, 15 (2018) 321-340.
- [3] M.J. Alam, O. Alam, P. Alam, M.J. Naim, A review on pyrazole chemical entity and biological activity, *Int. J. Pharm. Sci. Res.*, 6 (2015) 1433-1442.
- [4] R. Aggarwal, S. Kumar, P. Kaushik, D. Kaushik, G.K. Gupta, Synthesis and pharmacological evaluation of some novel 2-(5-hydroxy-5-trifluoromethyl-4,5-dihydropyrazol-1-yl)-4-(coumarin-3-yl)thiazoles, *Eur. J. Med. Chem.*, 62 (2013) 508-514.
- [5] F. Xie, G. Cheng, Y. Hu, Three-component, one-pot reaction for the combinatorial synthesis of 1,3,4-substituted pyrazoles, *J. Comb. Chem.*, 8 (2006) 286-288.
- [6] V.V. Arkhipov, M.M. Garazd, M.N. Smirnov, V.P. Khilya, Chemistry of modified flavonoids. 24. Synthesis of 4-aryloxy-3-(2-hydroxy-4-hydroxy/alkoxyphenyl) pyrazoles, *Chem. Heterocycl. Compd.*, 40 (2004) 183-187.
- [7] I.O. Ilhan, E. Saripinar, Y. Akcamur, Synthesis of some pyrazole-3-carboxylic acid-hydrazide and pyrazolopyridazine compounds, *J. Heterocycl. Chem.*, 42 (2005) 117-120.
- [8] A. Krishnaiah, B. Narsaiah, A novel approach to the synthesis of 5-trifluoromethyl-3-substituted pyrazoles, *J. Fluor. Chem.*, 115 (2002) 9-11.
- [9] E. Bisenieks, J. Uldrikis, G. Duburs, Reaction of 3, 5-carbonyl-substituted 1, 4-dihydropyridines with hydrazine hydrate, *Chem. Heterocycl. Compd.*, 40 (2004) 869-875.
- [10] U. Grošelj, A. Drobnič, S. Rečnik, J. Svete, B. Stanovnik, A. Golobič, N. Lah, I. Leban, A. Meden, S. Golič-Grdadolnik, 1,3-Dipolar cycloadditions to (5*Z*)-1-acyl-5-(cyanomethylidene)-imidazolidine-2, 4-diones: Synthesis and transformations of spirohydantoin derivatives, *Helv. Chim. Acta*, 84 (2001) 3403-3417.
- [11] K. Karrouchi, S. Radi, Y. Ramli, J. Taoufik, Y.N. Mabkhot, F.A. Al-Aizari, M. Ansari, Synthesis and pharmacological activities of pyrazole derivatives: A review, *Molecules*, 23 (2018) 134.
- [12] A. Ansari, A. Ali, M. Asif, S. Shamsuzzaman, Review: biologically active pyrazole derivatives, *New J. Chem.*, 41 (2017) 16-41.
- [13] L. Yet, Five-membered ring systems: With more than one *N* atom, in: *Progress in Heterocyclic Chemistry*, Elsevier, 2016, pp. 275-315.

- [14] K. Makino, H.S. Kim, Y. Kurasawa, Synthesis of pyrazoles and condensed pyrazoles, *J. Heterocycl. Chem.*, 36 (1999) 321-332.
- [15] S. He, L. Chen, Y.-N. Niu, L.-Y. Wu, Y.-M. Liang, 1,3-Dipolar cycloaddition of diazoacetate compounds to terminal alkynes promoted by $Zn(OTf)_2$: an efficient way to the preparation of pyrazoles, *Tetrahedron Lett.*, 50 (2009) 2443-2445.
- [16] A. Gioiello, A. Khamidullina, M.C. Fulco, F. Venturoni, S. Zlotzky, R. Pellicciari, New one-pot synthesis of pyrazole-5-carboxylates by 1,3-dipole cycloadditions of ethyl diazoacetate with α -methylene carbonyl compounds, *Tetrahedron Lett.*, 50 (2009) 5978-5980.
- [17] N. Jiang, C.J. Li, Novel 1,3-dipolar cycloaddition of diazocarbonyl compounds to alkynes catalyzed by $InCl_3$ in water, *Chem. Commun.*, (2004) 394-395.
- [18] F. Chen, F.-M. Liu, H. Shi, S.-L. Chen, A facile access to 1,3,4-trisubstituted pyrazoles via 1,3-dipolar cycloaddition of 3-arylsydnone with α,β -unsaturated ketones, *Monatsh. Chem.*, 144 (2013) 879-884.
- [19] S. Dadiboyena, E.J. Valente, A.T. Hamme, A novel synthesis of 1,3,5-trisubstituted pyrazoles through a spiro-pyrazoline intermediate via a tandem 1,3-dipolar cycloaddition/elimination, *Tetrahedron Lett.*, 50 (2009) 291-294.
- [20] R. Harigae, K. Moriyama, H. Togo, Preparation of 3,5-disubstituted pyrazoles and isoxazoles from terminal alkynes, aldehydes, hydrazines, and hydroxylamine, *J. Org. Chem.*, 79 (2014) 2049-2058.
- [21] J.-A. Jiang, W.-B. Huang, J.-J. Zhai, H.-W. Liu, Q. Cai, L.-X. Xu, W. Wang, Y.-F. Ji, 'One-pot' synthesis of 4-substituted 1,5-diaryl-1*H*-pyrazole-3-carboxylates via lithium tert-butoxide-mediated sterically hindered Claisen condensation and Knorr reaction, *Tetrahedron*, 69 (2013) 627-635.
- [22] M. Iizuka, Y. Kondo, Palladium-catalyzed alkynylcarbonylation of aryl iodides with the use of $Mo(CO)_6$ in the presence of tBu_3P ligand, *Eur. J. Org. Chem.*, 2007 (2007) 5180-5182.
- [23] S. Kovács, Z. Novák, Copper on iron promoted one-pot synthesis of β -aminoenones and 3,5-disubstituted pyrazoles, *Tetrahedron*, 69 (2013) 8987-8993.
- [24] T.T. Dang, T.T. Dang, C. Fischer, H. Görls, P. Langer, Synthesis of pyrazole-3-carboxylates and pyrazole-1,5-dicarboxylates by one-pot cyclization of hydrazone dianions with diethyl oxalate, *Tetrahedron*, 64 (2008) 2207-2215.
- [25] P. Lokhande, K. Hasanzadeh, S.G. Konda, A novel and efficient approach for the synthesis of new halo substituted 2-arylpyrazolo [4, 3-c] coumarin derivatives, *Eur. J. Chem.*, 2 (2011) 223-228.
- [26] X. Deng, N.S. Mani, Reaction of *N*-monosubstituted hydrazones with nitroolefins: a novel regioselective pyrazole synthesis, *Org. Lett.*, 8 (2006) 3505-3508.
- [27] X. Deng, N.S. Mani, Base-mediated reaction of hydrazones and nitroolefins with a reversed regioselectivity: a novel synthesis of 1,3,4-trisubstituted pyrazoles, *Org. Lett.*, 10 (2008) 1307-1310.

- [28] V.K. Aggarwal, J. de Vicente, R.V. Bonnert, A novel one-pot method for the preparation of pyrazoles by 1,3-dipolar cycloadditions of diazo compounds generated *in situ*, *J. Org. Chem.*, 68 (2003) 5381-5383.
- [29] E. Akbas, I. Berber, A. Sener, B. Hasanov, Synthesis and antibacterial activity of 4-benzoyl-1-methyl-5-phenyl-1*H*-pyrazole-3-carboxylic acid and derivatives, *Farmaco*, 60 (2005) 23-26.
- [30] B. Chandrakantha, A.M. Isloor, P. Shetty, S. Isloor, S. Malladi, H.K. Fun, Synthesis, characterization and antimicrobial activity of novel ethyl 1-(*N*-substituted)-5-phenyl-1*H*-pyrazole-4-carboxylate derivatives, *Med. Chem. Res.*, 21 (2011) 2702-2708.
- [31] N. Abunada, H. Hassaneen, N. Kandile, O. Miqdad, Synthesis and antimicrobial activity of some new pyrazole, fused pyrazolo[3,4-*d*]-pyrimidine and pyrazolo[4,3-*e*][1,2,4]- triazolo[1,5-*c*]pyrimidine derivatives, *Molecules*, 13 (2008) 1501-1517.
- [32] Y. Xu, X.H. Liu, M. Saunders, S. Pearce, J.M. Foulks, K.M. Parnell, A. Clifford, R.N. Nix, J. Bullough, T.F. Hendrickson, K. Wright, M.V. McCullar, S.B. Kanner, K.K. Ho, Discovery of 3-(trifluoromethyl)-1*H*-pyrazole-5-carboxamide activators of the M2 isoform of pyruvate kinase (PKM2), *Bioorg. Med. Chem. Lett.*, 24 (2014) 515-519.
- [33] A. Balbi, M. Anzaldi, C. Maccio, C. Aiello, M. Mazzei, R. Gangemi, P. Castagnola, M. Miele, C. Rosano, M. Viale, Synthesis and biological evaluation of novel pyrazole derivatives with anticancer activity, *Eur. J. Med. Chem.*, 46 (2011) 5293-5309.
- [34] G.M. Nitulescu, C. Draghici, A.V. Missir, Synthesis of new pyrazole derivatives and their anticancer evaluation, *Eur. J. Med. Chem.*, 45 (2010) 4914-4919.
- [35] M.A. El-Sayed, N.I. Abdel-Aziz, A.A. Abdel-Aziz, A.S. El-Azab, K.E. ElTahir, Synthesis, biological evaluation and molecular modeling study of pyrazole and pyrazoline derivatives as selective COX-2 inhibitors and anti-inflammatory agents. Part 2, *Bioorg. Med. Chem.*, 20 (2012) 3306-3316.
- [36] B. Maggio, G. Daidone, D. Raffa, S. Plescia, L. Mantione, V.M.C. Cutuli, N.G. Mangano, A. Caruso, Synthesis and pharmacological study of ethyl 1-methyl-5-(substituted 3,4-dihydro-4-oxoquinazolin-3-yl)-1*H*-pyrazole-4-acetates, *Eur. J. Med. Chem.*, 36 (2001) 737-742.
- [37] M.A. Abdelgawad, M.B. Labib, M. Abdel-Latif, Pyrazole-hydrazone derivatives as anti-inflammatory agents: Design, synthesis, biological evaluation, COX-1,2/5-LOX inhibition and docking study, *Bioorg. Chem.*, 74 (2017) 212-220.
- [38] A.E. Rashad, M.I. Hegab, R.E. Abdel-Megeid, J.A. Micky, F.M. Abdel-Megeid, Synthesis and antiviral evaluation of some new pyrazole and fused pyrazolopyrimidine derivatives, *Bioorg. Med. Chem.*, 16 (2008) 7102-7106.

- [39] S. Sidique, S.A. Shiryayev, B.I. Ratnikov, A. Herath, Y. Su, A.Y. Strongin, N.D. Cosford, Structure-activity relationship and improved hydrolytic stability of pyrazole derivatives that are allosteric inhibitors of West Nile Virus NS2B-NS3 proteinase, *Bioorg. Med. Chem. Lett.*, 19 (2009) 5773-5777.
- [40] C.M. Niswender, E.P. Lebois, Q. Luo, K. Kim, H. Muchalski, H. Yin, P.J. Conn, C.W. Lindsley, Positive allosteric modulators of the metabotropic glutamate receptor subtype 4 (mGluR4): Part I. Discovery of pyrazolo[3,4-*d*]pyrimidines as novel mGluR4 positive allosteric modulators, *Bioorg. Med. Chem. Lett.*, 18 (2008) 5626-5630.
- [41] B.K. Chan, A.A. Estrada, H. Chen, J. Atherall, C. Baker-Glenn, A. Beresford, D.J. Burdick, M. Chambers, S.L. Dominguez, J. Drummond, A. Gill, T. Kleinheinz, C.E. Le Pichon, A.D. Medhurst, X. Liu, J.G. Moffat, K. Nash, K. Scarce-Levie, Z. Sheng, D.G. Shore, H. Van de Poel, S. Zhang, H. Zhu, Z.K. Sweeney, Discovery of a highly selective, brain-penetrant aminopyrazole LRRK2 inhibitor, *ACS Med. Chem. Lett.*, 4 (2013) 85-90.
- [42] A. Dore, B. Asproni, A. Scampuddu, G.A. Pinna, C.T. Christoffersen, M. Langgard, J. Kehler, Synthesis and SAR study of novel tricyclic pyrazoles as potent phosphodiesterase 10A inhibitors, *Eur. J. Med. Chem.*, 84 (2014) 181-193.
- [43] P. Kushwaha, S. Fatima, A. Upadhyay, S. Gupta, S. Bhagwati, T. Baghel, M.I. Siddiqi, A. Nazir, K.V. Sashidhara, Synthesis, biological evaluation and molecular dynamic simulations of novel benzofuran-tetrazole derivatives as potential agents against Alzheimer's disease, *Bioorg. Med. Chem. Lett.*, 29 (2019) 66-72.
- [44] J. Hu, Y.D. Huang, T. Pan, T. Zhang, T. Su, X. Li, H.B. Luo, L. Huang, Design, synthesis, and biological evaluation of dual-target inhibitors of acetylcholinesterase (AChE) and phosphodiesterase 9A (PDE9A) for the treatment of Alzheimer's disease, *ACS Chem. Neurosci.*, 10 (2018) 537-551.
- [45] N. Gokhan-Kelekci, S. Yabanoglu, E. Kupeli, U. Salgin, O. Ozgen, G. Ucar, E. Yesilada, E. Kendi, A. Yesilada, A.A. Bilgin, A new therapeutic approach in Alzheimer's disease: some novel pyrazole derivatives as dual MAO-B inhibitors and antiinflammatory analgesics, *Bioorg. Med. Chem.*, 15 (2007) 5775-5786.
- [46] M.S. Malamas, J. Erdei, I. Gunawan, K. Barnes, Y. Hui, M. Johnson, A. Robichaud, P. Zhou, Y. Yan, W. Solvibile, J. Turner, K.Y. Fan, R. Chopra, J. Bard, M.N. Pangalos, New pyrazolyl and thienyl aminohydantoin s as potent BACE1 inhibitors: exploring the S2' region, *Bioorg. Med. Chem. Lett.*, 21 (2011) 5164-5170.
- [47] Y.T. Han, K. Kim, G.I. Choi, H. An, D. Son, H. Kim, H.J. Ha, J.H. Son, S.J. Chung, H.J. Park, J. Lee, Y.G. Suh, Pyrazole-5-carboxamides, novel inhibitors of receptor for advanced glycation end products (RAGE), *Eur. J. Med. Chem.*, 79 (2014) 128-142.

- [48] T.M. Acker, H. Yuan, K.B. Hansen, K.M. Vance, K.K. Ogden, H.S. Jensen, P.B. Burger, P. Mullasseril, J.P. Snyder, D.C. Liotta, S.F. Traynelis, Mechanism for noncompetitive inhibition by novel GluN2C/D N-methyl-D-aspartate receptor subunit-selective modulators, *Mol. Pharmacol.*, 80 (2011) 782-795.
- [49] T.M. Acker, A. Khatri, K.M. Vance, C. Slabber, J. Bacsa, J.P. Snyder, S.F. Traynelis, D.C. Liotta, Structure-activity relationships and pharmacophore model of a noncompetitive pyrazoline containing class of GluN2C/GluN2D selective antagonists, *J. Med. Chem.*, 56 (2013) 6434-6456.
- [50] M. Kawai, I. Sakurada, A. Morita, Y. Iwamuro, K. Ando, H. Omura, S. Sakakibara, T. Masuda, H. Koike, T. Honma, K. Hattori, T. Takashima, K. Mizuno, M. Mizutani, M. Kawamura, Structure-activity relationship study of novel NR2B-selective antagonists with arylamides to avoid reactive metabolites formation, *Bioorg. Med. Chem. Lett.*, 17 (2007) 5537-5542.
- [51] K. Anan, M. Masui, S. Hara, M. Ohara, M. Kume, S. Yamamoto, S. Shinohara, H. Tsuji, S. Shimada, S. Yagi, N. Hasebe, H. Kai, Discovery of orally bioavailable cyclohexanol-based NR2B-selective NMDA receptor antagonists with analgesic activity utilizing a scaffold hopping approach, *Bioorg. Med. Chem. Lett.*, 27 (2017) 4194-4198.
- [52] P. Conti, G. Grazioso, S.J. di Ventimiglia, A. Pinto, G. Roda, U. Madsen, H. Brauner-Osborne, B. Nielsen, C. Costagli, A. Galli, Synthesis of novel M1-substituted bicyclic pyrazole amino acids and evaluation of their interaction with glutamate receptors, *Chem. Biodivers.*, 2 (2005) 748-757.
- [53] P. Conti, A. Pinto, L. Tamborini, U. Madsen, B. Nielsen, H. Brauner-Osborne, K.B. Hansen, E. Landucci, D.E. Pellegrini-Giampietro, G. De Sarro, E. Donato Di Paola, C. De Micheli, Novel 3-carboxy- and 3-phosphonopyrazoline amino acids as potent and selective NMDA receptor antagonists: design, synthesis, and pharmacological characterization, *ChemMedChem*, 5 (2010) 1465-1475.
- [54] H. van de Waterbeemd, G. Camenisch, G. Folkers, J.R. Chretien, O.A. Raevsky, Estimation of blood-brain barrier crossing of drugs using molecular size and shape, and H-bonding descriptors, *J. Drug Target.*, 6 (1998) 151-165.
- [55] I. Khan, K.R. Garikapati, A.B. Shaik, V.K.K. Makani, A. Rahim, M.A. Shareef, V.G. Reddy, M. Pal-Bhadra, A. Kamal, C.G. Kumar, Design, synthesis and biological evaluation of 1, 4-dihydro indeno[1,2-c] pyrazole linked oxindole analogues as potential anticancer agents targeting tubulin and inducing p53 dependent apoptosis, *Eur. J. Med. Chem.*, 144 (2018) 104-115.
- [56] J.-M. Mussinu, S. Ruiu, A.C. Mulè, A. Pau, M.A.M. Carai, G. Loriga, G. Murineddu, G.A. Pinna, Tricyclic pyrazoles. Part 1: Synthesis and biological evaluation of novel 1,4-dihydroindeno[1,2-c]pyrazol-based ligands for CB1 and CB2 cannabinoid receptors, *Bioorg. Med. Chem.*, 11 (2003) 251-263.

- [57] D.G. van Greunen, W. Cordier, M. Nell, C. van der Westhuyzen, V. Steenkamp, J.-L. Panayides, D.L. Riley, Targeting Alzheimer's disease by investigating previously unexplored chemical space surrounding the cholinesterase inhibitor donepezil, *Eur. J. Med. Chem.*, 127 (2017) 671-690.
- [58] C.A. Lipinski, Lead- and drug-like compounds: the rule-of-five revolution, *Drug. Discov. Today. Technol.*, 1 (2004) 337-341.
- [59] A. Daina, O. Michielin, V. Zoete, SwissADME: a free web tool to evaluate pharmacokinetics, drug-likeness and medicinal chemistry friendliness of small molecules, *Sci. Rep.*, 7 (2017) 42717.
- [60] G.L. Ellman, K.D. Courtney, V. Andres, R.M. Featherstone, A new and rapid colorimetric determination of acetylcholinesterase activity, *Biochem. Pharmacol.*, 7 (1961) 88-95.
- [61] I.M. Eldeen, E.E. Elgorashi, J. van Staden, Antibacterial, anti-inflammatory, anti-cholinesterase and mutagenic effects of extracts obtained from some trees used in South African traditional medicine, *J. Ethnopharmacol.*, 102 (2005) 457-464.
- [62] Bruker, SHELXTL, Version 5.1 (includes XS, XL, XP and XSHELL); Bruker AXS Inc., Madison, Wisconsin, U.S.A, (1999).
- [63] C.F. Macrae, I.J. Bruno, J.A. Chisholm, P.R. Edgington, P. McCabe, E. Pidcock, L. Rodriguez-Monge, R. Taylor, J. van de Streek, P.A. Wood, Mercury CSD 2.0 - new features for the visualisation and investigation of crystal structures., *J. Appl. Cryst.*, 41 (2008) 466-470.
- [64] R.W. Hamilton, The antiarrhythmic and antiinflammatory activity of a series of tricyclic pyrazoles, *J. Het. Chem.*, 13 (1976) 545-553.

Chapter 6. Synthesis of donepezil as precursor for the development of β -secretase inhibitors for the treatment of Alzheimer's disease using flow conditions

Contributions to this chapter

All of the synthesis and compound characterization described in this chapter were performed by Mr DG van Greunen under the supervision of Dr DL Riley and Dr J-L Panayides. The synthetic work was undertaken in the Department of Chemistry at the University of Pretoria.

Synthesis of donepezil as precursor for the development of β -secretase inhibitors for the treatment of Alzheimer's disease using flow conditions

Divan G. van Greunen^a, Jenny-Lee Panayides^b, Darren L. Riley^{a,*}

^a *Department of Chemistry, Faculty of Natural and Agricultural Sciences, University of Pretoria, Lynnwood Road, Pretoria, South Africa*

^b *Pioneering Health Sciences, CSIR Biosciences, Meiring Naudé Road, Pretoria, South Africa*

* *Corresponding author. E-mail address: darren.riley@up.ac.za (D.L. Riley)*

ABSTRACT

The comparison of an improved conventional batch mode synthesis of donepezil **1**, an anti-Alzheimer's disease agent, with its partially flow chemistry alternative is reported in an effort to produce donepezil on a large scale as a precursor for the development of β -secretase inhibitors for the treatment of Alzheimer's disease. The stepwise and continuous flow synthesis of donepezil has been partially achieved where Stage 1 and Stage 3 has been optimised. Stage 1 has been completed where the benzylation reaction of ethyl isonipecotate **3** to access ethyl 1-benzylpiperidine-4-carboxylate **4** with an improve yield of 83% in forty-five minutes using flow conditions, compared to 79% in three hours using batch conditions, was achieved. Stage 3 was completed where the precursor (*E*)-2-[(1-benzylpiperidin-4-yl)methylene]-5,6-dimethoxy-2,3-dihydro-1*H*-inden-1-one **7** was reduced to donepezil **1** in a catalytic reductive hydrogenation reaction, using 10% Pd/C as catalyst, with a 80% yield in four-and-a-half hours using flow conditions, compared to 78% in six hours using batch conditions.

Key Words

Alzheimer's disease, batch chemistry, continuous flow chemistry, donepezil

6.1. INTRODUCTION

Donepezil **1** (Figure 6.1) the well-known acetylcholinesterase (AChE) inhibitor is currently used in the palliative treatment of Alzheimer's disease (AD) [1]. The chemical space surrounding donepezil **1** has been previously explored by the authors [2]. Unfortunately, further exploration of the chemical space surrounding **1** requires large amounts of this compound. As a result, a lot of interest was placed in the development of an improved means of synthesizing donepezil **1** and flow technology was considered to facilitate the synthesis of **1**.

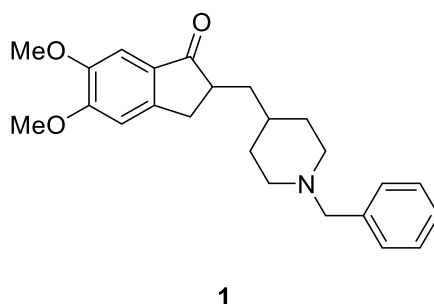


Figure 6.1. Donepezil.

The manufacturing of active pharmaceutical ingredients (API's) at minimal cost and of high quality, is the primary focus of process research and development in pharmaceutical companies [3-7]. As a result, process chemistry plays an important role in gaining a competitive advantage in pharmaceutical manufacturing [3, 8]. In our endeavour of drug discovery, our research group is also involved in the development of improved process routes for the development of pharmaceuticals and APIs, in this case flow chemistry. Flow chemistry incorporates the use of small reactors in which streams of substrates and reagents are united to react with each other in continual flowing streams in a highly controllable manner (heating, cooling, pressure, concentration, etc.). The latter has many advantages over that of traditional batch process chemistry, including: i) facile automation, ii) reproducibility, iii) safety and process reliability due to constant parameters including efficient mixing, temperature control, amount of reagents used, iv) multistep reactions can be conducted in continuous flow and shorter reaction time [9-13].

Commercially available flow chemistry equipment includes the following: i) Uniqsis FlowSyn, ii) Vapourtec R-Series, iii) Vapourtec E-Series, iv) FutureChemistry FlowStart Evo, v) Chemtrix Labtrix, vi) Syrris Asia and vii) Accendo Propel [9]. During this part of the study the Uniqsis FlowSyn Stainless Steel Flow reactor was utilized (Figure 6.2) [14].



Figure 6.2. Uniqsis FlowSyn Stainless Steel Flow reactor [14].

The current synthetic route utilised by our group to access donepezil **1** is a 5-step batch synthesis which affords **1** in an overall yield of 32% (**Scheme 6.1**) [2]. The overall batch synthesis is described in *Section 6.2.1*. The preparation of **1** has several drawbacks which include: i) a moderately yielding aldol condensation (Stage 4) and ii) a catalytic hydrogenation of an alkene, which causes unwanted debenylation of the target molecule's piperidine ring system (Stage 5). An alternative process route using flow technologies (**Scheme 6.2**) was therefore envisaged. The overall flow-based synthesis is described in *Section 6.2.2*. The approach is targeted at i) improving the benzylation of **3** by increasing the yield and decreasing the reaction time, ii) controlling the hydrogenation of the donepezil precursor **6** to selectively allow the reduction of the alkene without unwanted debenylation and iii) reducing the process to three steps by selectively reducing ester **4** to **6** and telescoping this directly into the aldol condensation to afford **7** in a single operation.

If successful, the flow-based route, in addition to potentially showing improvements to the process route, could also be used to facilitate drug discovery projects which require the modification of the donepezil **1** skeleton. One possible key area on donepezil **1** was identified as an example for future drug discovery projects. It has the potential when modified with a pharmacophore, to additionally act

as a β -secretase cleaving enzyme 1 (BACE1) inhibitor. Such a pharmacophore was identified by Huang and co-workers [15] in the development of the BACE1 inhibitor **2** (Figure 6.3). As part of a future project, it was hypothesized that by incorporating the spirocyclic pharmacophore onto donepezil **1**, inhibition of BACE1 may be achieved, while maintaining the affinity for AChE, thus affording a dual inhibitor.

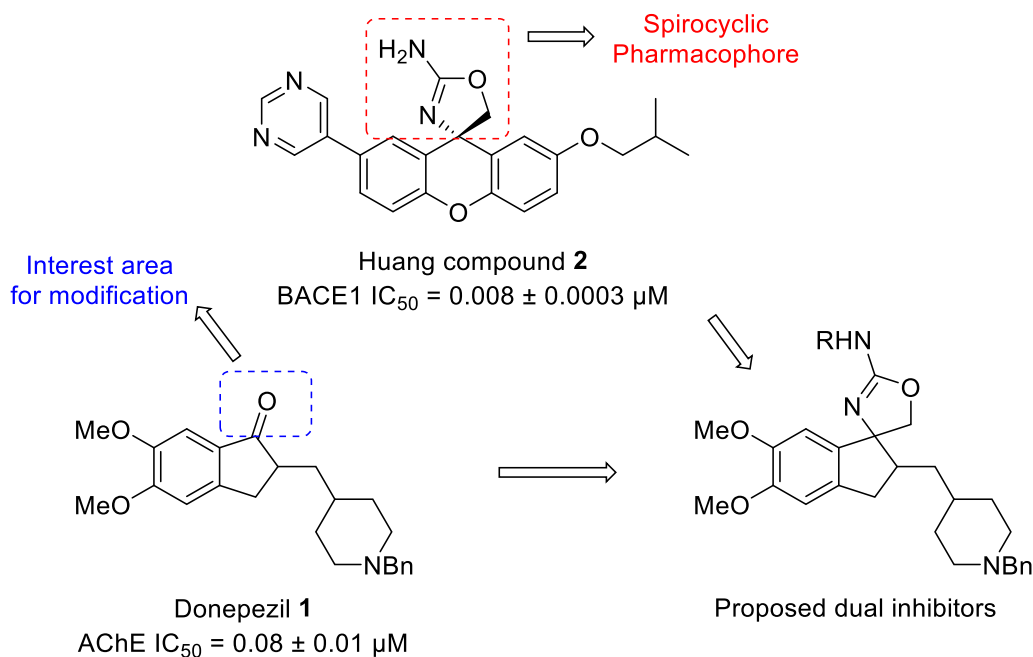


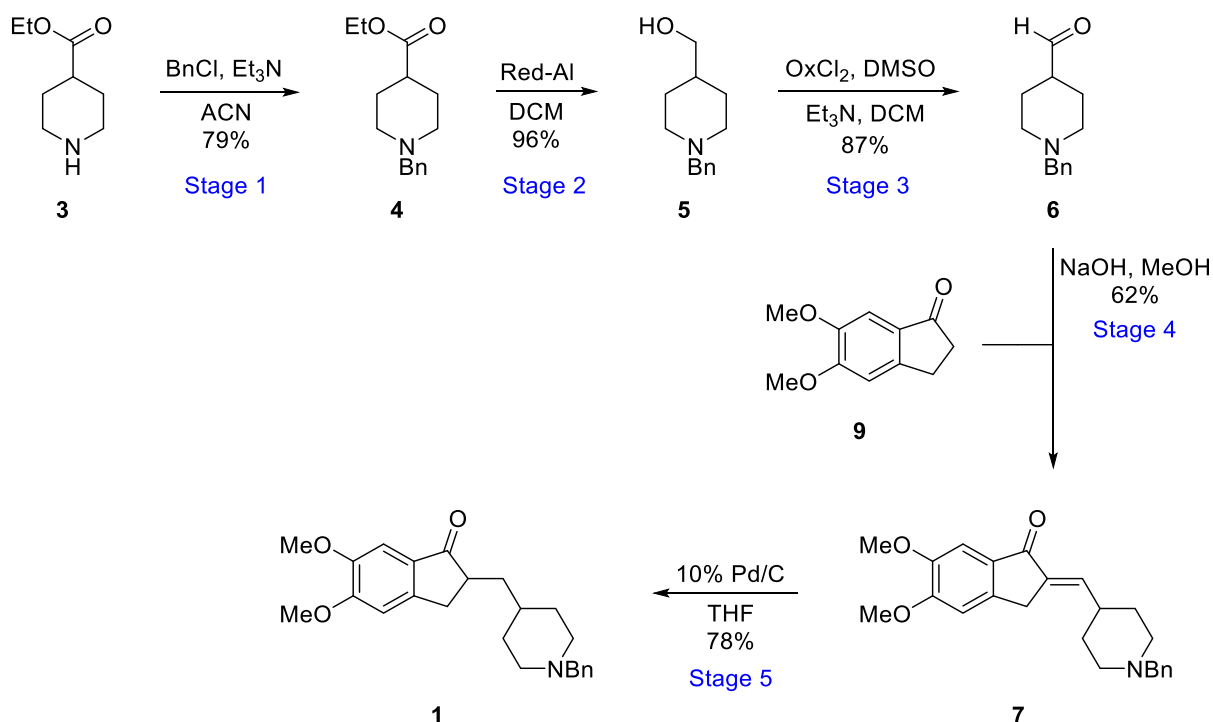
Figure 6.3. Proposed future modification of donepezil **1**.

It is envisaged that using flow chemistry, a shorter synthesis would be achieved which negates some of the draw-backs associated with the current route. In this study, progress towards the development of a continuous flow process route for donepezil **1** is described and contrasted against the analogous batch process route.

6.2. RESULTS AND DISCUSSION

6.2.1. Batch synthesis of donepezil

The synthesis of donepezil **1** (Scheme 6.1) using the traditional batch route can be divided into five distinct stages. The first stage involves a benzylation step in which ethyl isonipecotate **3** is reacted with benzyl chloride in the presence of triethylamine as base to afford the benzylated ester **4** in 79% yield in 3 hours [16]. Thereafter a Red-Al (sodium bis(2-methoxyethoxy)aluminium hydride)-mediated reduction of **4** was achieved at room temperature affording alcohol **5** in a yield of 96% [3], followed by the Swern oxidation at -78°C to afford 1-benzylpiperidine-4-carbaldehyde **6** in an 87% yield [3].



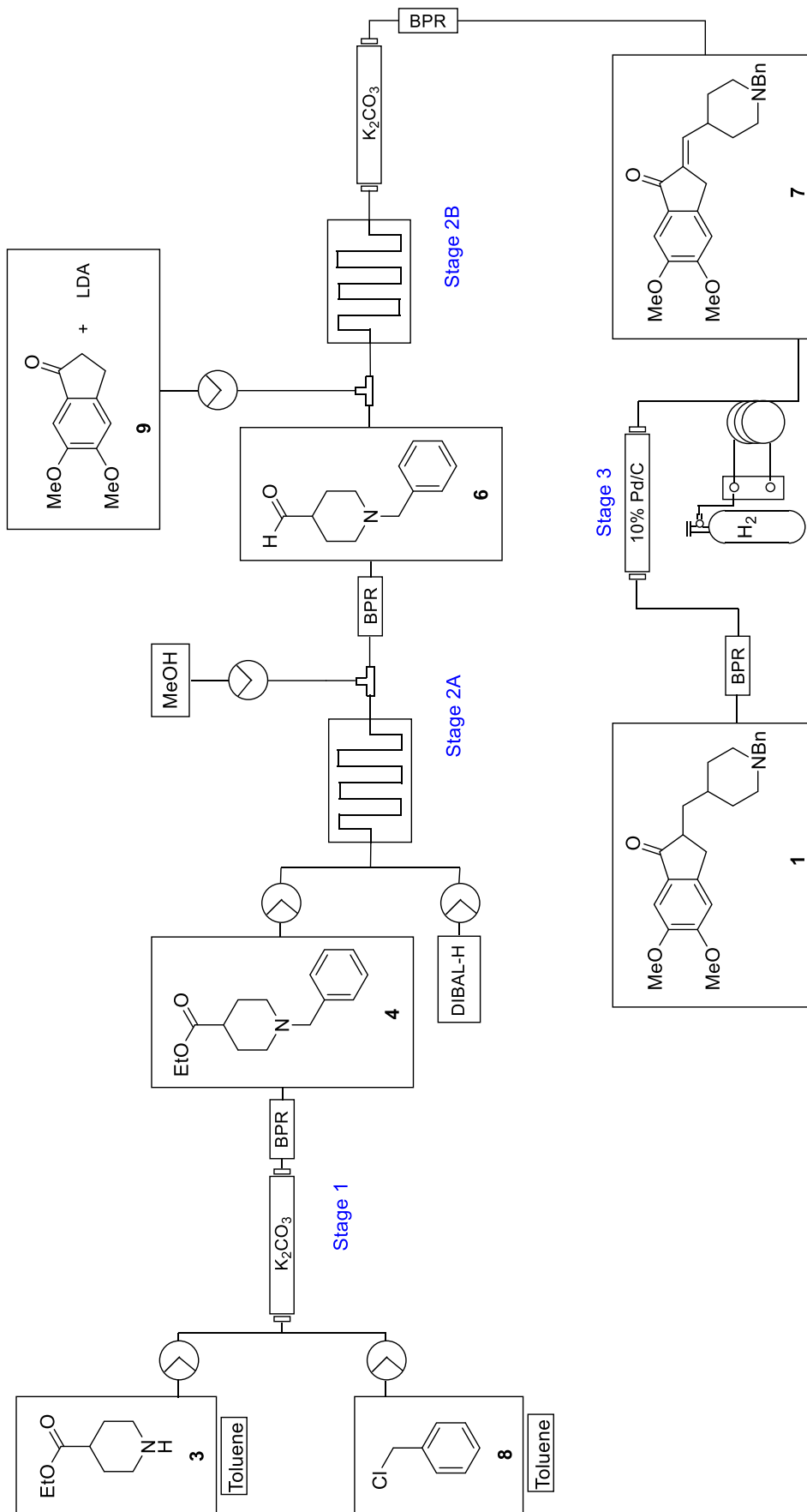
Scheme 6.1. Synthetic route to donepezil **1**.

The donepezil precursor **7** was prepared using an aldol condensation reaction between aldehyde **6** and 5,6-dimethoxy-1-indanone **9** (Scheme 6.1) under basic conditions to afford alkene **7** in 62% in 195 minutes [17]. The final stage of the synthesis was achieved through the catalytic hydrogenation of **7** using tetrahydrofuran as solvent to afford donepezil **1** in a 78% in 6 hours [1]. Tetrahydrofuran was chosen as solvent instead of the more commonly utilised protic solvents such as ethanol or methanol, as these significantly increased the amount of debenzylation. The batch synthesis of donepezil **1** was achieved in 32% over 5 steps with a reaction residence time of 16 hours 45 minutes.

6.2.2. Flow synthesis of donepezil

In the synthesis of donepezil **1** using a flow process (Scheme 6.2), it was attempted to develop a process in which the number of different solvents being used could be minimized, as well as the reaction time and the difficulty of workup procedures, thereby improving the overall synthesis yield of donepezil **1**.

The synthetic process route was envisaged to start off with Stage 1 in which the benzylation of **3** would be performed using pre-made solutions of **3** and benzyl chloride **8** in toluene, and pumping these through a packed-bed reactor (PBR) filled with potassium carbonate followed by a back-pressure regulator (BPR). Thereafter, the reaction stream would flow directly into Stage 2A and be combined

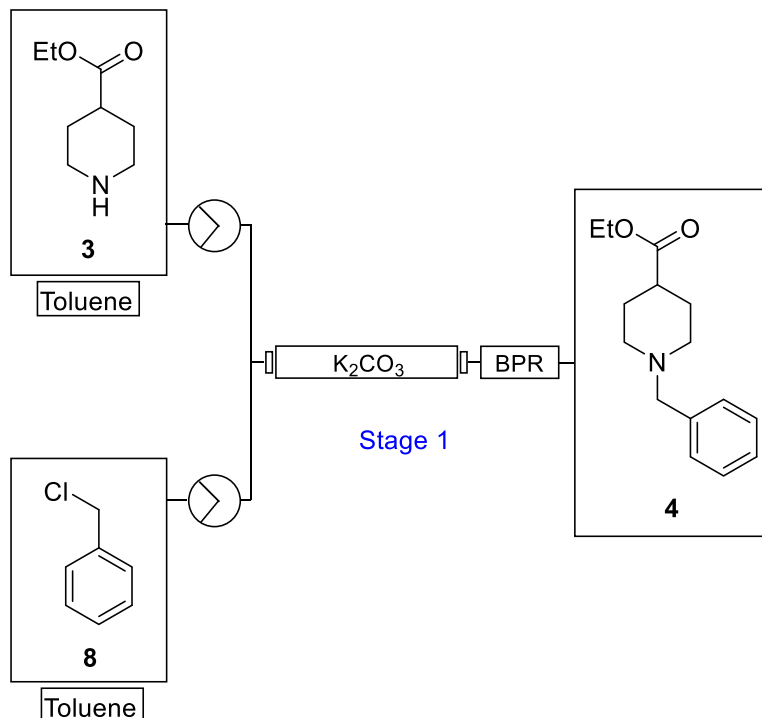


Scheme 6.2. Proposed flow process for donepezil 1.

Figure 6.4. Stage 1 stand-alone setup (left) and the K_2CO_3 packed column mounted on the column heating module (left and right).

In addition, it was also envisaged to use toluene instead of acetonitrile in the flow system as it would allow easy telescoping into Stage 2 (**Scheme 6.2**) where the DIBAL-H reductant utilised is commonly available as a 1 M solution in toluene. Unfortunately, when attempted in toluene the protonated form of **3** precipitates before neutralization with the potassium carbonate in the PBR, causing reactor fouling. As a result, it was decided to continue with the use of acetonitrile which did not cause the aforementioned precipitation issues.

The optimisation of Stage 1 was undertaken by performing temperature as well as residence time screening to find the optimum temperature and residence time at which the benzylation of **3** would proceed to completion. In a typical flow set-up (**Scheme 6.3**), a stock solution of ethyl isonipecotate **3** in acetonitrile (1 M) was combined with a stock solution of benzyl chloride **7** in acetonitrile (1 M) at a T-piece mixer in a 1:1 ratio. Thereafter, the reaction stream was passed through a PBR filled with potassium carbonate followed by a BPR. Results obtained are shown in **Table 6.1** and **Graph 6.1**.

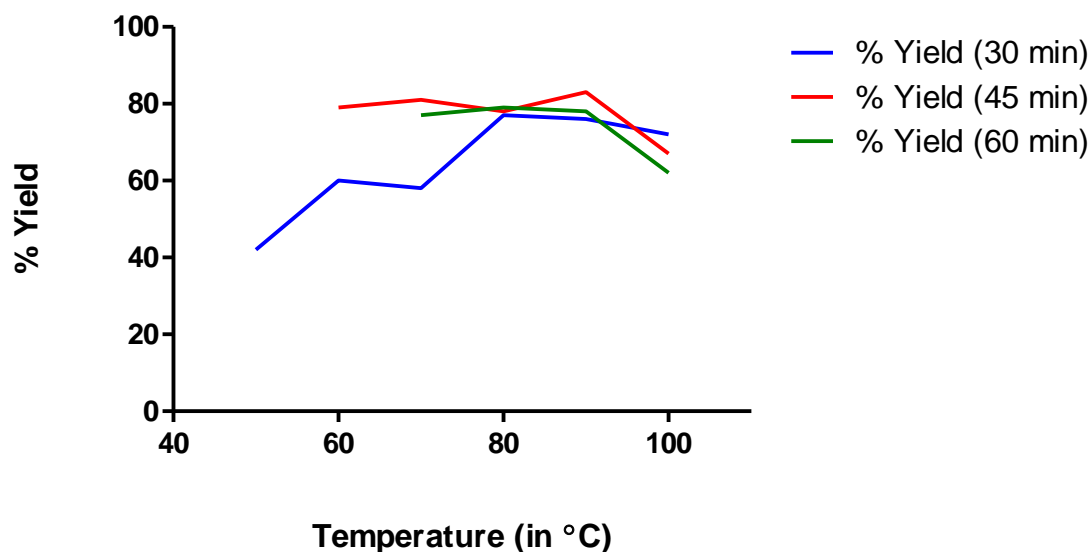


Scheme 6.3. Benzylation of ethyl isonipecotate **3** under flow conditions (Stage 1).

Table 6.1. Temperature and residence time study for Stage 1

| Entry | PBR Temp (°C) | Residence time (min) | Flow rate (mL.min ⁻¹) | % Yield |
|-------|------------------|----------------------------|--------------------------------------|---------|
| 1 | 50 | 30 | 0.183 | 42 |
| 2 | 60 | 30 | 0.183 | 60 |
| 3 | | 45 | 0.122 | 79 |
| 4 | 70 | 30 | 0.183 | 58 |
| 5 | | 45 | 0.122 | 81 |
| 6 | | 60 | 0.092 | 77 |
| 7 | 80 | 30 | 0.183 | 77 |
| 8 | | 45 | 0.122 | 78 |
| 9 | | 60 | 0.092 | 79 |
| 10 | 90 | 30 | 0.183 | 76 |
| 11 | | 45 | 0.122 | 83 |
| 12 | | 60 | 0.092 | 78 |
| 13 | 100 | 30 | 0.183 | 72 |
| 14 | | 45 | 0.122 | 67 |
| 15 | | 60 | 0.092 | 62 |

Comparison by temperature and residence time



Graph 6.1. Comparison of benzylation by temperature and residence time for Stage 1.

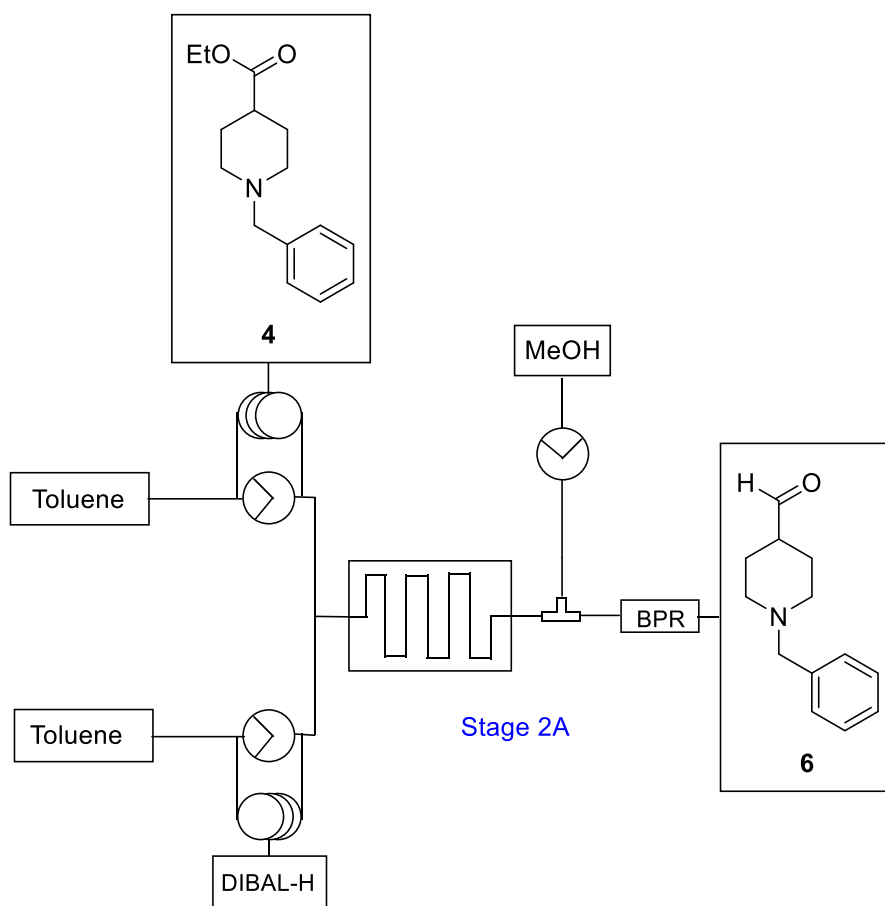
An optimum residence time was found to be 45 min at a temperature of 90 °C with a yield of 83%. It should, however, also be noted that entry 5 (45 min at 70 °C) is comparable with a yield of 81%. Interestingly, it was noted that the yield decreases at elevated temperatures, possibly due to product decomposition, this trend is seen with a distinct drop-off in yield observed at a temperature of 100 °C. As a result, it was decided to adopt the conditions from entry 5 in an effort to limit potential decomposition. The flow-based benzylation was completed in a quarter of the time (45 min) taken for the batch-based process (180 min) and in a comparable yield (81% vs. 79%). In addition, the flow-based process afforded pure material with no need for downstream processing and purification in which the same purification method of batch liquid-liquid extraction was used.

6.2.2.2. Stage 2A

In Stage 2A (**Scheme 6.4**) the reduction of ester **4** to the aldehyde **6** was attempted using DIBAL-H as a reducing agent adopting an approach previously described by Jamison and Webb [18]. Typically, reductions with DIBAL-H occur rapidly, and as a result, low temperatures are often employed to prevent over reduction to the alcohol oxidation level [18].

In attempts to develop a flow-based process it was decided to employ the use of injection loops to introduce the material as opposed to using reagent reservoirs. In doing so, it was easier to introduce moisture and air sensitive DIBAL-H into the system. The two injection loops (2 mL) were pre-loaded

with a solution of **4** (0.45M) in dried, degassed toluene and commercial DIBAL-H (0.5M) in toluene respectively. The reagent streams were mixed in a mixing chip cooled to $-82\text{ }^{\circ}\text{C}$ (**Figure 6.5**) at various flow rates (**Table 6.2**) affording residence times ranging from 10 to 360 sec. Unfortunately, in all instances trace amounts of the product could be detected by ^1H NMR spectroscopy; however, none of the unwanted over reduced material was observed. The results suggest that in contrast to the rapid reductions described by Jamison and Webb, ester **4** appears more robust and as such longer residence times and/or higher temperatures may be required. Alternatively, the reduction could potentially be achieved through an *in situ* Weinreb amide formation with a DIBAL-H and *N*-methylpiperazine mediated reduction [19]. Due to time constraints further investigations into the reduction of ester **4** could not be undertaken.



Scheme 6.4. Reduction of ethyl 1-benzylpiperidine-4-carboxylate **4** (Stage 2A).



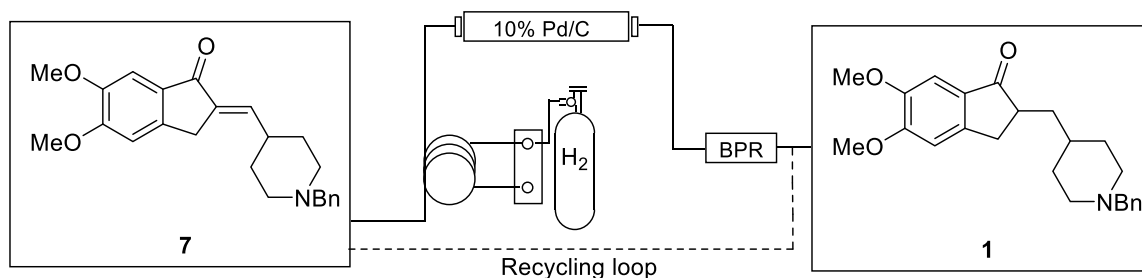
Figure 6.5. Stage 2A stand-alone setup with the mixing chip in the cold-bath at -82 °C.

Table 6.2. Flow rate study for Stage 2A

| Entry | Flow rate (mL.min ⁻¹) | Residence time (sec) | % Yield |
|-------|--------------------------------------|-------------------------|---------|
| 1 | 12.00 | 10 | - |
| 2 | 4.00 | 30 | - |
| 3 | 2.00 | 60 | - |
| 4 | 1.00 | 120 | - |
| 5 | 0.667 | 180 | - |
| 6 | 0.500 | 240 | - |
| 7 | 0.400 | 300 | - |

6.2.2.3. Stage 3

The catalytic reduction of the donepezil precursor **7** (**Scheme 6.5**) was performed by passing **7** (0.10 M, prepared by batch method) through a Gas Addition Module II (GAM II) and PBR containing 150 mg 10% Pd/C (**Figure 6.6**). The GAM II module is a gas-liquid coil reactor which permits gas to be introduced into reagent streams through an inner gas-permeable membrane that runs inside the whole length of the outer coil reactor tubing [14]. At first passage across a PBR housing containing the 10% Pd/C, both the desired product **1** and the debenzylated product were afforded, suggesting that the reduction of the alkene is faster than the debenzylation. At residence times short enough to prevent debenzylation there was incomplete reduction of the alkene **7**. It was therefore opted to use a small plug of Pd/C at a high flow rate, thereby giving minimum exposure to the catalyst. In this instance however, although there was no observed debenzylation of **7**, the reduction of **7** was limited. As such it was decided to use a recycling system in which the repeated exposure of precursor **7** to the catalyst bed was allowed, but never allowing prolonged exposure at any point in time. All reactions were performed at a total flow rate of 0.500 mL.min⁻¹ and recycled for 4.5 – 6 hours. Donepezil **1** was obtained through column chromatography. Results obtained are summarized in **Table 6.3** and **Graph 6.2**.



Scheme 6.5. Catalytic reduction of donepezil precursor **7** (Stage 3).

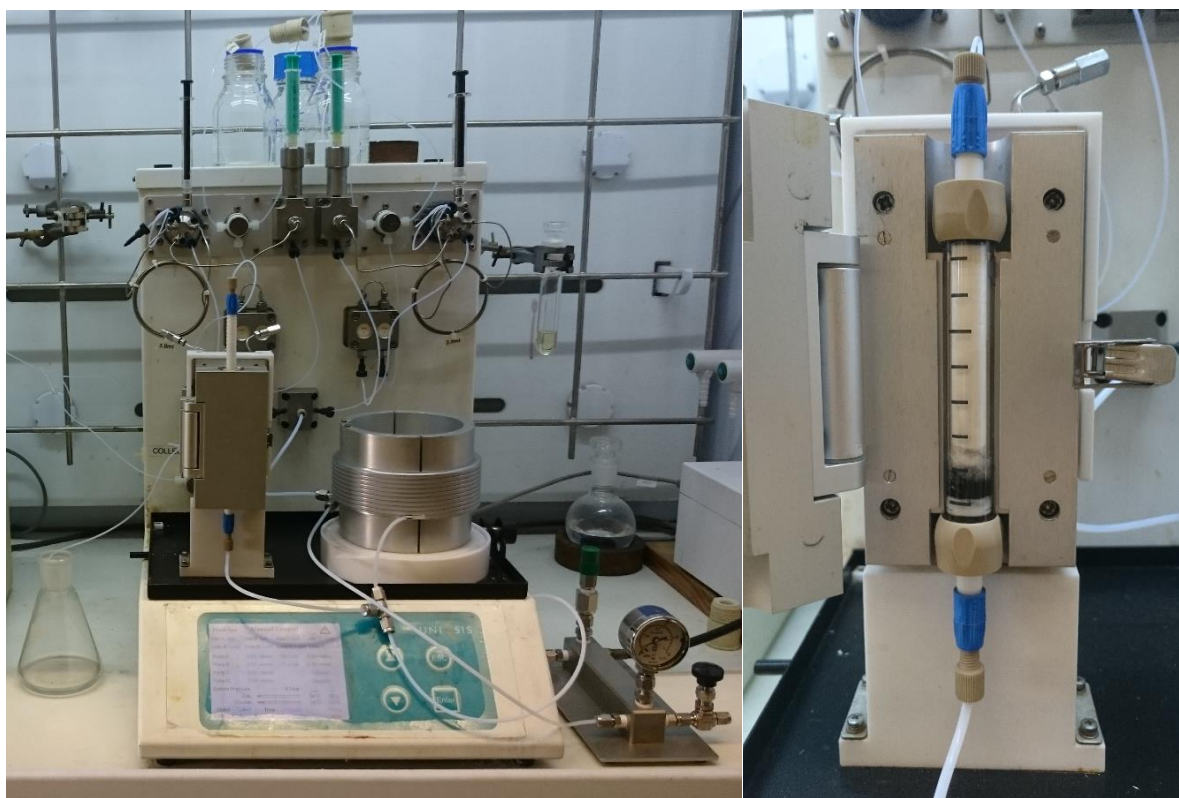
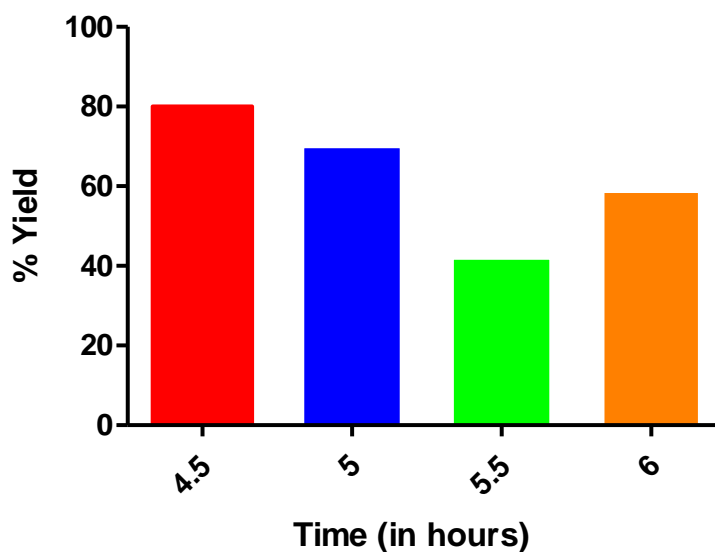


Figure 6.6. Stage 3 stand-alone setup with the GAM II mounted on the coil reactor (left) and the 10% Pd/C packed column mounted on the column heating module (left and right).

Table 6.3. Comparison of residence time at total flow rate of $0.500 \text{ mL}\cdot\text{min}^{-1}$

| Entry | Recycling time (h) | Coil residence time (min) | Column residence time (min) | Pressure (bar) | Debenzylation observed (Y/N) | % Yield |
|-------|--------------------|---------------------------|-----------------------------|----------------|------------------------------|---------|
| 1 | 6.00 | 12.00 | 12.00 | 2.7 | Y | 59 |
| 2 | 5.30 | 12.00 | 12.00 | 9.7 | Y | 42 |
| 3 | 5.00 | 12.00 | 12.00 | 4.8 | Y | 70 |
| 4 | 4.30 | 12.00 | 12.00 | 9.7 | N | 80 |

Comparison by residence time



Graph 6.2. Comparison of catalytic hydrogenation by residence time for Stage 3.

The optimum recycling time without any de-benzylation of the donepezil precursor **6** was 4 hours 30 minutes at a pressure of 9.7 bar at room temperature which provided a yield of 80%. The catalytic reduction of the donepezil precursor **7** (Scheme 6.5) was completed in less time (4.5 hours), in a comparable yield (80%) when compared to the batch process (6 hours, 78%). Furthermore, when compared to the batch process, the catalytic reduction in flow afforded the desired **1** without any observed debenzylation when performed at room temperature.

6.3. CONCLUSION

Under flow conditions, the highest yield obtained for the benzylation of ethyl isonipecotate **3** was 83% at 90 °C with a residence time of 45 minutes. In comparison, the batch process took 3 hours to complete with a comparable yield of 79%. Initial proof-of-concept studies for the DIBAL-H reduction were undertaken; however, at lower temperature with short residence times, no significant conversion was noted. The initial poor results suggest that optimisation of the residence time and temperature needs to be undertaken wherein runs with longer residence times need to be undertaken, potentially at higher temperatures. The reduction of the donepezil precursor **7** to afford the final product donepezil **1** was obtained with a yield of 80% after 4.5 hours with no observable debenzylation in flow, in comparison, the batch process was complete after 6 hours in a yield of 78%. At longer recycle times, minor debenzylation of donepezil **1** was observed which increased with increasing recycling time. Thus, with only two of the three steps completed for the flow process, the

yield of the individual steps was marginally improved, there was a reduction in the reaction times and in the case of the catalytic reduction it was shown to selectively reduce the alkene functionality without any unwanted debenzoylation being observed.

Future work will focus on i) optimisation of the DIBAL-H reduction of **4** to **6**, ii) development of a flow method for the aldol condensation of lithiated 5,6-dimethoxy-1-indanone **6** with the aldehyde **5** (from the DIBAL-H reduction of **4**), reducing the synthesis from 5 to 3 steps, and iii) upscaling of the synthesis of **1** for use as a drug discovery precursor.

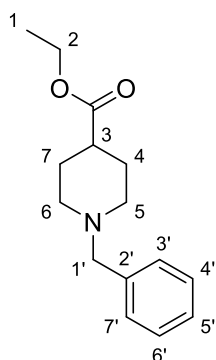
6.4. EXPERIMENTAL

6.4.1. General methods

Dry solvents were distilled under nitrogen before being used. Tetrahydrofuran and toluene were distilled from sodium metal wire with benzophenone added as indicator, acetonitrile and dichloromethane were distilled from calcium hydride. All reagents and solvents from commercial sources were used without further purification. ^1H NMR (300 MHz) and ^{13}C NMR (75 MHz) spectra were recorded on Bruker AVANCE-III-300 instrument using CDCl_3 . CDCl_3 contained tetramethylsilane as an internal standard. Chemical shifts, δ , are reported in parts per million (ppm), and splitting patterns are given as singlet (s), doublet (d), triplet (t), quartet (q), or multiplet (m). Coupling constants, J , are expressed in hertz (Hz). Mass spectra were recorded in ESI mode on a Waters Synapt G2 Mass Spectrometer at 70 eV and 200 mA. Samples were dissolved in acetonitrile (containing 0.1% formic acid) to an approximate concentration of 10 $\mu\text{g}/\text{mL}$. Infrared spectra were run on a Bruker ALPHA Platinum ATR spectrometer. The absorptions are reported on the wavenumber (cm^{-1}) scale, in the range 400 - 4000 cm^{-1} . The signals are reported: value (relative intensity, assignment if possible). Abbreviations used in quoting spectra are: v = very, s = strong, m = medium, w = weak, str = stretch. Melting points were measured on a Stuart Melting Point SMP10 microscope. The retention factor (R_f) values denoted are for thin layer chromatography (TLC) on aluminium-backed Macherey-Nagel ALUGRAM Sil G/UV₂₅₄ plates pre-coated with 0.25 mm silica gel 60, spots were visualised with UV light and basic KMnO_4 spray reagent. Chromatographic separations were performed on Macherey-Nagel Silica gel 60 (particle size 0.063 – 0.200 mm). Yields refer to isolated pure products unless stated otherwise. Flow reaction were conducted on a Uniqsis FlowSyn Stainless Steel reactor. Each compound is named either according to PerkinElmer's *ChemDraw Version 15.0.0.106* or according to common names. The numbering of compounds was not done according to priority, but rather to the author's convenience for characterization.

6.4.2. Batch synthesis of donepezil

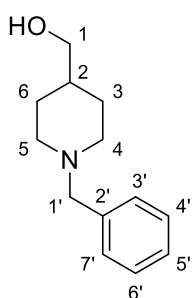
6.4.2.1. Ethyl 1-benzylpiperidine-4-carboxylate **4**



4

A mixture of ethyl isonipecotate **3** (10.00 g, 63.61 mmol, 1 eq.), benzyl chloride **7** (7.7 mL, 67 mmol, 1.05 eq.) and triethylamine (26.5 mL, 191 mmol, 3 eq.) in anhydrous acetonitrile (100 mL) was refluxed for 3 h after which time the reaction mixture was left to cool to room temperature and the solvent was evaporated *in vacuo*. The obtained oil was diluted with ethyl acetate (100 mL) and washed with a 10% aqueous solution of sodium hydroxide (3 x 50 mL) and water (50 mL). The organic layer was dried over anhydrous sodium sulfate, filtered and evaporated *in vacuo* to afford the product. The product was used without any further purification. (Yield 79%); Transparent orange oil. R_f 0.42 (1:3 ethyl acetate: hexane); ν_{\max} (neat)/ cm^{-1} 2944 (C-H str, m), 2801 (C-H str, m), 2760 (C-H str, m), 1728 (C=O str, s), 1448 (C-C str, m), 1168 (C-O str, s), 1046 (C-N str, m), 736 (C-H “oop”, s), 698 (C-H “oop”, s); $^1\text{H NMR}$ (300 MHz, CDCl_3); δ 7.41 – 7.15 (5H, m, ArH's), 4.13 (2H, t, $J = 7.1$ Hz, H-2), 3.51 (2H, s, H-1'), 2.87 (2H, dt, $J = 11.4, 3.1$ Hz, *H-5a & *H-6a), 2.30 (1H, tt, $J = 10.9, 4.2$ Hz, H-3), 2.05 (2H, td, $J = 11.3, 2.7$ Hz, *H-5b & *H-6b), 1.95 – 1.71 (4H, m, H-4 & H-5), 1.26 (3H, t, $J = 7.1$ Hz, H-1); $^{13}\text{C NMR}$ (75 MHz, CDCl_3); δ 175.3 (C=O), 138.5 (C-2'), 129.2 (C-3' & C-7'), 128.3 (C-4' & C-6'), 127.1 (C-5'), 63.4 (C-1'), 60.3 (C-2), 53.0 (C-5 & C-6), 41.3 (C-3), 28.4 (C-4 & C-7), 14.3 (C-1); HRMS m/z (ESI) ($\text{C}_{15}\text{H}_{21}\text{NO}_2$) 248.1682 ([M + H]⁺ requires 248.1645). *Assignments are interchangeable. Characterization of this compound compared well to literature [2].

6.4.2.2. (1-Benzylpiperidin-4-yl)methanol **5**

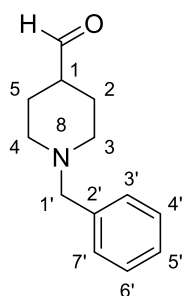


5

To a stirred solution of ethyl 1-benzyl-piperidine-4-carboxylate **4** (7.90 g, 32.5 mmol, 1.0 eq.) in anhydrous dichloromethane (100 mL), was added Red-Al (15.8 mL, 48.7 mmol, 1.5 eq., 60% weight in toluene) at 15 – 20 °C. The contents were stirred for 3 h at room temperature. The reaction was quenched by the slow addition of 10% aqueous sodium hydroxide (5 mL) and then diluted with water (100 mL). The contents were stirred for 30 min, and the organic layer was separated and the aqueous layer was extracted with dichloromethane (3 x 30 mL). The organic layers were combined, dried over anhydrous sodium sulfate, filtered and evaporated *in vacuo* to yield the product. The product was used without any further purification. (Yield 96%). Transparent viscous yellow oil. R_f 0.31 (9:1 dichloromethane: methanol); ν_{\max} (neat)/ cm^{-1} 3331 (O-H str, s, b), 2915 (C-H str, m), 2803 (C-H str, m), 1448 (C-C str, m), 1367 (C-H rock, m), 1112 (C-O str, s), 1040 (C-N str, m), 737 (C-H “oop”, s), 697 (C-H “oop”, s); $^1\text{H NMR}$ (300 MHz, CDCl_3); δ 7.35 – 7.19 (5H, m, Ar-H's), 3.50 (2H, s, H-1'), 3.46 (2H, d, $J = 6.4$ Hz, H-1), 2.91 (2H, d, $J = 11.6$ Hz, #H-4a & #H-5a), 2.53 (1H, s, OH), 1.96

(2H, td, $J = 11.7, 2.3$ Hz, $^{\#}\text{H-4b}$ & $^{\#}\text{H-5b}$), 1.70 (2H, d, $J = 13.9$ Hz, $^{\S}\text{H-3a}$ & $^{\S}\text{H-6a}$), 1.57 – 1.40 (1H, m, H-2), 1.28 (2H, m, $^{\S}\text{H-3b}$ & $^{\S}\text{H-6b}$); $^{13}\text{C NMR}$ (75 MHz, CDCl_3); δ 138.3 (C-2'), 129.4 (C-7' & C-3'), 128.3 (C-6' & C-4'), 127.1 (C-5'), 67.8 (C-1), 63.5 (C-1'), 53.5 (C-5 & C-4), 38.6 (C-2), 28.8 (C-3 & C-6); **HRMS m/z (ESI)** ($\text{C}_{13}\text{H}_{19}\text{NO}$) 206.1591 ($[\text{M} + \text{H}]^+$ requires 206.1539). $^{\#}$ Assignments are interchangeable. § Assignments are interchangeable. Characterization of this compound compared well to literature [2].

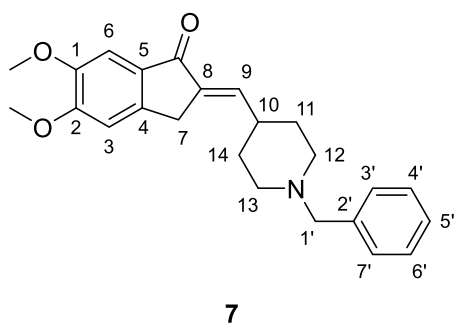
6.4.2.3. 1-Benzylpiperidine-4-carbaldehyde **6**



6

A solution of dimethyl sulfoxide (6.3 mL, 88 mmol, 3.2 eq.) in dichloromethane (10 mL) was added drop-wise to a pre-cooled solution of oxalyl chloride (3.3 mL, 38 mmol, 1.4 eq.) in dichloromethane (40 mL) and left to stir for 30 min. A solution of (1-benzylpiperidin-4-yl)methanol **5** (5.70 g, 27.8 mmol, 1 eq.) in dichloromethane (10 mL) was added drop-wise and stirred for 30 min. Triethylamine (20.3 mL, 147 mmol, 5.3 eq.) was then added and the solution was stirred for an additional 30 min. Upon warming the solution to room temperature, water (30 mL) was then added and the layers were separated. The organic layer was washed with brine (3 x 30 mL), dried over anhydrous sodium sulfate, filtered and evaporated *in vacuo* to afford the product. The product was used without any further purification (Yield 87%). Dark orange oil. R_f 0.27 (95:5 dichloromethane: methanol); ν_{max} (neat)/ cm^{-1} 2930 (C-H str, m), 2801 (H-C=O: C-H, m), 2758 (C-H str, m), 1720 (C=O str, s), 1448 (C-C str, m), 1365 (C-H rock, m), 1069 (C-O str, m), 976 (C-N str, m), 736 (C-H "oop", s), 697 (C-H "oop", s); $^1\text{H NMR}$ (300 MHz, CDCl_3); δ 9.63 (1H, d, $J = 1.1$ Hz, CHO), 7.32 – 7.20 (5H, m, Ar-H's), 3.48 (2H, s, H-1'), 2.80 (2H, dt, $J = 11.9, 4.0$ Hz, $^{\#}\text{H-3a}$ & $^{\#}\text{H-4a}$), 2.29 – 2.15 (1H, m, H-1), 2.09 (2H, td, $J = 11.2, 2.8$ Hz, $^{\#}\text{H-3b}$ & $^{\#}\text{H-4b}$), 1.86 (2H, dd, $J = 13.2, 4.1$ Hz, $^{\S}\text{H-2a}$ & $^{\S}\text{H-5a}$), 1.67 (2H, m, $^{\S}\text{H-2b}$ and $^{\S}\text{H-5b}$); $^{13}\text{C NMR}$ (75 MHz, CDCl_3); δ 204.1 (C=O), 138.3 (C-2'), 129.1 (C-7' & C-3'), 128.3 (C-6' & C-4'), 127.1 (C-5'), 63.3 (C-1'), 52.6 (C-4 & C-3), 48.1 (C-1), 25.5 (C-2 & C-5); **HRMS m/z (ESI)** ($\text{C}_{13}\text{H}_{17}\text{NO}$) 204.1427 ($[\text{M} + \text{H}]^+$ requires 204.1383). $^{\#}$ Assignments are interchangeable. § Assignments are interchangeable. Characterization of this compound compared well to literature [2].

6.4.2.4. (E)-2-[(1-Benzylpiperidin-4-yl)methylene]-5,6-dimethoxy-2,3-dihydro-1H-inden-1-one **7**

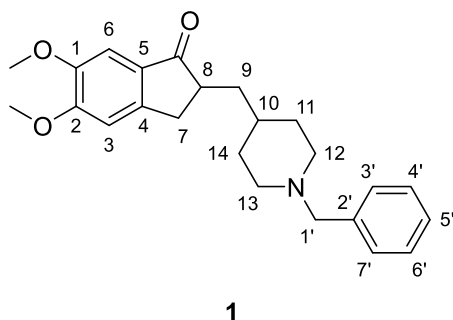


7

To a stirring solution of 5,6-dimethoxy-1-indanone **9** (3.75 g, 19.49 mmol, 1 eq.) in methanol (50 mL) at 40 - 45 °C, was added a mixture of sodium hydroxide (5.45 g, 136.34 mmol, 7 eq.) in methanol: water (50 mL, 4:1) drop-wise over 45 min. The resulting reaction mixture was left to stir for 30 min after which time a solution of 1-benzylpiperidine-4-carbaldehyde **6** (4.74 g, 23.31 mmol, 1.2 eq.) in methanol (20 mL) was

added drop-wise to the reaction mixture. The reaction mixture was left to stir for 2 h after which time the reaction was left to cool to room temperature. The solvent was evaporated *in vacuo* and the water (100 mL) was added to the resulting residue. The mixture was triturated for 30 min after which time the solids were filtered off and washed with additional water (50 mL), followed by a mixture of ice-cold methanol: acetone (30 mL, 1:1) to afford the product. The product was used without any further purification. (Yield 62%). Yellow solid. R_f 0.36 (95:5 dichloromethane: methanol); **mp** 171 – 174 °C (literature [17] 170 – 174 °C); **vmax (neat)/cm⁻¹** 2922 (=C-H str, m), 1686 (C=O str, s), 1643 (C=C str, s), 1594 (C-C str (in-ring), s), 1496 (C-H bend, m), 1452 (m), 1306 (C-H bend, s), 1245 (C-N str, m), 1124 (m), 978 (=C-H bend, m), 851 (C-H “oop”, m), 798 (s), 763 (s), 730 (s), 693 (s); **¹H NMR (300 MHz, CDCl₃)**; δ 7.35 – 7.19 (6H, m, Ar-H's & H-6), 6.88 (1H, s, H-3), 6.65 (1H, d, J = 9.7 Hz, H-9), 3.96 (3H, s, OCH₃), 3.91 (3H, s, OCH₃), 3.57 (2H, d, J = 1.3 Hz, H-7), 3.51 (2H, s, H-1'), 2.91 (2H, d, J = 11.6 Hz, H-13#), 2.39 – 2.24 (1H, m, H-10), 2.05 (2H, td, J = 11.3, 3.0 Hz, #H-11a & #H-14a), 1.65 (4H, dt, J = 14.5, 10.5 Hz, #H-11b & #H-14b); **¹³C NMR (75 MHz, CDCl₃)**; δ 192.6 (C=O), 155.4 (C-2), 149.6 (C-1), 144.6 (C-9), 139.9 (C-5), 138.4 (C-4), 135.7 (C-2'), 131.9 (C-8), 129.3 (C-7' & C-3'), 128.3 (C-6' & C-4'), 127.1 (C-5'), 107.3 (C-3), 105.1 (C-6), 63.6 (C-1'), 56.3 (OCH₃), 56.2 (OCH₃), 53.2 (C-12 & C-13), 37.4 (C-7), 31.3 (C-10), 29.6 (C-11 & C-14); **HRMS m/z (ESI)** (C₂₄H₂₇NO₃) 378.2073 ([M + H]⁺ requires 378.2064). #Assignments are interchangeable. Characterization of this compound compared well to literature [2].

6.4.2.5. *rac*-2-[(1-Benzylpiperidin-4-yl)methyl]-5,6-dimethoxy-2,3-dihydro-1*H*-inden-1-one **1** (Donepezil)



(*E*)-2-[(1-Benzylpiperidin-4-yl)methylene]-5,6-dimethoxy-2,3-dihydro-1*H*-inden-1-one **7** (1.48 g, 3.91 mmol, 1 eq.) was dissolved in tetrahydrofuran (35 mL) and stirred for 15 min at room temperature. 10% Pd/C (0.20 g, 50 mg/mmol) was then added to the reaction mixture. Hydrogen gas was pumped into the reaction vessel at 1 atm and left to stir until the disappearance of the starting material (6 h as monitored by

TLC). The catalyst was then removed by filtering the reaction mixture through celite. The solvent was then removed *in vacuo* to afford the crude product. The crude material was purified by column chromatography (95:5 dichloromethane: methanol as eluent) to afford the product. (Yield 78%). Viscous yellow oil. R_f 0.27 (95:5 dichloromethane: methanol); ν_{\max} (neat)/ cm^{-1} 2915 (C-H str, m), 1688 (C=O str, s), 1591 (C-C str (in-ring), s), 1496 (C-H bend, m), 1458 (m), 1306 (C-H bend, s), 1258 (C-N str, m), 1114 (m), 1031 (s), 847 (w), 804 (m), 730 (C-H “oop”, s), 694 (C-H “oop”, s); $^1\text{H NMR}$ (300 MHz, CDCl_3); δ 7.36 – 7.20 (5H, m, Ar-H's), 7.15 (1H, s, H-6), 6.84 (1H, s, H-3), 3.95 (3H, s, OCH_3), 3.89 (3H, s, OCH_3), 3.54 (2H, s, H-1'), 3.22 (1H, dd, $J = 17.6, 8.1$ Hz, H-8), 2.92 (2H, dd, $J = 11.3, 3.1$ Hz, H-7), 2.68 (2H, dt, $J = 11.3, 3.5$ Hz, $^{\#}\text{H-12a}$ & $^{\#}\text{H-13a}$), 2.01 (2H, t, $J = 11.7$ Hz, $^{\#}\text{H-12b}$ & $^{\#}\text{H-13b}$), 1.90 (1H, ddd, $J = 13.4, 7.5, 4.4$ Hz, $^{\#}\text{H-11a}$), 1.71 (2H, t, $J = 13.5$ Hz, $^{\#}\text{H-11b}$ & $^{\#}\text{H-14a}$), 1.38 (4H, m, $^{\#}\text{H-14b}$, H-10 & H-9 2H); ^{13}C (75 MHz, CDCl_3); δ 207.9 (C=O), 155.5 (C-2), 149.5 (C-1), 148.9 (C-4 & C-5), 129.5 (C-2'), 129.4 (C-7' & C-3'), 128.3 (C-6' & C-4'), 127.2 (C-5'), 107.5 (C-3), 104.5 (C-6), 63.4 (C-1'), 56.3 (OCH_3), 56.2 (OCH_3), 53.8 (C-12 & C-13), 45.5 (C-8), 38.8 (C-9), 34.4 (C-7), 33.5 (C-14), 32.8 (C-11), 31.7 (C-10); **HRMS** m/z (ESI) ($\text{C}_{24}\text{H}_{29}\text{NO}_3$) 380.2273 ([M + H]⁺ requires 380.2220). [#]Assignments are interchangeable. [§]Assignments are interchangeable. Characterization of this compound compared well to literature [2].

6.4.3. Flow synthesis of donepezil

6.4.3.1. General procedure for the synthesis of ethyl 1-benzylpiperidine-4-carboxylate **4**

A 10 mL glass OmnitFit™ column was loaded with potassium carbonate to a total volume of 5.5 mL. The column was mounted in a Uniqsis FlowSyn SS reactor heating block using the set-up shown in **Scheme 6.3** and **Figure 6.4**. The column was washed with anhydrous acetonitrile at 1.0 mL.min⁻¹ for 30 minutes. A stock solution containing ethyl isonipecotate **3** (1.0 M, 1.0 eq.) in anhydrous acetonitrile was mixed with a stock solution of benzyl chloride **7** (1.0 M, 1.0 eq.) in anhydrous acetonitrile in a 1:1 ratio at a T-piece mixer. Thereafter, the flow stream was passed through the glass OmnitFit™ column containing the potassium carbonate at temperatures ranging from 50 - 100 °C. Total flow rates varying

from 0.092 – 0.183 mL.min⁻¹ (T_R = 30 – 60 min) were used. A post-reaction wash of 12 mL with anhydrous acetonitrile was performed. The solvent was evaporated *in vacuo*. The obtained oil was diluted with ethyl acetate (20 mL) and washed with a 10 % aqueous solution of sodium hydroxide (3 x 15 mL) and water (15 mL). The organic layer was dried over anhydrous sodium sulfate, filtered and evaporated *in vacuo* to afford the product. The product was used without any further purification. (Yields 9 - 83%).

6.4.3.2. General procedure for the attempted synthesis of 1-benzylpiperidine-4-carbaldehyde **6**

A 2 mL glass mixing chip was cooled in a dry ice: acetone bath to -82 °C using the set-up shown in **Scheme 6.5** and **Figure 6.5**. The glass mixing chip was washed with anhydrous toluene at 1.0 mL.min⁻¹ for 30 min prior to commencement of the reactions. A stock solution containing ethyl 1-benzylpiperidine-4-carboxylate **4** (0.45 M, 1.0 eq.) in anhydrous toluene was mixed with a stock solution of DIBAL-H (0.5 M, 1.1 eq.) in anhydrous toluene in a 1:1 ratio within the glass mixing chip. Thereafter the flow stream was collected in a vial containing 15 mL of methanol. Total flow rates varying from 12.00 – 0.333 mL.min⁻¹ (T_R = 10 – 360 s) were used. A post-reaction wash of 6 mL with anhydrous toluene was performed. The solvent was evaporated *in vacuo*. The obtained oil was diluted with ethyl acetate (20 mL) and washed with water (3 x 15 mL). The organic layer was dried over anhydrous sodium sulfate, filtered and evaporated *in vacuo* to afford the crude material.

6.4.3.3. General procedure for the synthesis of donepezil **1**

A 10 mL glass OmnitFit™ column was loaded with 150 mg of 10% Pd/C together with celite to a total volume of 5.5 mL. The column was mounted in a Uniqsis FlowSyn SS reactor heating block whereas the GAM II module (6.0 mL) was mounted on the coil heating module using the set-up shown in **Scheme 6.5** and **Figure 6.6**. The glass OmnitFit™ column and GAM II module were washed with tetrahydrofuran at 0.2 mL.min⁻¹ for 1 hour maintaining a hydrogen pressure of 2.0 bar and a system pressure ranging from 2.7 – 9.7 bar (depending on the back-pressure regulator). A stock solution containing (*E*)-2-[(1-benzylpiperidin-4-yl)methylene]-5,6-dimethoxy-2,3-dihydro-1*H*-inden-1-one **7** (0.05 M) in tetrahydrofuran was passed through the GAM II module followed by the flow stream passing through the glass OmnitFit™ column containing the 10% Pd/C at temperatures ranging from 21 - 27 °C. Thereafter the flow stream was recycled for 4.5 – 6 hours and then collected. A total flow rate of 0.500 mL.min⁻¹ was used with residence times of 12.00 min (GAM II module) and 11.00 min (OmnitFit™ column). A post-reaction wash with tetrahydrofuran was performed at a flow rate of 0.500 mL.min⁻¹ for 45 min. The solvent was evaporated *in vacuo*. The obtained oil was diluted with ethyl acetate (20 mL) and washed with water (3 x 15 mL). The organic layer was dried over anhydrous sodium sulfate, filtered and evaporated *in vacuo* to afford the crude material. The crude material was

purified by column chromatography (95:5 dichloromethane: methanol as eluent) to afford the product (Yields 42 – 80%).

6.5. ACKNOWLEDGEMENTS

This work was supported by the National Research Foundation (NRF) of South Africa (Thuthuka grant number 87893), the University of Pretoria (University, Science Faculty Research Councils and Research and Development Program) and the Council for Scientific and Industrial Research (CSIR), South Africa. Opinions expressed in this publication and the conclusions arrived at, are those of the authors, and are not necessarily attributed to the NRF. The authors would like to gratefully acknowledge Ms Madelien Wooding (University of Pretoria) for LC-MS services.

6.6. CONFLICT OF INTEREST

The authors declare no conflict of interest.

6.7. APPENDIX E. SUPPLEMENTARY INFORMATION

Appendix E can be found as a separate document on the CD.

6.8. REFERENCES

- [1] H. Sugimoto, Y. Iimura, Y. Yamanishi, K. Yamatsu, Synthesis and structure-activity relationships of acetylcholinesterase inhibitors: 1-Benzyl-4-[(5,6-dimethoxy-1-oxoindan-2-yl)methyl]piperidine hydrochloride and related compounds, *J. Med. Chem.*, 38 (1995) 4821-4829.
- [2] D.G. van Greunen, W. Cordier, M. Nell, C. van der Westhuyzen, V. Steenkamp, J.-L. Panayides, D.L. Riley, Targeting Alzheimer's disease by investigating previously unexplored chemical space surrounding the cholinesterase inhibitor donepezil, *Eur. J. Med. Chem.*, 127 (2017) 671-690.
- [3] N. Niphade, A. Mali, K. Jagtap, R.C. Ojha, P.J. Vankawala, V.T. Mathad, An improved and efficient process for the production of donepezil hydrochloride: Substitution of sodium hydroxide for n-butyl lithium via phase transfer catalysis, *Org. Process Res. Dev.*, 12 (2008) 731-735.
- [4] T. Fukuyama, H. Chiba, H. Kuroda, T. Takigawa, A. Kayano, K. Tagami, Application of continuous flow for DIBAL-H reduction and n-BuLi mediated coupling reaction in the synthesis of eribulin mesylate, *Org. Process Res. Dev.*, 20 (2015) 503-509.
- [5] L. Malet-Sanz, F. Susanne, Continuous flow synthesis. A pharma perspective, *J. Med. Chem.*, 55 (2012) 4062-4098.
- [6] J.P. McMullen, C.H. Marton, B.D. Sherry, G. Spencer, J. Kukura, N.S. Eyke, Development and scale-up of a continuous reaction for production of an active pharmaceutical ingredient intermediate, *Org. Process Res. Dev.*, 22 (2018) 1208-1213.

- [7] J.C. McWilliams, A.D. Allian, S.M. Opalka, S.A. May, M. Journet, T.M. Braden, The evolving state of continuous processing in pharmaceutical API manufacturing: A survey of pharmaceutical companies and contract manufacturing organizations, *Org. Process Res. Dev.*, 22 (2018) 1143-1166.
- [8] M. Baumann, I.R. Baxendale, The synthesis of active pharmaceutical ingredients (APIs) using continuous flow chemistry, *Beilstein J. Org. Chem.*, 11 (2015) 1194-1219.
- [9] J.C. Pastre, D.L. Browne, S.V. Ley, Flow chemistry syntheses of natural products, *Chem. Soc. Rev.*, 42 (2013) 8849-8869.
- [10] J. Wegner, S. Ceylan, A. Kirschning, Flow chemistry - A key enabling technology for (multistep) organic synthesis, *Adv. Synth. Catal.*, 354 (2012) 17-57.
- [11] R.J. Ingham, C. Battilocchio, D.E. Fitzpatrick, E. Sliwinski, J.M. Hawkins, S.V. Ley, A systems approach towards an intelligent and self-controlling platform for integrated continuous reaction sequences, *Angew. Chem. Int. Ed. Engl.*, 54 (2015) 144-148.
- [12] J. Yoshida, Y. Takahashi, A. Nagaki, Flash chemistry: Flow chemistry that cannot be done in batch, *Chem. Commun.*, 49 (2013) 9896-9904.
- [13] V. Hessel, D. Kralisch, N. Kockmann, T. Noel, Q. Wang, Novel process windows for enabling, accelerating, and uplifting flow chemistry, *ChemSusChem*, 6 (2013) 746-789.
- [14] http://www.uniqsis.com/securedocs/common/FlowSyn_brochure.pdf, ([Accessed 2019/02/06]).
- [15] H. Huang, D.S. La, A.C. Cheng, D.A. Whittington, V.F. Patel, K. Chen, T.A. Dineen, O. Epstein, R. Graceffa, D. Hickman, Y.H. Kiang, S. Louie, Y. Luo, R.C. Wahl, P.H. Wen, S. Wood, R.T. Fremeau, Jr., Structure- and property-based design of aminooxazoline xanthenes as selective, orally efficacious, and CNS penetrable BACE inhibitors for the treatment of Alzheimer's disease, *J. Med. Chem.*, 55 (2012) 9156-9169.
- [16] D. Manetti, L. Di Cesare Mannelli, S. Dei, N. Galeotti, C. Ghelardini, M.N. Romanelli, S. Scapecchi, E. Teodori, A. Pacini, A. Bartolini, F. Gualtieri, Design, synthesis, and preliminary pharmacological evaluation of a set of small molecules that directly activate Gi proteins, *J. Med. Chem.*, 48 (2005) 6491-6503.
- [17] R.J.R. Rao, A.K.S. Bhujanga Rao, Y.L.N. Murthy, Efficient and industrially viable synthesis of donepezil, *Synth. Commun.*, 37 (2007) 2847-2853.
- [18] D. Webb, T.F. Jamison, Diisobutylaluminum hydride reductions revitalized: a Fast, robust, and selective continuous flow system for aldehyde synthesis, *Org. Lett.*, 14 (2012) 568-571.
- [19] K. Hagiya, S. Mitsui, H. Taguchi, A facile and selective synthetic method for the preparation of aromatic dialdehydes from diesters- via the amine-modified SMEAH reduction system, *Synthesis*, 2003 (2003) 823-828.

Chapter 7. Conclusion, and limitations and future work

7.1. THESIS CONCLUSION

In this study, four different series of compounds, consisting of ninety-one analogues, were synthesized as novel compounds against biomarkers of AD. These included; (i) series 1: *N*-benzylpiperidine carboxamide derivatives; (ii) series 2: 1-(5,6-dimethoxy-8*H*-indeno[1,2-*d*]thiazole-2-yl)urea derivatives; (iii) series 3: 1-amino-3-(indeno[1,2-*b*]indol-5(10*H*)-yl)propan-2-ol derivatives; and series 4: 6,7-dimethoxy-1-phenyl-1,4-dihydroindeno[1,2-*c*]pyrazole-3-carboxamide derivatives. All compounds were evaluated for activity against acetylcholinesterase (AChE), the major biomarker of AD. Derivatized compounds of series 1 were assessed for activity against butyrylcholinesterase (BuChE). Derivatized compounds of series 3 were assessed for activity against the amyloid precursor protein cleaving enzyme 1 (BACE1).

Compound **25** (IC₅₀ = 5.94 μM) and compound **33** (IC₅₀ = 0.41 μM), of series 1 (Chapter 2) were found to be the most active against *EeAChE* using Ellman's assay method. Replacement of the carbonyl groups with that of an imine, together with the alteration in the position of the nitrogen in the heterocycle of compound **33**, led to the synthesis of more potent inhibitors against AChE due to its higher inhibition of *EeAChE*. These compounds demonstrated *in vitro* selectivity for AChE rather than BuChE.

Of the compounds in series 2 (Chapter 3), compound **35**, a thiazole with a urea linker, was found to have the highest inhibitory potential against AChE with an IC₅₀ value of 12.74 ± 2.33 μM. The benzyl group derivatives, with substituents on the *para*-position, showed better inhibitory activity than the aryl group derivatives. In the case of halogen substituents on the aryl derivatives, fluorine substituents in the *ortho*-position showed better inhibitory activity. Elongated substituents on the benzyl derivatives, with longer alkyl chains resulted in increased inhibitory activity of compound **35** vs. compound **39**.

In series 3 (Chapter 4), seventeen novel 1-amino-3-(indeno[1,2-*b*]indol-5(10*H*)-yl)propan-2-ol derivatives were synthesized with the target being BACE1 inhibition. Compound **24** was found to have the highest inhibitory activity (91%) against human BACE1. Compound **25** had the best inhibitory activity against *EeAChE* with an IC₅₀ value of 13.50 ± 1.41 μM. It was observed that by substituting the planar benzyl group (compound **9**, 42% inhibition) with that of a rigid cyclohexyl- and methyl group (compound **25**, 86% inhibition) or a 1,2,3,4-tetrahydronaphthalene group (compound **22**, 71% inhibition), the inhibition of BACE1 increased substantially which suggests that cyclic aliphatic systems may be good substituents in the development of BACE1 inhibitors.

Series 4 (Chapter 5) consisted of twenty-four novel 6,7-dimethoxy-1-phenyl-1,4-dihydroindeno[1,2-c]pyrazole-3-carboxamide derivatives which were synthesized as possible NMDA antagonists. These compounds were not observed to have AChE activity and that the compounds will in future undergo screening for NMDA.

Under flow conditions (Chapter 6), the highest yield obtained for the benzylation of ethyl isonipecotate **3** was 83% at 90 °C with a residence time of 45 minutes. In comparison the batch process took 3 hours to complete with a comparable yield of 79%. Initial proof-of-concept studies for the DIBAL-H reduction of compound **4** were undertaken, however, at lower temperature with short residence times no significant conversion was noted. The initial poor results suggest that optimisation of the residence time and temperature need to be undertaken wherein runs with longer residence times need to be undertaken, potentially at higher temperatures. The reduction of the donepezil precursor, compound **7** to afford the final product donepezil **1**, was obtained with a yield of 80% after 4.5 hours with no observable debenylation in flow. In comparison, the batch process was complete after 6 hours in a yield of 78%. At longer recycle times, minor debenylation of donepezil **1** was observed which increased with increasing recycling time. Thus, with only two of the three steps completed for the flow process, the yield of the individual steps was marginally improved, there was a reduction in the reaction times and in the case of the catalytic reduction it was shown to selectively reduce the alkene functionality without any unwanted debenylation being observed.

7.2. LIMITATIONS AND FUTURE WORK

Due to time constraints, it was unable to obtain A β -aggregation assay information in Chapter 2. However, this information will be obtained prior to the submission of the article for publication. Further studies will be conducted on structural changes on the newly identified lead compound, 1-benzyl-*N*-(1-methyl-3-oxo-2-phenyl-2,3-dihydro-1*H*-pyrazol-4-yl) piperidine-4-carboxamide **25** (IC₅₀ = 5.94 μ M). Substitutions like a (di)methoxy substitution on the phenyl ring might improve the activity and it would be worth to explore it further.

Assay studies on glycogen synthase kinase 3 (GSK-3) could not be performed due the enzyme assay kit being expensive at this stage (Chapter 3). Additional inhibition assay studies will be performed on GSK-3 in order to find a possible dual inhibitor of both AChE and GSK-3. Compound **35**, the strongest *Ee*AChE inhibitor of series 3, only have a moderate *Ee*AChE inhibition activity of IC₅₀ = 12.74 μ M. It would be of great benefit to perform addition molecular modelling as well as synthesis of other elongated derivatives of compound **35** such as: propoxy, isopropoxy, *N*-methyl, *N*-ethyl, *N,N*-dimethyl and *N,N*-diethyl groups.

Due to the relative cytotoxicity of the compounds synthesized in Chapter 4, further studies will be conducted to determine the effect of less bulky substituents on the cytotoxicity as well as the inhibitory effect on BACE1. Additional work, such as the substitution of benzyl groups with that of phenyl or aliphatic groups, are also of great interest in which BACE1 activity as well as the cytotoxicity of these inhibitors may be affected.

The fourth series of compounds could not be evaluated against NMDA due to a collaboration agreement not being concluded at this stage (Chapter 5). Assessment of the antagonistic properties of these compounds on NMDA need to be concluded prior to submission of the article for publication. Although this series of compounds with aryl/benzyl substitutions did not display any inhibition of *EeAChE*, further exploration will be done with other aliphatic groups such as *N*-alkyl groups and other *N*-heterocycles.

Initial proof-of-concept for the DIBAL-H reduction has been undertaken in Stage 2a of the total synthesis of donepezil **1** (Chapter 6), but requires further optimisation. Further work will be attempting to incorporate the aldol condensation of lithiated 5,6-dimethoxy-1-indanone **9** with 1-benzylpiperidine-4-carbaldehyde **6** from the DIBAL-H reduction of ethyl 1-benzylpiperidine-4-carboxylate **4**. Thus, affording an overall total synthesis of 3 steps compared to the traditional batch synthesis of 5 steps. Stage 1 has been optimized and completed; it will be then attempted to link the three individual stages into one continuous flow synthesis. Completion of the donepezil synthesis will enable the mass production of donepezil **1** for the development of donepezil derivatives which may contain dual inhibitory ability of AChE and BACE1.